CRANFIELD UNIVERSITY

MONICA PATRICIA DA SILVA SANTOS

CALCIUM LOOPING FOR PULP AND PAPER INDUSTRY DECARBONISATION AND HYDROGEN PRODUCTION FROM BIOMASS AND WASTE

SCHOOL OF WATER, ENERGY AND ENVIRONMENT
Energy And Power

PhD
Academic Year: 2019 - 2022

Supervisor: Dr. Dawid Hanak
Associate Supervisor: Prof. Vasilije Manovic
August 2022

CRANFIELD UNIVERSITY

SCHOOL OF WATER, ENERGY AND ENVIRONMENT
Energy And Power

PhD

Academic Year 2019 - 2022

MONICA PATRICIA DA SILVA SANTOS

CALCIUM LOOPING FOR PULP AND PAPER INDUSTRY DECARBONISATION AND HYDROGEN PRODUCTION FROM BIOMASS AND WASTE

Supervisor: Dr. Dawid Hanak
Associate Supervisor: Prof. Vasilije Manovic
August 2022

This thesis is submitted in partial fulfilment of the requirements for the degree of PhD

ABSTRACT

Global CO_2 emissions from fossil fuels have been rising for more than a century. Nevertheless, to meet the ambitious targets set by the Paris Agreement, greenhouse gas emissions must be substantially reduced. The improvement of energy efficiency, implementation of carbon capture and reduction of fossil fuel dependency can play an important role. Of the CO_2 capture technologies, amine scrubbing is the most mature technology; however, calcium looping has shown to be a promising one. Thus, this research aimed to assess the techno-economic feasibility of calcium lopping as a carbon capture technology for combined heat, power and hydrogen production from biomass and/or waste. First, a new concept for the conversion of the pulp and paper industry to carbon-negative that relies on the inherent CO_2 capture capability of the Kraft process was proposed. This concept has shown that a pulp and paper plant can turn from importer to electricity exporter with the cost of CO_2 avoided of 39.0 €/t_{CO_2}. Second, in the pulp and paper industry, two carbon capture and storage routes were compared, calcium looping retrofitted to the pulp and paper plant and calcium looping coupled with black liquor gasification. The latter was assessed for H_2 production and for electricity generation with a gas turbine combined cycle or solid-oxide fuel cell. The last alternative has shown that the pulp and paper plant can also become a net electricity export asset at the expense of the cost of CO_2 avoided, 50.8 €/t_{CO_2}. On the contrary, the alternative for H_2 production presented the highest energy penalty but the lowest cost of CO_2 avoided (48.8 €/t_{CO_2}). Third, the feasibility of calcium looping for H_2 production and *in-situ* CO_2 capture was assessed for waste-to-energy conversion in a greenfield scenario. However, this resulted in a significantly higher levelised cost of hydrogen (5.0 €/kg_{H_2}) compared to that estimated for conventional gasification (2.7 €/kg_{H_2}). Although calcium looping is more cost-efficient for carbon capture in a retrofitted scenario, this technology can become a competitive technology for hydrogen production in a greenfield scenario.

Keywords: Calcium looping, carbon capture, sorption-enhanced gasification, techno-economic analysis, waste-to-energy

DECLARATION

I declare that no part of the work referred to in the thesis has been submitted for any other degree or professional qualification of this or any other institution.

Five papers were published in peer-reviewed journals and are part of this submission. These journal papers were published by Elsevier and Springer that allow reuse and reproduction of the entire published material in an unchanged form in the PhD Thesis.

Elsevier[1]

"Theses and dissertations which contain embedded PJAs [Published Journal Article] as part of the formal submission can be posted publicly by the awarding institution with DOI links back to the formal publications on ScienceDirect."

Springer[2]

"Authors have the right to reuse their article's Version of Record, in whole or in part, in their own thesis. Additionally, they may reproduce and make available their thesis, including Springer Nature content, as required by their awarding academic institution. Authors must properly cite the published article in their thesis according to current citation standards."

1 Elsevier (2021), Article Sharing, Elsevier B.V., available online: https://www.elsevier.com/about/policies/sharing (last accessed: 24/11/2021)

2 Springer (2021), Author reuse, Springer Nature, available online: https://www.springer.com/gp/rights-permissions/obtaining-permissions/882 (last accessed: 14/12/2021)

To my husband Carlos Eduardo

ACKNOWLEDGEMENTS

Undertaking the PhD during a pandemic, part of it carried out under lockdown, was a challenge, and it would have been tougher without the support of some people, who shall be referenced next.

I would like to express my sincere gratitude to my primary supervisor Dr. Dawid Hanak for his guidance, availability, patience and mainly for trying to keep me always motivated. I could not imagine a better supervisor.

To my associate supervisor Prof. Vasilije Manovic, I would like to thank his valuable comments and encouragement.

To my special friend Sonia, that even being apart I know she is always there for me, I am so grateful for her continuous friendship too.

Thanks to the group “Putos grandes da primaria” for all the chats and video calls that made me feel closer to my homeland, Portugal.

To Francesco (just because he did not want to be mentioned), I am thankful for all the shared laughs and for always reminding me “how smart I am”.

I would like to thank my parents, Jose and Maria Adelaide, for their wise teaching that we should always follow our dreams, no matter if we need to restart again and again… Thanks indeed for showing me that nothing is possible without persistent work.

To my husband Carlos Eduardo for being my anchor over the years, for supporting my return to academia and in the end for being proud of me!

I gratefully thank the UK Engineering and Physical Sciences Research Council for financial support of the project "Clean heat, power and hydrogen from biomass and waste" (EPSRC reference: EP/R513027/1).

TABLE OF CONTENTS

LIST OF FIGURES

LIST OF TABLES

NOMENCLATURE

Notations and symbols

a_1, a_2	sorbent maximum average conversion model fitting parameter	[-]
b	sorbent maximum average conversion model fitting parameter	[-]
e_{CO_2}	direct CO_2 emissions from the plant	[kg_{CO_2}/ADt] or [kg_{CO_2}/kg_{H_2}]
$e_{CO_2,e}$	specific CO_2 emissions associated with power generation	[$kg_{CO_2}/MW_{el}h$]
$e_{CO_2,eq}$	equivalent CO_2 emissions	[kg_{CO_2}/ADt] or [kg_{CO_2}/kg_{H_2}]
f_1, f_2	sorbent maximum average conversion model fitting parameter	[-]
f_i	reaction extent	[-]
$i_{P\&C}$	piping and integration costs indicator	[%]
$\dot{m}_{Air}$	inlet air flowrate	[kg/s]
$\dot{m}_{BL}$	black liquor flowrate	[t/d]
$\dot{m}_{CO_2}$	flowrate of CO_2	[kg/s]
$\dot{m}_{DG}$	dry gas flowrate	[kg/s]
$\dot{m}_F$	fuel flowrate	[kg/s]
$\dot{m}_i$	flowrate of component i	[kg/s] or [t/h] or [kg/h]
$\dot{m}_{News}$	newsprint production per year	[ADt/y]
$\dot{m}_{O_2}$	O_2 production rate	[kg/s]
$\dot{m}_{Pulp}$	pulp production per year	[ADt/y]
n	cost exponent for the correction of capacity	[-]
q	direct fuel consumption	[MJ_{LHV}/ADt]
q_{eq}	equivalent fuel consumption	[MJ_{LHV}/ADt]
r	discount rate	[%]
r_0	fraction of never calcined limestone in the system	[-]
t	project lifetime	[y]

A_j	heat exchanger area of equipment j	[m^2]
AC	cost of CO_2 avoided	[€/t_{CO_2}]
ADt	air dried tonne	
AMP	2-amino-2-methyl-1-propanol	
AS	amine scrubbing	
ASU	air separation unit	
BAT	best available technologies	
BECCS	bioenergy combined with carbon capture and storage	
BFB	bubbling fluidised bed	
BFG	blast furnace gas	
BLG	black liquor gasification	
BLG-CaL	black liquor gasification with calcium looping	
BLG-CaL-GT	black liquor gasification with gas turbine combined cycle	
BLG-CaL-H_2	black liquor gasification with H_2 production	
BLG-CaL-SOFC	black liquor gasification with solid oxide fuel cell	
BLG-CCS	black liquor gasification with CO_2 capture	
BLG-CC-CCS	black liquor gasification combined cycle with CO_2 capture	
BLG-CC-NCC	black liquor gasification combined cycle without CO_2 capture	
BMW	biodegradable municipal waste	
BOFG	basic oxygen furnace gas	
C_j	capital cost of equipment j	[€]
Ca-LP	calcium looping integrated in the lime production	
CaL	calcium looping	
CaL-CLC	calcium looping coupled with chemical looping combustion	
CCS	carbon capture and storage	
CCU	carbon capture utilisation	

CCUS	carbon capture, usage and storage	
CEPCI	chemical engineering plant cost index	
CF_t	discounted cash flows through the project lifetime	[€]
CHP	combined heat & power	
CL	chemical looping	
CLC	chemical looping combustion	
COG	coke oven gas	
COS	carbonyl sulphide reactor	
Dea	deaerator	
DEA	diethanolamine	
DEPG	dimethyl ether of polyethylene glycol	
DFB	dual fluidised bed	
DME	dimethylether	
DPA	diisopropanolamine	
DRI-EAF	direct reduced iron electric arc furnace	
EE	equivalent energy consumption	[MJ_{th}/kg_{CO_2}]
EII	energy-intensive industry	
EPC	engineering procurement and construction	[€]
EU ETS	European Union Emissions Trading System	
EUA	CO_2 emission allowance	
F_0	make-up rate (fresh limestone and lime mud)	[kmol/s]
F_R	sorbent looping rate	[kmol/s]
G	generator	
GHG	greenhouse gases	
GT	gas turbine	
HP	high pressure	
HRSG	heat recovery steam generator	
HTS	high-temperature shift reactor	
HX	heat exchanger	
IP	intermediate pressure	

IGCC	integrated gasification combined cycle	
LCOH	levelised cost of hydrogen	[€/kg_{H_2}]
LCON	levelised cost of market product, newsprint	[€/ADt]
LCOP	levelised cost of market product, pulp	[€/ADt]
LHV	lower heating value	[kJ/kg]
LO-CAT	liquid oxidation catalyst	
LTS	low-temperature shift reactor	
MDEA	methyl diethanolamine	
MEA	monoethanolamine	
MSW	municipal solid waste	
NGCC	natural gas combined cycle	
NMP	N-methyl-2-pyrrolidone	
NPV	net present value	[€]
O&M	Operation and maintenance	
Oxy	oxy-fuel combustion	
OCAPEX	other capital cost	[€]
P_e	specific energy or electric power	[MJ/ADt] or [[MW_{el}h/ADt] or [MW_{el}h/kg_{H_2}] or [MW_{el}]
P_{net}	net power output	[MW_{el}]
PA	physical absorption	
PC	project contingency	[€]
PSA	pressure swing adsorption	
$\dot{Q}_j$	heat flux of equipment j	[kW_{th}]
Q_{LHV}	thermal energy of fuel	[MW]
Q_{th}	thermal energy of steam	[MW]
S	target capacity	[ADt/d]
SBR	steam-to-biomass ratio	[kg/kg]
S/C	molar steam-to-carbon ratio	[mol/mol]
SEG	sorption-enhanced gasification	
SEWGS	sorption-enhanced water gas shift	
SMR	steam methane reforming	

SPECCA	specific primary energy consumption for CO_2 avoided	$[MJ_{LHV}/kg_{CO_2}]$
T	temperature	[°C]
TCR	total capital requirement	[€]
TEA	triethanolamine	
TGR	top gas recycling	
TIC	total installed cost	[€]
TPC	total plant cost	[€]
VPSA	vacuum pressure swing adsorption	
$W_{el,gross}$	gross electric power output	$[MW_{el}]$
$W_{el,net}$	net electric power output	$[MW_{el}]$
$\dot{W}_j$	brake power requirement/output of equipment j	$[kW_{el}]$
WGS	water-gas shift	
WGSR	water-gas shift reaction	
WtE	waste-to-energy	
X_{ave}	average sorbent conversion	[-]
ZnO	zinc oxide bed	

Greek Letters

η_e	electric efficiency	[-]
$\eta_{el,\ gross}$	gross power efficiency	[-]
$\eta_{el,\ net}$	net power efficiency	[-]
$\eta_{el,\ tot}$	total efficiency	[-]
η_{H_2}	H_2 production efficiency	[-]
λ	excess amount of air	[-]

Subscripts

0	reference value
calc	calciner
cap	pulp and paper plant with CO_2 capture
carb	carbonator

e	electric
eq	equivalent
ref	reference pulp and paper plant without CO_2 capture
ArC	air compressor
AGR	acid gas removal
ASU	air separation unit
AXPH	air preheater
BRKP	brake power
Claus	Claus sulphur plant
CCU	CO_2 compression unit
COND	condensate
CW	fresh water
Dea	deaerator
DG	dry gas
ECON	economiser
FC	fuel compressor
FP	fuel preparation
Gasf	conventional steam gasification
GT	gas turbine
H_2Comp	H_2 compressor at 60 bar
H_2PV	H_2 pressure vessel
H_2StorComp	H_2 compressor at 700 bar
HPST	high-pressure steam turbine
HPW	high-pressure water
HRSG	heat recovery steam generator
IPST	intermediate-pressure steam turbine
LPST	low-pressure steam turbine
LPW	low-pressure water
LS	live steam
MTPD	metric tonne per day
OXPH	oxygen preheater
SC	steam cycle
SGE	syngas expander

SST	small steam turbine
ST	steam turbine
SyngasPH	syngas preheater

1 INTRODUCTION

1.1 Background and motivation

Global CO_2 emissions from fossil fuels have been rising for more than a century, with a sharp rise in the last 60 years with the exception of 2020 due to the Covid-19 pandemic (Ritchie and Roser, 2020). Figure 1-1 shows the CO_2 emitted from fossil fuels between 1900 and 2020. Though this reduction was an exception, the global energy-related CO_2 emissions bounced close to the pre-pandemic level in 2021 and were just 1.2% lower than the peak in 2019 (IEA, 2021a).

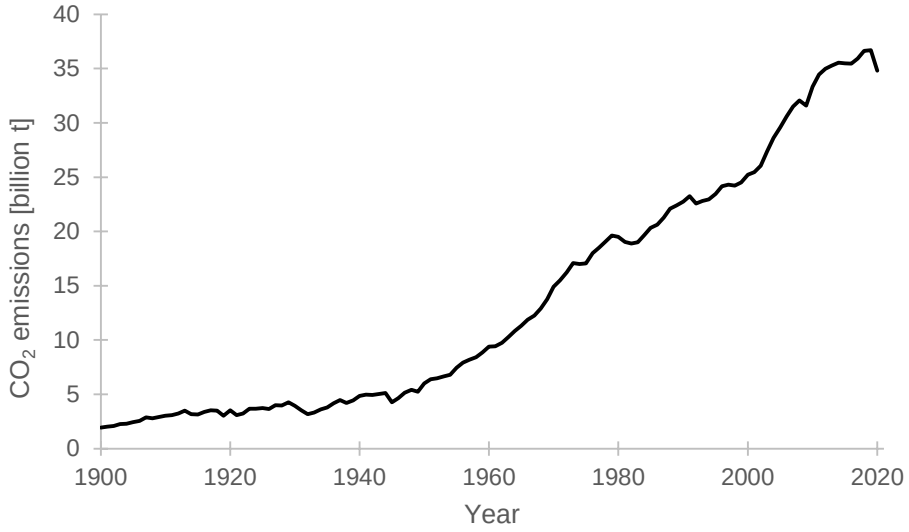

Figure 1-1: Global historical CO_2 emissions from fossil fuels 1900–2020 (Ritchie and Roser, 2020)

As shown in Figure 1-2, just four industries, so-called energy-intensive industries (EIIs), were responsible for around 68% of the industrial CO_2 emissions in 2018. The share of CO_2 emissions by these industries was 26.4%, 25.1%, 14.3% and 2.0% for cement, iron and steel, chemicals and petrochemicals and pulp and paper industry, respectively.

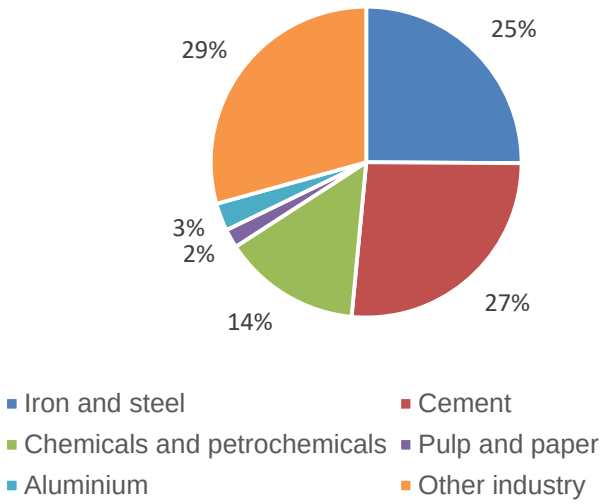

Figure 1-2: Share of industrial direct CO_2 emissions in 2018 (IEA, 2020a)

For some of these EIIs, the CO_2 emissions are inherent to the process and their reduction could just be reached by a decrease in production. For example, in the cement industry, 60% of CO_2 emissions result from the conversion of limestone into CO_2 and CaO (Barker et al., 2009). Besides, the cement demand is rising in emerging markets, such as India and some African countries (IEA, 2020b). In 2020, India contributed to 8% of the global production of cement (4.3 Gt), being the second-largest producer. It is also expected that the economic growth of these countries, besides the association of Southeast Asian countries, will drive the market and, thus, the steel demand (IEA, 2021b). In the Net Zero Scenario, a 4% increase in global steel production is foreseen by 2030. Under the same scenario (2020–2030), the production of high-value chemicals, methanol and ammonia is also expected to rise by 31%, 28% and 11%, respectively (IEA, 2021c). Similarly to the previous EIIs, it is forecasted that the paper and paperboard demand will keep growing at 1.5% per year until 2030 (IEA, 2020c).

Even though some progress has been achieved in reducing CO_2 emissions from EIIs, the current progress is not on track to meet the target set in the Paris agreement. Unless significant mitigation measures are implemented, the global net-zero CO_2 emissions will not be reached by 2050 and the set global warming of 1.5 °C above the pre-industrial level will be behind. In 2100, the latter could

reach 3 °C or 5 °C in the worst-case scenario (Peters and Hausfather, 2020). Therefore, such deep decarbonisation implies the need for electrification, improvements in energy efficiency, mentality and behaviour change, wide implementation of carbon capture and storage (CCS) and the decrease of fossil fuels dependence (IEA, 2021d). The latter can be achieved by switching to nuclear, hydropower, geothermal, marine energy, solar power, hydrogen and hydrogen-based fuels.

At present, hydrogen production contributes to the emission of around 830 million tonnes of CO_2 *per annum* (IEA, 2021e). Importantly, 96% of the total hydrogen production still relies on fossil fuels. In the UK, as of 2019, 49% of hydrogen was produced *via* steam methane reforming, 29% *via* partial oil oxidation and 18% *via* coal gasification. These shares are represented in Figure 1-3 (Statista, 2021a).

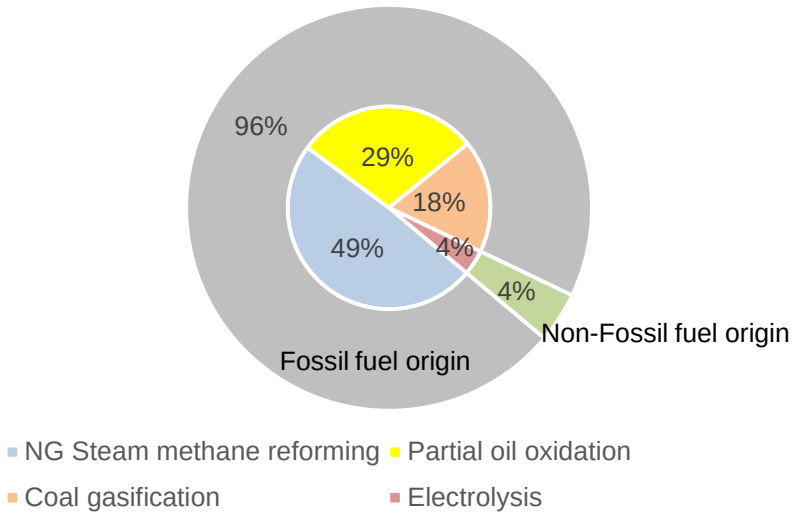

Figure 1-3: Share of hydrogen production by technology in the UK for the year 2019 (Statista, 2021a)

Thus, hydrogen production itself is not the solution to CO_2 emissions mitigation but can play an important role. Such can be characterised by producing from fossil fuel and coupled with carbon capture and storage, so-called blue hydrogen, or from renewables-based solutions, so-called green hydrogen (IRENA, 2020). Unfortunately, the high production costs have been a hurdle in the acceptance of the latter option.

Unfortunately, there is no single solution that would allow achieving complete industrial decarbonisation, which is necessary to reduce the impact of climate change. Still, between the four EIIs, the pulp and paper industry presents a clear advantage. As most of the CO_2 emissions from that industry are of biogenic origin, which is considered carbon neutral in the European Union Emissions Trading System (EU ETS), this industry can become carbon-negative if decarbonisation measures are implemented (Möllersten et al., 2004). For this reason, the implementation of CCS technologies in this industry has not attracted the same level of attention as that paid to the others EIIs. Nevertheless, the retrofit of the pulp and paper industry with CCS may completely decarbonise this industry (Gerres et al., 2019). Moreover, this industry can simultaneously reduce fossil dependence by using the by-product black liquor as an energy source. The potential of using black liquor as a feedstock to produce H_2, integrated with CO_2 capture and thus, reduce the CO_2 emissions, was shown by Andersson and Harvey (2006). Since then, more studies have shown the feasibility of hydrogen production with CO_2 capture from black liquor (Darmawan et al., 2019; Naqvi, Yan and Dahlquist, 2012).

Yet while biomass and bio-based waste play an important role in the decarbonisation of the pulp and paper industry, the extensive use of biomass as renewable energy raises some serious questions about its sustainability. In this case, biomass is defined as the forest biomass and crops, such as sugar, starch, oil, and lignocellulosic. Currently, biomass is used to produce food, animal feed and bioenergy. Therefore, there is a competition between biomass and land for bioenergy production as well as for food and animal feed production. Besides, the competition extends to other resources such as water, capital and labour (Muscat et al., 2020). Consequently, biomass residues, fats-oils-grease, wastewater sludge, manure and wastes resultants from food, agriculture and landfill should be the primary feedstock for bioenergy production (Foster et al., 2021).

Moreover, it is estimated that approximately 2.0 billion tonnes of municipal solid waste (MSW) is now produced *per annum*. This figure would reach 3.4 billion

tonnes in 2050 (Kaza et al., 2018). Only the households in the UK contributed to around 26 million tonnes of waste produced in 2019 (Department for Environment Food and Rural Affairs, 2021). Figure 1-4 shows the amount of MSW and the amount of biodegradable municipal waste (BMW) that was sent to landfills in the UK between 2010 and 2019 (Department for Environment Food and Rural Affairs, 2021). Although the amount of landfilled waste has been decreasing, such a reduction was more accentuated at the beginning of the decade. In 2019, around 14 million tonnes of MSW were sent to landfills, of which almost 50% were biodegradable waste (6.63 million tonnes). In the same year, the first UK municipal waste gasification commercial demonstration plant started its operation in Aldridge. In some European countries like Finland, Germany, Italy, Norway and Sweden, waste gasification plants have already been in operation for years (Molino, Chianese and Musmarra, 2016). According to Foster et al. (2021), the use of waste can play an important role in the decarbonisation of the UK energy market. Hence, the production of clean energy vectors from non-fossil fuels associated with CCS deployment needs to be explored.

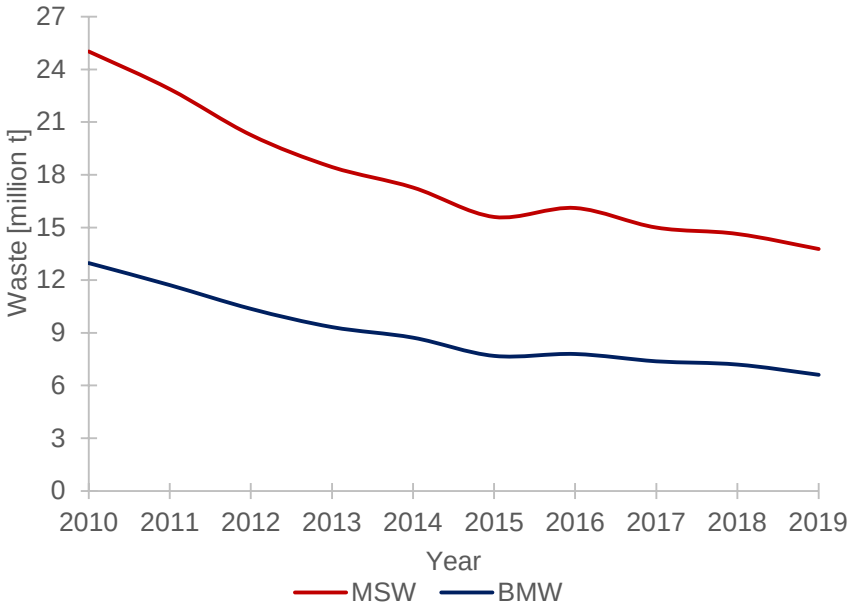

Figure 1-4: Waste sent to landfill in the UK. MSW and BMW correspond to municipal solid waste and biodegradable municipal waste, respectively (Department for Environment Food and Rural Affairs, 2021)

1.2 Aim and objectives

This research aims to examine the techno-economic feasibility of calcium looping (CaL) as a carbon capture technology for combined heat, power and hydrogen production from biomass and/or waste. To achieve this aim, the following measurable objectives have been established:

1. Conduct a comprehensive review of carbon capture technologies across the EIIs, focusing on solid looping cycle technology.
2. Develop a model in Aspen Plus®/CADSIM Plus® to represent a retrofit of a pulp and paper plant with CCS and validate it against the literature data.
3. Develop and validate the process model of hydrogen production from black liquor (by-product from pulp and paper industry) gasification with CO_2 capture.
4. Evaluate the techno-economic feasibility of CaL retrofit to the pulp and paper industry, as a carbon capture route or as a hydrogen production route.
5. Assess the applicability of CaL for hydrogen production with CO_2 capture from another feedstock, MSW.
6. Examine the effect of sorbent selection on the techno-economic performance of the hydrogen production route.

1.3 Novelty and linkage of project outputs

The project outputs delivered during this PhD project contributed to the publication of five high-impact factor peer-reviewed publications. Figure 1-5 shows the linkage between the project outputs.

The concept of solid looping cycles, such as chemical looping (CL) and CaL, has been known for 20 years. The development of solid looping technology has accelerated in the last decade. Therefore, the role of CaL as a CO_2 capture route in the decarbonisation of main EIIs has been reviewed and compared with more mature CCS technologies (Publication 1, objective 1). The current literature has shown CaL as a promising technology for decarbonisation across iron and steel

(Tian et al., 2018), cement (De Lena et al., 2019) and petroleum refining (Morin and Béal, 2005) industries. Furthermore, Tian et al. (2018) and De Lena et al. (2019) showed that when CaL is implemented, these industries can take advantage of their inherent decarbonisation potential at lower energy requirements and CO_2 avoided costs. Despite being the fourth most-emitting EII, it was found that the decarbonisation of the pulp and paper industry has not been thoroughly assessed and the viability of using the CaL process in this industry has not been explored.

For that reason, a new concept for decarbonisation of the pulp and paper industry, where the inherent carbon capture capability of the Kraft process is exploited, has been proposed (Publication 2). The performance of the reference pulp and paper plant was assessed using the existing CADSIM Plus® model. The flue gases properties and input data for the CaL model were benchmarked against the literature (Nwaoha and Tontiwachwuthikul, 2019; Onarheim et al., 2017a). The CaL retrofit to the reference pulp and paper plant was modelled in Aspen Plus® (Objective 2). The model was based on the one developed by Hanak et al. (2015) and validated with data from a 1.7 MW_{th} pilot plant at INCAR-CSIC (Sánchez-Biezma et al., 2013a). The techno-economic performance of the retrofitted pulp and paper plant was compared with that of the reference pulp and paper plant (Objective 4). It was found that the reference pulp and paper plant can turn from electricity importer to electricity exporter with an estimated cost of CO_2 avoided of 39.0 €/t_{CO_2}. Besides, the pulp and paper industry has a high potential to become a carbon-negative industry, which with a change of policies would make CCS implementation feasible in this industry.

Since the techno-economic feasibility of the proposed system has shown encouraging results, the possibility of implementing CO_2 capture coupled with black liquor gasification (BLG) was proposed. Black liquor is a by-product produced in the Kraft process. Usually, it is combusted in the recovery boiler to recover inorganic chemicals and produce process utilities (steam and electricity). To date, the viability of BLG has been considered for the production of biofuels (Andersson, Lundgren and Marklund, 2014; Carvalho et al., 2018), higher-value

products such as ammonia (Akbari, Oyedun and Kumar, 2018) and polygeneration of biofuels, steam and electricity (Ferreira and Balestieri, 2015; Pettersson and Harvey, 2012; Zhang et al., 2011). Although the latter studies have assessed the integration of BLG with CO_2 capture, none of them has considered the application of solid looping cycles. Besides, Darmawan et al. (2018) have studied the technical viability of BLG coupled with CL, but the economic feasibility of such a process still needs to be assessed. Therefore, the techno-economic feasibility of BLG coupled with CaL was assessed (Publication 3, objective 4). To accomplish this objective, the BLG model was developed in Aspen Plus® and integrated with the CaL model developed above (Objective 3). The BLG model was optimised to match the syngas composition under the experimental gasification conditions described by Carlsson et al. (2010). Three co-production options were also evaluated, considering BLG with H_2 production (BLG-CaL-H_2), BLG with gas turbine combined cycle (BLG-CaL-GT) or BLG with solid oxide fuel cell (BLG-CaL-SOFC) for electricity production. This route was then compared, from the thermodynamic and economic points of view, with CaL retrofit to the same reference pulp and paper plant. Although BLG-CaL was found to be a viable route for CCS, the thermodynamic performance showed that pulp and paper plant integrated with CaL or integrated with BLG-CaL with SOFC presented the best overall performance. The economic assessment revealed that the former presented the lowest cost of CO_2 avoided, 39.0 €/t_{CO_2}. However, from the three options of BLG integrated with CaL, the hydrogen production has shown to have the lowest cost of CO_2 avoided, 48.0 €/t_{CO_2} even though it had the highest energy penalty.

The results obtained for BLG coupled with CaL showed that a by-product from the pulp and paper industry is a viable feedstock for energy production. Although BLG-CaL is feasible for H_2 and power production, the H_2 production option is achievable at a lower cost of CO_2 avoided. Furthermore, and based on the works performed by He et al. (2009), Zhou et al. (2014), Hu et al. (2015), Irfan et al. (2019) and Martínez et al. (2020), waste-to-energy (WtE) conversion has been shown to be a promising route to simultaneously tackle climate change and reduce waste landfilling. These authors showed that sorption-enhanced

gasification (SEG) of MSW can be successfully employed for syngas production. Although the integration of CaL with BLG for H_2 production was assessed in a retrofit scenario, in this case, the possibility of H_2 production in a greenfield scenario was explored. The former was assessed in a retrofit scenario to carry out a comparative study between two different routes for pulp and paper decarbonisation, CaL or BLG-CaL. The concept of SEG, gasification integrated with CaL, for H_2 production was studied for another type of waste, MSW (Objective 5). Importantly, SEG has shown to be feasible for the production of synthetic fuel in a 30 kW_{th} bubbling fluidised bed (BFB) pilot plant (Martínez et al., 2020a). However, its commercialisation is dependent on the hydrogen production costs, which are still very limited due to the lack of economic assessments for this technology. Based on the first assessment for SEG of biomass carried out by Schweitzer et al. (2018), the cost of H_2 production ranges between 6 €/kg_{H_2} and 10 €/kg_{H_2}. Such a cost is almost 6 times higher compared to steam methane reforming (1.1–2.6 €/kg_{H_2} with CO_2 capture) that is the most commonly used and least expensive technology for hydrogen production. However, it needs to be stressed that MSW presents some advantages relative to biomass, as there is no feedstock cost, no competition with food production and use of land. The use of MSW as feedstock for hydrogen production also reduces the volume of waste sent to the landfill. Finally, there is a possibility of an additional profit by introducing a gate fee that can offset the added cost of SEG. For these reasons, it was pertinent to evaluate the techno-economic feasibility of H_2 production through SEG of MSW. To perform a direct and fair comparison, the techno-economic performance of SEG was benchmarked with conventional steam gasification of MSW. It was found that the levelised cost of hydrogen (*LCOH*) was higher for SEG (5.0 €/kg_{H_2}) than that of conventional gasification (2.7 €/kg_{H_2}). However, the *LCOH* estimated of the MSW SEG was lower than the figures reported for biomass SEG (Publication 4). Also, the cost of CO_2 avoided was in the range for steam methane reforming. Such results indicated the potential of SEG to produce low-carbon H_2 and that it would be appropriate to continue this field research to find a way to decrease the cost of H_2 production, which can be achieved by increasing the H_2 productivity.

The H_2 production enhancement can be accomplished by replacing the sorbent with one with a higher CO_2 sorption capacity or with improved cyclic stability (Objective 6). The CO_2 sorbent used for H_2 production in SEG, the limestone, is widely available at a low cost. However, the loss in the adsorption capacity along the cycles is one of the main drawbacks of using natural limestone as a sorbent for SEG. The requirement of high temperatures during the calcination to achieve complete regeneration is another drawback. Dolomite is another inexpensive natural CO_2 sorbent that has been shown to have an enhanced performance after several cycles of carbonation/calcination (Zhen-Shan et al., 2008). This superiority can be attributed to the MgO that at the calcination/carbonation conditions is inert and, therefore, acts as a support component improving the cycle stability of the sorbent (Valverde, Sanchez-Jimenez and Perez-Maqueda, 2015). Another advantage of dolomite is the slightly lower temperature necessary to achieve a complete regeneration (850 °C against 900 °C required by limestone). Furthermore, sorbent doping with an inert material such as MgO, Al_2O_3, La_2O_3, TiO_2 and SiO_2 or with inorganic salts like chlorides of Na, Mg, K and Ca is another way to enhance the sorption capacity. Recently, Xu et al. (2017) and González, Kokot-Blamey and Fennell (2020) have shown that limestone doped with seawater, a naturally abundant and cheap solution, improved the cycle stability and, therefore, the sorption capacity. The techno-economic assessment of the MSW SEG performed for three sorbents, including natural limestone, doped limestone with seawater and dolomite, showed that doped limestone is a promising option to replace natural limestone. The former presented the same *LCOH* (5.0 €/kg_{H_2}) as the latter, even if with a cost of CO_2 avoided slightly higher (117.7 €/t_{CO_2} against 114.9 €/t_{CO_2}), for doped and natural limestone, respectively (Publication 5). It should be noted that the price of doped limestone (58.0 €/t) was assumed to be 5 times the price of natural limestone (11.6 €/t). Yet, it was found that a reduction in doped limestone price to below 42.6 €/t would reduce the cost of CO_2 avoided for a figure lower than that obtained for natural limestone (114.9 €/t_{CO_2}).

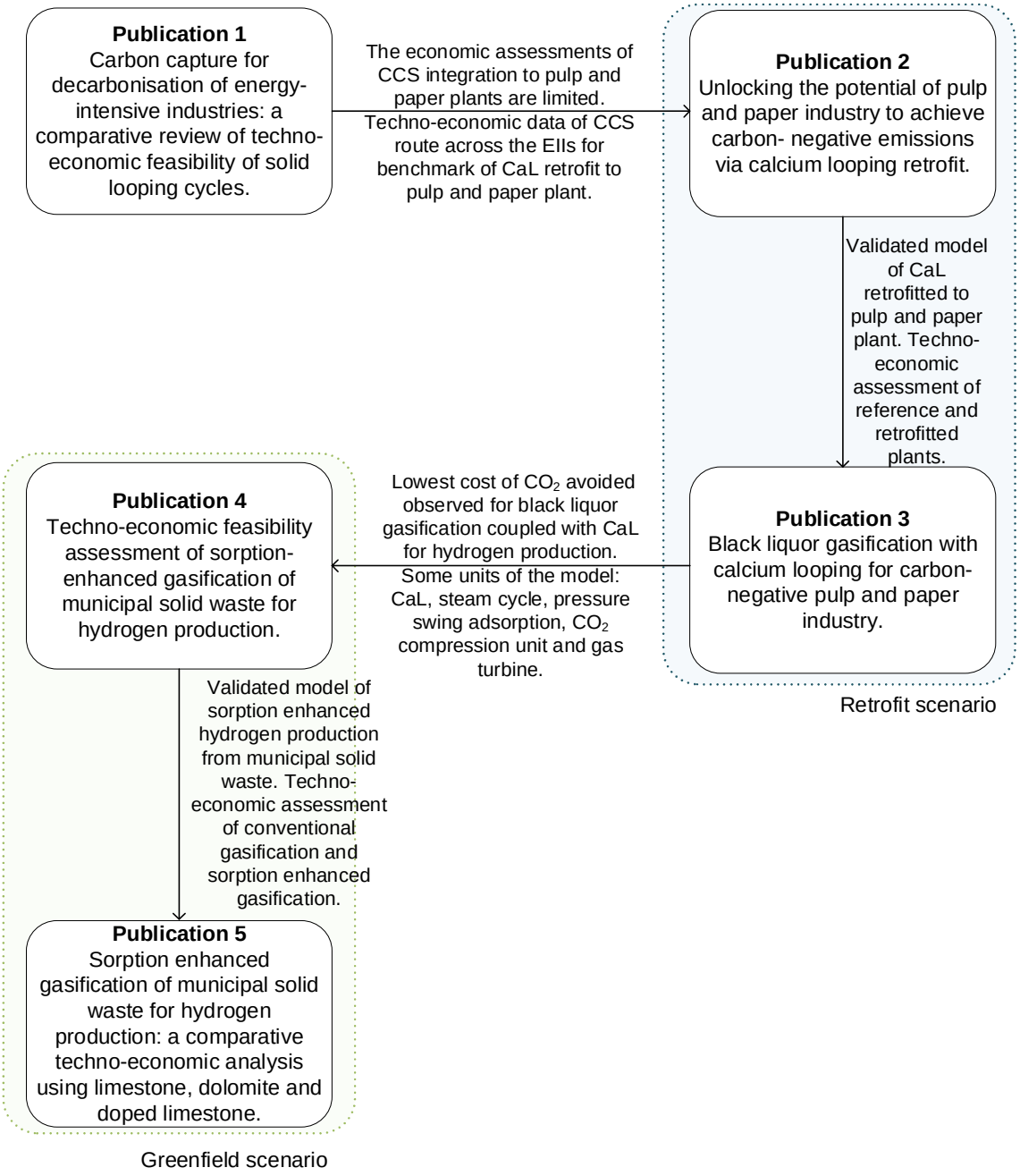

Figure 1-5: Interconnections of the project outputs

1.4 Outline of PhD thesis

The PhD thesis, Figure 1-6, has been organised into eight chapters that were defined based on the six objectives described in Section 1.2. Five of these chapters have been written in paper format.

The content of each chapter is briefly explained below. The background and motivation of this PhD project, as well as the aim and main objectives defined to deliver this thesis, are presented in Chapter 1.

A comprehensive review of the state-of-art in carbon capture technology for the decarbonisation of the main four EIIs, including iron and steel, cement, petroleum refining and pulp and paper industries, is presented in Chapter 2. This review was carried out with a particular focus on the solid looping cycle, calcium looping. The feasibility of using CaL to decarbonise the EIIs was also benchmarked with other carbon capture technologies based on the techno-economic assessment.

Since CaL has never been considered in the pulp and paper industry, its feasibility for the decarbonisation of this industry was assessed in Chapter 3. The feasibility of CaL retrofit to pulp and paper plant was assessed by comparing the thermodynamic and economic performance of the pulp and paper plant with and without CO_2 capture. The CO_2 capture concept proposed in this chapter leveraged the inherent CO_2 capture capability of the Kraft process. The techno-economic viability of such a layout was thoroughly assessed. Furthermore, the development and validation of CaL retrofitted to the pulp and paper process, as well as its techno-economic performance, were also described.

Based on the data published in the literature, CaL is a promising CO_2 capture technology across different industries, including the power industry and EIIs. Also, the technical viability of BLG coupled with CL for co-production of H_2 and power was presented in the literature. Therefore, a comparative study of two different CaL retrofit routes to the pulp and paper industry was carried out in Chapter 4. The process model described in Chapter 3 was adapted to retrofit the pulp and paper plant with CO_2 capture and hydrogen or power production. The first route, the Kraft process retrofitted with CaL for CO_2 capture, was compared with the second one, BLG integrated with CaL for simultaneous CO_2 capture and H_2 or power production.

To assess the applicability of the SEG production route to other feedstocks, the SEG of MSW was evaluated in Chapter 5. The techno-economic feasibility of H_2

production through SEG of MSW was benchmarked with the conventional steam gasification of MSW.

As the integration of CO_2 capture resulted in an economic penalty, the possible improvement of the performance was evaluated in Chapter 6 by considering alternative CO_2 capture sorbents. Since dolomite, similarly to limestone, is widely available at a low cost, it was the first sorbent selected. The second one was limestone doped with seawater. In both cases, the techno-economic performance was compared with SEG using natural limestone as sorbent, as well as, with the techno-economic performance of conventional steam gasification.

Chapter 7 presented the main outputs from each chapter, followed by a general discussion. The contribution to knowledge in the research field was also provided in this chapter. The concluding remarks and the overall implications of this PhD project were provided in Chapter 8. This chapter also presented recommendations for future work.

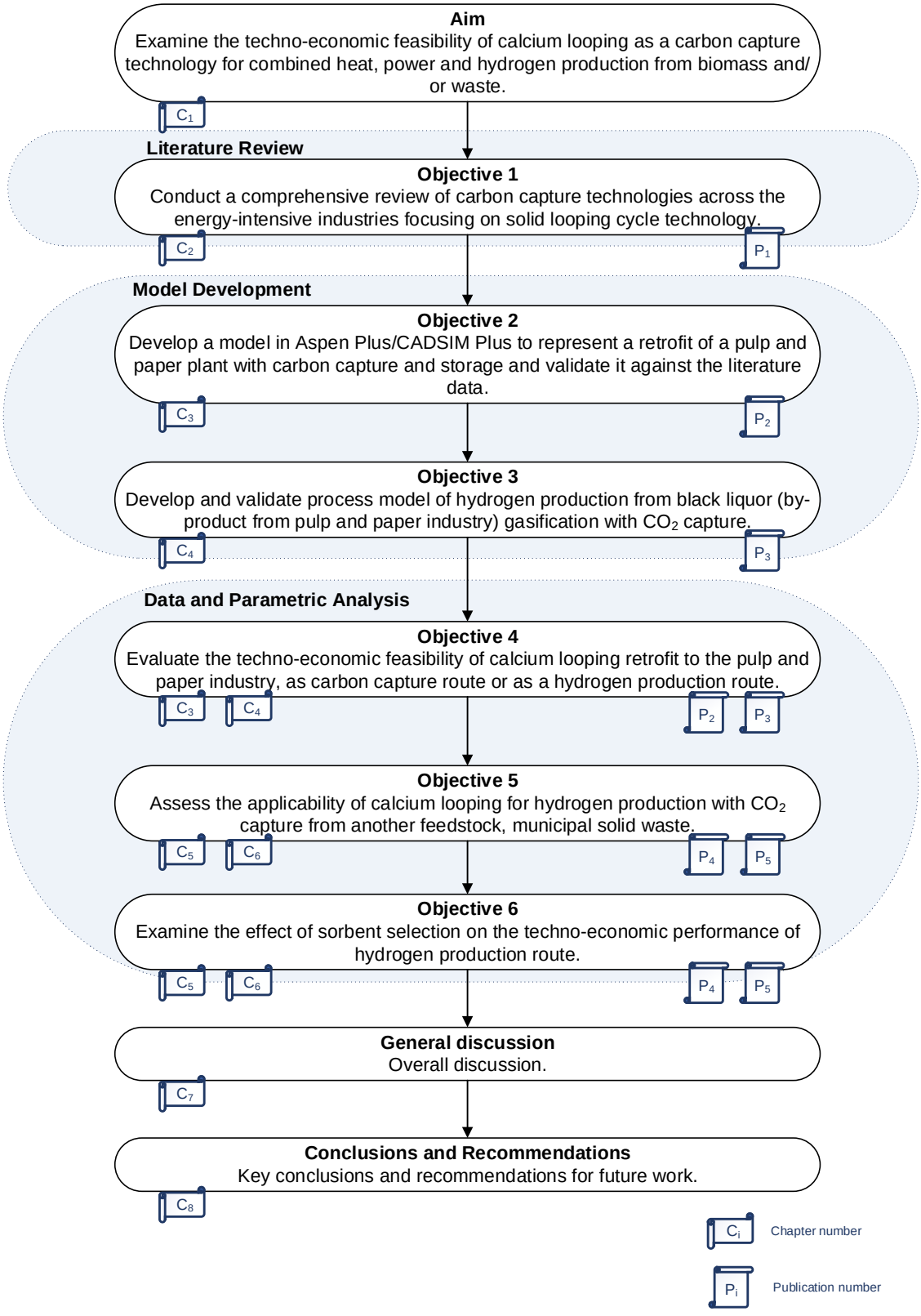

Figure 1-6: The structure of the PhD thesis mapped against the objectives and the connection of the objectives with the peer-reviewed papers

1.5 List of publications

1.5.1 Peer-reviewed journal publications

Santos, M.P.S. and Hanak, D.P. (2022) ‘Sorption-enhanced gasification of municipal solid waste for hydrogen production: a comparative techno-economic analysis using limestone, dolomite and doped limestone’, *Biomass Conversion and Biorefinery.*

Santos, M.P.S. and Hanak, D.P. (2022) ‘Carbon capture for decarbonisation of energy intensive industries: a review of techno-economic feasibility’, *Frontiers of Chemical Science and Engineering*.

Santos, M.P.S. and Hanak, D.P. (2022) ‘Techno-economic feasibility assessment of sorption-enhanced gasification of municipal solid waste for hydrogen production’ *International Journal of Hydrogen Energy*, 47(10), pp. 6586–6604.

Santos, M.P.S., Manovic, V. and Hanak, D.P. (2021) ‘Unlocking the potential of pulp and paper industry to achieve carbon-negative emissions via calcium looping retrofit’, *Journal of Cleaner Production*, 280, p. 124431.

Santos, M.P.S., Manovic, V. and Hanak, D.P. (2021) ‘Black liquor gasification with calcium looping for carbon-negative pulp and paper industry’, International *Journal of Greenhouse Gas Control*, 110, p. 103436.

1.5.2 Other publications

Santos, Mónica P.S. and Hanak, Dawid P. (2020) Trade article: Can an energy-intensive industry become negative? Process Industry Informer magazine (https://www.processindustryinformer.com/can-an-energy-intensive-industry-become-carbon-negative).

1.6 References

Akbari, M., Oyedun, A.O. and Kumar, A. (2018) ‘Ammonia production from black liquor gasification and co-gasification with pulp and waste sludges: A techno-economic assessment’, *Energy*, 151, pp. 133–143.

Andersson, E. and Harvey, S. (2006) ‘System analysis of hydrogen production

from gasified black liquor', *Energy*, 31(15), pp. 3426–3434.

Andersson, J., Lundgren, J. and Marklund, M. (2014) 'Methanol production via pressurized entrained flow biomass gasification – Techno-economic comparison of integrated vs. stand-alone production', *Biomass and Bioenergy*, 64, pp. 256–268.

Barker, D.J., Turner, S.A., Napier-Moore, P.A., Clark, M. and Davison, J.E. (2009) 'CO_2 Capture in the Cement Industry', *Energy Procedia*, 1(1), pp. 87–94.

Carlsson, P., Wiinikka, H., Marklund, M., Grönberg, C., Pettersson, E., Lidman, M. and Gebart, R. (2010) 'Experimental investigation of an industrial scale black liquor gasifier. 1. The effect of reactor operation parameters on product gas composition', *Fuel*, 89(12), pp. 4025–4034.

Carvalho, L., Lundgren, J., Wetterlund, E., Wolf, J. and Furusjö, E. (2018) 'Methanol production via black liquor co-gasification with expanded raw material base – Techno-economic assessment', *Applied Energy*, 225, pp. 570–584.

Darmawan, A., Ajiwibowo, M.W., Biddinika, M.K., Tokimatsu, K. and Aziz, M. (2019) 'Black liquor-based hydrogen and power co-production: Combination of supercritical water gasification and syngas chemical looping', *Applied Energy*, 252, p. 113446.

Darmawan, A., Ajiwibowo, M.W., Yoshikawa, K., Aziz, M. and Tokimatsu, K. (2018) 'Energy-efficient recovery of black liquor through gasification and syngas chemical looping', *Applied Energy*, 219, pp. 290–298.

Department for Environment Food and Rural Affairs (2021) '*Crown copyright 2021*', (July), pp. 1–25.

Ferreira, E.T.D.F. and Balestieri, J.A.P. (2015) 'Black liquor gasification combined cycle with CO_2 capture – Technical and economic analysis', *Applied Thermal Engineering*, 75, pp. 371–383.

Foster, W., Azimov, U., Gauthier-Maradei, P., Molano, L.C., Combrinck, M., Munoz, J., Esteves, J.J. and Patino, L. (2021) 'Waste-to-energy conversion

technologies in the UK: Processes and barriers – A review', *Renewable and Sustainable Energy Reviews*, 135, p. 110226.

Gerres, T., Chaves Ávila, J.P., Llamas, P.L. and San Román, T.G. (2019) 'A review of cross-sector decarbonisation potentials in the European energy intensive industry', *Journal of Cleaner Production*, 210, pp. 585–601.

González, B., Kokot-Blamey, J. and Fennell, P. (2020) 'Enhancement of CaO-based sorbent for CO_2 capture through doping with seawater', *Greenhouse Gases: Science and Technology*, 10(5), pp. 878–883.

Hanak, D.P., Biliyok, C., Anthony, E.J. and Manovic, V. (2015) 'Modelling and comparison of calcium looping and chemical solvent scrubbing retrofits for CO_2 capture from coal-fired power plant', *International Journal of Greenhouse Gas Control*, 42, pp. 226–236.

He, M., Xiao, B., Liu, S., Guo, X., Luo, S., Xu, Z., Feng, Y. and Hu, Z. (2009) 'Hydrogen-rich gas from catalytic steam gasification of municipal solid waste (MSW): Influence of steam to MSW ratios and weight hourly space velocity on gas production and composition', *International Journal of Hydrogen Energy*, 34, pp. 2174–2183.

Hu, M., Guo, D., Ma, C., Hu, Z., Zhang, B., Xiao, B., Luo, S. and Wang, J. (2015) 'Hydrogen-rich gas production by the gasification of wet MSW (municipal solid waste) coupled with carbon dioxide capture', *Energy*, 90, pp. 857–863.

IEA (2021a) *Global energy-related CO_2 emissions, 1990-2021, IEA, Paris*. Available at: https://www.iea.org/data-and-statistics/charts/global-energy-related-co2-emissions-1990-2021 (Accessed: 27 October 2021).

IEA (2020a) *Industry direct CO_2 emissions in the Sustainable Development Scenario, 2000-2030, IEA, Paris*. Available at: https://www.iea.org/data-and-statistics/charts/industry-direct-co2-emissions-in-the-sustainable-development-scenario-2000-2030 (Accessed: 15 June 2021).

IEA (2020b) *Cement, IEA, Paris*. Available at: https://www.iea.org/reports/cement (Accessed: 29 June 2021).

IEA (2021b) *Iron and Steel, IEA, Paris*. Available at: https://www.iea.org/reports/iron-and-steel (Accessed: 28 April 2022).

IEA (2021c) *Chemicals, IEA, Paris*. Available at: https://www.iea.org/reports/chemicals (Accessed: 28 April 2022).

IEA (2020c) *Pulp and Paper, IEA, Paris*. Available at: https://www.iea.org/reports/pulp-and-paper (Accessed: 15 June 2021).

IEA (2021d) *Net Zero by 2050: A Roadmap for the Global Energy Sector*.

IEA (2021e) *Global Hydrogen Review 2021*.

IRENA (2020) *Green hydrogen. A guide to policy making*.

Irfan, M., Li, A., Zhang, L., Wang, M., Chen, C. and Khushk, S. (2019) 'Production of hydrogen enriched syngas from municipal solid waste gasification with waste marble powder as a catalyst', *International Journal of Hydrogen Energy*, 44, pp. 8051–8061.

Kaza, S., Yao, L.C.., Bhada-Tata, P. and Van Woerden, F. (2018) *What a Waste 2.0 : A Global Snapshot of Solid Waste Management to 2050.* Washington, DC: Urban Development;. Washington, DC: World Bank.

De Lena, E., Spinelli, M., Gatti, M., Scaccabarozzi, R., Campanari, S., Consonni, S., Cinti, G. and Romano, M.C. (2019) 'Techno-economic analysis of calcium looping processes for low CO_2 emission cement plants', *International Journal of Greenhouse Gas Control*, 82, pp. 244–260.

Martínez, I., Grasa, G., Callén, M.S., López, J.M. and Murillo, R. (2020) 'Optimised production of tailored syngas from municipal solid waste (MSW) by sorption-enhanced gasification', *Chemical Engineering Journal*, 401, p. 126067.

Molino, A., Chianese, S. and Musmarra, D. (2016) 'Biomass gasification technology: The state of the art overview', *Journal of Energy Chemistry*, 25(1), pp. 10–25.

Möllersten, K., Gao, L., Yan, J. and Obersteiner, M. (2004) 'Efficient energy systems with CO_2 capture and storage from renewable biomass in pulp and paper

mills', *Renewable Energy*, 29(9), pp. 1583–1598.

Morin, J.-X. and Béal, C. (2005) 'Chemical Looping Combustion of Refinery Fuel Gas with CO_2 Capture', in D.C. Thomas and S.M. Benson (ed.) *Carbon Dioxide Capture for Storage in Deep Geologic Formations, Volume 1*. Elsevier, pp. 647–654.

Muscat, A., de Olde, E.M., de Boer, I.J.M. and Ripoll-Bosch, R. (2020) 'The battle for biomass: A systematic review of food-feed-fuel competition', *Global Food Security*, 25, p. 100330.

Naqvi, M., Yan, J. and Dahlquist, E. (2012) 'Energy conversion performance of black liquor gasification to hydrogen production using direct causticization with CO_2 capture', *Bioresource Technology*, 110, pp. 637–644.

Nwaoha, C. and Tontiwachwuthikul, P. (2019) 'Carbon dioxide capture from pulp mill using 2-amino-2-methyl-1-propanol and monoethanolamine blend: Techno-economic assessment of advanced process configuration', *Applied Energy*, 250, pp. 1202–1216.

Onarheim, K., Santos, S., Kangas, P. and Hankalin, V. (2017) 'Performance and costs of CCS in the pulp and paper industry part 1: Performance of amine-based post-combustion CO_2 capture', *International Journal of Greenhouse Gas Control*, 59, pp. 58–73.

Peters, G.P. and Hausfather, Z. (2020) 'Emissions - the "business as usual" story is misleading', *Nature*, 577, pp. 618–620.

Pettersson, K. and Harvey, S. (2012) 'Comparison of black liquor gasification with other pulping biorefinery concepts – Systems analysis of economic performance and CO_2 emissions', *Energy*, 37(1), pp. 136–153.

Ritchie, H. and Roser, M. (2020) *CO_2 and Greenhouse Gas Emissions. Published online at OurWorldInData.org.* Available at: https://ourworldindata.org/co2-and-other-greenhouse-gas-emissions (Accessed: 10 February 2022).

Sánchez-Biezma, A., Paniagua, J., Diaz, L., Lorenzo, M., Alvarez, J., Martínez,

D., Arias, B., Diego, M.E. and Abanades, J.C. (2013) ‘Testing postcombustion CO_2 capture with CaO in a 1.7 MW_{th} pilot facility’, *Energy Procedia*, 37, pp. 1–8.

Schweitzer, D., Albrecht, F.G., Schmid, M., Beirow, M., Spörl, R., Dietrich, R.-U. and Seitz, A. (2018) ‘Process simulation and techno-economic assessment of SER steam gasification for hydrogen production’, *International Journal of Hydrogen Energy*, 43(2), pp. 569–579.

Statista (2021) *Distribution of hydrogen production methods in the United Kingdom (UK) as of 2019*. Available at: https://www.statista.com/statistics/457795/uk-hydrogen-production-share-by-method/ (Accessed: 26 October 2021).

Tian, S., Jiang, J., Zhang, Z. and Manovic, V. (2018) ‘Inherent potential of steelmaking to contribute to decarbonisation targets via industrial carbon capture and storage’, *Nature Communications*, 9(1), pp. 1–8.

Valverde, J.M., Sanchez-Jimenez, P.E. and Perez-Maqueda, L.A. (2015) ‘Ca-looping for postcombustion CO_2 capture: A comparative analysis on the performances of dolomite and limestone’, *Applied Energy*, 138, pp. 202–215.

Xu, Y., Luo, C., Zheng, Y., Ding, H., Zhou, D. and Zhang, L. (2017) ‘Natural Calcium-Based Sorbents Doped with Sea Salt for Cyclic CO_2 Capture’, *Chemical Engineering and Technology*, 40(3), pp. 522–528.

Zhang, G., Yan, J., Jin, H. and Dahlquist, E. (2011) ‘Integrated Black Liquor Gasification Polygeneration System with CO_2 Capture in Pulp and Paper Mills to Produce Methanol and Electricity’, *International Journal of Green Energy*, 8(2), pp. 275–293.

Zhen-Shan, L., Ning-Sheng, C., Li, Z., Cai, N. and Croiset, E. (2008) ‘Process Analysis of CO_2 Capture from Flue Gas Using Carbonation/Calcination Cycles’, *AIChE Journal*, 54(7), pp. 1912–1925.

Zhou, C., Stuermer, T., Gunarathne, R., Yang, W. and Blasiak, W. (2014) ‘Effect of calcium oxide on high-temperature steam gasification of municipal solid waste’, *Fuel*, 122, pp. 36–46.

2 CARBON CAPTURE FOR DECARBONISATION OF ENERGY-INTENSIVE INDUSTRIES: A COMPARATIVE REVIEW OF TECHNO-ECONOMIC FEASIBILITY OF SOLID LOOPING CYCLES*

Abstract

Carbon capture and storage will play a crucial role in industrial decarbonisation. However, the current literature presents a large variability in the techno-economic feasibility of CO_2 capture technologies. Consequently, reliable pathways for carbon capture deployment in energy-intensive industries are still missing. This work provides a comprehensive review of the state-of-the-art CO_2 capture technologies for decarbonisation of the iron and steel, cement, petroleum refining, and pulp and paper industries. Amine scrubbing was shown to be the least feasible option, resulting in the average avoided CO_2 cost of between 62.7 €/t_{CO_2} for the pulp and paper and 104.6 €/t_{CO_2} for the iron and steel industry. Its average equivalent energy requirement varied between 2.7 (iron and steel) and 5.1 MJ_{th}/kg_{CO_2} (cement). Retrofits of emerging calcium looping were shown to improve the overall viability of CO_2 capture for industrial decarbonisation. Calcium looping was shown to result in the average avoided CO_2 cost of between 32.7 €/t_{CO_2} (iron and steel) and 42.9 €/t_{CO_2} (cement). Its average equivalent energy requirement varied between 2.0 MJ_{th}/kg_{CO_2} (iron and steel) and 3.7 MJ_{th}/kg_{CO_2} (pulp and paper). Such performance demonstrated the superiority of calcium looping for industrial decarbonisation. Further work should focus on standardising the techno-economic assessment of technologies for industrial decarbonisation.

Keywords: Industrial CO_2 emissions, CCS deployment, carbonate looping, net-zero industry, carbon capture benchmarks

*Santos, M.P.S. and Hanak, D.P. (2022) 'Carbon capture for decarbonisation of energy intensive industries: a review of techno-economic feasibility', *Frontiers of Chemical Science and Engineering*

2.1 Introduction

CO_2, whose residence time in the atmosphere is around 100 years (Griffin and Hammond, 2019), is one of the six greenhouse gases (GHG) targeted by the Paris Agreement, signed by 197 countries. These countries are committed to reduce their GHG emissions and keep global warming at least well-below 2°C. Therefore, to comply with this agreement, the net GHG emissions need to become zero or even negative between 2055 and 2080 (Rogelj et al., 2018). For that reason, several routes for decarbonisation have been identified, including improvement in the material and energy efficiencies, reduction of dependence on fossil fuels and implementation of CCS (Gerres et al., 2019; IPCC, 2015; McGrail et al., 2012). Since the major contributors to the global CO_2 emissions are iron and steel, cement, petroleum refining and pulp and paper industries, decarbonisation of these industries must be prioritised to comply with the Paris Agreement. Due to their high energy demand, these industries are classified as EIIs. It needs to be emphasised that these four industries are responsible for around 68% of the industrial direct CO_2 emissions (IEA, 2020a) and accounted for around 20% of the global direct CO_2 emissions in 2016 (Bataille, 2019).

The decarbonisation of these industries is crucial to reaching net-zero emissions, as evident in the previous review papers published in recent years (Bataille et al., 2018; Fennell et al., 2012; Gerres et al., 2019; Koytsoumpa, Bergins and Kakaras, 2018; Kuramochi et al., 2012; Leeson et al., 2017; Markewitz et al., 2012; Napp et al., 2014; Nurdiawati and Urban, 2021; Rissman et al., 2020; Yang, Meerman and Faaij, 2021). The scope and main conclusions of these reviews are summarised in Table 2-1. Although some of the reviews include comprehensive appraisals of EIIs, there are significant limitations that need to be addressed. Fennell et al. (2012) have conducted an overview of the economic performance of CCS for EIIs. However, their review accounted only for a limited number of studies. Kuramochi et al. (2012) have performed a comprehensive review that compared the techno-economic feasibility of CCS technologies in selected industries. However, the development of these technologies was in an early stage at the time this review was published. Markewitz et al. (2012) have

compared the efficiency, energy consumption and technical viability of the main CCS routes for industrial decarbonisation without focusing on a specific industry. Napp et al. (2014) have also carried out an extensive review of EIIs decarbonisation, but did not include a complete detail and analysis of the CO_2 capture technologies due to the lack of available data. The application of CCS to different EIIs was covered in detail in the systematic review carried out by Leeson et al. (2017). However, the main goal of that review was to compare the economic performance of CCS technologies, neglecting their thermodynamic performance. Moreover, Yang, Meerman and Faaij (2021) have done a comprehensive review about CCS and bioenergy combined with CCS (BECCS). However, it only focused on the environmental and economic performance, neglecting the thermodynamic performance presented by each CCS technology. Although CaL has been recently shown as promising CCS technology by integration on the iron and steel and pulp and paper industries, it was not considered by Yang, Meerman and Faaij (2021). Moreover, that review considered only the economic assessments carried out one decade ago.

Other comprehensive reviews of EIIs decarbonisation have also been published in the last five years (Bataille et al., 2018; Gerres et al., 2019; Nurdiawati and Urban, 2021; Rissman et al., 2020). Nevertheless, these focused on appraising all the available routes and policies for deep decarbonisation of EIIs. As a result, the CCS option was not evaluated in detail. Furthermore, Nurdiawati and Urban (2021) have based their work on the Swedish industrial scenario and the considered technology options were selected specifically for the iron and steel and cement industries. Koytsoumpa, Bergins and Kakaras (2018) have only analysed the high-level CCS options (i.e. pre- and post-combustion capture) and have not focused on a particular technology. Furthermore, despite being the fourth most polluting EII, the pulp and paper industry was considered in 50% of the reviews in the current literature (Bataille et al., 2018; Gerres et al., 2019; Leeson et al., 2017; Nurdiawati and Urban, 2021; Yang, Meerman and Faaij, 2021). Although carbon capture is forecasted to play a critical role in industrial decarbonisation, the recent progress in this field has not been thoroughly reviewed, analysed and discussed. Significant progress has been made in

reducing the energy intensity and improving the economics of CCS, especially in the past 5 years. However, the majority of the reviews in this area were published between 2012–2017. As a result, the data and analysis presented in these reviews focus solely on the early-stage development of the CCS technologies. Solid looping cycles were recently shown to have a high potential to decarbonise energy and industrial systems, showing a techno-economic superiority compared with other CCS technologies. In the energy sector, the retrofits of CaL to power plants were shown to reduce the efficiency penalty associated with CCS as a result of availability of high grade heat (Hanak, Anthony and Manovic, 2015). It is important to emphasise that limestone, the most commonly considered sorbent for CaL, is also used in the iron and steel (Tian et al., 2018), the cement (De Lena et al., 2019), and the pulp and paper (Santos, Manovic and Hanak, 2021) industries. Therefore, these industries can take advantage of their inherent decarbonisation potential at lower energy requirements and CO_2 avoided costs when CaL is implemented. For example, the retrofit of CaL in the cement industry was shown to result in the CO_2 avoided cost of 58.6 €$_{2014}$/t_{CO_2}, which was around 25% lower than that of amine scrubbing retrofit (80.2 €$_{2014}$/t_{CO_2}). Such a decrease in the cost of CO_2 avoided due to CaL retrofit can reach up to 70% in the iron and steel industry (12.5–15.8 €$_{2010}$/t_{CO_2}, CaL against 45–60 €$_{2010}$/t_{CO_2}, amine scrubbing).

This work aims to present a comprehensive review of CCS technologies for the decarbonisation of the EIIs, with the main focus on solid looping cycles. Although the concept of solid looping cycles has been known for 20 years, the development of this technology has only intensified in the last decade. For this reason, this review does not include studies published before 2009. This work aims to critically appraise the viability of solid looping cycles, particularly CaL, as a route for decarbonisation of EIIs. For this reason, a techno-economic comparative assessment of CCS for the four EIIs was performed. As shown later in this review, the current literature presents large discrepancies in the key performance indicators used to assess the CCS retrofits to EIIs. Therefore, to achieve as fair comparison as possible, this work considered the cost of CO_2 avoided as the key economic performance indicator and the equivalent energy consumption as the

thermodynamic performance indicator. Finally, because this field is of commercial interest, this work also provides an overview of recent developments in CaL and compares its performance with other, more mature CCS technologies. It should be noted that, although membrane-based technology has been shown recently promising results in the iron and steel (Baker et al., 2018; Ramírez-Santos et al., 2018; Yun, Jang and Kim, 2021) and cement (Baker et al., 2018; Ferrari et al., 2021; Gardarsdottir et al., 2019; Voldsund et al., 2019) it was not included in this review due to fewer research studies published across the four EIIs.

Table 2-1: A summary of the review studies about energy-intensive industries decarbonisation

Review author	Review scope	Main conclusions
Kuramochi et al. (2012)	• Extensive review about the CO_2 capture technologies applied to three industries, iron and steel, cement, petroleum refineries and petrochemicals; • Techno and economic assessment of the technologies, based on standardisation of performance parameters; • Estimation of potential reduction of CO_2 emissions and respective costs for what they categorised as short/medium term and long term technologies.	• No dominant technology for any of the industries analysed; • The costs could be so diverse that for the cement industry, they could vary from 29.2 €/t_{CO_2} to 141.5 €/t_{CO_2} avoided when the carbon capture is obtained by CaL applied to the pre-calciner or by absorption with monoethanolamine (MEA), respectively; • Short-mid-term technologies may have a cost of 43.2–70.2 €/t_{CO_2}, above 70.2 €/t_{CO_2} and 54.0–64.8 €/t_{CO_2} avoided in the iron and steel, cement and refining industries, respectively; • Long-term technologies could be achieved at lower cost, 32.4–59.4 €/t_{CO_2}, 27.0–59.4 €/t_{CO_2} and 32.4 €/t_{CO_2} avoided in the iron and steel, cement and refining industries, respectively; • The economic feasibility of these technologies is strongly dependent to the power market once the excess electricity produced is exported to the grid.
Markewitz et al. (2012)	• Overview of CO_2 capture, transport and utilisation; • Comparison of efficiency, energy consumption and technical viability of the main routes available for CCS; • Assessment of environmental impact of CCS technologies; • Summary of the largest CCS projects worldwide.	• At that time, there was no best CCS technology, but gas separation by membranes and solid looping cycles were seen as promising technologies; • The CO_2 use as a raw material could have an effective contribution to a decrease in CO_2 emissions.
Fennell et al. (2012)	• Brief review about the costs of CCS application to five industries, iron and steel, cement, refinery, biomass and high purity sources.	• Unlike the power industry and due to the heterogeneity of the processes involved in petrochemical industries, the costs could reach 150.9 €/t_{CO_2} avoided; • The cost of cement decarbonisation could be as low as 17.2 €/t_{CO_2} avoided when CaL is employed; • In the cement and iron and steel industries, which involve high-temperature processes, the integration of solid looping cycles seems to be the distinctive solution for the deep decarbonisation of these two industries.

Review author	Review scope	Main conclusions
(Napp et al., 2014)	• Comprehensive review about decarbonisation of three industrial industries, iron and steel, cement and refineries; • Review of the energy-efficient technologies in these industries as well as the potential of their implementation; • Assessment of different routes for these industries decarbonisation; • Discussion about the policies that should be adopted as a strategy to mitigate CO_2 emissions.	• An energy/emissions monitorisation system should be implemented and the best available technologies (BAT); • Fuel switching, CCS capture, co-location of industries and re-design of the processes were proposed as routes for these industries decarbonisation; • The replacement of fossil fuel by biomass and wastes should be encouraged and CCS should be seen as an option for deep decarbonisation.
(Leeson et al., 2017)	• Exhaustive review about different CCS technologies employed in five industries, iron and steel, cement, refining and petrochemical, pulp and paper and high purity sources; • Technical and economic assessment of these technologies; • A mathematical model was proposed to estimate the costs of CCS implementation until 2050; • A sensitivity analysis was also performed.	• The studies about the costs of CCS implementation were scarce and practically non-existent for the pulp and paper industry; • Costs in the other industries could vary from 17.8–106.8 €/t_{CO_2} avoided, which contributes to a high economic uncertainty associated with these technologies and consequently to the delay of its commercialisation; • Delaying CCS implementation will lead to higher costs.
(Bataille et al., 2018)	• Review of technologies and policies available to reduce CO_2 emissions in pulp and paper, iron and steel and cement.	• The biomass conversion in heat and power for the pulp and paper plant seems to be the key to decarbonise this industry; • Unlike the previous industry, in the steelmaking process and refining industry, there is not a dominant route although the replacement of fossil fuel by biomass combined with CCS is mentioned (IRENA, 2014); • In the cement industry, the carbon capture, usage and storage (CCUS) employing CaL is the most straightforward route to decrease CO_2 emissions; • Even though some of the technologies are near commercial, policies and incentives to research must be put in practice to reach the Paris agreement targets.
(Koytsoumpa, Bergins and Kakaras, 2018)	• Evaluation of carbon capture utilisation (CCU) technologies as well as the potential of use pre- and post-combustion capture in the thermal power, EIIs and other industries;	• The CO_2 utilisation in conjunction with the use of incentives in implementing carbon capture technologies must be seen as a route to follow.

Review author	Review scope	Main conclusions
	• Detailed list of commercial projects where carbon capture was already implemented and proved that is a feasible option in the CO_2 emissions abatement.	
(Gerres et al., 2019)	• Comprehensive review of decarbonisation of seven industries, iron and steel, cement, petrochemical, pulp and paper, ceramics, glass and food; • Roadmap for the deep decarbonisation of these industries and their potential to reach the imposed targets until 2050.	• CCS, biomass and bio-based waste, process heat provision, alternative feedstock, electrolysis, combined heat & power (CHP), industrial ovens and membrane process were the main routes identified; • CCS was the only trans-sectional option that had the potential to mitigate the CO_2 emissions with a potential between 25% to 55% for total decarbonisation; • All the work done so far is not enough for deep decarbonisation and there is no yet a dominant technology being necessary to develop new technologies.
(Rissman et al., 2020)	• Review of technologies and policies to reach net greenhouse gas emissions by 2050–2070 in the cement, iron and steel, chemical, and plastics industries.	• Use of mineral and chemical admixtures, re-design building techniques to decrease the demand for concrete, improvement of the thermal efficiency of processes during cement production, fuel switching, electrification of cement kilns and CCS were the main options to full decarbonisation of cement industry; • In the iron and steel industry, the implementation of CCS and the replacement of fossil fuels by hydrogen or direct electrolysis were the main paths for reducing the CO_2 emissions of this industry; • Development of clean processes, by avoiding the use of fossil fuels, the use of biomass feedstocks and recycled chemicals, and the use of CO_2 as feedstock, the improvement of separation technologies and CCS were identified as the main routes to decarbonise the chemical and plastics industry; • Although the low carbon technologies will become cheaper, they are not enough for deep decarbonisation across the studied industries. Certain policies such as carbon pricing, government incentives for research, development and deployment, and energy efficiency or emissions standards should be adopted.
(Nurdiawati and Urban, 2021)	• Review of technical options, policies and barries to decarbonise the iron and steel, mining, cement and refinery industries, taking the Swedish case as reference.	• Electrification, fuel switching to low carbon fuels, CCS and when possible, a fossil free production are necessary deep decarbonisation of EIIs; • The use of less raw materials, improvement of material efficiency and implementation of circular economy were also identified as decarbonisation pathways; • There is necessary keep going development of decarbonisation technologies and its test at large scale in order to reach the commercial viability;

Review author	Review scope	Main conclusions
(Yang, Meerman and Faaij, 2021)	• Comprehensive review of decarbonisation of five industries, iron and steel, cement, petrochemical, pulp and paper and hydrogen; • Techno and economic assessment of the technologies CCS or BECCS based on a standardisation of performance parameters; • Estimation of CO_2 mitigation potential and respective costs.	• The incentive of low carbon technologies should be a priority, which can be achieved by implementation of new policies and incentives. • CCS only had the CO_2 mitigation potential up to 74% however, this figure could reach the 2548% for BECCS implementation in pulp and paper industry; • The iron and steel, pulp and paper and hydrogen could become carbon-negative industries; • These results could be achieved with a CO_2 avoided cost lower than 100 €/t_{CO_2}; • There were some discrepancies in literature regarding the potential and the economic assessment of the reviewed technologies.

2.2 Overview of CCS

CCS is a chain of processes from the CO_2 capture to its transport and long-lived storage, with the CO_2 capture being the most expensive and energy-intensive step (Dean et al., 2011; Hills, Florin and Fennell, 2016). Across the main industries, three routes have been identified as CO_2 capture strategies: pre-combustion capture, post-combustion and oxy-fuel (Damen et al., 2006; Markewitz et al., 2012; van Straelen et al., 2009). The principle of each CO_2 capture approach is presented in Figure 2-1. In pre-combustion capture, CO present in the syngas produced by reforming or partial oxidation is converted to CO_2 and then separated from H_2 at high pressure. The post-combustion capture involves the removal of CO_2 from the flue gases at low CO_2 partial pressure. It is considered an end-of-pipe solution that can be retrofitted to existing systems without major modifications to the plant layout. Yet, due to the heterogeneity of industries, some processes have more than one CO_2 emissions point. As a result, the flue gases from different parts of the process may need to be combined before CO_2 capture (Leeson et al., 2017), reducing the technical viability of the post-combustion capture. The oxy-fuel combustion process assumes that the fuel combustion takes place in pure O_2 rather than air. This leads to a higher CO_2 purity due to the absence of N_2. Another advantage of the absence of N_2 is the reduction of NO_x emissions.

As shown in Figure 2-1, the pre- and post-combustion capture require CO_2 separation from the syngas or the flue gas, respectively. Depending on the gas streams characteristics, the following physical-chemical separation processes have been employed in the CO_2 abatement (Feron and Hendriks, 2005):

- gas-liquid separation that involves physical or chemical absorption with solvents, called solvent scrubbing;
- gas-solid separation that is based on adsorption by solid adsorbents;
- membrane-based separation; and
- cryogenic, where the gases are cooled to a very low temperature and the CO_2 is separated.

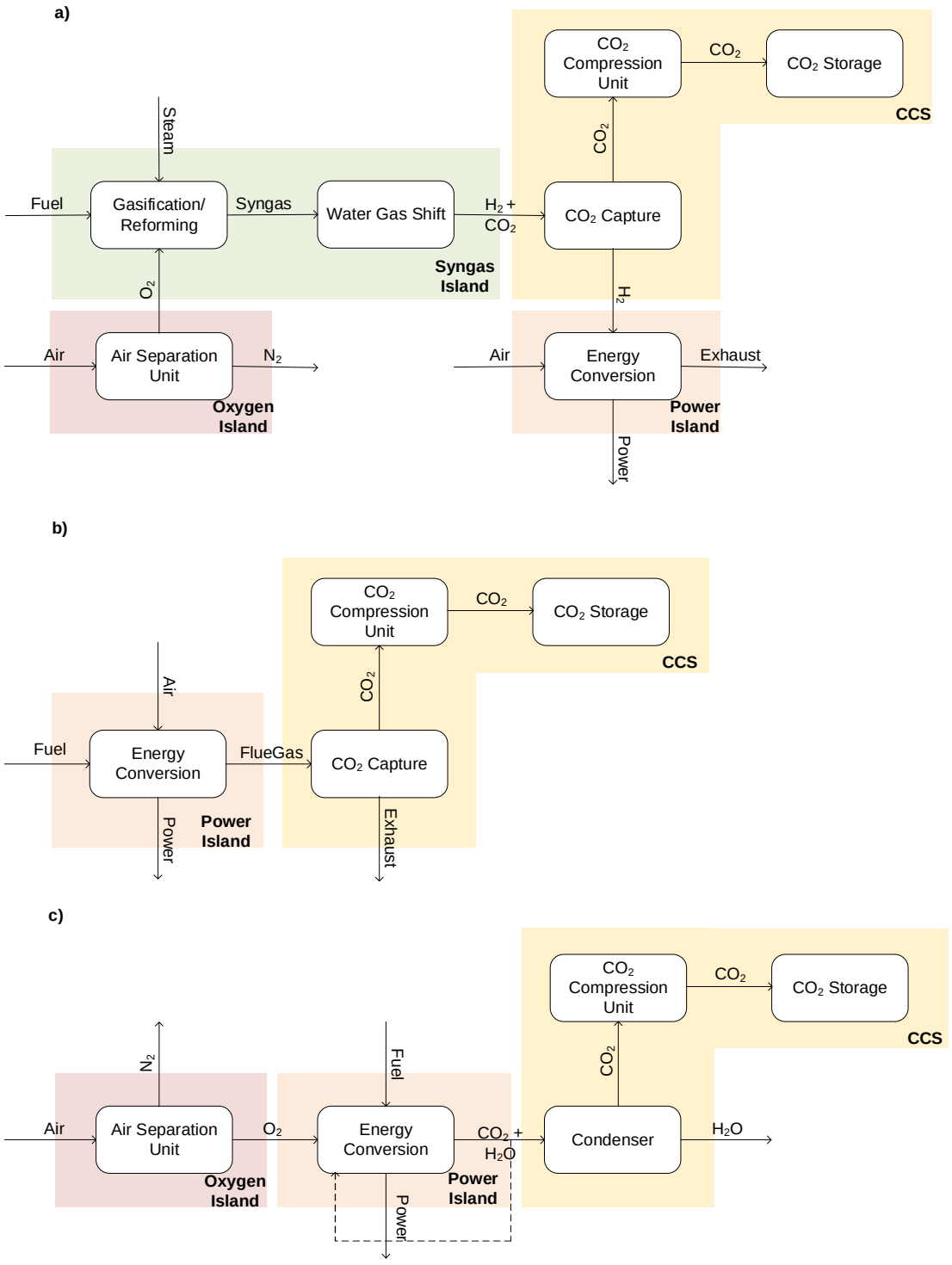

Figure 2-1: Block flow diagrams for a) pre-combustion capture, b) post-combustion capture, and c) oxy-fuel combustion CO_2 capture

Among the abovementioned separation processes, amine scrubbing is the most mature technology (Voldsund et al., 2019). Initially proposed by Bottoms (1930)

to separate the acidic gases present in a gaseous mixture, amine scrubbing has been used as CO_2 separation technology for several decades (Dean et al., 2011). This CCS technology use MEA or methyl diethanolamine (MDEA) as the most common solvents. However, diethanolamine (DEA), dominoethoxyethanol (DGA), diisopropanolamine (DPA), triethanolamine (TEA) and Ucarsol® are also among the chemical solvents considered for chemical solvent scrubbing (Koytsoumpa, Bergins and Kakaras, 2018). In physical scrubbing, the nature of the solvents is more diverse and solvents such as dimethyl ether of polyethylene glycol (DEPG), methanol (MeOH), N-methyl-2-pyrrolidone (NMP) and propylene carbonate can be used (Koytsoumpa, Bergins and Kakaras, 2018). Nevertheless, some issues have been identified with this technology in the power industry. These issues include:

- the solvent degradation at higher temperatures;
- adverse reactions with some components in the flue gas, such as SO_2 and O_2 (Dean et al., 2011);
- the expensive solvent production (Rao and Rubin, 2002a);
- the solvent concentration limited to 30 $\%_{wt}$ (MEA) due to corrosion issues (Shao and Stangeland, 2009);
- the efficiency penalty of 9.5% to 12.5% (Xu et al., 2010); and
- the generation of high volumes of hazardous wastes, mainly heat-stable salts and carbamate polymers, as a consequence of the thermal and oxidative degradation of the solvent (Dean et al., 2011; Nurrokhmah, Mezher and Abu-Zahra, 2013).

Amine scrubbing has been extensively studied across EIIs (Arasto et al., 2013; Farla, Hendriks and Blok, 1995; McGrail et al., 2012; Nwaoha and Tontiwachwuthikul, 2019; Onarheim et al., 2017b; van Straelen et al., 2009; Tsupari et al., 2013; Wiley, Ho and Bustamante, 2011), but due to high costs and the abovementioned issues, the use of hot potassium and ammonia-based solvents has also been studied as an alternative to amine-based solvents (Koytsoumpa, Bergins and Kakaras, 2018; Voldsund et al., 2019). NH_3 is less corrosive and subject to lower rates of degradation compared to amine-based

solvents. It also presents a higher CO_2 absorption capacity and requires less energy once the regeneration is carried out at lower temperatures. However, due to its high volatility and slower kinetics, ammonia scrubbing was deemed not to be a feasible option for the decarbonisation of the EIIs (Han et al., 2013).

Oxy-fuel combustion is another technology at a relatively high technology readiness level (Arasto et al., 2013; Rodríguez, Murillo and Abanades, 2012a; Tsupari et al., 2013; Wiley, Ho and Bustamante, 2011) and close to its commercialisation (Hanak, Anthony and Manovic, 2015). Since a high CO_2 purity stream is produced during fuel combustion in O_2/CO_2 environment, this technology does not require a CO_2 separation process that constitutes its main advantage. However, to keep the desired purity of CO_2, potential air infiltration into the boiler should be minimised, implying high safety procedures (Blamey et al., 2010). Moreover, the O_2 production by a cryogenic air separation unit increases the costs associated with this technology (Anthony, 2008). Despite the advantage of oxy-fuel compared with amine scrubbing, it is not commercialised due to the issues mentioned and the lack of consistent economic data (Leeson et al., 2017).

To overcome the drawbacks of mature CCS technologies, emerging technologies have been developed. Recently, solid looping cycles, such as CL and CaL, have been shown to be a promising technology for the decarbonisation of EIIs (Morin and Béal, 2005; Santos, Manovic and Hanak, 2021; Tian et al., 2018; Voldsund et al., 2019). Furthermore, the extensive review performed by (Adánez et al., 2018) on chemical looping combustion (CLC) of solid fuels has concluded that EIIs, such as the pulp and paper and cement industries, are potential industries to apply CLC. As it was shown by Berdugo Vilches et al. (2017), a circulating fluidised bed gasifier can be coupled to a bubbling bed boiler and operate as a CLC unit. In such a case, the former assumes the function of a fuel reactor and the latter works as air reactor, while generating heat. Since the energy demand of these two industries is met by using boilers, the implementation of CLC would be suitable with a minor need for retrofitting.

2.2.1 Solid looping cycles

The most common layout of the solid looping cycles consists of two interconnected fluidised beds. A metal oxide is used as an O_2 carrier (i.e. Cu, Ni) or CO_2 carrier (i.e. CaO, MgO) in chemical or carbonate looping, respectively. The carrier circulates between the two reactors in alternate cycles of reduction-oxidation or carbonation-calcination, which is the most commonly studied configuration. Nevertheless, recently in the iron and steel industry, Fernández, Spallina and Abanades (2020) have proposed using packed-bed reactors. In such a configuration, the gas, instead of sorbent, circulates between the reactors. Generally, the oxidation and carbonation reactions are exothermic, whereas the reduction and calcination reactions are endothermic, except in the CuO/Cu cycle (de Diego et al., 2007). The regenerator reactor can be fed with solid, liquid or gas fuels of renewable (i.e. biomass) or non-renewable (i.e. natural gas) origin.

A combination of heat, electricity, chemicals and fuels can be generated by solid looping processes (Darmawan et al., 2018, 2019; Wang et al., 2015; Zafar, Mattisson and Gevert, 2005; Zhao et al., 2017). Depending on the target output, solid looping processes can be classified as the following (Zhao et al., 2017):

- CLC or CaL if the generation of heat or electricity is the main purpose; or
- chemical looping gasification or calcium looping gasification , with the note that gasification can also be referred to as a reforming process when steam or CO_2 is added to the reactor to enhance their reforming reactions (Zhao et al., 2017). Energy vectors (i.e. hydrogen) and fuels (i.e. syngas) are the main products in such processes.

It should be noted that the difference between gasification and combustion processes is the extent of carbonaceous fuel oxidation. In the gasification process of solid fuels, carbon is first partially oxidised to carbon monoxide (CO) and then further water-gas shift (WGS) reaction takes place to promote the formation of H_2 and CO_2. In the reforming process of gaseous fuels, light hydrocarbons (i.e. CH_4) are first broken down to syngas comprising a mixture of H_2/CO/CO_2, followed by the WGS reaction. Conversely, the combustion process involves the complete oxidation of the fuel to CO_2 while the H_2 on it is oxidised to water vapour (H_2O).

2.2.1.1 Chemical Looping

CL employs a metal oxide as an oxygen carrier that transfers oxygen between the two reactors. Nickel, copper, iron, manganese and cobalt-based oxygen carriers have been studied as oxygen carriers (Mattisson, Järdnäs and Lyngfelt, 2003; Zafar, Mattisson and Gevert, 2005). The following characteristics must be presented by them (Hossain and de Lasa, 2008):

- be reactive in reduction and oxidation steps;
- should be able to fulfil stoichiometric combustion;
- be stable at high temperatures, even after a large number of cycles;
- its structure should not be affected by the friction resultant from the fluidisation;
- be fluidisable and should avoid the formation of clusters;
- be eco-friendly and no hazardous to operators; and
- be viable economically.

Figure 2-2 presents a basic scheme of this technology. In the first reactor, called the air reactor, the reduced metal oxide is oxidised and the regenerated oxygen carrier returns to the fuel reactor. This step is represented by Eq. (2-1).

$$\text{Air reactor: } Me_xO_{y-1}(s) + \frac{1}{2}O_2(g) \rightarrow Me_xO_y(s) \qquad \textbf{(2-1)}$$

Then, the oxidised oxygen carrier is fed to the fuel reactor, where it is reduced on contact with the fuel to produce a stream of CO_2 and water vapour, according to Eq. (2-2).

$$\text{Fuel reactor: Fuel} + nMe_xO_y(s) \rightarrow nMe_xO_{y-1}(s) + H_2O(g) + CO_2(g) \qquad \textbf{(2-2)}$$

The water vapour is then condensed and a high-purity CO_2 stream is sent for compression, avoiding the need for additional separation processes. The cost of these separation processes can be varied depending on the partial pressure of CO_2 and the technology used (Fennell et al., 2012).

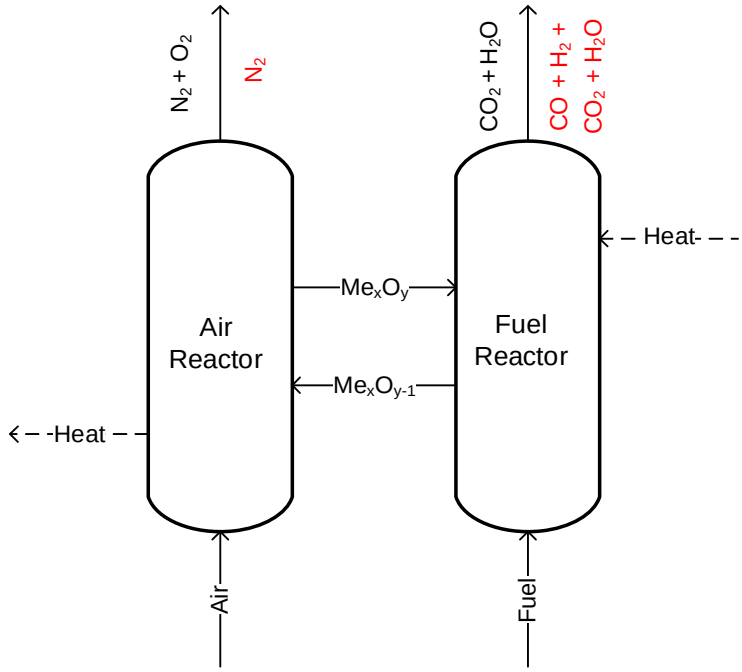

Figure 2-2: Simplified scheme of chemical looping process (black text: products from chemical looping combustion; red text: products from chemical looping gasification)

2.2.1.2 Calcium Looping

CaL was initially proposed by Shimizu et al. (1999) as a CCS option for the decarbonisation of the power industry. Since calcium carbonate ($CaCO_3$) is formed during the carbonation reaction, the CaL is also known as carbonate looping (Hilz et al., 2017; Rolfe et al., 2018). The concept of this technology is shown in Figure 2-3. The CO_2 from the flue gas or syngas is captured by the sorbent (i.e. CaO), which circulates between the two reactors, leading to the formation of $CaCO_3$ in the carbonator. The decomposition of $CaCO_3$ to CaO and CO_2 takes place in the calciner, which requires high-grade heat provided by the oxy-fuel combustion. As shown in Eq. (2-3) and Eq. (2-4), this process is based on the reversible reaction between CaO and CO_2.

Carbonator reactor: $CaO(s) + CO_2(g) \rightarrow CaCO_3(s)$ ΔH=-178 kJ/mol **(2-3)**

Calciner reactor: $CaCO_3(s) \rightarrow CaO(s) + CO_2(g)$ ΔH=178 kJ/mol **(2-4)**

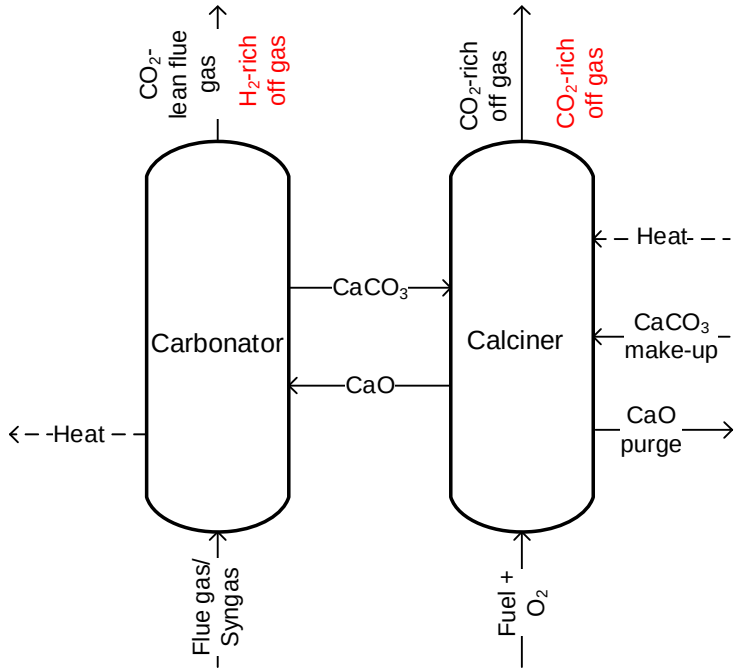

Figure 2-3: Simplified scheme of calcium looping technology. Black: products from calcium looping, red: products from calcium looping gasification

In the first reactor, the so-called carbonator, the CO_2 is removed from the flue gas or syngas at 600–750 °C. In the second reactor, the so-called calciner, the decomposition of the formed carbonate takes place at 870–950 °C and a CO_2-rich gas is produced (Ozcan et al., 2015). CaL, involves oxy-combustion in the calciner to provide heat for sorbent regeneration to ensure the high-purity of the CO_2 stream. This technology also presents the following advantages over mature amine scrubbing (Dean et al., 2011):

- use of fluidised beds, a well-known technology at large scale (Cuenca and Anthony, 1995);
- the thermal energy released in the carbonator can be recovered to produce steam, which is one of the key benefits of this technology (Arias et al., 2013);
- the low cost and high availability of the natural sorbents, limestone;
- the sorption capacity of limestone-based sorbents after a large number of cycles is higher than that for many synthetic sorbents (Blamey et al., 2010);

- the sorbent is SO_2 selective which contributes to a partial desulphurisation of the stream; and
- the purged CaO can be used as raw material in the cement and iron and steel industries (Tian et al., 2018).

However, the reactivity decay of the sorbent over the cycles is the main challenge of CaL (Erans et al., 2016; Grasa and Abanades, 2006). The loss in the adsorption capacity is attributed to the sorbent sintering during the calcination (Borgwardt, 1989; Sun et al., 2007) that is exacerbated by high temperatures, long cycles, high CO_2 and steam partial pressures and by contaminations (Borgwardt, 1989). Moreover, due to abrasion and fragmentation, a small fraction of sorbent particles can leave the calciner. Therefore, the fresh sorbent is continuously fed to it (Perejón et al., 2016). As the $CaCO_3$ decomposition to CaO and CO_2 at high pressure requires temperatures higher than 900°C (Baker, 1962), another challenge of this technology is to find a less energy-intensive process for sorbent regeneration. To overcome this limitation, a new configuration was developed, first proposed by Lyon (1984). He has suggested that the coupling of a solid looping cycle, Fe/FeO, can deliver the heat required in the calcination step. This was provided by the exothermic oxidation of the Fe to FeO with air, which took place in the same fixed bed reactor as the calcination. Although this new loop met the calcination heat requirement, the CO_2 emissions problem was still unsolved. This was because the CO_2 formed during the calcination was diluted by the N_2 present in the air and thus released to the atmosphere. Then Abanades et al. (2010) proposed the replacement of Fe/FeO by CuO/Cu, known as Ca-Cu chemical looping. In this case, the heat requirement for the $CaCO_3$ decomposition was delivered *via* oxidation of fuel in the reaction with CuO that was produced in another reactor through the oxidation of Cu to CuO with air. Consequentely, a CO_2-rich stream is produced in the integrated calciner and fuel reactor, since there is no dilution by N_2.

To date, solid looping cycles have been extensively researched in the power industry, and some CaL and CLC pilot scale units were already built and assessed: the 1.7 MW_{th} pilot in La Pereda (Arias et al., 2013), the 0.2 MW_{th} facility

in Stuttgart University (Dieter et al., 2014), the 1 MW_{th} unit in Darmstadt (Ströhle et al., 2014), the 1.9 MW_{th} pilot in Taiwan (Chang et al., 2014), the 120 kW_{th} CLC unit in Wien University (Mayer et al., 2018), the 100 kW_{th} CLC unit in Chalmers University (Lyngfelt and Linderholm, 2017), the 3 MW_{th} CLC unit at ALSTOM labs (Abdulally et al., 2014) and more recently, the 3 MW_{th} CLC unit in China (CHEERS project) (Yazdanpanah et al., 2019). However, the effectiveness of this technology does not limit just to the power industry. Regarding the EIIs, CaL has been intensively explored in the cement industry by CEMEX in Mexico (Fennell et al., 2012) and in the past few years, the feasibility of its integration in the steelmaking process has also been studied by Fernández, Spallina and Abanades (2020) and Tian et al. (2018). Regarding the petrochemical and pulp and paper industries, CaL has not received much interest and only a few papers were found in the literature.

2.3 Carbon capture for decarbonisation of energy-intensive industries

2.3.1 Considerations

In this review, the CO_2 capture technologies for decarbonisation of the EIIs were compared with respect to their techno-economic performance. The thermodynamic performance of the entire system was evaluated using an equivalent energy consumption (*EE*, MJ_{th}/kg_{CO_2}), defined in Eq. (2-5). This is because the considered CCS technologies require energy of different quality: thermal energy of fuel (Q_{LHV}), thermal energy of steam (Q_{th}) and electrical energy (P_e). To ensure a fair comparison, the electric energy was converted to thermal energy using an electric efficiency of 45.9% (De Lena et al., 2019). To convert the steam energy to the same basis of calculation, it was assumed that steam was produced in a boiler with an efficiency of 90% (Fernández, Spallina and Abanades, 2020). The $\dot{m}_{CO_2}$ is the flowrate of CO_2 captured (kg/s).

$$EE = \frac{\left(Q_{LHV} \pm \frac{Q_{th}}{0.90} \pm \frac{P_e}{0.459}\right)_{CCS} - \left(Q_{LHV} \pm \frac{Q_{th}}{0.90} \pm \frac{P_e}{0.459}\right)_{Ref}}{\dot{m}_{CO_2}} \quad \textbf{(2-5)}$$

Depending on the technology and level of excess heat integration of the plant, some terms in Eq. (2-5) can be zero. The plus and minus signs represent an input or output of the plant, respectively. The equivalent energy consumption accounts for the heat requirement for solvent regeneration in the case of chemical and physical absorption. In the case of vacuum pressure swing adsorption and oxy-fuel combustion, the equivalent energy consumption accounts for the power required by sorbent regeneration and the air separation unit (ASU), respectively. The power requirement for the CO_2 compression unit is also accounted for all technologies, whenever is available. For solid looping cycles, the equivalent energy consumption is defined only as the thermal energy requirement met by the fuel consumption (Q_{LHV}), since these technologies integrate a steam cycle to recover the waste heat to meet their electrical energy requirement.

The economic performance was evaluated using the cost of CO_2 avoided (*AC*). For the sake of clarity, this metric is defined in Figure 2-4. The cost of CO_2 avoided is defined as the cost associated with reducing the CO_2 emissions from the reference plant due to the CCS retrofit, excluding the additional CO_2 that needs to be captured to offset the energy penalty of the CCS retrofit.

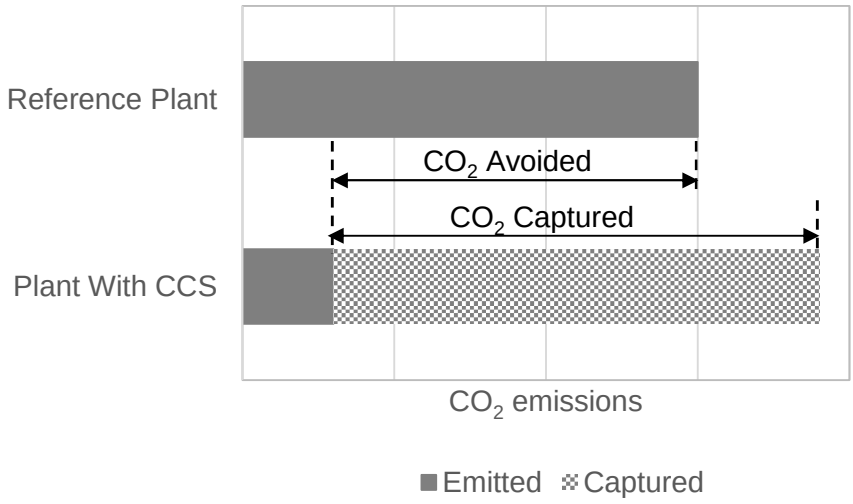

Figure 2-4: Difference between CO_2 avoided and CO_2 captured

All the costs reported in this review were adjusted to the year 2017 by using the Chemical Engineering Plant Cost Index (*CEPCI*), Eq. (2-6), and reported in Euro (€). The subscript *i* refers to the year of reported data. If a different currency is

used in the reviewed studies, the costs were updated to the year 2017 and then converted to Euro.

$$AC_{2017} = AC_i \frac{CEPCI_{2017}}{CEPCI_i} \quad \textbf{(2-6)}$$

2.3.2 Iron and steel industry overview

The iron and steel industry is one of the main contributors to GHG emissions, accounting for 25.1% of the industrial CO_2 emissions in the world in 2018 (IEA, 2020a). Although the steel scrap-based production, which is based on secondary or recycled steelmaking process, generates around 4.5 times less CO_2 (Croezen and Korteland, 2010), the ore-based production is still expected to prevail, at least, in the next decade. It is due to the increasing steel demand and still low recycling rates of steel scrap (IEA, 2020d). Regardless of the steelmaking process, the following steps are present: raw material preparation, iron production and finally the steel production. Blast furnace, smelt reduction or direct reduction are the three main processes in iron production (Ho, Allinson and Wiley, 2011). The ore-based production is carried out mainly through blast furnace-basic oxygen furnace (BF-BOF) or direct reduced iron electric arc furnace (DRI-EAF) (WorldSteel Association, 2021). The iron production *via* BF-BOF is represented in Figure 2-5. As can be seen, to meet the energy requirement of the iron and steel production, the off gases from other operations are combusted in the power plant. This power plant can account for around 50% of the overall CO_2 emissions, while the blast furnace, the coke and sinter plants contribute to 26%, 13% and 10% of the total CO_2 emitted by this steelmaking plant, respectively (Bender et al., 2018). According to Wiley et al. (2013), the CO_2 concentration in the flue gases can vary from 8%$_{vol}$ in the gas released in the sinter plant to 27%$_{vol}$ in the exhaust gas from the coke plant. The flue gas from the blast furnace can contain up to 22%$_{vol}$ of CO_2. In 2004, to seek deep decarbonisation of the iron and steel industry, 48 European companies from 15 countries joined efforts and formed a consortium called ULCOS (Eurofer: The European Steel Association, 2013). These partners have identified new iron and steelmaking processes, such as blast furnace with top gas recycling (TGR), smelting reduction (HIsarna), direct

reduction (ULCORED) and electrolysis (ULCOWIN) to mitigate CO_2 emissions (Croezen and Korteland, 2010). In the first process, TGR, O_2 is introduced in the blast furnace instead of air, eliminating N_2 presence and thus, increasing the CO_2 concentration in the flue gas. The second process, HIsarna, was developed to produce a high CO_2 purity stream *via* ore reduction with coal in pure oxygen rather than air. The ULCORED process relies on the production of direct-reduced iron by using natural gas, coke oven gas, or syngas from coal/biomass gasification as a reducing agent. Similarly to the two previous routes, this process also needs to be coupled with CCS, but there is only one CO_2 source point (shaft furnace). The ULCOWIN process is a carbon-free technique where the iron oxides are reduced electrochemically. According to Van Der Stel et al. (2013) and Eurofer: The European Steel Association (2013), TGR and HIsarna process combined with CCS present a potential for CO_2 abatement that could reach the 60% and 80%, respectively. In case of ULCOWIN, the potential CO_2 reduction can achieve the 98% when the electricity required to the process is generated from non-fossil fuel sources. Over the years, several CO_2 capture technologies have been assessed.

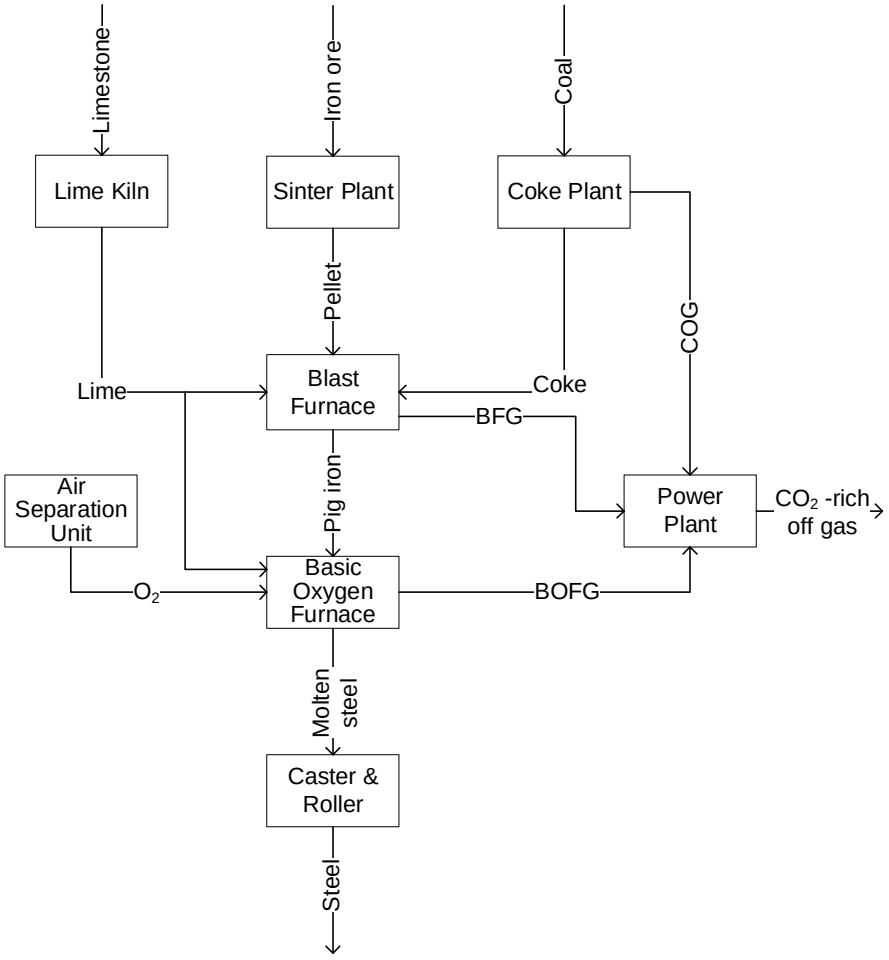

Figure 2-5: Block flow diagram of an iron and steel plant with steel production *via* blast furnace-basic oxygen furnace. BFG, blast furnace gas; BOGF, basic oxygen furnace gas; COG, coke oven gas

2.3.2.1 Chemical absorption (post-combustion amine scrubbing)

As mentioned above, after the power plant, the blast furnace is one of the main contributors to CO_2 emissions in iron and steel plants. For this reason, several researchers have been studying the CO_2 abatement measures for this specific part of the process. Ho, Allinson and Wiley (2011) have estimated the capture costs associated with CO_2 capture from a conventional blast furnace by amine scrubbing (MEA). It should be mentioned that the estimated costs only include the cost associated with CO_2 capture, and the transport and storage costs were not included in their estimation. They concluded that the cost of CO_2 avoided was around 59.7 €/t_{CO_2}, with an equivalent energy consumption of 3.3 MJ_{th}/kg_{CO_2}.

However, replacing the conventional blast furnace with the Corex process could reduce the cost of CO_2 avoided to 45.6 €/t_{CO_2}. In this process, the smelt reduction process uses O_2 and coal instead of air and coke, which takes place in two separate reactors. These reactors, reduction shaft and the melter gasifier substitute the sinter and coke plants. This alternative resulted in a decrease in the equivalent energy consumption of around 7% (3.1 MJ_{th}/kg_{CO_2}). The lower cost and power consumption was due to higher CO_2 concentration and no requirement for pre-treatment of flue gas.

Ho, Bustamante and Wiley (2013) performed the techno-economic feasibility assessment of the amine scrubbing retrofit that used MEA as a solvent. This study has compared the CO_2 avoided cost for CO_2 capture from the flue gas of the TGR and Hismelt processes with the largest volume of CO_2. In this case, it was the flue gas of the blast furnace and the smelt reduction vessel, respectively. The costs associated with CO_2 transport and storage were neglected. This study concluded that CO_2 capture from the TGR was the least expensive option, resulting in the cost of CO_2 avoided of 35.1 €/t_{CO_2}. Such figure was 34.3% lower than 53.4 €/t_{CO_2} reported for the Hismelt process. Interestingly, the energy requirement for both processes was comparable and reported to be 3.1 MJ_{th}/kg_{CO_2} and 3.3 MJ_{th}/kg_{CO_2} for the TGR and Hismelt process, respectively.

Tsupari et al. (2013) have studied the economic feasibility of amine scrubbing retrofit to the iron and steelmaking plant. The CO_2 capture from the largest source of emissions, power plant and blast furnace hot stoves, was evaluated. This study compared three different solvents, including MEA, advanced amine and low-temperature regeneration amine (“Low T”), as well as five different layouts for heat integration for solvent regeneration. Depending on the level of waste heat integration, the equivalent energy consumption was shown to fall between 0.5 MJ_{th}/kg_{CO_2} (MEA) and 4.3 MJ_{th}/ kg_{CO_2} (MEA). In the former case, the heat for solvent regeneration was covered by the waste heat from the steel plant. This, however, resulted in the lowest CO_2 capture capacity. The highest equivalent energy consumption, and subsequently the capture rate, was found for the case where all the steam produced in the iron and steelmaking plant was used for

solvent regeneration. However, in such a case, no electricity was generated and the entire electricity requirement of the plant was met by the grid electricity. This study has also found that the electricity price played an important role in the cost of CO_2 avoided. If the price of electricity was fixed at 80 €/MWh, the cost of CO_2 avoided was between 81.5–164.1 €/t_{CO_2} ("Low T" solvent) and between 91.3–180.6 €/t_{CO_2} (MEA). Nevertheless, if the cost of electricity increased to 100 €/MWh, the corresponding cost of CO_2 avoided would also increase to between 90.3–186.4 €/t_{CO_2} and 92.2–205.8 €/t_{CO_2} for the "Low T" solvent and MEA, respectively. The "Low T" solvent presented lower costs due to lower heat duty for solvent regeneration, 3.4 MJ_{th}/kg_{CO_2} against 3.0 MJ_{th}/kg_{CO_2}, which translated into a lower energy penalty.

Dreillard et al. (2017) have compared the techno-economic performance of three different amines when employed to capture CO_2 from the flue gases of TGR and blast furnace. A conventional amine (MEA) with two different concentrations (30 $\%_{wt}$ and 40 $\%_{wt}$) and a demixing solvent (blend amines) were selected as solvent. The latter involves the change of phase during the process. Their study has shown that the heat requirement for solvent regeneration of demixing solvent was lower by 20–25% and 6–9% than the one for MEA 30 $\%_{wt}$ and MEA 40 $\%_{wt}$, respectively. This translated into an energy consumption in the range between 3.4 MJ_{th}/kg_{CO_2} (MEA) and 2.7 MJ_{th}/kg_{CO_2} (demixing solvent) for blast furnace case and between 3.3 MJ_{th}/kg_{CO_2} (MEA) and 2.4 MJ_{th}/kg_{CO_2} (demixing solvent) for TGR case. Such a reduction in the energy requirement can be explained by a higher CO_2 partial pressure in the flue gas from TGR. It should be noted that in both cases, there was no heat integration. Yet, it was not possible to estimate the equivalent energy consumption based on the data provided in their study. Similarly, the cost of CO_2 captured was reduced by 20–28% when the MEA 30 $\%_{wt}$ was replaced by the demixing solvent. The cost of CO_2 captured decreased from 67.0 €/t_{CO_2} to 53.4 €/t_{CO_2} and from 56.6 €/t_{CO_2} to 40.9 €/t_{CO_2} to capture the CO_2 from blast furnace and TGR, respectively.

The CO_2 mitigation by amine scrubbing (MEA) was also assessed by Garðarsdóttir et al. (2018). They have estimated the CO_2 capture costs and energy consumption associated with the CO_2 capture from the power plant's flue gas. The equivalent energy consumption for the CO_2 capture was 4.8 MJ_{th}/kg_{CO_2}, which was higher than reported in previous studies. This can be attributed to the different levels of heat utilisation for solvent regeneration, which also impacts the CO_2 capture cost. Consequently, the cost of CO_2 captured estimated in this study was 51.4 €/t_{CO_2}. It needs to be noted that this study reported the cost of CO_2 captured that, in general, are lower than the CO_2 avoided cost. This is because the former also includes the additional CO_2 that needs to be captured to offset the energy penalty of the CCS retrofit (Figure 2-4).

Finally, Cormos et al. (2020) have performed a techno-economic analysis of the CO_2 capture retrofit to the power plant, blast furnace hot stoves and lime and coke production *via* the amine scrubbing using MDEA as a solvent. Their study estimated the CO_2 avoided cost of 73.5 €/t_{CO_2}. This figure is slightly higher than that reported in previous studies. However, as opposed to previous studies by Ho, Allinson and Wiley (2011) and Ho, Bustamante and Wiley (2013), this study accounted for the CO_2 transport and storage costs, showing the need for the complete life cycle costing of the CCS chains. Furthermore, the equivalent energy associated with the CO_2 capture was -1.6 MJ_{th}/kg_{CO_2}. This means that the net power output of the plant retrofitted with CO_2 capture is higher than the one for the reference plant. This is the case because this study considered implementing a gas turbine that generated additional electricity and the steel plant off-gases were used to meet the heat and power requirements.

2.3.2.2 Physical absorption (Selexol)

To reduce the energy penalty associated with CCS, the low CO_2 partial pressure flue gas from iron and steel production can be pressurised and the CO converted into CO_2 *via* WGS reaction, thus increasing the CO_2 concentration. Physical absorption using Selexol as a solvent was the technology evaluated by Ho, Allinson and Wiley (2011) for such a case. This study has compared the Selexol process retrofit to the blast furnace and the Corex process. They estimated the

cost of CO_2 avoided of 52.7 €/t_{CO_2} and 28.1 €/t_{CO_2}, for blast furnace and Corex process, respectively. Similarly, the equivalent energy consumption for the Corex process was almost half (1.2 MJ_{th}/kg_{CO_2}) of that estimated for the blast furnace (2.4 MJ_{th}/kg_{CO_2}). This is due to the higher content of CO in the Corex process stream before the water gas shift reaction (44%) compared to the CO content in the gas from the blast furnace (21%).

2.3.2.3 Vacuum pressure swing adsorption

Based on their previous studies, Ho, Bustamante and Wiley (2013) have studied the implementation of vacuum pressure swing adsorption (VPSA), using zeolite 13X as adsorbent, as an alternative to reduce the cost of CO_2 capture. The economic feasibility of CO_2 capture from the flue gas, with the largest volume of CO_2, of 4 different processes, including conventional blast furnace, TGR, Hismelt and Corex, were compared. These points are normally selected due to economy of scale and, therefore, are likely to be prioritised for decarbonisation. The CO_2 capture was carried out at 1.5 bar and the adsorbent regeneration took place at 0.05 bar. Their study showed that the cost of CO_2 avoided from the flue gas of the TGR and Corex processes were the lowest among the considered processes, and were estimated to be around 26.7 €/t_{CO_2}. The cost of CO_2 avoided from the flue gas of the blast furnace and the Hismelt processes were estimated to be around 31.6 €/t_{CO_2} and 35.1 €/t_{CO_2}, respectively. The estimated equivalent energy consumption was estimated to be between 1.8 MJ_{th}/kg_{CO_2} (Corex) and 2.4 MJ_{th}/kg_{CO_2} (Hismelt).

2.3.2.4 Solid looping cycles

Conversely to the other EII, such as cement, the solid looping cycles were considered for the decarbonisation of the iron and steel industry only recently. Therefore, techno-economic assessments are still very scarce. The integration of CaL to the iron and steel plant was proposed for the first time by Tian et al. (2016a). In the considered process, the Ca and Fe ions in the iron slag were first separated using acetic acid. Then, the Fe-rich stream was recycled to the blast furnace and the Ca-rich stream, after precipitation and dry-distillation, was fed to

the calciner. The spent CaO was recycled to the blast furnace. They concluded that the steel slag-derived sorbent could be employed as a CO_2 sorbent, presenting higher reactivity and lower degradation compared to limestone. Depending on the synthesis process, four of the steel slag-derived samples presented a CO_2 uptake between 0.08 $g_{CO_2}/g_{sorbent}$ and 0.11 $g_{CO_2}/g_{sorbent}$ while the limestone stabilised for 0.07 $g_{CO_2}/g_{sorbent}$ after 15 cycles. However, the enhanced CO_2 capture performance resulted in a higher cost of sorbent purchase that could be compensated by selling two by-products, high-purity CaO and acetone. Again, depending on the steel slag-derived sorbent synthesis, the final cost of this would result in values between 57.7 €/t and 145.7 €/t compared to 102.0 €/t for limestone.

Based on their previous work, Tian et al. (2016b) have proposed a combined Ca-Fe looping to capture the CO_2 released from the blast furnace during the iron production. The heat required to drive the endothermic reaction in the calciner was provided by the FeO oxidation. Similar to their previous work, the spent sorbent was utilised in the iron process as the CaO could be used in the blast furnace. The developed CaO-based, Fe-functionalised sorbent presented a medium CO_2 sorption capacity, around 0.16 $g_{CO_2}/g_{sorbent}$, but very good cycling stability.

High energy consumption due to temperatures of around 900 °C during the calcination can be avoided by integrating calcium and chemical looping. In that case, the existing iron and steel power plant can be replaced by a steam cycle power plant. However, in order to produce a high-purity CO_2 stream, the ASU is still required by the oxy-fuel combustion, which is an energy-intensive process. To avoid the ASU requirement, Fernández et al. (2017) and Martínez et al. (2018) have proposed the combined Ca-Cu looping for H_2 production with CO_2 capture. In this process, the H_2 production was carried out by sorption-enhanced water gas shift (SEWGS) and the heat required for the sorbent regeneration was met by reducing CuO to Cu. They concluded that this new process could effectively contribute to the CO_2 abatement in the iron and steel industry. The CO_2 direct emissions could be reduced in 30% by implementing the Ca-Cu process into the

blast furnace. Furthermore, the part of the energy input could be recovered by the integration of high heat grade for electricity production.

A new Ca-Cu looping configuration was also considered by Fernández, Spallina and Abanades (2020). While in the previous work by Fernández et al. (2017), the blast furnace off-gas was used for H_2 production, in case of the new configuration, the coke oven gas and basic oxygen furnace gas were also used as reducing gas. This resulted in up to a 40% increase in the H_2-rich stream production that could be used for on-site power generation or to produce sponge iron, thus increasing the steel plant capacity. Unfortunately, the potential of CaL coupled with chemical looping cycles (Ca-CLC) was not completely demonstrated. Although Fernández, Spallina and Abanades (2020) have reported a specific energy consumption of around 1.5 MJ_{th}/kg_{CO_2}, only Martínez et al. (2018) have compared this technology with other CCS technologies. They found that the energy penalty associated with CO_2 capture was reduced when Ca-Cu looping was employed, the electricity imported from the grid decreased by more than a half, from 185.4 kWh/t_{HRC} (MEA) to 69.1 kWh/t_{HRC} (Ca-Cu looping). Unfortunately, no economic analysis was performed to assess the viability of such a process.

Tian et al. (2018) were the first authors to present economic data on solid looping integration to the iron and steel industry. They have proposed a new decarbonisation concept that relies on the inherent CO_2 capture capability of the steelmaking process. The CO_2 emissions of the power plant, where the coke oven gas and blast furnace gas are combusted, were captured at the lime kiln. The integration of CaL in the lime production (Ca-LP), resulted in the cost of CO_2 avoided of between 12.9 €/t_{CO_2} and 16.3 €/t_{CO_2}, with an equivalent energy consumption of 2.8 MJ_{th}/kg_{CO_2}. Such figures seem to be the best option in the mid- and long-term.

Cormos et al. (2020) have evaluated the CaL potential to capture the CO_2 from the power plant, blast furnace, hot stoves, lime and coke production. Because this work considered the decarbonisation of four points without integration of CaL in the iron and steel process, unlike what was considered in the previous work,

the operating costs were higher. Their study presented the CO_2 avoided cost of 68.9 €/t_{CO_2} and the energy penalty of 1.3 MJ_{th}/kg_{CO_2}. The former figure is 4–5 times higher, while the latter figure is more than 50% lower than the values reported by Tian et al. (2018). This can be attributed to the implementation of a combined gas turbine.

2.3.2.5 Discussion

The CO_2 capture from the flue gas of the blast furnace, one of the main sources of CO_2 emissions in this industry, has been extensively studied. The comparative techno-economic performance of the CO_2 capture technologies for decarbonisation of this industry is represented in Figure 2-6. It should be noted that only the studies that reported both thermodynamic and economic performance data are represented in that figure. Amine scrubbing, the most commonly studied technology, presents the highest mean cost of CO_2 avoided (104.6 €/t_{CO_2}) and the highest mean equivalent energy consumption (2.7 MJ_{th}/kg_{CO_2}). The range for the equivalent energy consumption for this technology was wide, reflecting the different levels of waste heat integration considered. The current literature shows that using alternative solvents, for example, replacing MEA with MDEA, can reduce the heat regeneration duty and, thus, the cost associated with CO_2 capture. However, the major cost reductions reported in the literature result from consideration of alternative technologies, such as the vacuum pressure swing adsorption or emerging CaL. The retrofits of these technologies to the iron and steel plants resulted in the mean cost of CO_2 avoided of as low as 30.0 €/t_{CO_2} and 32.7 €/t_{CO_2}, respectively. However, the techno-economic assessments of using alternative CO_2 capture technologies for decarbonisation of the iron and steel industry are still very limited. It needs to be emphasised that even for amine scrubbing, the current literature presents a large discrepancy in the results of the techno-economic assessments, with the cost of CO_2 avoided reported to vary between 35.1 €/t_{CO_2} and 205.8 €/t_{CO_2}. This can be attributed to the selection of system boundaries, different assumptions and methods used in the economic assessment, as confirmed by Tsupari et al. (2013). Furthermore, the techno-economic performance indicators also depend

on the volume and composition of the flue gas to be treated. Although it is difficult to choose the best technology and, to date, the studies are very limited, CaL appears to be a promising option for the decarbonisation of the iron and steel industry. The concept Ca-LP, proposed by Tian et al. (2018), showed a CO_2 avoided cost in the range as low as 12.9–16.3 €/t_{CO_2} due to the heat waste recovery and the reduction in the material cost once the limestone used as the sorbent is fully integrated into the steelmaking process. Regardless of the limited number of assessments presented in the current literature, Fernández, Spallina and Abanades (2020) showed that combined Ca-CLC is a promising technology for decarbonisation of the iron and steel industry, mostly because of its low specific energy consumption of around 1.5 MJ_{th}/kg_{CO_2}.

Although not discussed in this work, SEWGS technology was shown to be also a promising CO_2 capture technology in the iron and steel industry (Gazzani, Romano and Manzolini, 2015; Manzolini et al., 2020). Manzolini et al. (2020) have shown that SEWGS can be employed in an iron and steel plant to capture the CO_2 from the off-gases and produce H_2. The H_2 is then burnt in the power plant to meet the electricity requirement of the iron and steel plant. They have compared the SEWGS performance with that of a conventional amine scrubbing and found that the former presents a lower cost of CO_2 avoided (33 €/t_{CO_2} against 38 €/t_{CO_2} for amine scrubbing) and lower specific energy consumption for CO_2 avoided (1.9 MJ_{th}/kg_{CO_2} against 2.5 MJ_{th}/kg_{CO_2} for amine scrubbing).

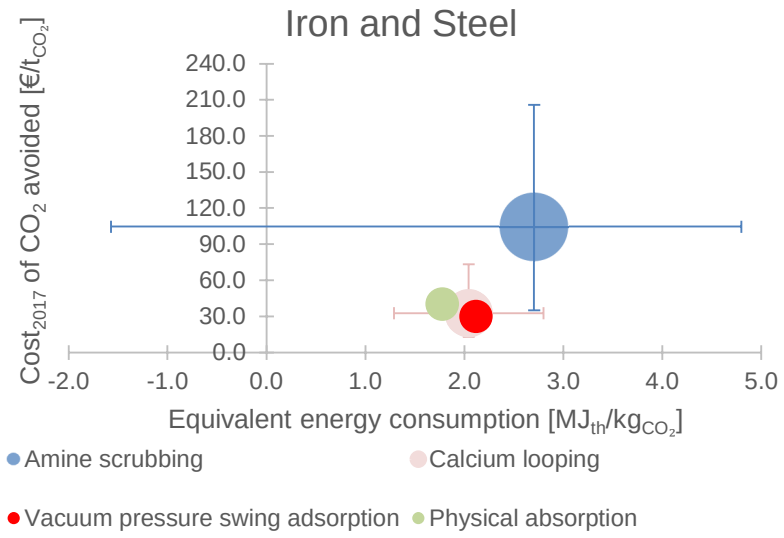

Figure 2-6: Techno-economic performance of different CO_2 capture technologies for decarbonisation of iron and steel industry: equivalent energy consumption vs mean CO_2 avoided cost. (Error bars represent the range of figures found in the literature. The bubbles without error bars have only one source. The area of each bubble is proportional to the number of studies reviewed.)

2.3.3 Cement industry overview

The cement industry accounted for around 26.4% of the total global industry emissions in 2018 (IEA, 2020a). 40% of these emissions are released during the heat generation for the kiln and the remaining 60% results from the calcination process (Barker et al., 2009; Dean et al., 2011; Favier, Scrivener and Habert, 2019), in which limestone is converted into CO_2 and CaO at >900°C. The CO_2 content in the exhaust stream after the raw mill, depending on the level of air leaking in the system, can reach up to 22%$_{vol}$ (Voldsund et al., 2019). Figure 2-7 shows the simplified process of a cement plant. Since limestone is the cheapest raw material available for cement production, the abatement of these 60% emissions can only be achieved with a decrease in production (Favier, Scrivener and Habert, 2019; Leeson et al., 2017). Although cement production has decreased in China, which is the largest cement producer globally (2.3 bn tonnes per year), the Indian and some African countries are emerging markets (IEA, 2020b). Therefore, the mitigation of CO_2 emissions from cement production can only be achieved by CCS. Because the flue gas produced in this industry include

a high content of CO_2, the application of CCS appears to be a feasible decarbonisation option (Bataille et al., 2018; Gerres et al., 2019).

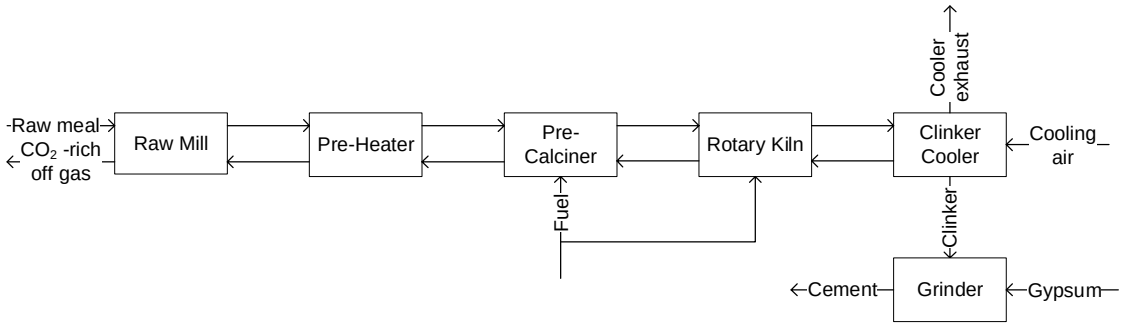

Figure 2-7: Block flow diagram of a cement plant

2.3.3.1 Chemical absorption (post-combustion amine scrubbing)

Barker et al. (2009) were one of the first to study the feasibility of amine scrubbing (MEA) integration in the cement industry. They found that the cost of CO_2 avoided (116.8 €/t_{CO_2}) for this process was higher than that for coal-fired power plants (42.4 €/t_{CO_2}). This can be attributed to the lower volume of CO_2 emissions produced by the cement plant, the requirement of a unit for SO_x and NO_x removal, being normally part of existing power plants, and the need for installing a steam generator. The major cost of amine scrubbing is associated with the steam supply for the stripper. It was found that the CO_2 capture translated into an equivalent energy consumption of 5.2 MJ_{th}/kg_{CO_2}, for a CO_2 capture rate of 77%, where the extra energy demand was met by coal-fired CHP. However, the study by Barker et al. (2009) showed that the replacement of MEA by other amine solvents with lower heat duty of regeneration and the location of cement plant in an industry cluster with CO_2 capture, enhancing the CO_2 transport scale, could reduce the cost of CO_2 avoided up to 50% (in case of the latter).

The CO_2 avoided cost associated with amine scrubbing (MEA) implementation in a cement plant was also estimated by Ho, Allinson and Wiley (2011) and Atsonios et al. (2015). Their work showed lower costs of CO_2 avoided (59.7 €/t_{CO_2} and 72.4 €/t_{CO_2}, respectively) than that reported by Barker et al. (2009). However, their work did not account for the transport and storage costs. Ho, Allinson and Wiley

(2011) have estimated an energy penalty of 1.5 MJ_{el}/kg_{CO_2}, which corresponds to an equivalent energy consumption of 3.3 MJ_{th}/kg_{CO_2}. They concluded that this figure could be reduced by considering solvents with a lower energy requirement, such as MDEA, or utilisation of the excess heat available in the cement plant, which was not considered in this work. A higher value was obtained by Atsonios et al. (2015), as the estimated equivalent energy consumption was 4.4 MJ_{th}/kg_{CO_2}. While Ho, Allinson and Wiley (2011) assumed that the steam and power required for the carbon capture was delivered by an external source (CHP plant), Atsonios et al. (2015) considered an on-site coal-fired boiler to meet the heat requirement for solvent regeneration.

Gomez et al. (2014) have compared the economic performance of a cement plant using amine scrubbing as CO_2 capture. Two kinds of amines, the conventional MEA and a phase-change amine (demixing solvent) were considered as solvent. They have found that the cost of CO_2 capture was reduced by around 50% with the phase-change amine (43.9 €/t_{CO_2}) when compared with the conventional MEA (89.1 €/t_{CO_2}). Unfortunately, there was not enough data available to estimate the equivalent energy consumption. However, the authors have found that the heat requirement for solvent regeneration, met by steam, was lower for the phase-change amine.

Zhou et al. (2016) have done a comparative study between amine scrubbing (MEA) with CHP and amine scrubbing with imported steam and electricity. Assuming an 85% CO_2 capture rate, they concluded the cost of CO_2 avoided was comparable in both cases. The second option was marginally less expensive (68.3–113.1 €/t_{CO_2} against 78.5–128.4 €/t_{CO_2}), mainly due to lower capital costs and the higher CO_2 avoided. The latter was due to the lower electricity emission factor assumed for the electricity imported, since the indirect emissions associated with the electricity and steam required by the CO_2 capture plant were also accounted on the estimation of CO_2 avoided. An equivalent energy requirement of 8.1 MJ_{th}/kg_{CO_2} and 5.3 MJ_{th}/kg_{CO_2} was found for the first and second options, respectively. These figures are higher than the values reported

above with similar configurations. This can be explained by different assumptions made in these studies, such as electric efficiency and specific heat requirement for solvent regeneration. The lower energy consumption for the configuration with energy import compared to that with on-site generation is in agreement with the previous results. Since the heat and power production on-site results in a rise of CO_2 produced and then captured, this translates into a higher energy requirement.

A conventional amine, MEA, was the solvent selected by Gardarsdottir et al. (2019) to capture 90% of the CO_2 present in the flue gas stream from the cement kiln. This required an equivalent energy consumption of 5.2 MJ_{th}/kg_{CO_2}, the same figure obtained by Barker et al. (2009). The former considered that 96% of the steam required for solvent generation was delivered by a natural gas-fired boiler and the remaining by the waste heat. Regarding the economic analysis, a comparable figure with the previous works was obtained, 78.5 €/t_{CO_2}.

The techno-economic analysis of retrofit amine scrubbing (MEA) to cement industry was also assessed by Markewitz et al. (2019). Four different cases were compared. In two of them, the plant was an electricity and steam importer, but with different levels of flue gas air leak, in the third case, the steam was provided by an on-site coal boiler, and in the fourth, a coal-fired CHP plant was implemented. They found that the heat requirement demand varied between 3.5–3.8 MJ_{th}/kg_{CO_2}, for case 2 and case 3 and 4, respectively. Similar to the heat demand, the equivalent energy consumption did not differ too much for the different cases (4.8–5.2 MJ_{th}/kg_{CO_2}). As shown by the previous work of Zhou et al. (2016), cases 1 and 2 (with energy import) presented the lowest equivalent energy consumption, 4.8 MJ_{th}/kg_{CO_2} and 4.9 MJ_{th}/kg_{CO_2}. Regarding the economic analysis, they concluded that the second case is the cheapest (80.8 €/t_{CO_2}), while in cases 1, 3 and 4, the cost of CO_2 avoided were 85.6 €/t_{CO_2}, 120.5 €/t_{CO_2} and 106.9 €/t_{CO_2}, respectively.

Cormos et al. (2020) performed a techno-economic analysis for CO_2 capture by amine scrubbing (MDEA) with CHP to meet the additional energy requirement.

The estimated equivalent energy consumption was around 4.8 MJ_{th}/kg_{CO_2}. This figure is lower than the previous studies (Barker et al., 2009; Gardarsdottir et al., 2019; Markewitz et al., 2019) where on-site CHP was considered as the source to meet the additional energy demand but still comparable. The cost of CO_2 avoided was estimated to be around 86.9 €/t_{CO_2}.

2.3.3.2 Oxy-fuel combustion

Unlike post-combustion amine scrubbing, oxy-fuel combustion technology requires some modification in the cement production process. Because the fuel combustion with air is replaced by a mixture of O_2 with recycled CO_2, an ASU is required. Furthermore, the retrofit of oxy-fuel combustion to cement process alters the gas temperature, the heat exchange between gas and reactor, and the bed material that affect the quality of clinker (Carrasco-Maldonado et al., 2016; ECRA, 2012). Therefore, the pre-calciner and/or rotary kiln, depending on type of oxy-fuel combustion (partial or full), need to be adapted or redesigned and a second pre-heater is required in parallel with the first pre-heater, in case of partial oxy-fuel combustion (Carrasco-Maldonado et al., 2016). Barker et al. (2009) evaluated the cost associated with oxy-fuel combustion retrofitted to the pre-calciner in the cement industry. They concluded that to achieve a capture rate of 52%, the cost of CO_2 avoided (43.7 €/t_{CO_2}) was almost 1/3 of post-combustion amine scrubbing. Similarly to the cost, the equivalent energy consumption (1.8 MJ_{th}/kg_{CO_2}) was less than 1/3 of the energy requirement of MEA. However, the latter could achieve a higher CO_2 capture rate (77%).

Rodríguez, Murillo and Abanades (2012) also studied the feasibility of pre-calciner replacement by an oxy-fuel circulating fluidised bed calciner. They estimated a cost of CO_2 avoided of 13.8 €/t_{CO_2} with extra electricity consumption, compared with the reference plant, in the range 0.5–0.7 MJ_{el}/kg_{CO_2}. Nonetheless, this additional requirement due to CO_2 capture was covered by the integration of the Rankine cycle for the recovery of the heat waste. The estimated equivalent energy consumption was 1.2 MJ_{th}/kg_{CO_2} for a CO_2 capture rate of 89%. It should be mentioned that although the cost of CO_2 avoided was around half of the figure

estimated by Barker et al. (2009), it did not take into account the costs associated with CO_2 transport and storage.

The retrofitting of oxy-fuel combustion to pre-calciner was also assessed by Zhou et al. (2016). Their study reported values between 38.7 €/t_{CO_2} and 62.2 €/t_{CO_2}, which are comparable with those estimated by Barker et al. (2009). Similar to this study, the authors also concluded this cost was around half of the cost for post-combustion amine scrubbing and the equivalent energy consumption (2.0 MJ_{th}/kg_{CO_2}) was less than half of the figure obtained for MEA, in the case of electricity and steam import. However, this performance was obtained with a lower capture rate (62% against 85%) because only the CO_2 from the calciner was captured and thus, the CO_2 from the kiln was released to the atmosphere.

Gardarsdottir et al. (2019) proposed the integration of oxy-fuel combustion in cement plant, but in that case, the CO_2 released during the fuel burnt in the kiln was also captured which means the process conditions were changed. They have estimated a CO_2 avoided cost of around 41.5 €/t_{CO_2}, almost half of post amine scrubbing cost. This figure was also confirmed by previous studies. It should be emphasised that in that case, the CO_2 emissions from the kiln were also captured. As proposed by Rodríguez, Murillo and Abanades (2012), the extra electricity requirement (0.7 MJ_{el}/kg_{CO_2}) was covered by the power generated by a Rankine cycle. The equivalent energy consumption was 1.7 MJ_{th}/kg_{CO_2}, which was in agreement with the values obtained in the previous studies.

2.3.3.3 Solid looping cycles

For the integration of the solid looping cycles in the cement plants, two configurations have been studied over the years. In the tail-end process, the CO_2 is captured from the flue gases *via* the post-combustion route. In the integrated process, the CaL purge stream, which comprises mainly CaO, is used as a feed stream in the cement plant, the carbonator is integrated with the pre-heater of the clinker production process and the oxy-fuel calciner replaces the pre-calciner of a conventional cement plant. As CaL has been extensively explored in the power industry, which along cement industry is a major contributor for CO_2 emissions,

Romeo et al. (2011) proposed the integration of power and cement plants with a common CaL process. This new layout benefitted from the waste energy from the carbonation reaction and clinker cooling, which was used to produce extra power in the steam cycle, and the CaO from the CaL was integrated with the cement process. The equivalent energy consumption was estimated to be around 0.7 MJ_{th}/kg_{CO_2}, for a CO_2 capture rate of 94%. The cost of CO_2 avoided associated with this symbiosis was 12.0 €/t_{CO_2}, which is lower than for a standalone cement or power plant with CO_2 capture. It should be noted that this figure neglected the CO_2 transport and storage costs.

Rodríguez, Murillo and Abanades (2012) have proposed the substitution of cement pre-calciner by CaL process, this was an oxy-fuel calciner connected with a carbonator. In this case, part of the CaO formed in the calciner was directed to the carbonator, where the CO_2, from flue gas generated in the kiln, was captured. The remaining CaO stream was fed to the kiln to produce the clinker as in the conventional process. Although the integration of CaL to cement process showed an electrical penalty comprised between 0.6 and 0.7 MJ_{el}/kg_{CO_2}, mainly due to ASU and CO_2 compression, this was covered by the waste heat recovery. This translated into an equivalent energy consumption of 1.3 MJ_{th}/kg_{CO_2} with 99% of the CO_2 emissions captured. The CO_2 avoided cost was as low as 22.3 €/t_{CO_2}. However, this cost would be higher if the costs associated with CO_2 transport and storage had been included.

The techno-economic feasibility of retrofitting CaL to a cement plant was also evaluated by Atsonios et al. (2015). In this study, the authors took into consideration the technical specifications of the cement process. They showed that fuel composition, sulphur (S) content, plays an important role in the CaL performance and CaO purge quality. They found that coal with lower S content was the fuel that minimised the fresh limestone make-up. The specific heat requirement for sorbent regeneration was 4.6 MJ_{th}/kg_{CO_2} which is slightly higher than the one for MEA regeneration (4.3 MJ_{th}/kg_{CO_2}) in the same work. However, this heat was then recovered in the steam cycle to produce electricity, sold to the

grid. For this case, they estimated a cost of CO_2 avoided of 70.1 €/t_{CO_2}, which is higher than previous works as well as the equivalent energy consumption (3.0 MJ_{th}/kg_{CO_2}). Likely the previous ones, this figure did not include CO_2 transport and storage costs.

Since CaL technology has an energy penalty due to ASU, Diego, Arias and Abanades (2016) proposed a new concept that not requires one. In order to minimise the calciner heat requirements, a double CaL was implanted. In the first cycle, the flue gases from the cement plant and air-fired combustor, were fed to the carbonator, where the CO_2 was captured, and then the $CaCO_3$ was preheated before entering the calciner. Here, the heat requirements were met by a stream of hot CaO, previously overheated in the air-fired combustor, constituting the second looping. In that case, the CaO stream was a heat carrier. The estimated equivalent energy consumption, for a capture rate of 94%, was 1.6 MJ_{th}/kg_{CO_2}. However, this figure could be reduced to 0.9 MJ_{th}/kg_{CO_2} if the capture efficiency was reduced to 58%. The cost of CO_2 avoided estimated for both cases was 39.1 and 25.2 €/t_{CO_2}, respectively. As these figures are comparable to those reported for a single CaL scheme, it is difficult to justify the superiority of the new scheme.

As mentioned before, two approaches can be adapted to retrofit CaL into a cement plant, integrated and tail-end. De Lena et al. (2019) compared three different levels of integration, 100%, 50% and 20%. It should be mentioned that when there is no full integration, it is considered a tail-end process. The technical analysis showed that the CaL 100% integrated had the lowest extra electricity consumption of 0.8 MJ_{el}/kg_{CO_2} against 0.9 MJ_{el}/kg_{CO_2} for only 20% of integration, though, the latter was the only option that resulted in an electricity exporter. The equivalent energy consumption ranged between 2.5 MJ_{th}/kg_{CO_2} (full integration) to 2.9 MJ_{th}/kg_{CO_2} (20% of integration). They estimated a cost of CO_2 avoided in the range 51.0–57.4 €/t_{CO_2} for partial and full integration, respectively, although the latter with a CO_2 capture rate around 3.2 points percent higher than the case with 20% of integration.

Cormos et al. (2020) have also studied the feasibility of CaL as a tail-end technology for the retrofit of the cement plant. As proposed by the previous authors, the extra electricity demand to drive the CaL plant was generated by a steam cycle that recovered the high-grade heat available in the process. This study reported a similar cost (57.8 €/t_{CO_2}) to that estimated by De Lena et al. (2019), though with a higher equivalent energy consumption (3.9 MJ_{th}/kg_{CO_2}) and a lower CO_2 capture rate (90%). It is important to note that the estimated cost for CaL was 33% lower than the figure obtained in the same study for amine scrubbing.

2.3.3.4 Discussion

CaL has been extensively studied in the cement industry as an end-pipe technology or fully integrated into the process. As can be seen from the techno-economic comparison between the CO_2 capture technologies (Figure 2-8), the cheapest technology is the oxy-fuel combustion (40.0 €/t_{CO_2}) followed by CaL (42.9 €/t_{CO_2}). Amine scrubbing presents the highest mean cost (92.0 €/t_{CO_2}) as well as the highest equivalent energy consumption 5.1 MJ_{th}/kg_{CO_2}, which is mainly due to the high heat requirement for amine regeneration. Unlike the iron and steel industry, where the heat requirement for solvent regeneration or at least part of it can be met by the integration of waste heat, in the cement industry, this needs to be delivered by an external source such, as a boiler or a CHP plant implemented on-site or be off-site but delivering the required energy. The results showed that the implementation of a boiler or CHP on-site results in higher equivalent energy consumption since the CO_2 emissions generated by them are also captured at the CO_2 capture plant. Although CaL and oxy-fuel combustion also result in an energy penalty, the additional fuel demand in the calciner for CaL and the electricity demand of the ASU for both technologies, a part of high-heat grade can be recovered with a Rankine cycle. Although oxy-fuel combustion resulted in the lowest equivalent energy consumption (1.7 MJ_{th}/kg_{CO_2} versus 2.2 MJ_{th}/kg_{CO_2} for CaL), the CO_2 capture rate is, in general, lower than the values reported for CaL technology. In summary, CaL is a feasible technology for this

industry and an alternative to overcome the high efficiency penalty presented by amine scrubbing.

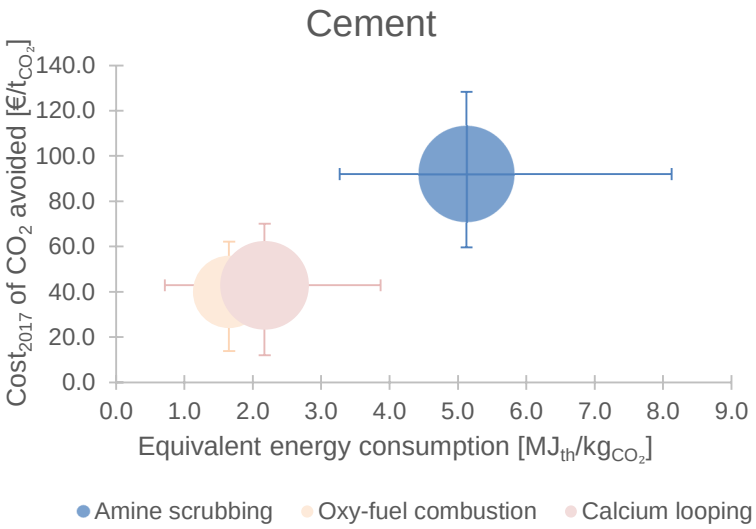

Figure 2-8: Techno-economic performance of different CO_2 capture technologies for decarbonisation of cement industry: equivalent energy consumption vs mean CO_2 avoided cost. (Error bars represent the range of figures found in the literature. The area of the bubble is proportional to the number of works reviewed.)

2.3.4 Petroleum refining industry overview

Accounting for 14.3% of the industrial CO_2 emissions in the world in 2018 (IEA, 2020a), petroleum refineries are the largest industrial worldwide energy consumer (IEA, 2020). These industries require 15%$_{vol}$ of the total primary demand for oil and 9%$_{vol}$ of gas consumed globally. Johansson et al. (2012) categorised the EU refineries by size, considering the simple refinery designs with no conversion units through to the complex refinery designs that consider hydrocracking and catalytic cracking processing units. The latter can also accommodate an integrated gasification combined cycle (IGCC) for the conversion of solids and heavy fuels into heat and power along with lighter products. Figure 2-9 represents a simple diagram of a refinery with conversion. The main challenge in the petroleum industry is the fact that the CO_2 emissions come from a range of diverse sources, leading to variable CO_2 content in the exhaust gases. According to van Straelen et al. (2010), between 20 to 60% of the

CO_2 emissions are released by furnaces and boilers. The remainder part comes from different sources: the utilities (electricity and steam) produced to feed the refinery (can be between 20% and 50% of the total emissions), the fluid catalytic cracker (20–35% of the total emissions), and from other sources during H_2 manufacturing (5–20% of the total emissions). The type of fuel burnt also plays an important role in the flue gas composition (Bains, Psarras and Wilcox, 2017). In general, the CO_2 concentration varies from $4\%_{vol}$ in the CHP gas turbine, and can reach $20–99\%_{vol}$ in the gas stream from the pressure swing adsorption (PSA) unit used in the H_2 purification (van Straelen et al., 2010). Then, a combination of multiple flue gases, to be treated in a single CCS unit, may be necessary which is not simple to accommodate in the plant and thus has not been tested yet (Leeson et al., 2017). The demand for chemical products, such as high-value chemicals, ammonia and methanol, has been increasing and this growth is expected to continue (IEA, 2020e). As these heavily rely on fossil fuels, CCS is a viable route to decarbonise the petroleum refining industry.

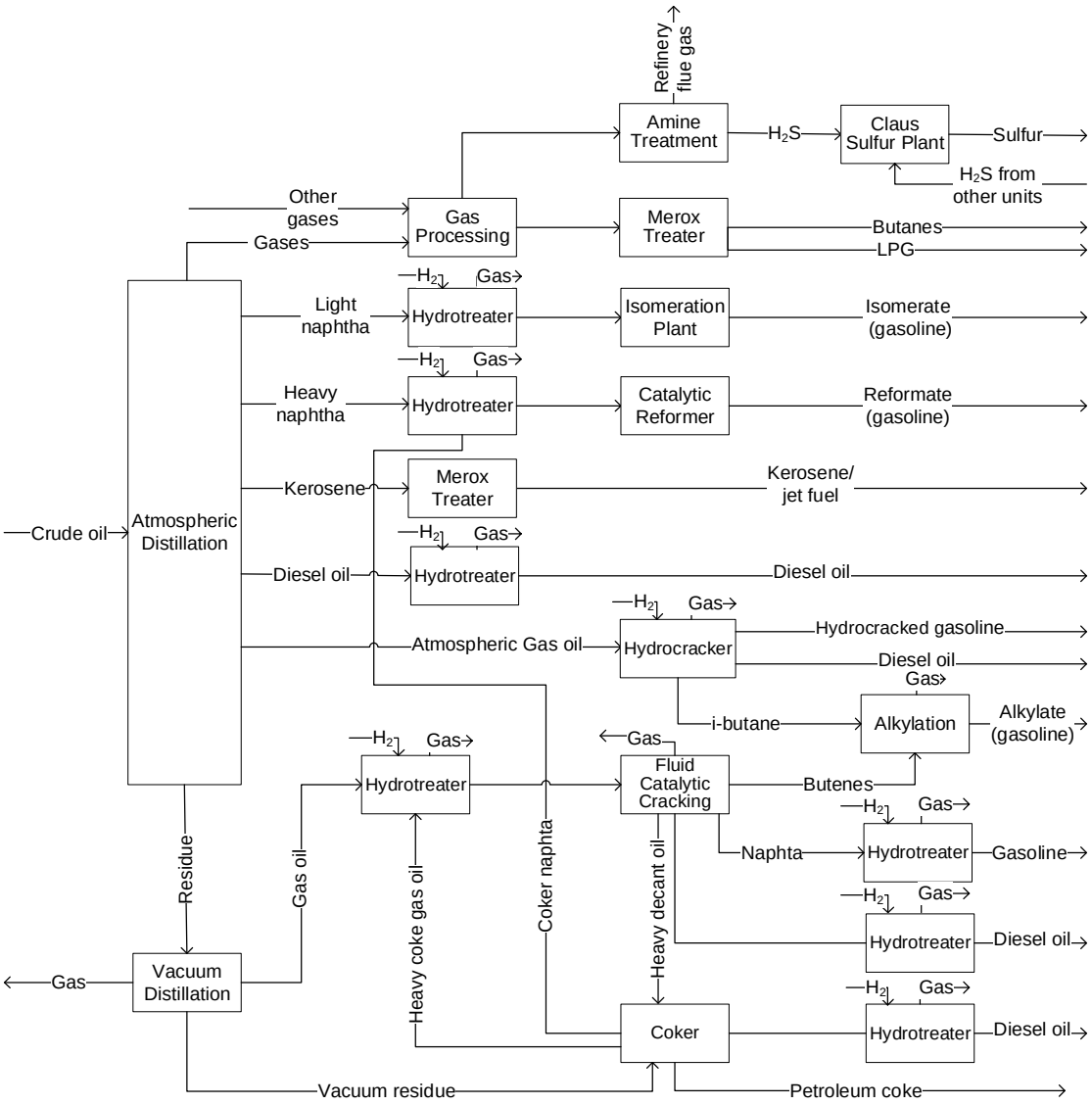

Figure 2-9: Block flow diagram of a conversion refinery plant

2.3.4.1 Chemical absorption (Amine scrubbing)

Amine scrubbing has been the most studied CCS technology in the petroleum refining industry. The costs associated with the retrofit of the post-combustion amine scrubbing (MEA) into a complex refinery was assessed by van Straelen et al. (2010). They have studied the cost of CO_2 avoided for different CO_2 emissions point sources, with a diverse volume of gas to be treated and CO_2 concentration. For a capture rate between 85% and 90% of a stream with 8%$_{vol}$ to 9%$_{vol}$ of CO_2, the cost of CO_2 avoided was in the range 97.2–129.6 €/t_{CO_2}, although these costs did not include the cost of CO_2 transport and storage. These figures correspond

to a combined stack, corresponding to 40% of the total CO_2 emissions of the refinery. Due to the scale of flue gases streams to be treated, the CO_2 capture plant would require the implementation of a dedicated utility plant, being a boiler with a Rankine cycle steam turbine the most feasible option. In that case, the equivalent energy consumption would be 3.8 MJ_{th}/kg_{CO_2}. They concluded that CO_2 capture costs depend strongly on the volume gas to be treated and its CO_2 concentration. If the annual CO_2 captured (8%$_{vol}$ CO_2 content in the flue gas) dropped from 2000 kt to 500 kt the cost of CO_2 avoided increased by around 20%. The reduction in the level of CO_2 in the flue gas, from 12%$_{vol}$ to 8%$_{vol}$ translated into a rise up to 25% on the cost of CO_2 avoided.

Ho, Allinson and Wiley (2011) also studied the economic feasibility of CO_2 capture from a combined stack with 9%$_{vol}$ of CO_2 concentration. They concluded that the implementation of a CO_2 capture unit, post-combustion amine scrubbing (MEA), introduced an electrical power penalty of 1.6 MJ_{el}/kg_{CO_2}, which translated into an equivalent energy consumption of 3.5 MJ_{th}/kg_{CO_2}. For a 90% of capture rate, the cost of CO_2 avoided was equal to 76.3 €/t_{CO_2}, a lower figure than the one reported by van Straelen et al. (2010). Since the CO_2 concentration and volume captured (1000 kt per year) were similar and in both cases, the cost associated with the CO_2 transport and storage was excluded, this difference maybe is due to the different route assumed for the source of energy to meet the energy requirement by the CO_2 capture plant. While these authors assumed that the energy was delivered by an external source, the previous study considered the implementation of a CHP plant.

Berghout, van den Broek and Faaij (2013) compared the retrofits of the pre- and post-combustion amine scrubbing in five different plants (two refineries, two petrochemical plants and a steam reforming hydrogen plant) in a long- (2040–2050) and short- (2020–2025) term analysis. Therefore, the latter assumes that commercially ready CO_2 capture technologies are employed and the former considers new technologies still in development. While MEA was selected as the solvent for the post-combustion retrofits, a mixture of methyl diethanolamine and 3%$_{wt}$ of piperazine was chosen in pre-combustion. This was justified by higher

absorption capacity, chemical stability and lower regeneration heat requirement. In the post-combustion, the CO_2 present in the flue gases (4–16%$_{vol}$ CO_2 concentration) from furnaces, boilers and the catalytic cracker, depending on the plant type, was captured. In the pre-combustion capture, the CO_2 was captured from a high-pressure gas leaving the steam methane reformer, followed by the WGS reactor. The main techno-economic results are shown in Table 2-2. As can be seen for refineries, the equivalent energy consumption was the lowest for pre-combustion (between 1.1 MJ_{th}/kg_{CO_2} and 1.2 MJ_{th}/kg_{CO_2}) retrofits than for post-combustion for either short- (3.4–4.0 MJ_{th}/kg_{CO_2}) and long-term (2.6–3.3 MJ_{th}/kg_{CO_2}). This can be attributed to the selection of a solvent with lower regeneration duty in the pre-combustion and the waste heat from H_2 production was enough to meet the energy requirement for the solvent regeneration, though this was achieved with high fuel consumption and high CO_2 emissions. Regarding the chemical plant, the equivalent energy requirement was again lower for pre-combustion (1.1 MJ_{th}/kg_{CO_2}) than post-combustion at short- (4.0–4.7 MJ_{th}/kg_{CO_2}) and long-terms (2.1–3.3 MJ_{th}/kg_{CO_2}) for both plants. Even though the cost is dependent on CO_2 concentration and volume to be treated, in general, pre-combustion presented higher CO_2 avoided costs (89.6–172.1 €/t_{CO_2}) than post-combustion (71.1–120.5 €/t_{CO_2}) due to higher fuel and capital costs. Regarding the H_2 plant, the post-combustion energy requirement in the short- and long-term (5.8 MJ_{th}/kg_{CO_2} and 4.8 MJ_{th}/kg_{CO_2}) was higher than the figure reported for pre-combustion (3.1 MJ_{th}/kg_{CO_2}) and higher costs of CO_2 avoided, too. This can be explained by the lower heat solvent regeneration used in the pre-combustion, which had an impact on energy requirement and so, on the energy expenses. Furthermore, in the pre-combustion, the CO_2 was captured from a high-pressure gas rather than a flue gas at atmospheric pressure. However, these figures were obtained at the expense of a lower CO_2 capture rate (56%, pre-combustion, against 80 and 89%, post-combustion). It should be noted that the specific CO_2 emissions factors for the additional fuel and electricity imported (in this case at short- and long-term) were accounted in calculation of the CO_2 emissions captured.

Table 2-2: CO_2 capture rate, equivalent energy consumption and cost of CO_2 avoided for post- and pre-combustion

		Post-combustion		Pre-combustion
		Short-term	**Long-term**	**Short-term**
Refineries	CO_2 capture rate [%]	86–85	89–79	82–72
	Equivalent energy consumption [MJ_{th}/kg_{CO_2}]	3.4–4.0	2.6–3.3	1.1–1.2
	Cost of CO_2 avoided [€/t_{CO_2}]	78.3–82.4	71.1	89.6–92.7
Chemical Plants	CO_2 capture rate [%]	80–84	80–88	100
	Equivalent energy consumption [MJ_{th}/kg_{CO_2}]	4.7–4.0	3.3–2.1	1.1
	Cost of CO_2 avoided [€/t_{CO_2}]	94.8–120.5	83.5–98.9	117.5–172.1
Steam Reforming H_2 plant	CO_2 capture rate [%]	80	89	56
	Equivalent energy consumption [MJ_{th}/kg_{CO_2}]	5.8	4.8	3.1
	Cost of CO_2 avoided [€/t_{CO_2}]	117.5	101.0	62.8

Post-combustion amine scrubbing (a mixture of MDEA and piperazine) was also considered by Fernández-Dacosta et al. (2017) to assess the techno-economic feasibility of CO_2 capture (with an efficiency of 95%) from an H_2 plant in a refinery. They evaluated two scenarios, CCS and CCUS. In the latter, 10% of the CO_2 captured was used for polyol production. Unlike in previous studies that the CO_2 avoided cost was estimated, these authors determined the break-even CO_2 cost, 49.2 €/t_{CO_2}, which accounts for the CO_2 captured instead of avoided. This figure means that implementation of CCS would be economically more attractive than without CO_2 capture. Regarding CCUS, they concluded that could be a feasible option since part of CO_2 is replacing an expensive feedstock. The equivalent energy consumption was around 4.1 MJ_{th}/kg_{CO_2} for both cases, which is comparable with the values reported by other authors.

2.3.4.2 Oxy-fuel combustion

As mentioned before, Berghout, van den Broek and Faaij (2013) have compared different CO_2 capture technologies in five plants in a long- (2040–2050) and short-

(2020–2025) term analysis. In the case of oxy-fuel combustion, this study assessed the performance of CO_2 capture retrofit to two refineries and two chemical plants. The oxy-fuel combustion was applied to the boilers, furnaces and catalytic cracker. The techno-economic performance in a short- and long-term analysis is present in Table 2-3. Although the oxy-fuel combustion presented the highest consumption of electricity, due mainly to the ASU, this technology presented the lowest cost in the refineries and chemical plants. Namely, the cost of CO_2 avoided was 24.7–58.7 €/t_{CO_2} and 38.1–127.8 €/t_{CO_2}, respectively. The equivalent energy consumption was shown to range between 1.9 MJ_{th}/kg_{CO_2} (long-term) and 2.8 MJ_{th}/kg_{CO_2} (short-term) for the refineries, with a CO_2 capture rate between 65% and 76%. For the chemical plants, the energy consumption was higher in the range 2.7–3.9 MJ_{th}/kg_{CO_2} (short-term) and 2.2–5.2 MJ_{th}/kg_{CO_2} (long-term), but higher CO_2 capture rates were achieved (88–100%).

Table 2-3: CO_2 capture rate, equivalent energy consumption and cost of CO_2 avoided for oxy-fuel combustion

		Short-term	Long-term
Refineries	CO_2 capture rate [%]	65–73	70–76
	Equivalent energy consumption [MJ_{th}/kg_{CO_2}]	2.6–2.8	1.9–2.2
	Cost of CO_2 avoided [€/t_{CO_2}]	53.6–58.7	24.7–31.9
Chemical Plants	CO_2 capture rate [%]	100–95	100–88
	Equivalent energy consumption [MJ_{th}/kg_{CO_2}]	2.7–3.9	2.2–5.2
	Cost of CO_2 avoided [€/t_{CO_2}]	82.4–127.8	38.1–74.2

2.3.4.3 Discussion

Unlike the two previous EIIs, in the last decade, very few techno-economic data have been published in the literature for the petroleum refining industry. To date, amine scrubbing was the most studied technology, while solid looping technology has not been widely considered for this industry. Only one paper was found in the literature (Morin and Béal, 2005), dated for more than one decade and then not reviewed in this study. CLC was the technology studied in the referred paper

and no data about CaL was found. Regarding the economic feasibility, oxy-fuel combustion seems to be the least expensive technology with a mean CO_2 avoided cost of around 80.6 €/t_{CO_2} against 102.4 €/t_{CO_2} for amine scrubbing, Figure 2-10. It should be noted that only the results of one source, for oxy-fuel combustion, is represented in this figure. Once again, some discrepancies are visible in the CO_2 avoided costs, which is strongly dependent on the volume of gas to be treated and CO_2 concentration. This is particularly important in this industry due to its heterogeneity and numerous points of CO_2 emissions. Although the oxy-fuel combustion presents the lowest mean cost, as well as the lowest equivalent energy consumption (3.0 MJ_{th}/kg_{CO_2} against 3.2 MJ_{th}/kg_{CO_2} for amine scrubbing), the implementation of this technology can be limited to individual sources of CO_2. On the contrary, deployment of the amine scrubbing, as an end-pipe technology, can be retrofitted to capture the CO_2 from combining streams. It is worthwhile to mention that the mean equivalent energy consumption for amine scrubbing is very similar to oxy-fuel combustion because the pre-combustion was shown to offer better opportunities for heat integration.

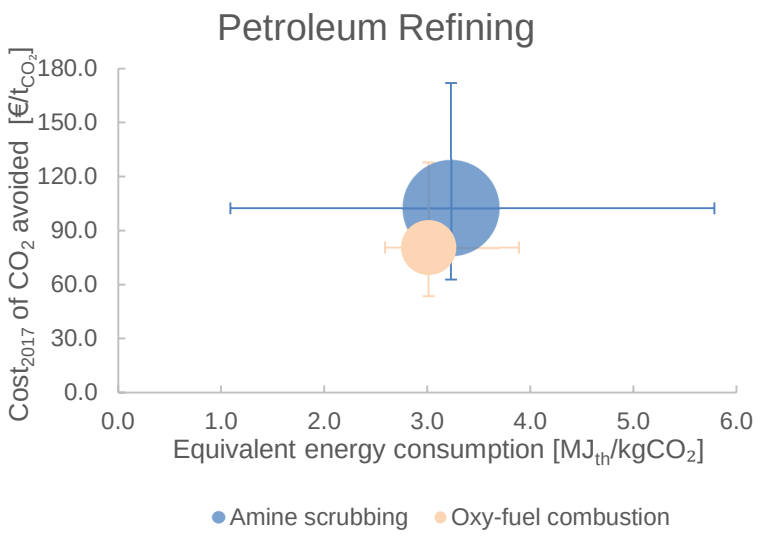

Figure 2-10: Techno-economic performance of different CO_2 capture technologies for decarbonisation of petroleum refining industry: equivalent energy consumption vs mean CO_2 avoided cost. (Error bars represent the range of figures found in the literature. The area of the bubble is proportional to the number of works reviewed.)

2.3.5 Pulp and paper industry overview

The pulp and paper industry is the 4th energy-intensive industry, being responsible for 2% of the global industry emissions in 2018 (IEA, 2020a). These CO_2 emissions are released along the process, and for the extraction, manufacturing and transport of raw materials (Möllersten, Yan and Westermark, 2003). Although the CO_2 emissions depend on the operation conditions, the recovery boiler is the major contributor to the CO_2 released in the pulp and paper plants. The CO_2 produced in the recovery boiler during the black liquor combustion accounts for up to 75% of the total CO_2 emissions (Garðarsdóttir et al., 2018). The power boiler, whose purpose, along with the recovery boiler, is to meet the heat and power requirements of the plant, is another source of CO_2 emissions. The remaining CO_2 emissions are released during the calcination of lime mud and the combustion of fuel, usually of fossil origin, in the lime kiln. The highest concentration of CO_2 occurs in the flue gas produced in the lime kiln, around 20%$_{vol}$, while the recovery and power boiler generates lower CO_2 purity streams, 13%$_{vol}$ and 12%$_{vol}$, respectively (Nwaoha and Tontiwachwuthikul, 2019; Onarheim et al., 2017a; Santos, Manovic and Hanak, 2021).

Although paper and paperboard production has increased by more than 25% in the last two decades, energy consumption has seen a rise of only 6%. This can be explained by the fact that more recycled paper has been produced (IEA, 2020c). However, in order to achieve deep decarbonisation, CCS has been appointed as a path to follow in this industry (Gerres et al., 2019). The simplified process of a pulp and paper plant is represented in Figure 2-11.

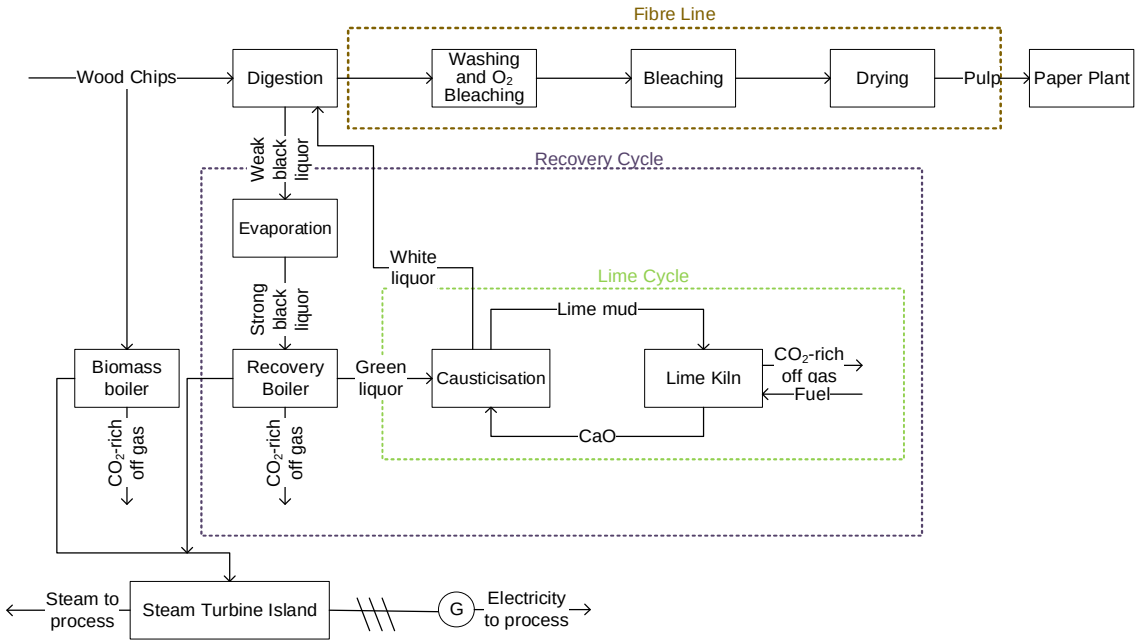

Figure 2-11: Block flow diagram of a pulp and paper plant

2.3.5.1 Chemical absorption (post-combustion amine scrubbing)

In the last decade, amine scrubbing has been the focus of attention in 85% of the studies carried out about CCS retrofitted to pulp and paper plants.

Hektor and Berntsson (2009) evaluated the techno-economic feasibility of CO_2 capture from the flue gases in the recovery boiler by amine scrubbing (MEA), with a CO_2 capture rate of 90%. This study was performed for a pulp plant and for an integrated pulp and paper plant. Since this technology demands steam for the solvent regeneration, five different configurations have been assessed to satisfy this additional steam requirement: 1) upgrade of biofuel boiler, 2) implementation of a natural gas combined cycle (NGCC) to replace the biofuel boiler; 3) recovery of low-grade heat available by a heat pump and 4) thermal process integration with a larger biofuel boiler or 5) with NGCC. They concluded that for the integrated pulp and paper plant, NGCC and the process integration with NGCC alternatives were the best options in terms of thermodynamic performance, as these resulted in an energy surplus. It should be noted that the reference plant was an electricity importer. These two options have an equivalent energy consumption of -0.9 MJ_{th}/kg_{CO_2} and -0.8 MJ_{th}/kg_{CO_2}, respectively. The negative

sign means the CO_2 capture does not represent an energy penalty for the plant because the CO_2 capture was associated with an improvement of the process (implementation of NGCC). The remaining options required additional electricity importation, which translated into an equivalent energy consumption between 2.4 and 3.4 MJ_{th}/kg_{CO_2}. Under different energy market scenarios, they concluded that to capture 90% of CO_2 emissions, the CO_2 avoided cost ranged between 32.9 €/t_{CO_2} and 57.9 €/t_{CO_2} for the pulp plant and between 22.7 €/t_{CO_2} and 75.0 €/t_{CO_2} for the integrated pulp and paper plant, for a future scenario in 2020. These costs are only valid for transportation until 500 km. It is noteworthy that the costs were estimated based on the CO_2 allowance price of 27 €/t_{CO_2} and 43 €/t_{CO_2} that reflect the current trends in CO_2 pricing.

Application of amine scrubbing, Fluor Corporation's Econamine FG Plus®, into a primary recovery boiler was also assessed by McGrail et al. (2012). As mentioned previously, this technology requires additional steam, which the authors fulfilled with a larger biomass boiler, integrated in the power island ($37MW_{el}$), that replaced the existing natural gas and hog boilers. This boiler meets the steam requirements for both the paper and CCS plants, whereas producing enough steam to ensure an electricity surplus. This new design would permit to work without CO_2 capture and thus the additional steam used to produce more electricity. Comparing the new plant with and without CO_2 capture, the equivalent energy consumption was 2.2 MJ_{th}/kg_{CO_2}. They estimated a CO_2 avoided cost of around 52.5 €/t_{CO_2}, in the same order of magnitude as the previous work, but only 62% of CO_2 is captured.

A detailed evaluation of amine scrubbing (MEA), retrofitted to a pulp plant and integrated pulp and paper plant, was carried out by Onarheim et al. (2017a). They assessed different six CO_2 capture configurations, CO_2 capture from 1) recovery boiler, 2) power boiler, 3) lime kiln and stream combinations from 4) recovery and power boilers, 5) recovery boiler plus lime kiln and 6) recovery and power boilers plus lime kiln, which corresponded to an overall CO_2 capture rate between 9.1% (configuration 3 in both cases) and 90% (configuration 6 in the pulp plant). They found that the excess energy of the standalone pulp plant was enough for the

CCS unit. However, in the integrated pulp and paper plant, this did not meet the energy requirements for configurations 1 and 4–6. Depending on the capture level, the equivalent energy consumption was within the range 2.0–3.0 MJ_{th}/kg_{CO_2} for the pulp plant. On the other hand, the integrated pulp and paper plant has shown an equivalent energy consumption between 2.2 MJ_{th}/kg_{CO_2} and 5.4 MJ_{th}/kg_{CO_2}. Similarly, to the study of Hektor and Berntsson (2009) the cost associated with the integrated pulp and paper plant was higher than for a standalone pulp plant. The cost of CO_2 avoided, assessed under various market scenarios, was in the range of 72.4–90.7 €/t_{CO_2} for the first one, while the second plant presented costs comprised between 53.0 €/t_{CO_2} and 67.3 €/t_{CO_2}. These figures are valid for an overall CO_2 capture rate between 60% and 90%.

Garðarsdóttir et al. (2018) have assessed the cost associated with CO_2 capture, amine scrubbing (MEA), in a pulp and paper plant in Sweden. They found that, for a CO_2 capture rate of 90%, the cost of CO_2 capture was 63.0 €/t_{CO_2}, which had slightly favoured affected by an increase in CO_2 concentration. This translated into an equivalent energy requirement of 5.0 MJ_{th}/kg_{CO_2}, which is in agreement with the results obtained by Onarheim et al. (2017a). Note that these figures correspond only to the capture of CO_2 from the flue gases produced by the recovery boiler, with a CO_2 concentration of 13%$_{vol}$.

Amine scrubbing was also studied by Nwaoha and Tontiwachwuthikul (2019), which proposed the use of 2-amino-2-methyl-1-propanol blend with a conventional MEA to capture the flue gas from recovery boiler, lime kiln and power boiler. Although it was not possible to estimate the equivalent energy consumption, this would be lower for the cases where the 2-amino-2-methyl-1-propanol blend with a conventional MEA is used, once its regeneration duty (3.2–4.7 MJ_{th}/kg_{CO_2}) is lower than MEA (4.2–5.2 MJ_{th}/kg_{CO_2}). They have compared the performance of the blend with the one by a single MEA under different configurations. They found that the cost of CO_2 captured was lower for the cases which in the 2-amino-2-methyl-1-propanol blend with a conventional MEA was used (108.0–110.5 €/t_{CO_2}), compared to 115.1–123.3 €/t_{CO_2} (MEA). They have

also concluded that the costs of CO_2 captured could be reduced with new 2-amino-2-methyl-1-propanol-based amine blends and the process configurations proposed in this study.

2.3.5.2 Solid looping cycles (Calcium looping)

The CaL retrofit to a pulp and paper plant was proposed for the first time by Santos, Manovic and Hanak (2021). The inherent decarbonisation of the Kraft process, by integration of CaL in the existing lime cycle, was techno-economically assessed for different design configurations and under market scenarios. They found that an integrated pulp and paper plant could turn from an electricity importer to an electricity exporter. The equivalent energy consumption estimated was 3.7 MJ_{th}/kg_{CO_2}. This study showed that the CaL performance is superior to post-combustion amine scrubbing, once the retrofit of latter to pulp and paper plant in general translated in a decrease of net power production if the retrofit of CCS to the plant is not linked to any process improvement. Furthermore, in some cases, the implementation of an auxiliary boiler is necessary to meet the energy requirement. The CO_2 avoided cost to capture 90% of the CO_2 emitted by the plant, was 39.0 €/t_{CO_2}, under the baseline scenario.

2.3.5.3 Discussion

From the four EIIs, the pulp and paper industry has been the one with less attention being paid by the researchers. As a result, the techno-economic data of CO_2 capture retrofitted to this industry is scarce. Only two technologies, amine scrubbing and CaL, were assessed to date. Figure 2-12 shows the equivalent energy consumption versus the cost of CO_2 avoided. However, to ensure a fair comparison, only the data for integrated pulp and paper plants are represented. CaL presented the lowest mean avoided cost (39.0 €/t_{CO_2}) against amine scrubbing (62.7 €/t_{CO_2}). This can be explained by the reduction of material costs, as part of fresh limestone is replaced by lime mud from the Kraft process, and the plant achieves an additional revenue from sales of the electricity exported to the grid. While the equivalent energy consumption is similar for both technologies (2.9 MJ_{th}/kg_{CO_2}against 3.7 MJ_{th}/kg_{CO_2} for amine scrubbing and CaL,

respectively), CaL presents a clear advantage to amine scrubbing. Since the CaL temperatures (600–900 °C) are higher than amine scrubbing (40–50 °C), there is a higher heat recovery potential. This was confirmed by Santos, Manovic and Hanak (2021), who showed that an importer pulp and paper industry could turn into an electricity exporter by integration of CaL in the lime cycle. As can be seen in Figure 2-12, the range of equivalent energy consumption for amine scrubbing is high due to the different configurations assumed to deliver the additional energy requirement by the CCS plant. The cases that consider the upgrade of the reference plant present the lowest equivalent energy requirement, with the cases with NGCC implementation showing values below zero since the efficiency of the process is enhanced.

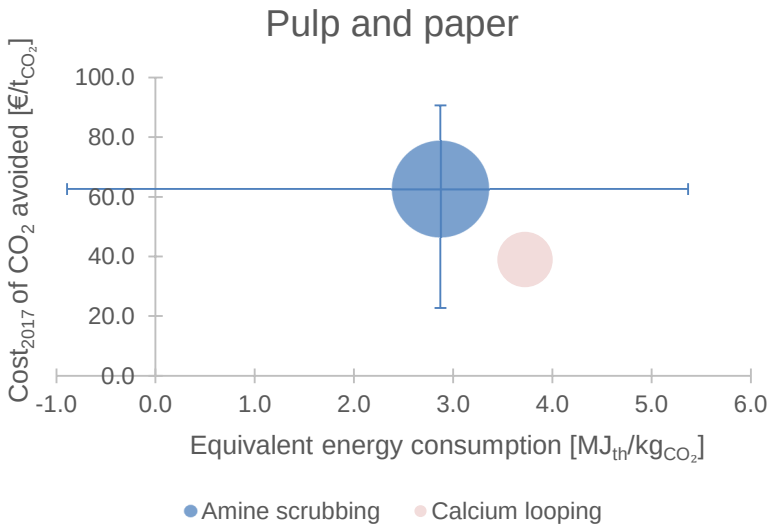

Figure 2-12: Techno-economic performance of different CO_2 capture technologies for decarbonisation of pulp and paper industry: equivalent energy consumption vs mean CO_2 avoided cost. (Error bars represent the range of figures found in the literature. The bubble without error bars has only one source. The area of the bubble is proportional to the number of works reviewed.)

2.4 Perspective for decarbonisation of energy-intensive industries

As can be seen in Figure 2-13, the current literature shows a substantial uncertainty in the estimates of the cost of CO_2 avoided for CCS. The most mature technology, amine scrubbing, is also the technology that presents higher costs

associated with the highest uncertainty. The cost of CO_2 avoided varies between 22.7 €/t_{CO_2} (pulp and paper) and 205.8 €/t_{CO_2} (iron and steel). Although there is limited evidence in the current literature, these costs could be reduced by using phase-change amines. These are promising amines as their regeneration heat requirement has been shown to be lower than that for conventional amines. On the other hand, the costs associated with CO_2 capture using CaL were shown to be one of the lowest for the three industries analysed (iron and steel, cement and pulp and paper). It is noteworthy to mention that these figures are based on studies considering natural CaO-based sorbents. These sorbents are characterised with lower sorbent cost but have a high rate of degradation compared to synthetic sorbents. The consideration of synthetic sorbents with higher sorption capacity would overcome this drawback, but at the expense of higher sorbent costs. The CO_2 avoided cost varied between 12.0 €/t_{CO_2} and 73.5 €/$t_{CO_2}$for cement and iron and steel industries, respectively. In the pulp and paper industry, the cost falls within this range. Nevertheless, it should be noted the economic feasibility evaluation is very limited for the iron and steel industry and the pulp and paper industry, with only one economic assessment published to date for the latter one. Besides, because there is no standardised methodology for techno-economic assessment, a transparent and fair comparison of the different technologies for decarbonisation of EIIs is challenging. It is, therefore, crucial to standardise the assumptions and assessment frameworks for techno-economic assessment, as well as, to systematically assess the uncertainty in techno-economic performance *via* stochastic modelling. Such an approach would account for the uncertainty associated with the technology operating conditions and the market conditions. There is some evidence in the current literature indicating that these challenges are gradually being addressed. Garcia and Berghout (2019) have proposed a cost method to assess the CCS costs in the cement and iron and steel industries, which could be extended to the other two EIIs. More recently, Roussanaly et al. (2021) have proposed some recommendations that should be taken into consideration for a fair comparison between economic studies. These guidelines can be applied to different industries. It is also important to emphasise that beyond the standardised techno-

economic assessments, it is crucial to assess the impact of the integration of CO_2 capture technology in the industrial process on product quality. This is especially important when the CO_2 capture technology requires modification of the original process, such as in the case of oxy-combustion and CaL retrofits.

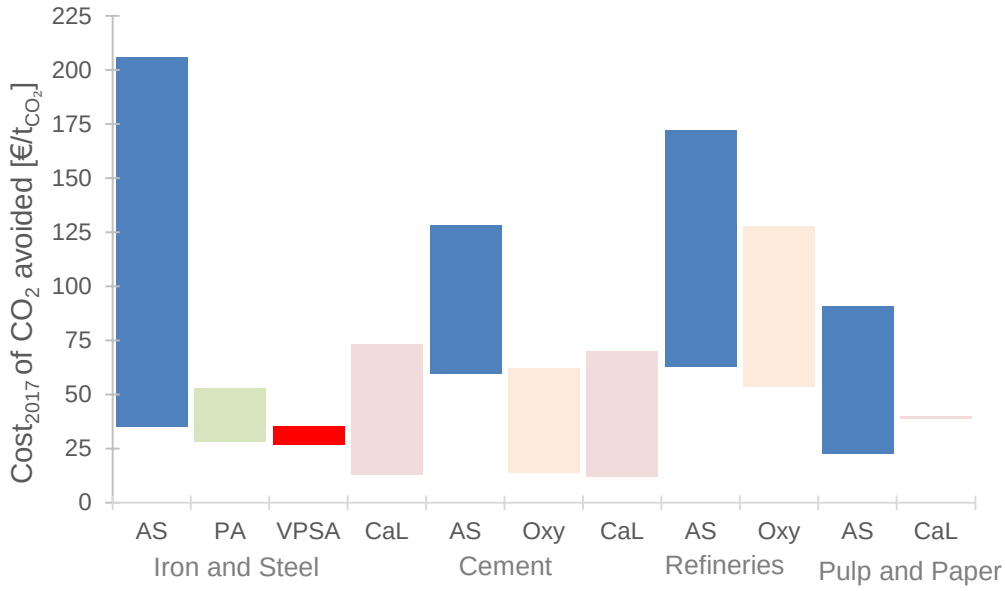

Figure 2-13: Cost of CO_2 avoided of each technology for Energy Intensive Industries. AS: amine scrubbing; PA: physical absorption; VPSA: vacuum pressure swing adsorption; CaL: calcium looping; Oxy: oxy-fuel combustion

2.5 Conclusions

This work presented a review of the state-of-the-art in CCS technology for decarbonisation of the main four EIIs, including iron and steel, cement, petroleum refining and pulp and paper industries. Only the papers published in the academic literature in the last decade were reviewed.

CCS is a feasible option for the decarbonisation of the four EIIs analysed, presenting costs as low as 12.0 €/t_{CO_2} (CaL retrofitted to cement industry) and 205.8 €/t_{CO_2} for amine scrubbing implementation in the iron and steel industry. A direct comparison between CO_2 capture technologies is difficult to be done since there is no methodology and assumptions standardisation, which has an impact in the techno-economic performance. Regarding the economic analysis, while

some authors estimated the cost accounting for the CO_2 avoided, others considered the cost of CO_2 captured. Furthermore, the costs of CO_2 transport and storage, in some studies, are also neglected. Besides, the estimation of the specific energy consumption of each technology is a tough task because, in some studies, it is not clear what is taken into account as the power consumption required for CO_2 compression. Therefore, a wide range in the thermodynamic and economic analysis was observed and the identification of the best CO_2 capture technology is challenging. Thus, these observed discrepancies cause some uncertainty and, therefore, a delay in the technology deployment at a commercial scale.

The review of the current literature has indicated that, to date, there is no dominant CO_2 capture technology. However, high-temperature solid looping cycles seem to be an emerging technology with the potential to be implemented across the EIIs studied, excluding petroleum refining due to lack of data. Importantly, one of the main drawbacks of amine scrubbing, which is the high-heat requirement for solvent regeneration, could be overcome by new amines and new configurations. However, as this technology operates at lower temperatures than solid looping cycles, the heat recovery potential is significantly diminished, resulting in lower overall process efficiency. Furthermore, some authors showed that CaL can also be integrated into iron and steel, cement and pulp and paper, using the inherent potential of the process for CO_2 capture. Since the limestone used as a sorbent in CaL is partial or totally integrated in the industrial process, there is a reduction in the material cost too. Further work should focus on standardising the techno-economic assessment of technologies for industrial decarbonisation to support industry and policy decision makers in deriving reliable decarbonisation pathways.

2.6 References

Abanades, J.C., Murillo, R., Fernandez, J.R., Grasa, G. and Martínez, I. (2010) 'New CO_2 Capture Process for Hydrogen Production Combining Ca and Cu Chemical Loops', *Environmental Science & Technology*, 44(17), pp. 6901–6904.

Abdulally, I., Beal, C., Andrus, H.E., Epple, B., Lyngfelt, A. and White, B. (2014)

‘Alstom’s Chemical Looping Technology, Program Update.’, *In 11th Annual Conference on Carbon Capture Utilization & Sequestration Pittsburgh*. Pittsburgh, Pennsylvania.

Adánez, J., Abad, A., Mendiara, T., Gayán, P., de Diego, L.F. and García-Labiano, F. (2018) ‘Chemical looping combustion of solid fuels’, *Progress in Energy and Combustion Science*, 65, pp. 6–66.

Anthony, E.J. (2008) ‘Solid Looping Cycles: A New Technology for Coal Conversion’, *Industrial & Engineering Chemistry Research*, 47, pp. 1747–1754.

Arasto, A., Tsupari, E., Kärki, J., Pisilä, E. and Sorsamäki, L. (2013) ‘Post-combustion capture of CO_2 at an integrated steel mill – Part I: Technical concept analysis’, *International Journal of Greenhouse Gas Control*, 16, pp. 271–277.

Arias, B., Diego, M.E., Abanades, J.C., Lorenzo, M., Diaz, L., Martínez, D., Alvarez, J. and Sánchez-Biezma, A. (2013) ‘Demonstration of steady state CO_2 capture in a 1.7MW_{th} calcium looping pilot’, *International Journal of Greenhouse Gas Control*, 18, pp. 237–245.

Atsonios, K., Grammelis, P., Antiohos, S.K., Nikolopoulos, N. and Kakaras, E. (2015) ‘Integration of calcium looping technology in existing cement plant for CO_2 capture: Process modeling and technical considerations’, *Fuel*, 153, pp. 210–223.

Bains, P., Psarras, P. and Wilcox, J. (2017) ‘CO_2 capture from the industry sector’, *Progress in Energy and Combustion Science*, 63, pp. 146–172.

Baker, E.H. (1962) ‘87. The calcium oxide–carbon dioxide system in the pressure range 1—300 atmospheres’, *Journal of the Chemical Society*, , pp. 464–470.

Baker, R.W., Freeman, B., Kniep, J., Huang, Y.I. and Merkel, T.C. (2018) ‘CO_2 Capture from Cement Plants and Steel Mills Using Membranes’, *Industrial & Engineering Chemistry Research*, 57(47), pp. 15963–15970.

Barker, D.J., Turner, S.A., Napier-Moore, P.A., Clark, M. and Davison, J.E. (2009) ‘CO_2 Capture in the Cement Industry’, *Energy Procedia*, 1(1), pp. 87–94.

Bataille, C. (2019) ‘Low and zero emissions in the steel and cement industries Barriers, technologies and policies’, *Organisation for Economic Co-operation and Development OECD*, , pp. 2–42.

Bataille, C., Åhman, M., Neuhoff, K., Nilsson, L.J., Fischedick, M., Lechtenböhmer, S., Solano-Rodriquez, B., Denis-Ryan, A., Stiebert, S., Waisman, H., Sartor, O. and Rahbar, S. (2018) ‘A review of technology and policy deep decarbonization pathway options for making energy-intensive industry production consistent with the Paris Agreement’, *Journal of Cleaner Production*, 187, pp. 960–973.

Bender, M., Roussiere, T., Schelling, H., Schuster, S. and Schwab, E. (2018) ‘Coupled Production of Steel and Chemicals’, *Chemie-Ingenieur-Technik*, 90(11), pp. 1782–1805.

Berdugo Vilches, T., Lind, F., Rydén, M. and Thunman, H. (2017) ‘Experience of more than 1000 h of operation with oxygen carriers and solid biomass at large scale’, *Applied Energy*, 190, pp. 1174–1183.

Berghout, N., van den Broek, M. and Faaij, A. (2013) ‘Techno-economic performance and challenges of applying CO_2 capture in the industry: A case study of five industrial plants’, *International Journal of Greenhouse Gas Control*, 17, pp. 259–279.

Blamey, J., Anthony, E.J., Wang, J. and Fennell, P.S. (2010) ‘The calcium looping cycle for large-scale CO_2 capture’, *Progress in Energy and Combustion Science*, 36(2), pp. 260–279.

Borgwardt, R.H. (1989) ‘Sintering of nascent calcium oxide’, *Chemical Engineering Science*, 44, pp. 53–60.

Bottoms, R. (1930) *Process For Separating Acidic Gases*.

Carrasco-Maldonado, F., Spörl, R., Fleiger, K., Hoenig, V., Maier, J. and Scheffknecht, G. (2016) ‘Oxy-fuel combustion technology for cement production - State of the art research and technology development’, *International Journal of Greenhouse Gas Control*, 45, pp. 189–199.

Chang, M.-H., Chen, W.-C., Huang, C.-M., Liu, W.-H., Chou, Y.-C., Chang, W.-C., Chen, W., Cheng, J.-Y., Huang, K.-E. and Hsu, H.-W. (2014) 'Design and Experimental Testing of a 1.9MW_{th} Calcium Looping Pilot Plant', *Energy Procedia*, 63, pp. 2100–2108.

Cormos, A.-M., Dragan, S., Petrescu, L., Sandu, V. and Cormos, C.-C. (2020) 'Techno-Economic and Environmental Evaluations of Decarbonized Fossil-Intensive Industrial Processes by Reactive Absorption & Adsorption CO_2 Capture Systems', *Energies*, 13(5), p. 1268.

Croezen, H. and Korteland, M. (2010) *Technological developments in Europe. A long-term view of CO_2 efficient manufacturing in the European region*. Delft.

Cuenca, M.A. and Anthony, E.J. (1995) *Pressurized Fluidized Bed Combustion of Coal.*First edit.Springer Science+Business Media Dordrecht (ed.) Chapman & Hall.

Damen, K., Troost, M. Van, Faaij, A. and Turkenburg, W. (2006) 'A comparison of electricity and hydrogen production systems with CO_2 capture and storage. Part A: Review and selection of promising conversion and capture technologies', *Progress in Energy and Combustion Science*, 32(2), pp. 215–246.

Darmawan, A., Ajiwibowo, M.W., Biddinika, M.K., Tokimatsu, K. and Aziz, M. (2019) 'Black liquor-based hydrogen and power co-production: Combination of supercritical water gasification and syngas chemical looping', *Applied Energy*, 252, p. 113446.

Darmawan, A., Ajiwibowo, M.W., Yoshikawa, K., Aziz, M. and Tokimatsu, K. (2018) 'Energy-efficient recovery of black liquor through gasification and syngas chemical looping', *Applied Energy*, 219, pp. 290–298.

Dean, C.C., Blamey, J., Florin, N.H., Al-Jeboori, M.J. and Fennell, P.S. (2011) 'The calcium looping cycle for CO_2 capture from power generation, cement manufacture and hydrogen production', *Chemical Engineering Research and Design*, 89(6), pp. 836–855.

de Diego, L.F., García-Labiano, F., Gayán, P., Celaya, J., Palacios, J.M. and

Adánez, J. (2007) ‘Operation of a 10 kW_{th} chemical-looping combustor during 200 h with a CuO-Al_2O_3 oxygen carrier’, *Fuel*, 86, pp. 1036–1045.

Diego, M.E., Arias, B. and Abanades, J.C. (2016) ‘Analysis of a double calcium loop process configuration for CO_2 capture in cement plants’, *Journal of Cleaner Production*, 117, pp. 110–121.

Dieter, H., Bidwe, A.R., Varela-Duelli, G., Charitos, A., Hawthorne, C. and Scheffknecht, G. (2014) ‘Development of the calcium looping CO_2 capture technology from lab to pilot scale at IFK, University of Stuttgart’, *Fuel*, 127, pp. 23–37.

Dreillard, M., Broutin, P., Briot, P., Huard, T. and Lettat, A. (2017) ‘Application of the DMXTM CO_2 Capture Process in Steel Industry’, *Energy Procedia*, 114, pp. 2573–2589.

ECRA (2012) *Report on Phase III. ECRA CCS Project.* Düsseldorf, Germany: European Cement Research Academy.

Erans, M., Beisheim, T., Manovic, V., Jeremias, M., Patchigolla, K., Dieter, H., Duan, L. and Anthony, E.J. (2016) ‘Effect of SO_2 and steam on CO_2 capture performance of biomass-templated calcium aluminate pellets’, *Faraday Discussions*, 192, pp. 97–111.

Eurofer: The European Steel Association (2013) *A Steel Roadmap For A Low Carbon Europe 2050*.

Farla, J.C.M., Hendriks, C.A. and Blok, K. (1995) ‘Carbon dioxide recovery from industrial processes’, *Climatic Change*, 29(4), pp. 439–461.

Favier, A., Scrivener, K. and Habert, G. (2019) ‘Decarbonizing the cement and concrete sector: integration of the full value chain to reach net zero emissions in Europe’, *IOP Conference Series: Earth and Environmental Science*, 225(1), p. 012009.

Fennell, P.S., Florin, N., Napp, T. and Hills, T. (2012) ‘CCS from industrial sources’, *Sustainable Technologies, Systems & Policies*, (CCS Workshop), p. 17.

Fernández-Dacosta, C., van der Spek, M., Hung, C.R., Oregionni, G.D., Skagestad, R., Parihar, P., Gokak, D.T., Strømman, A.H. and Ramirez, A. (2017) 'Prospective techno-economic and environmental assessment of carbon capture at a refinery and CO_2 utilisation in polyol synthesis', *Journal of CO_2 Utilization*, 21, pp. 405–422.

Fernández, J.R., Martínez, I., Abanades, J.C. and Romano, M.C. (2017) 'Conceptual design of a Ca–Cu chemical looping process for hydrogen production in integrated steelworks', *International Journal of Hydrogen Energy*, 42(16), pp. 11023–11037.

Fernández, J.R., Spallina, V. and Abanades, J.C. (2020) 'Advanced Packed-Bed Ca-Cu Looping Process for the CO_2 Capture From Steel Mill Off-Gases', *Frontiers in Energy Research*, 8(146), pp. 1–13.

Feron, P.H.M. and Hendriks, C.A. (2005) 'CO_2 Capture Process Principles and Costs', *Oil & Gas Science and Technology*, 60(3), pp. 451–459.

Ferrari, M.-C., Amelio, A., Nardelli, G.M. and Costi, R. (2021) 'Assessment on the Application of Facilitated Transport Membranes in Cement Plants for CO_2 Capture', *Energies*, 14(16), p. 4772.

Garcia, M. and Berghout, N. (2019) 'Toward a common method of cost-review for carbon capture technologies in the industrial sector: cement and iron and steel plants', *International Journal of Greenhouse Gas Control*, 87, pp. 142–158.

Gardarsdottir, S., De Lena, E., Romano, M., Roussanaly, S., Voldsund, M., Pérez-Calvo, J.-F., Berstad, D., Fu, C., Anantharaman, R., Sutter, D., Gazzani, M., Mazzotti, M. and Cinti, G. (2019) 'Comparison of Technologies for CO_2 Capture from Cement Production—Part 2: Cost Analysis', *Energies*, 12, p. 542.

Garðarsdóttir, S.Ó., Normann, F., Skagestad, R. and Johnsson, F. (2018) 'Investment costs and CO_2 reduction potential of carbon capture from industrial plants – A Swedish case study', *International Journal of Greenhouse Gas Control*, 76, pp. 111–124.

Gazzani, M., Romano, M.C. and Manzolini, G. (2015) 'CO_2 capture in integrated

steelworks by commercial-ready technologies and SEWGS process', *International Journal of Greenhouse Gas Control*, 41, pp. 249–267.

Gerres, T., Chaves Ávila, J.P., Llamas, P.L. and San Román, T.G. (2019) 'A review of cross-sector decarbonisation potentials in the European energy intensive industry', *Journal of Cleaner Production*, 210, pp. 585–601.

Gomez, A., Briot, P., Raynal, L., Broutin, P., Gimenez, M., Soazic, M., Cessat, P. and Saysset, S. (2014) 'ACACIA Project – Development of a Post-Combustion CO_2 Capture Process. Case of the DMXTM Process', *Oil & Gas Science and Technology – Revue d'IFP Energies nouvelles*, 69(6), pp. 1121–1129.

Grasa, G.S. and Abanades, J.C. (2006) 'CO_2 Capture Capacity of CaO in Long Series of Carbonation/Calcination Cycles', *Industrial & Engineering Chemistry Research*, 45, pp. 8846–8851.

Griffin, P.W. and Hammond, G.P. (2019) 'Industrial energy use and carbon emissions reduction in the iron and steel sector: A UK perspective', *Applied Energy*, 249, pp. 109–125.

Han, K., Ahn, C.K., Lee, M.S., Rhee, C.H., Kim, J.Y. and Chun, H.D. (2013) 'Current status and challenges of the ammonia-based CO_2 capture technologies toward commercialization', *International Journal of Greenhouse Gas Control*, 14, pp. 270–281.

Hanak, D.P., Anthony, E.J. and Manovic, V. (2015) 'A review of developments in pilot-plant testing and modelling of calcium looping process for CO_2 capture from power generation systems', *Energy & Environmental Science*, 8(8), pp. 2199–2249.

Hektor, E. and Berntsson, T. (2009) 'Reduction of greenhouse gases in integrated pulp and paper mills: Possibilities for CO_2 capture and storage', *Clean Technologies and Environmental Policy*, 11(1), pp. 59–65.

Hills, T., Florin, N. and Fennell, P.S. (2016) 'Decarbonising the cement sector: A bottom-up model for optimising carbon capture application in the UK', *Journal of Cleaner Production*, 139, pp. 1351–1361.

Hilz, J., Helbig, M., Haaf, M., Daikeler, A., Ströhle, J. and Epple, B. (2017) ‘Long-term pilot testing of the carbonate looping process in 1 MW_{th} scale’, *Fuel*, 210, pp. 892–899.

Ho, M.T., Allinson, G.W. and Wiley, D.E. (2011) ‘Comparison of MEA capture cost for low CO_2 emissions sources in Australia’, *International Journal of Greenhouse Gas Control*, 5, pp. 49–60.

Ho, M.T., Bustamante, A. and Wiley, D.E. (2013) ‘Comparison of CO_2 capture economics for iron and steel mills’, *International Journal of Greenhouse Gas Control*, 19, pp. 145–159.

Hossain, M.M. and de Lasa, H.I. (2008) ‘Chemical-looping combustion (CLC) for inherent CO_2 separations-a review’, *Chemical Engineering Science*, 63, pp. 4433–4451.

IEA (2020a) *Industry direct CO_2 emissions in the Sustainable Development Scenario, 2000-2030, IEA, Paris*. Available at: https://www.iea.org/data-and-statistics/charts/industry-direct-co2-emissions-in-the-sustainable-development-scenario-2000-2030 (Accessed: 15 June 2021).

IEA (2020b) *Iron and Steel Technology Roadmap, IEA, Paris*.

IEA (2020c) *Cement, IEA, Paris*. Available at: https://www.iea.org/reports/cement (Accessed: 29 June 2021).

IEA (2020d) *Chemicals, IEA, Paris*. Available at: https://www.iea.org/reports/chemicals (Accessed: 29 September 2021).

IEA (2020e) *Pulp and Paper, IEA, Paris*. Available at: https://www.iea.org/reports/pulp-and-paper (Accessed: 15 June 2021).

IPCC (2015) ‘Summary for Policymakers and Technical Summary’, in *Climate Change 2014 Mitigation of Climate Change*. Cambridge, United Kingdom and New York, NY, USA: Cambridge University Press, pp. 1–30.

IRENA (2014) *Renewable Energy in Manufacturing-A technology roadmap for REmap 2030*.

Johansson, D., Rootzén, J., Berntsson, T. and Johnsson, F. (2012) ‘Assessment of strategies for CO_2 abatement in the European petroleum refining industry’, *Energy*, 42(1), pp. 375–386.

Koytsoumpa, E.I., Bergins, C. and Kakaras, E. (2018) ‘The CO_2 economy: Review of CO_2 capture and reuse technologies’, *The Journal of Supercritical Fluids*, 132, pp. 3–16.

Kuramochi, T., Ramírez, A., Turkenburg, W. and Faaij, A. (2012) ‘Comparative assessment of CO_2 capture technologies for carbon-intensive industrial processes’, *Progress in Energy and Combustion Science*, 38, pp. 87–112.

Leeson, D., Mac Dowell, N., Shah, N., Petit, C. and Fennell, P.S. (2017) ‘A Techno-economic analysis and systematic review of carbon capture and storage (CCS) applied to the iron and steel, cement, oil refining and pulp and paper industries, as well as other high purity sources’, *International Journal of Greenhouse Gas Control*, 61, pp. 71–84.

De Lena, E., Spinelli, M., Gatti, M., Scaccabarozzi, R., Campanari, S., Consonni, S., Cinti, G. and Romano, M.C. (2019) ‘Techno-economic analysis of calcium looping processes for low CO_2 emission cement plants’, *International Journal of Greenhouse Gas Control*, 82, pp. 244–260.

Lyngfelt, A. and Linderholm, C. (2017) ‘Chemical-Looping Combustion of Solid Fuels – Status and Recent Progress’, *Energy Procedia*., Vol.114, pp. 371–386.

Lyon, R.K. (1984) *Method and apparatus for unmixed combustion as an alternative to fire*.

Manzolini, G., Giuffrida, A., Cobden, P.D., van Dijk, H.A.J., Ruggeri, F. and Consonni, F. (2020) ‘Techno-economic assessment of SEWGS technology when applied to integrated steel-plant for CO_2 emission mitigation’, *International Journal of Greenhouse Gas Control*, 94, p. 102935.

Markewitz, P., Kuckshinrichs, W., Leitner, W., Linssen, J., Zapp, P., Bongartz, R., Schreiber, A. and Müller, T.E. (2012) ‘Worldwide innovations in the development of carbon capture technologies and the utilization of CO_2’, *Energy and*

Environmental Science, 5, pp. 7281–7305.

Markewitz, P., Zhao, L., Ryssel, M., Moumin, G. and Wang, Y. (2019) ‘Carbon Capture for CO_2 Emission Reduction in the Cement Industry in Germany’, *Energies*, 12, p. 2432.

Martínez, I., Fernández, J.R., Abanades, J.C. and Romano, M.C. (2018) ‘Integration of a fluidised bed Ca–Cu chemical looping process in a steel mill’, *Energy*, 163, pp. 570–584.

Mattisson, T., Järdnäs, A. and Lyngfelt, A. (2003) ‘Reactivity of Some Metal Oxides Supported on Alumina with Alternating Methane and Oxygen–Application for Chemical-Looping Combustion’, *Energy & Fuels*, 17, pp. 643–651.

Mayer, K., Schanz, E., Pröll, T. and Hofbauer, H. (2018) ‘Performance of an iron based oxygen carrier in a 120 kW_{th} chemical looping combustion pilot plant’, *Fuel*, 217, pp. 561–569.

McGrail, B.P., Freeman, C.J., Brown, C.F., Sullivan, E.C., White, S.K., Reddy, S., Garber, R.D., Tobin, D., Gilmartin, J.J. and Steffensen, E.J. (2012) ‘Overcoming business model uncertainty in a carbon dioxide capture and sequestration project: Case study at the Boise White Paper Mill’, *International Journal of Greenhouse Gas Control*, 9, pp. 91–102.

Möllersten, K., Yan, J. and Westermark, M. (2003) ‘Potential and cost-effectiveness of CO_2 reductions through energy measures in Swedish pulp and paper mills’, *Energy*, 28(7), pp. 691–710.

Morin, J.-X. and Béal, C. (2005) ‘Chemical Looping Combustion of Refinery Fuel Gas with CO_2 Capture’, in D.C. Thomas and S.M. Benson (ed.) *Carbon Dioxide Capture for Storage in Deep Geologic Formations, Volume 1*. Elsevier, pp. 647–654.

Napp, T.A., Gambhir, A., Hills, T.P., Florin, N. and Fennell, P.. (2014) ‘A review of the technologies, economics and policy instruments for decarbonising energy-intensive manufacturing industries’, *Renewable and Sustainable Energy Reviews*, 30, pp. 616–640.

Nurdiawati, A. and Urban, F. (2021) ‘Towards deep decarbonisation of energy-intensive industries: A review of current status, technologies and policies’, *Energies*, 14(9), p. 2408.

Nurrokhmah, L., Mezher, T. and Abu-Zahra, M.R.M. (2013) ‘Evaluation of Handling and Reuse Approaches for the Waste Generated from MEA-based CO_2 Capture with the Consideration of Regulations in the UAE’, *Environmental Science & Technology*, 47(23), pp. 13644–13651.

Nwaoha, C. and Tontiwachwuthikul, P. (2019) ‘Carbon dioxide capture from pulp mill using 2-amino-2-methyl-1-propanol and monoethanolamine blend: Techno-economic assessment of advanced process configuration’, *Applied Energy*, 250, pp. 1202–1216.

Onarheim, K., Santos, S., Kangas, P. and Hankalin, V. (2017a) ‘Performance and cost of CCS in the pulp and paper industry part 2: Economic feasibility of amine-based post-combustion CO_2 capture’, *International Journal of Greenhouse Gas Control*, 66, pp. 60–75.

Onarheim, K., Santos, S., Kangas, P. and Hankalin, V. (2017b) ‘Performance and costs of CCS in the pulp and paper industry part 1: Performance of amine-based post-combustion CO_2 capture’, *International Journal of Greenhouse Gas Control*, 59, pp. 58–73.

Ozcan, D.C., Macchi, A., Lu, D.Y., Kierzkowska, A.M., Ahn, H., Müller, C.R. and Brandani, S. (2015) ‘Ca–Cu looping process for CO_2 capture from a power plant and its comparison with Ca-looping, oxy-combustion and amine-based CO_2 capture processes’, *International Journal of Greenhouse Gas Control*, 43, pp. 198–212.

Perejón, A., Romeo, L.M., Lara, Y., Lisbona, P., Martínez, A. and Valverde, J.M. (2016) ‘The Calcium-Looping technology for CO_2 capture: On the important roles of energy integration and sorbent behavior’, *Applied Energy*, 162, pp. 787–807.

Ramírez-Santos, Á.A., Bozorg, M., Addis, B., Piccialli, V., Castel, C. and Favre, E. (2018) ‘Optimization of multistage membrane gas separation processes.

Example of application to CO_2 capture from blast furnace gas', *Journal of Membrane Science*, 566, pp. 346–366.

Rao, A.B. and Rubin, E.S. (2002) 'A Technical , Economic , and Environmental Assessment of Amine-Based CO_2 Capture Technology for Power Plant Greenhouse Gas Control', *Environ. Sci. Technol.*, 36, pp. 4467–4475.

Rissman, J., Bataille, C., Masanet, E., Aden, N., Morrow, W.R., Zhou, N., Elliott, N., Dell, R., Heeren, N., Huckestein, B., Cresko, J., Miller, S.A., Roy, J., Fennell, P., Cremmins, B., Koch Blank, T., Hone, D., Williams, E.D., de la Rue du Can, S., Sisson, B., Williams, M., Katzenberger, J., Burtraw, D., Sethi, G., Ping, H., Danielson, D., Lu, H., Lorber, T., Dinkel, J. and Helseth, J. (2020) 'Technologies and policies to decarbonize global industry: Review and assessment of mitigation drivers through 2070', *Applied Energy*, 266, p. 114848.

Rodríguez, N., Murillo, R. and Abanades, J.C. (2012) 'CO_2 Capture from Cement Plants Using Oxyfired Precalcination and/or Calcium Looping', *Environmental Science & Technology*, 46(4), pp. 2460–2466.

Rogelj, J., Popp, A., Calvin, K. V., Luderer, G., Emmerling, J., Gernaat, D., Fujimori, S., Strefler, J., Hasegawa, T., Marangoni, G., Krey, V., Kriegler, E., Riahi, K., Van Vuuren, D.P., Doelman, J., Drouet, L., Edmonds, J., Fricko, O., Harmsen, M., Havlík, P., Humpenöder, F., Stehfest, E. and Tavoni, M. (2018) 'Scenarios towards limiting global mean temperature increase below 1.5 °C', *Nature Climate Change*, 8(4), pp. 325–332.

Rolfe, A., Huang, Y., Haaf, M., Pita, A., Rezvani, S., Dave, A. and Hewitt, N.J. (2018) 'Technical and environmental study of calcium carbonate looping versus oxy-fuel options for low CO_2 emission cement plants', *International Journal of Greenhouse Gas Control*, 75, pp. 85–97.

Romeo, L.M., Catalina, D., Lisbona, P., Lara, Y. and Martinez, A. (2011) 'Ca looping technology : current status , developments and future directions', *Greenhouse Gas Sci Technol*, 1, pp. 72–82.

Roussanaly, S., Berghout, N., Fout, T., Garcia, M., Gardarsdottir, S., Nazir, S.M.,

Ramirez, A. and Rubin, E.S. (2021) ‘Towards improved cost evaluation of Carbon Capture and Storage from industry’, *International Journal of Greenhouse Gas Control*, 106, p. 103263.

Santos, M.P.S., Manovic, V. and Hanak, D.P. (2021) ‘Unlocking the potential of pulp and paper industry to achieve carbon-negative emissions via calcium looping retrofit’, *Journal of Cleaner Production*, 280, p. 124431.

Shao, R. and Stangeland, A. (2009) *Amines Used in CO_2 Capture - Health and Environmental Impacts*.

Shimizu, T., Hirama, T., Hosoda, H., Kitano, K., Inagaki, M. and Tejima, K. (1999) ‘A Twin Fluid-Bed Reactor for Removal of CO_2 from Combustion Processes’, *Chemical Engineering Research and Design*, 77, pp. 62–68.

Van Der Stel, J., Louwerse, G., Sert, D., Hirsch, A., Eklund, N. and Pettersson, M. (2013) ‘Top gas recycling blast furnace developments for “green” and sustainable ironmaking’, *Ironmaking and Steelmaking*, 40(7), pp. 483–489.

van Straelen, J., Geuzebroek, F., Goodchild, N., Protopapas, G. and Mahony, L. (2009) ‘CO_2 capture for refineries, a practical approach’, *Energy Procedia*, 1, pp. 179–185.

van Straelen, J., Geuzebroek, F., Goodchild, N., Protopapas, G. and Mahony, L. (2010) ‘CO_2 capture for refineries, a practical approach’, *International Journal of Greenhouse Gas Control*, 4, pp. 316–320.

Ströhle, J., Junk, M., Kremer, J., Galloy, A. and Epple, B. (2014) ‘Carbonate looping experiments in a $1MW_{th}$ pilot plant and model validation’, *Fuel*, 127, pp. 13–22.

Sun, P., Grace, J.R., Lim, C.J. and Anthony, E.J. (2007) ‘The effect of CaO sintering on cyclic CO_2 capture in energy systems’, *AIChE Journal*, 53(9), pp. 2432–2442.

Tian, S., Jiang, J., Yan, F., Li, K., Chen, X. and Manovic, V. (2016a) ‘Highly efficient CO_2 capture with simultaneous iron and CaO recycling for the iron and

steel industry', *Green Chemistry*, 18(14), pp. 4022–4031.

Tian, S., Jiang, J., Zhang, Z. and Manovic, V. (2018) 'Inherent potential of steelmaking to contribute to decarbonisation targets via industrial carbon capture and storage', *Nature Communications*, 9(1), pp. 1–8.

Tian, S., Li, K., Jiang, J., Chen, X. and Yan, F. (2016b) 'CO_2 abatement from the iron and steel industry using a combined Ca-Fe chemical loop', *Applied Energy*, 170, pp. 345–352.

Tsupari, E., Kärki, J., Arasto, A. and Pisilä, E. (2013) 'Post-combustion capture of CO_2 at an integrated steel mill – Part II: Economic feasibility', *International Journal of Greenhouse Gas Control*, 16, pp. 278–286.

Voldsund, M., Gardarsdottir, S., De Lena, E., Pérez-Calvo, J.-F., Jamali, A., Berstad, D., Fu, C., Romano, M., Roussanaly, S., Anantharaman, R., Hoppe, H., Sutter, D., Mazzotti, M., Gazzani, M., Cinti, G. and Jordal, K. (2019) 'Comparison of Technologies for CO_2 Capture from Cement Production—Part 1: Technical Evaluation', *Energies*, 12(3), p. 559.

Wang, P., Means, N., Shekhawat, D., Berry, D. and Massoudi, M. (2015) 'Chemical-looping combustion and gasification of coals and oxygen carrier development: A brief review', *Energies*, 8(10), pp. 10605–10635.

Wiley, D.E., Ho, M.T. and Bustamante, A. (2011) 'Assessment of opportunities for CO_2 capture at iron and steel mills: An Australian perspective', *Energy Procedia*, 4, pp. 2654–2661.

WorldSteel Association (2021) *About Steel*. Available at: https://www.worldsteel.org/about-steel.html (Accessed: 14 June 2021).

Xu, G., Jin, H.G., Yang, Y.P., Xu, Y.J., Lin, H. and Duan, L. (2010) 'A comprehensive techno-economic analysis method for power generation systems with CO_2 capture', *International Journal of Energy Research*, 34(4), pp. 321–332.

Yang, F., Meerman, J.C. and Faaij, A.P.C. (2021) 'Carbon capture and biomass in industry: A techno-economic analysis and comparison of negative emission

options', *Renewable and Sustainable Energy Reviews*, 144, p. 111028.

Yazdanpanah, M., Guillou, F., Bertholin, S. and Zhang, A. (2019) 'Demonstration of Chemical Looping Combustion (CLC) with Petcoke Feed for Refining Industry in a 3 MW_{th} Pilot Plant', *SSRN Electronic Journal*, 33, pp. 1–8.

Yun, S., Jang, M.-G. and Kim, J.-K. (2021) 'Techno-economic assessment and comparison of absorption and membrane CO_2 capture processes for iron and steel industry', *Energy*, 229, p. 120778.

Zafar, Q., Mattisson, T. and Gevert, B. (2005) 'Integrated Hydrogen and Power Production with CO_2 Capture Using Chemical-Looping Reforming Redox Reactivity of Particles of CuO, Mn_2O_3, NiO, and Fe_2O_3 Using SiO_2 as a Support', *Industrial & Engineering Chemistry Research*, 44, pp. 3485–3496.

Zhao, X., Zhou, H., Sikarwar, V.S., Zhao, M., Park, A.H.A., Fennell, P.S., Shen, L. and Fan, L.S. (2017) 'Biomass-based chemical looping technologies: The good, the bad and the future', *Energy and Environmental Science*, 10(9), pp. 1885–1910.

Zhou, W., Jiang, D., Chen, D., Griffy-Brown, C., Jin, Y. and Zhu, B. (2016) 'Capturing CO_2 from cement plants: A priority for reducing CO_2 emissions in China', *Energy*, 106, pp. 464–474.

3 UNLOCKING THE POTENTIAL OF PULP AND PAPER INDUSTRY TO ACHIEVE CARBON-NEGATIVE EMISSIONS *VIA* CALCIUM LOOPING RETROFIT*

Abstract

Pulp and paper is considered to be the fourth most energy-intensive industry worldwide. However, as most of the CO_2 emissions are of biomass origin, this sector has the potential to become a carbon-negative industry. This study proposes a new concept for conversion of the pulp and paper industry to carbon-negative that relies on the inherent CO_2 capture capability of the Kraft process. The techno-economic performance of the proposed carbon-negative system, based on calcium looping retrofitted to a pulp and paper plant, was evaluated. The effect of calcium looping design specifications and cost assumptions on the thermodynamic and economic performance were evaluated. Under the initial design assumptions, the reference pulp and paper plant was shown to turn from electricity importer to electricity exporter with the cost of CO_2 avoided equal to 39.0 €/t_{CO_2}. The parametric study showed that an increase in the fresh limestone make-up rate resulted in a linear increase of the specific primary energy consumption for CO_2 avoided and a reduction in the amount of electricity exported to the electric grid. This translates into an increase in the price of pulp and newsprint, and the cost of CO_2 avoided. This study has also demonstrated that the pulp and paper industry has high potential to become carbon-negative. It has been shown that carbon capture and storage would become economically viable in this industry if the negative CO_2 emissions are recognised and a negative CO_2 emissions credit of at least 41.8 €/t_{CO_2} is implemented.

Keywords: Pulp and paper, calcium looping, carbon capture, techno-economic analysis, negative CO_2 emissions credit

---

*Santos, M.P.S., Manovic, V. and Hanak, D.P. (2021) 'Unlocking the potential of pulp and paper industry to achieve carbon-negative emissions via calcium looping retrofit', *Journal of Cleaner Production*, 280, p. 124431.

3.1 Introduction

The pulp and paper industry generated 0.2 Gt of direct CO_2 emissions in 2017, accounting for 6% of industrial GHG emissions in the UK (Griffin, Hammond and Norman, 2018). It is considered as one of the main EIIs, consuming 31,659 ktoe of primary energy in 2014 (Eurostat, 2016). However, the pulp and paper industry can become carbon-negative due to the origin of its CO_2 emissions, which are mainly from biomass (Möllersten et al., 2004). This can be achieved by capturing and storing CO_2 or by using it as a raw material in other industries (Kuparinen, Vakkilainen and Tynjälä, 2019). As biomass is the primary source of energy in the pulp and paper plant, the CO_2 emissions are considered carbon neutral, assuming the biomass is sustainably sourced, and integrated in a closed carbon cycle. During plant photosynthesis, biogenic CO_2 is captured from the atmosphere. Importantly, biogenic emissions are accountable in agriculture, forestry and other land-use and not in the energy sector (IPCC, 2015). Therefore, these emissions are not currently included in the EU ETS. Consequently, there is no incentive to implement CCS technologies by this industry (Onarheim et al., 2017b).

CCS is considered as a feasible route to deep decarbonisation of EIIs (Gerres et al., 2019). The techno-economic feasibility of industrial CCS technologies has been thoroughly studied in the iron and steel (Garðarsdóttir et al., 2018; Tian et al., 2018), cement (De Lena et al., 2019; Rolfe et al., 2018) and petrochemical (Fernández-Dacosta et al., 2017; Yao et al., 2018) industries. Nevertheless, economic assessments of CCS integration to pulp and paper plants are limited Table 3-1.

Table 3-1: Literature data on economic assessments of carbon capture and storage integration to pulp and paper plants

Reference	CCS integration	CO_2 capture cost [€/t_{CO_2}]
Möllersten et al. (2006)	Pre-combustion physical absorption + CHP	18–27 €/t_{CO_2}
		43 €/t_{CO_2} (long CO_2 transport distances)
Hektor and Berntsson (2009)	Amine scrubbing + CHP	29–51 €/t_{CO_2} (pulp plant)
		20–66 €/t_{CO_2} (integrated pulp and paper plant)
McGrail et al. (2012)	Post-combustion amine scrubbing	52.5 €/t_{CO_2}
Onarheim et al. (2017a)	Post-combustion amine scrubbing	71–89 €/t_{CO_2} (integrated pulp and paper plant)
		52–66 €/t_{CO_2} (pulp plant)
Nwaoha and Tontiwachwuthikul (2019)	Post-combustion amine scrubbing	114.8–117.4 €/t_{CO_2} (AMP)
		122.5–131 €/t_{CO_2} (MEA)
Kuparinen et al. (2019)	CO_2 capture and utilisation + MEA	≤50 €/t_{CO_2}

Möllersten et al. (2006) have performed a preliminary assessment of the potential integration of pre-combustion physical absorption in both the pulp plant and integrated pulp and paper plant with CHP generation. They found that the cost of CO_2 capture and storage, if the points of capture and storage are located in the same place, is in the range of 18–27 €/t_{CO_2}. However, the CCS cost can increase to 43 €/t_{CO_2} for long transport distances (above 1000 km). Application of amine scrubbing for CO_2 capture from flue gas of the recovery boiler was assessed by Hektor and Berntsson (2009). They studied five possible configurations that combined CO_2 capture with CHP to overcome the additional steam demand. The extra energy demand was achieved by the following alternatives: upgrade biomass boiler, replace biomass boiler by NGCC, upgrade low-grade heat from the plant with a heat pump, process integration with a larger biomass boiler, or process integration combined with NGCC. Considering these scenarios, their study reported values of 29–51 €/t_{CO_2} for the pulp plant and 20–66 €/t_{CO_2} for the integrated pulp and paper plant. The techno-economic feasibility of retrofitting a pulp and paper plant with post-combustion amine scrubbing was also evaluated by McGrail et al. (2012). They have proposed replacing two existing natural gas-

fired boiler and hog boiler with a larger biomass boiler. The latter would meet the additional demand for steam of the CCS unit. They concluded that the CO_2 capture cost was around 52.5 €/t_{CO_2}. Onarheim et al. (2017a) have performed a comprehensive study to assess the techno-economic performance of retrofitting post-combustion amine scrubbing to both a pulp plant and integrated pulp and paper plant. They found that the cost associated with the integrated pulp and paper plant (71–89 €/t_{CO_2}) was higher than for a standalone pulp plant (52–66 €/t_{CO_2}) when 60–90% of the total CO_2 emissions were captured for both plants. For CO_2 capture rates below 60%, which implied only the CO_2 from the multi-fuel boiler and lime kiln flue gases was captured, these costs increased to 92 €/t_{CO_2} for the standalone pulp plant and 93 €/t_{CO_2} for the integrated pulp and paper plant. The costs associated with a retrofit of the pulp plant with post-combustion amine scrubbing were also estimated by Nwaoha and Tontiwachwuthikul (2019). They also compared the use of a conventional MEA solvent with 2-amino-2-methyl-1-propanol (AMP) solvent for different process configurations. The use of AMP-MEA resulted in lower costs, in the range of 114.8–117.4 €/t_{CO_2}, compared to 122.5–131.0 €/t_{CO_2} when MEA was used. Kuparinen et al. (2019) evaluated CO_2 capture and its potential on-site utilisation in the pulp plant and pulp and paper plant. They concluded that CO_2 capture is a feasible option for the pulp and paper industry, and estimated that the cost of CO_2 avoided can be below 50 €/t_{CO_2} if MEA was used as solvent (Kuparinen, Vakkilainen and Hamaguchi, 2017). However, such a low cost of CO_2 avoided was obtained because CO_2 was utilised on-site for production of bioproducts, such as tall oil, lignin and precipitated $CaCO_3$.

The review of the current literature has indicated that, to date, amine scrubbing was the only CCS technology considered for retrofits in pulp and paper plants. However, this technology has presented some challenges in the power industry, such as thermal degradation and adverse reactions of solvent with flue gas impurities such as NO_2, SO_2 and O_2 (Dean et al., 2011), the cost of solvent (Rao and Rubin, 2002b), solvent concentration limited to 30 $\%_{wt}$ (MEA) (Shao and Stangeland, 2009), high efficiency penalties of 9.5% to 12.5% points (Xu et al.,

2010), and high volumes of waste generated (Dean et al., 2011). Therefore, more energy efficient and less expensive capture technologies have been explored. CaL has emerged as one of the promising technologies for decarbonisation of the power and industrial sectors. Importantly, the cost of CO_2 avoided from the CaL process has been shown to be as low as 20.5 €/t_{CO_2} when implemented in the cement industry (Rodríguez, Murillo and Abanades, 2012b). This figure is one-third to one-sixth that reported for amine scrubbing retrofits in the cement industry (60.5–107 €/t_{CO_2}) (Barker et al., 2009; Ho, Allinson and Wiley, 2011). Ca-based sorbents, such as limestone (~95%$_{wt}$ $CaCO_3$), are the most considered sorbents for CaL. Importantly, $CaCO_3$ is the main compound of lime mud, a waste from the Kraft process in the pulp and paper industry. Furthermore, Sun et al. (2013) have shown that lime mud from the lime kiln can be successfully used as CO_2 adsorbent in CaL. Therefore, it is pertinent to assess the feasibility of using CaL for CO_2 capture in the pulp and paper industry.

The aim of this work is to assess the techno-economic feasibility of CaL retrofitted to a pulp and paper plant. The concept of the Kraft process with inherent CO_2 capture was proposed by integrating CaL in the existing lime cycle. In order to investigate the influence of CaL design specifications and economic assumptions on the techno-economic performance of the retrofitted process, a sensitivity analysis was carried out. The economic performance of the retrofitted pulp and paper plant was benchmarked against amine scrubbing. The impact of recognising negative CO_2 emissions on the cost of CO_2 avoided was also evaluated.

3.2 Process and model description

In this work, an integrated pulp and paper plant was selected as a reference plant, considering a process model developed in CADSIM Plus®. It was assumed that the reference plant produces 1000 ADt (air-dried tonnes, 90% dry content) of bleached pulp per day, 375 ADt/d of thermomechanical pulp and 450 ADt/d of newsprint. As some of the Kraft pulp and the thermomechanical pulp are consumed on-site, only 925 ADt/d of bleached pulp and newsprint are sold to the market.

3.2.1 Kraft process

The Kraft process involves conversion of raw wood into pulp, mainly cellulose fibres, which occurs in digesters with a solution of NaOH and Na_2S, so-called white liquor. The pulp is then separated from the solution, called black liquor, and forwarded to the fibre line. In order to recover the inorganic chemicals and produce steam for the entire process, the black liquor is burnt in a recovery boiler. This stage can generate 75% of the total CO_2 released in the plant (Garðarsdóttir et al., 2018). The molten black liquor (mainly Na_2CO_3 and Na_2S) is then dissolved in water to produce the green liquor. This solution is sent to a slaker where it is mixed with the lime (CaO) burnt in the lime kiln. At this point CaO is converted to $Ca(OH)_2$, which reacts with Na_2CO_3 to produce NaOH and $CaCO_3$. While the white liquor (mainly NaOH and Na_2S) is sent to the pulp digester to restart the cycle, the precipitated $CaCO_3$, called lime mud, is calcined in the lime kiln. Since this reaction is endothermic, the heat required to sustain it is generated by combustion of fossil fuels. The flue gas released during this step has the highest CO_2 concentration (~20%$_{vol}$), which is partially biogenic due to CO_2 formed during lime mud calcination. Importantly, the CO_2 emissions related to the calcination of the fresh limestone make-up are of fossil origin. The remaining CO_2 emissions come from the multi-fuel boiler that produces steam and/or electricity for the plant. Depending on the type of fuel used, the CO_2 emissions produced by this unit can be biogenic or of fossil origin. In that case the multi-fuel boiler refers to both the hog and power boilers. Unlike flue gas from the lime kiln, the multi-fuel and recovery boilers generate flue gas with lower CO_2 concentration (between 10–13%$_{vol}$). Table 3-2 shows the breakdown of the total CO_2 emissions produced by the pulp and paper plant. It can be observed that 4% of the total CO_2 emissions are of fossil origin and come primarily from the lime kiln. Around 34% of CO_2 from the lime kiln is of fossil origin, mostly because of the requirement for natural gas combustion, which is valid for the specific case study considered in this work. Although the main fuels are of fossil origin, methanol, tall oil, hydrogen, turpentine and strong odorous gases may also be burnt in the lime kilns (Kuparinen and Vakkilainen, 2017). Although the main fuels in the recovery and hog boilers are black liquor and wood, natural gas is also burnt during start-up. As around 96%

of the total CO_2 emissions are biogenic, this industry has high potential to become a carbon-negative industry if CCS is implemented.

Table 3-2: CO_2 emissions breakdown for the pulp and paper plant without carbon capture and storage

Parameter	Recovery boiler	Hog boiler	Power boiler	Lime kiln
Biogenic CO_2 [t/d]	2299.7	823.0	-	191.4
Fossil CO_2 [t/d]	0.2	0.2	48.1	99.1
Total CO_2 [t/d]	2299.9	823.2	48.1	290.5

The reference pulp and paper plant consists mainly of a fibre line, the recovery and lime cycles, and the biomass and power boilers used to generate steam, which is then combined with that produced by the recovery boiler and sent to the steam turbine island. Part of steam is used in the process and the remaining part is converted to electricity that is used on-site. Due to the integration of paper production, which is an energy intensive process (Kuparinen, Vakkilainen and Tynjälä, 2019; Möllersten, Gao and Yan, 2006; Onarheim et al., 2017b), the considered plant needs to import additional electricity from the electric grid. Although not depicted in the diagram (Figure 3-1), an air separation unit and a bleach chemical plant are also part of the plant to provide O_2 and ClO_2 to the fibre line. In this work, the concept of the Kraft process with inherent CO_2 capture is proposed for the integrated pulp and paper plant, as presented in the simplified block diagram in Figure 3-1. The proposed concept considers CO_2 capture by integration of CaL in the lime cycle. The existing lime kiln is replaced by a kiln of larger capacity, interconnected with the add-on carbonator, as shown in Figure 3-1. It is important to note that this is a general concept and that in a real application the process should be designed considering the causticisation requirements.

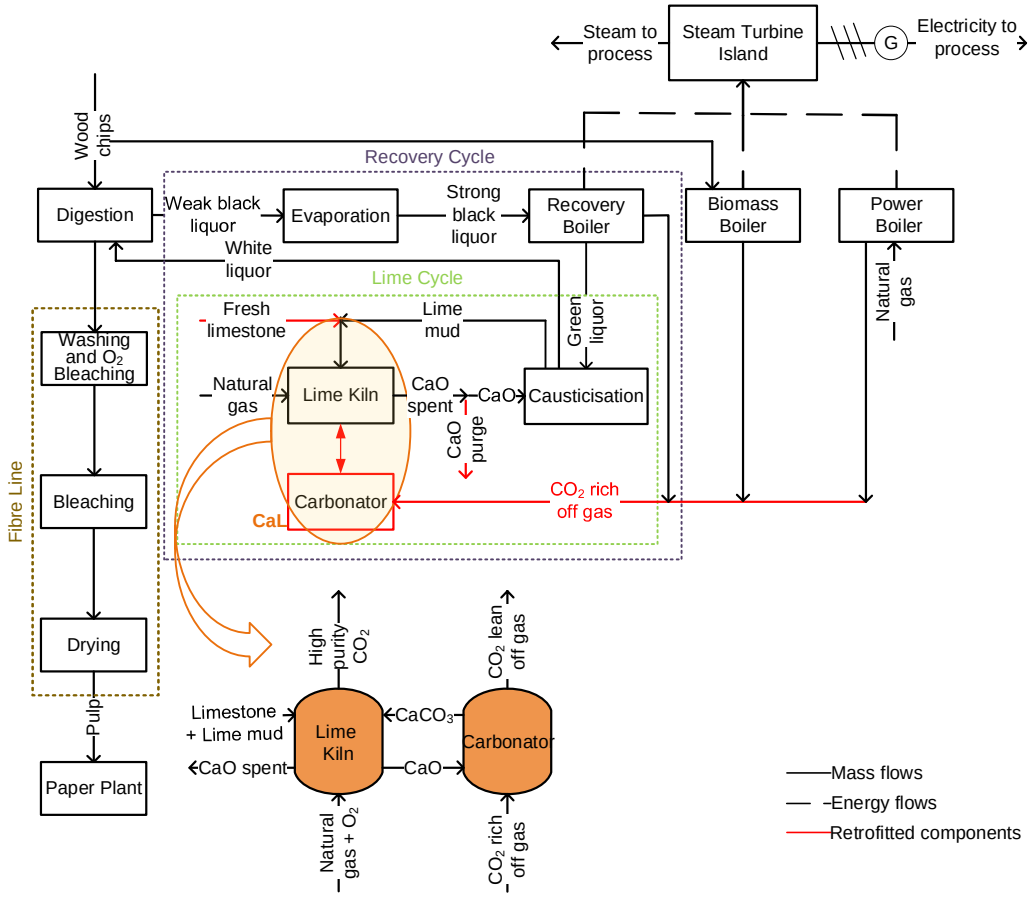

Figure 3-1: Kraft process concept with inherent CO_2 capture

3.2.2 Reference pulp and paper plant model development

The performance of the reference pulp and paper plant was assessed using existing CADSIM Plus® model. Since the lime kiln was represented as a black box in CADSIM Plus®, it was modelled in Aspen Plus® to obtain the flue gas composition. The lime kiln was represented by two Gibbs reactors connected in series, where the Gibbs free-energy minimisation model was used to predict the equilibrium composition of the gas product. Natural gas combustion with air, which occurs in the first reactor, supplies the energy to achieve the desired temperature for calcination. The fuel rate was assumed based on the specific energy requirement of 6.5 GJ/t_{CaO}, which was fixed in the CADSIM Plus® model (Schorcht et al., 2013). To ensure complete combustion of fuel, 12% excess air was assumed. In the second reactor, the lime mud is heated with the combustion gas to the calcination temperature (900 °C). The mass and energy balances of

the reference pulp and paper plant, which were used as input data to the CaL model, were validated against literature data (Table 3-3) (Nwaoha and Tontiwachwuthikul, 2019; Onarheim et al., 2017a). The results of the lime kiln modelled in Aspen Plus® are also shown in Table 3-3. It can be concluded that the characteristics of the flue gas from the recovery boiler, power boiler, biomass boiler and lime kiln are comparable to those reported in the literature. The differences observed between the flue gas compositions can be attributed to the different operating conditions and type of fuel burnt in the plant. As mentioned previously, the power boiler can burn biogenic or fossil fuels and, depending on that, the flue gas composition will vary. Therefore, the power and biomass boiler results, whose fuel is natural gas and hog, respectively, are compared with the multi-fuel boiler. Natural gas is also burnt in the recovery and biomass boilers during start-up.

Table 3-3: Properties and composition of the flue gases in the reference pulp and paper plant

Parameter	This work				Literature data (Nwaoha and Tontiwachwuthikul, 2019; Onarheim et al., 2017a)					
					Recovery boiler		Multi-fuel boiler		Lime kiln	
	Recovery boiler	Power boiler	Hog boiler	Lime Kiln	Data[3]	Data[4]	Biomass[3]	Biomass + NG[4]	Data[3]	Data[4]
Temperature [°C]	210.0	150.0	130.0	204.0	184.0	185.0/192.0	189.0	163.0	250.0	196.0/207.0
Mass flow [MTPD]	11070.5	330.3	3957.0	1035.5	-	-	-	-	-	-
Mass flow [t/ADt]	11.1	0.3	4.0	1.0	10.2	2.0/4.5	1.9	3.1	0.9	0.4/0.4
N_2 [$\%_{vol}$]	63.5	71.7	56.6	43.3	67.6	58.1/54.9	53.4	59.7	47.4	53.6/55.8
O_2 [$\%_{vol}$]	1.7	0.7	0.8	1.2	2.3	8.3/6.1	1.7	10.1	1.2	9.6/8.9
H_2O [$\%_{vol}$]	21.4	18.4	29.8	37.7	17.0	20.9/24.1	32.7	19.3	30.9	22.9/21.6
CO_2 [$\%_{vol}$]	13.3	9.2	12.8	17.3	13.0	12.7/14.9	12.1	10.9	20.4	13.9/13.7
SO_x [ppm]	152.1	0.0	18.9	N/A	60.0	27.2/31.0	40.0	N/A	50.0	19.9/24.2
NO_x [ppm]	N/A	N/A	N/A	31.7	125.0	N/A	150.0	N/A	175.0	0.7/1.2

3 (Onarheim et al., 2017a)

4 (Nwaoha and Tontiwachwuthikul, 2019)

3.2.3 Model development and integration

The retrofit of the reference pulp and paper plant with CO_2 capture can be achieved in the lime production without affecting the rest of the Kraft process. The flue gas streams from recovery, power and biomass boilers are merged and directed to the carbonator where the carbonation reaction, Eq. (3-1), takes place. During this step, CO_2 is captured by lime produced in the lime kiln. The decomposition of $CaCO_3$ into CaO and CO_2, Eq. (3-2), which occurs in the lime kiln (calciner), requires heat that is generated by oxy-fuel combustion. Thus, the sorbent circulates between the two reactors in alternate cycles of carbonation-calcination.

$$\text{Carbonator reactor: } CaO(s) + CO_2(g) \rightarrow CaCO_3(s) \quad \Delta H = -178 \text{ kJ/mol} \qquad \textbf{(3-1)}$$

$$\text{Calciner reactor: } CaCO_3(s) \rightarrow CaO(s) + CO_2(g) \quad \Delta H = 178 \text{ kJ/mol} \qquad \textbf{(3-2)}$$

The process model used in this work to simulate CaL integration to the pulp and paper plant, comprising a CaL process, a CO_2 compression unit (CCU) and a steam cycle, was modelled in Aspen Plus®. The CaL model was developed based on the work by Hanak et al. (2015) and validated with data from the 1.7 MW_{th} pilot plant at INCAR-CSIC (Sánchez-Biezma et al., 2013b). The calciner, which was modelled as a Gibbs reactor, and the carbonator, which was modelled as a stoichiometric reactor, are the main components of the CaL process (Figure 3-1). As the conversion of the sorbent decreases over the carbonation-calcination cycles (Fennell et al., 2007; Grasa and Abanades, 2006), fresh limestone is fed, called make-up stream (F_0), to maintain the desired average conversion in the carbonator. In the pulp and paper plant, the make-up stream comprises lime mud from the causticisation process and fresh limestone, and part of the spent CaO is sent back to the causticisation. The maximum average conversion (X_{ave}), Eq. (3-3), which depends on the carbonation (f_{carb}) and calcination extent (f_{calc}), the make-up rate (F_0), the solid looping rate (F_R) and the sorbent characteristics (a_1, a_2, f_1, f_2 and b), is estimated using the model proposed by Rodríguez et al. (2010). Considering the results presented by Sun et al. (2013), which showed at lab scale that lime mud can be employed as CO_2 sorbent, limestone was selected as the

sorbent that best represents lime mud behaviour. The sorbent characteristics were selected based on the measurements from 1.7 MW_{th} INCAR-CSIC pilot plant (Sánchez-Biezma et al., 2013b).

$$X_{ave} = (F_0+F_R r_0) f_{calc} \left[\frac{a_1 f_1^2}{F_0+F_R f_{carb} f_{calc}(1-f_1)} + \frac{a_2 f_2^2}{F_0+F_R f_{carb} f_{calc}(1-f_2)} + \frac{b}{F_0} \right] \quad \textbf{(3-3)}$$

The gas stream generated in the calciner contains CO_2 and water vapour, which is condensed, and then a high-purity CO_2 stream is available for compression. This stream is initially compressed to 80 bar, above the critical pressure, in a multi-stage compressor. Then, the CO_2-rich stream is cooled to 25°C and compressed to 110 bar, which are the requirements for pipeline transport (Metz et al., 2005).

As a result of the exothermic reaction in the carbonator, a large amount of high-grade heat is available for recovery in a heat recovery steam generator (HRSG) and can be used to generate additional electricity in the steam cycle. The steam cycle, based on a superheated Rankine cycle without reheat, was modelled in Aspen Plus®. It was validated with the CADSIM Plus® model (Table 3-4), considering fresh water flowrate, steam temperature and pressure and the electricity generated by each turbine. The results were in good agreement between the two models, as the difference between compared parameters was less than 5%. In further analysis, it was assumed that live steam enters the high-pressure turbine at 593°C and 154 bar (Dryden, 1982). Furthermore, a heat exchanger network was introduced to maximise energy recovery (Figure 3-2). Importantly, the intermediate-pressure steam produced by the boilers is not represented in this simplified diagram.

Table 3-4: Steam cycle validation with CADSIM Plus® data

Parameter	Fresh water flowrate [t/d]		Temperature [°C]		Pressure [bar]		Power [kW_{el}]	
	CADSIM Plus®	Model	CADSIM Plus®	Model	CADSIM Plus®	Model	CADSIM Plus®	Model
High-pressure turbine	-	-	427.0	436.0	59.6	59.6	-	-
Intermediate-pressure turbine	-	-	244.0	255.0	11.7	11.7	22393.0	23374.0
First low-pressure turbine	-	-	181.0	190.0	4.8	4.8	6262.5	6450.0
Second low-pressure turbine	-	-	90.0	90.0	0.7	0.7	1131.3	1135.4
Condenser	5304.1	5344.6						

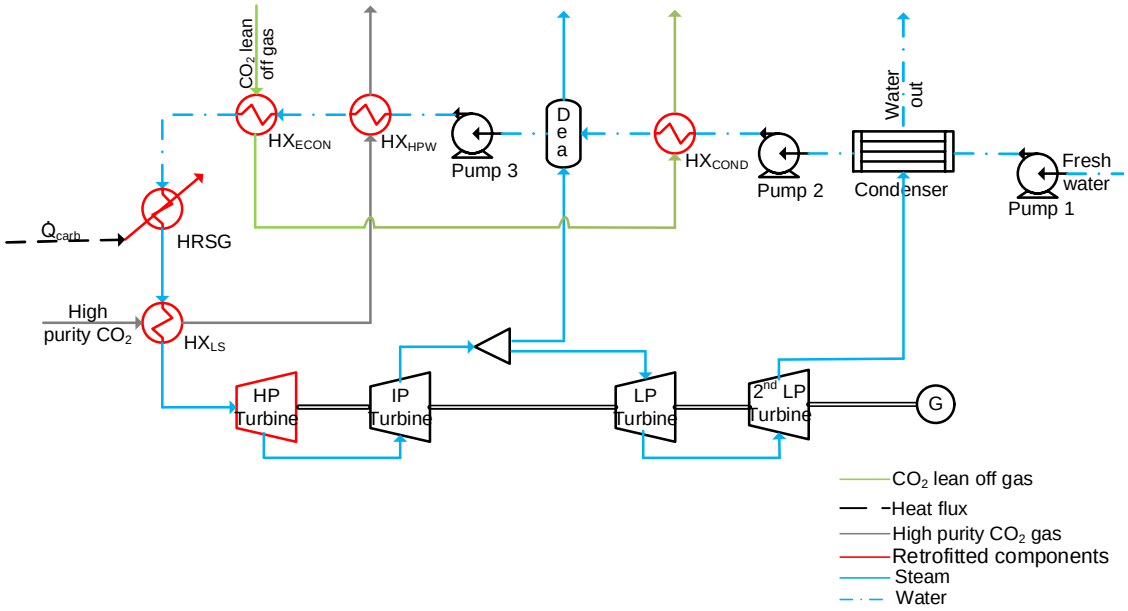

Figure 3-2: Calcium looping heat network. Dea: deaerator; G: generator; HP: high pressure; HRSG: heat recovery steam generator; HX: heat exchanger; IP: intermediate pressure; LP: low pressure; $\dot{Q}_{carb}$: heat flux of carbonator

A cryogenic ASU was not modelled in detail in this work, but its energy requirement was considered in the techno-economic assessment. It was assumed that the energy requirement to produce 1 t of O_2 at 95%$_{vol}$ purity is 200 $kW_{el}h$ (Romano, 2013). The main design conditions and thermodynamic assumptions used in modelling the proposed system are summarised in Table 3-5.

Table 3-5: Calcium looping model assumptions

Unit operation	Parameter	Value
Calcium looping		
Carbonator	Temperature [°C]	650.0
	Carbonated sorbent fraction [-]	0.7
	CO_2 capture on carbonator [%]	90.0
Lime kiln (Calciner)	Temperature [°C]	900.0
	Calcined sorbent fraction [-]	0.95
	Excess oxygen [$\%_{vol,dry}$]	2.5
	Relative make-up [-]	0.04
Steam Cycle		
Live Steam	Temperature [°C]	593.0
	Pressure [bar]	154.0
High-pressure turbine	Isentropic efficiency [%]	92.0
	Mechanical efficiency [%]	99.8
Intermediate-pressure turbine	Isentropic efficiency [%]	77.5
	Mechanical efficiency [%]	96.5
Low-pressure turbine	Isentropic efficiency [%]	59.0
	Mechanical efficiency [%]	96.5
Second low-pressure turbine	Isentropic efficiency [%]	60.0
	Mechanical efficiency [%]	98.0
Condenser	Feed water temperature [℃]	10.0
CO_2 compression unit		
Compressors	Polytropic efficiency [%]	80.0
	Mechanical efficiency [%]	99.6
	Intercooler temperature [°C]	40.0
Pump	Isentropic efficiency [%]	80.0
	Mechanical efficiency [%]	99.6
CO_2 final stream	Temperature [°C]	25.0
	Pressure [bar]	110.0
	Purity level [%]	>95.0
Fresh material (Hanak and Manovic, 2018)	Limestone (95.0%$_{wt}$ $CaCO_3$, 3.5%$_{wt}$ $MgCO_3$, 0.6%$_{wt}$ SiO_2, 0.4%$_{wt}$ Fe_2O_3, 0.5%$_{wt}$ Al_2O_3)	
Fuel (Hanak and Manovic, 2018)	Natural gas (93.1%$_{vol}$ CH_4, 3.2%$_{vol}$ C_2H_6, 0.7%$_{vol}$ C_3H_8, 0.4%$_{vol}$ C_4H_{10}, 1.0%$_{vol}$ CO_2, 1.6%$_{vol}$ N_2)	

3.3 Techno-economic feasibility assessment

To assess the effect of the CaL process integration with the reference pulp and paper plant, the process models presented in section 3.2 were used to assess the techno-economic performance of the reference pulp and paper plant with and without CO_2 capture.

3.3.1 Thermodynamic performance indicators

Three parameters were used to evaluate the effect of CaL integration to the pulp and paper plant, including the net power output (P_{net}), the equivalent fuel consumption (q_{eq}) and the specific primary energy consumption for CO_2 avoided (*SPECCA*). The equivalent fuel consumption is defined in Eq.(3-4) as the sum of direct (q) and indirect fuel consumption of the pulp and paper plant. The latter is defined as the fuel consumption associated with the electricity imported (P_e) and depends on the electric efficiency (η_e) of the power generation.

$$q_{eq} = q + \frac{P_e}{\eta_e} \quad \textbf{(3-4)}$$

The equivalent CO_2 emissions ($e_{CO_2,eq}$), given by Eq.(3-5), are calculated as the sum of direct $\left(e_{CO_2}\right)$ and indirect $\left(P_e \cdot e_{CO_2,e}\right)$ emissions. The latter is related to the electricity imported from the electric grid, thus depending on the specific CO_2 emissions source of the power plant ($e_{CO_2,e}$).

$$e_{CO_2,eq} = e_{CO_2} + P_e \cdot e_{CO_2,e} \quad \textbf{(3-5)}$$

If the retrofitted pulp and paper plant becomes a net electricity producer, the second term of Eq. (3-5) is negative and, therefore, results in negative indirect CO_2 emissions (De Lena et al., 2019). *SPECCA* is defined in Eq. (3-6), where the subscripts ref and cap correspond to reference pulp and paper plant without CO_2 capture and pulp and paper plant with CO_2 capture, respectively.

$$SPECCA = \frac{q_{eq,cap} - q_{eq,ref}}{e_{CO_2,eq,ref} - e_{CO_2,eq,cap}} \quad \textbf{(3-6)}$$

It should be noted that the characteristics of the power generation, electric efficiency (η_e) and the specific CO_2 emissions have an impact on *SPECCA.* For that reason, estimation of the indirect CO_2 emissions is based on the average non-CHP energy mix in the 27 EU Member States and the UK in 2015 ($e_{CO_2,e}$ = 262 $kg_{CO_2}/MW_{el}h$ and η_e = 45.9%) (De Lena et al., 2019).

3.3.2 Economic performance indicators

Three economic parameters were selected to evaluate the effect of CaL integration to the pulp and paper plant: the levelised cost of pulp (*LCOP*), the levelised cost of newsprint (*LCON*) and the cost of CO_2 avoided (*AC*). In order to estimate the *LCOP* and *LCON*, the net present value (*NPV*) method was applied, as defined by Eq. (3-7) (Onarheim et al., 2017b). As a result, the levelised cost of product (pulp, newsprint) is the minimum sale price of that product at which *NPV* is zero. At such point, the present value of revenue from the sales of pulp, newsprint and potentially electricity are equal to the present values of expenditures.

$$NPV = \sum_{t=1}^{n} \frac{CF_t}{(1+r)^t} - TCR \qquad \textbf{(3-7)}$$

The *NPV* method considers the discounted cash flow (CF_t) through the project lifetime (*t*), the total capital requirement (*TCR*) and the project interest rate (*r*). The economic assumptions made to estimate *NPV* are presented in Table 3-6. In order to simplify the calculations, inflation was not taken into account during the project lifetime. Thus, the market price of pulp and newsprint, as well as the price of raw materials and utilities are kept constant.

Table 3-6: Economic model assumptions

Parameter	Value
Expected lifetime [y] (Martínez et al., 2014a; Yang et al., 2010)	25.0
Project interest rate [%] (Martínez et al., 2014a; Yang et al., 2010)	8.8
Capacity factor [%] (Martínez et al., 2014a; Yang et al., 2010)	80.0
CO_2 emission allowance price [€/t_{CO_2}] (Business Inside, 2020a)	23.74
Average GBP/EUR exchange rate 2017 (Bank of England, 2019)	1.1418

3.3.3 Cost estimation for pulp and paper plant

Since economic studies on the pulp and paper industry are scarce, estimation of capital and operating costs of the pulp and paper plant is based on research published by Onarheim et al. (2017a). These costs were calculated using Eqs. (3-8)-(3-11). TCR_{ref}, Eq. (3-8), is the sum of the total plant cost (TPC_{ref}) and other capital costs ($OCAPEX$) which comprise spare parts, start-up, additional fuel costs, operation and maintenance, chemicals, owner's costs, working capital and interest during construction. These are calculated as a fraction of TPC_{ref}, Eq. (3-9).

$$TCR_{ref} = TPC_{ref} + OCAPEX \quad \textbf{(3-8)}$$

In order to account for unexpected expenditures, a contingency plan (PC) was considered that, along with the total invested cost (TIC_{ref}), constitutes TPC_{ref}.

$$TPC_{ref} = TIC_{ref} + PC \quad \textbf{(3-9)}$$

TIC_{ref} was assessed using a scaling law that is the empirical correlation between the cost and the scale of the plant, as shown in Eq. (3-10).

$$\frac{C}{C_0} = \left(\frac{S}{S_0}\right)^n \quad \textbf{(3-10)}$$

In this empirical correlation, C represents the actual capital cost and S is the target capacity. The corresponding variables with the subscript 0 refer to the reference value. A cost exponent for the correction of capacity (n) of 0.6 was considered. Furthermore, as the reference capital cost (C_0) was reported for the year 2005, the scaled capital cost was adjusted to the year 2017 by using the Chemical Engineering Plant Cost Index, as shown in Eq. (3-11) (CEPCI, 2020).

$$C_{2017} = C_{2005}\frac{CEPCI_{2017}}{CEPCI_{2005}} \quad \textbf{(3-11)}$$

All the assumptions used to estimate the capital and operating costs are presented in Table 3-7.

Table 3-7: Assumptions for capital and operating cost estimation of the reference pulp and paper plant

Parameter	Value
$CEPCI_{2005}$ (CEPCI, 2020)	468.2
$CEPCI_{2017}$ (CEPCI, 2020)	567.5
Cost exponent for correction of capacity (Onarheim et al., 2017b)	0.6
Project Contingency (*PC*) [€] (Onarheim et al., 2017b)	10.0% of TIC_{ref}
Other CAPEX	
Spare parts [€] (Onarheim et al., 2017b)	1.0% of TPC_{ref}
Start-up CAPEX [€] (Onarheim et al., 2017b)	2.0% of TPC_{ref}
Additional fuel costs [€] (Onarheim et al., 2017b)	2.1% of TPC_{ref}
Operation and maintenance [€] (Onarheim et al., 2017b)	25.0% of TPC_{ref}
Chemicals and others [€] (Onarheim et al., 2017b)	8.3% of TPC_{ref}
Owner's cost [€] (Onarheim et al., 2017b)	7.0% of TPC_{ref}
Interest during construction, charged annually [€] (Onarheim et al., 2017b)	8.0% of TPC_{ref}
Working capital [€] (Onarheim et al., 2017b)	0.2% of TPC_{ref}
Fixed operating costs [€] (Onarheim et al., 2017b)	5.7% of TCR_{ref}
Waste and disposal [€/y] (Onarheim et al., 2017b)	11.1% of TCR_{ref}
Raw materials and feedstock	
Wood unit cost [€/m^3] (Onarheim et al., 2017b)	40.0
NaOH unit cost [€/t] (Onarheim et al., 2017b)	370.0
H_2O_2 unit cost [€/t] (Onarheim et al., 2017b)	500.0
$NaClO_3$ unit cost [€/t] (Onarheim et al., 2017b)	500.0
H_2SO_4 unit cost [€/t] (Onarheim et al., 2017b)	50.0
Methanol unit cost [€/t] (Onarheim et al., 2017b)	350.0
Limestone unit cost [€/t] (Lisbona et al., 2010; Martínez et al., 2014a; Yang et al., 2010)	6.0
Natural gas unit cost [€/GJ] (Perry, Green and Maloney, 2007)	3.0
Hog fuel unit cost [€/m^3] (Onarheim et al., 2017b)	18.8
Unit cost of electricity imported from the grid [€/$MW_{el}h$] (BEIS, 2019)	87.3
Cooling water unit cost [€/m^3] (Onarheim et al., 2017b)	0.1
Process water unit cost [€/m^3] (Onarheim et al., 2017b)	0.1

The operating costs include the fixed and variable components. The former were assumed as a fraction of the TCR_{ref}, while the latter include the costs of raw materials, chemicals, utilities and costs related to waste disposal. Most economic assumptions were based on the data reported by Onarheim et al. (2017b). The utilities, raw materials and feedstock prices were also obtained from the same

study, except for the price of sorbent, natural gas and the electricity imported from the electric grid. The cost of electricity (87.3 €/$MW_{el}h$) was taken as the mean annual price of electricity to industrial consumers for the year 2017 (BEIS, 2019).

3.3.4 Cost estimation for calcium looping

Besides the costs associated directly with CaL, the cost of the ASU (C_{ASU}), the cost of CCU (C_{CCU}) and the costs related to the steam cycle (C_{SC}) must be also considered. Although the reference plant has an ASU, it is assumed that a new ASU is required to cover the O_2 demand of CaL. The sum of these costs, given by Eq. (3-12), constitute the total capital requirement of the capture plant (TCR_{cap}).

$$TCR_{cap} = C_{CaL} + C_{ASU} + C_{CCU} + C_{SC} \quad \textbf{(3-12)}$$

The C_{ASU} and C_{CCU} were estimated based on correlations available in the literature, where the O_2 flowrate and the brake power requirement were used as scaling factors. The investment cost of the CaL and the steam cycle are based on the individual costs of their components, presented in Eq. (3-13) and Eq. (3-14).

$$C_{CaL} = (1 + i_{P\&C})(C_{calc} + C_{carb} + C_{FP} + C_{Fan}) \quad \textbf{(3-13)}$$

As shown in Eq. (3-13), it was assumed that the investment cost of CaL also accounts for the piping and integration cost, which is estimated using the piping and integration cost indicator ($i_{P\&C}$) of 5% (Michalski, Hanak and Manovic, 2019).

$$C_{SC} = C_{HPW} + C_{ECON} + C_{LS} + C_{COND} + C_{HRSG} + C_{ST} \quad \textbf{(3-14)}$$

The individual cost of each component, including calciner, carbonator, fuel preparation, fan and heat exchangers was determined from the correlations summarised in Table 3-8. Furthermore, all assumptions considered in the estimation of the CaL costs are also included in Table 3-7. It is worth noting that the fixed and variables costs were assumed to be 1 and 2% of TCR_{cap}. Although the costs associated with sorbent and fuel and the CO_2 transport and storage cost are not included in these fractions, they are considered in the calculations.

Table 3-8: Assumptions for capital and operating cost estimation of calcium looping

Unit operation	Cost correlation
Air separation unit [O_2 production rate, $\dot{m}_{O_2}$ (kg/s)] (Atsonios et al., 2013)	$C_{ASU} = 2.926e7\left(\frac{\dot{m}_{O_2}}{28.9}\right)^{0.7}$
CO_2 compression unit [Brake power requirement, $\dot{W}_{CCU,BRK}$ (kW_{el})] (Kreutz et al., 2005b)	$C_{CCU} = 1.22914e7\left(\frac{\dot{W}_{CCU,BRK}}{13000}\right)^{0.67}$
Steam turbine [Brake power output, $\dot{W}_{ST,BRK}$, (kW_{el})] (Aminyavari et al., 2016)	$C_{ST} = 3744.3\left(\dot{W}_{ST,BRK}\right)^{0.7} - 61.3\left(\dot{W}_{ST,BRK}\right)^{0.95}$
Heat exchanger high-pressure water [Heat exchange area, A_{HPW} (m^2)] (Lee et al., 2014)	$C_{HPW} = 130\left(\frac{A_{HPW}}{0.093}\right)$
Economiser [Heat exchange area, A_{ECON} (m^2)] (Lee et al., 2014)	$C_{ECON} = 130\left(\frac{A_{ECON}}{0.093}\right)$
Heat exchanger live steam [Heat exchange area, A_{LS} (m^2)] (Shirazi et al., 2012)	$C_{LS} = 2290(A_{LS})^{0.6}$
Heat exchanger condensate [Heat exchange area, A_{COND} (m^2)] (Lee et al., 2014)	$C_{COND} = 130\left(\frac{A_{COND}}{0.093}\right)$
Heat recovery steam generator [Heat exchange area, A_{HRSG} (m^2)] (Lee et al., 2014)	$C_{HRSG} = 130\left(\frac{A_{HRSG}}{0.093}\right)$
Calciner [Calciner heat flux, $\dot{Q}_{calc}$ (kW_{th})] (Michalski, Hanak and Manovic, 2019)	$C_{calc} = 13140\ (\dot{Q}_{cal})^{0.67}$
Carbonator [Carbonator heat flux, $\dot{Q}_{carb}$ (kW_{th})] (Michalski, Hanak and Manovic, 2019)	$C_{carb} = 16591\ \left(\dot{Q}_{carb}\right)^{0.67}$
Fuel preparation system [Fuel flowrate $\dot{m}_{FP}$ (kg/s)] (Michalski, Hanak and Manovic, 2019)	$C_{FP} = 14158479\ (\dot{m}_{FP})^{0.24}$
Fan [Brake power requirement, $\dot{W}_{Fan,BRK}$ (kW_{el})] (Michalski, Hanak and Manovic, 2019)	$C_{Fan} = 103193\left(\frac{\dot{W}_{Fan,BRK}}{445}\right)^{0.67}$
Fixed operating costs [€] (Martínez et al., 2014a; Yang et al., 2010)	1.0% of TCR_{Cap}
Variable operating costs [€] (Martínez et al., 2014a; Yang et al., 2010)	2.0% of TCR_{Cap}
Limestone price [€/t] (Lisbona et al., 2010; Martínez et al., 2014a; Yang et al., 2010)	6.0
Natural gas price [€/GJ] (Perry, Green and Maloney, 2007)	3.0
Electricity exported to the grid [€/MW_{el}h] (Onarheim et al., 2017b)	40.0
CO_2 transport and storage cost [€/t_{CO_2}] (Romano et al., 2012)	7.0
Piping and integration costs indicator [%] (Michalski, Hanak and Manovic, 2019)	5.0

As mentioned above, the third economic parameter used to evaluate the proposed system is the cost of CO_2 avoided (*AC*), defined in Eq. (3-15). This

figure is calculated based on the levelised costs of pulp and newsprint and the equivalent CO_2 emissions ($e_{CO_2,eq}$) of the pulp and paper plant with and without CO_2 capture. It is also dependent on the annual pulp and newsprint production, $\dot{m}_{Pulp}$ and $\dot{m}_{News}$, respectively.

$$AC = \frac{\left[\dot{m}_{Pulp}\frac{LCOP}{(\dot{m}_{Pulp}+\dot{m}_{News})} + \dot{m}_{News}\frac{LCON}{(\dot{m}_{Pulp}+\dot{m}_{News})}\right]_{cap} - \left[\dot{m}_{Pulp}\frac{LCOP}{(\dot{m}_{Pulp}+\dot{m}_{News})} + \dot{m}_{News}\frac{LCON}{(\dot{m}_{Pulp}+\dot{m}_{News})}\right]_{ref}}{e_{CO_2,eq,ref} - e_{CO_2,eq,cap}} \quad \textbf{(3-15)}$$

3.4 Results and discussion

The techno-economic feasibility of the proposed system was evaluated using the parameters reported in Section 3.3 and the design specifications presented in Table 3-5. To establish a direct comparison basis, the key indicators were estimated for both the reference and the retrofitted pulp and paper plants. To study the impact of CaL design specifications on the thermodynamic and economic performance, a parametric study was carried out.

3.4.1 Techno-economic performance

The thermodynamic analysis (Table 3-9) revealed that integration of CaL increases the on-site power requirement from 70.0 MW_{el} to 118.7 MW_{el}. In the base case, 85% of the total power required by CaL was associated with the power requirement of the ASU and CCU. Regardless of the increased power requirement, the amount of electricity generated overcame the energy demand of the retrofitted pulp and paper plant. In contrast to previous studies (Kuparinen, Vakkilainen and Tynjälä, 2019; Möllersten, Gao and Yan, 2006; Onarheim et al., 2017b), in which integration of amine scrubbing reduces the net power output, this study showed that integration of CaL led to an increase in the net power output. While the operation of the reference pulp and paper plant relied on electricity import of 27.7 MW_{el}, the retrofitted pulp and paper plant became a net electricity export asset, exporting 9.6 MW_{el} of electricity to the electric grid. Therefore, the additional energy input required in CaL, reflected in 35% increase in the equivalent fuel consumption, is recovered in the steam cycle. Although there are no *SPECCA* data available for the pulp and paper industry, the specific primary energy consumption is more than double (5.7 MJ_{LHV}/kg_{CO_2}) compared to

the figures reported for the iron and steel industry (2.8 MJ_{LHV}/kg_{CO_2}) (Tian et al., 2018) and the cement industry (2.39–3.27 MJ_{LHV}/kg_{CO_2}) (De Lena et al., 2019; Rolfe et al., 2018). It should be noted that the latter value, presented by De Lena et al. (2019), corresponds to a total CaL integration; for the tail-end case, this value increased to 4.42 MJ_{LHV}/kg_{CO_2} avoided. The relative make-up of fresh sorbent (F_0/F_R) can explain the difference observed between this work and previous studies. This difference can also be attributed to the fact that the *SPECCA* considers the indirect CO_2 emissions. Therefore, the emissions associated with electricity import or export, the efficiency and emissions of the reference power generation have an impact on the final figure. Nevertheless, this work demonstrated that CaL is superior to post-combustion amine scrubbing that requires a heat duty of 3–5.25 MJ_{LHV}/kg_{CO_2} for the solvent regeneration only (Cormos, 2015; Kuparinen, Vakkilainen and Tynjälä, 2019; Nwaoha and Tontiwachwuthikul, 2019).

The economic evaluation showed that the levelised costs of pulp and newsprint are 728.3 €/ADt and 374.5 €/ADt without CCS and 824.4 €/ADt and 411.1 €/ADt with CCS, respectively. Thus, the levelised costs of pulp and newsprint increase by 13% and 10%, respectively, on retrofit of CaL. It is noteworthy that the effect of limestone replacement by lime mud was considered in the economics evaluation, as use of lime mud can reduce the cost of fresh sorbent by up to 30%. The estimated CO_2 avoided cost is 39.0 €/t_{CO_2} (Table 3-9). This figure is comparable with the initial techno-economic studies considering amine scrubbing (Hektor and Berntsson, 2009; McGrail et al., 2012) and physical absorption (Möllersten, Gao and Yan, 2006). However, when compared with recent studies, which relied on up-to-date costs, the cost of CO_2 avoided for CaL is lower by around 50% and 65% than for post-combustion amine scrubbing (52–131 €/t_{CO_2}) (Nwaoha and Tontiwachwuthikul, 2019; Onarheim et al., 2017b). The superior economic performance of CaL can provide sufficient incentives for the pulp and paper industry to invest in CCS.

Table 3-9: Summary of techno-economic performance

Parameter	Reference pulp and paper plant	Retrofitted pulp and paper plant
Thermodynamic assessment		
Gross power output [MW_{el}]	42.3	128.3
On-site power requirement [MW_{el}]	70.0	118.7
Net power output [MW_{el}]	-27.7	9.6
Equivalent fuel consumption [MJ_{LHV}/ADt]	30086	40551
SPECCA [MJ_{LHV}/kg_{CO_2} avoided]	-	5.7
Economic assessment		
Levelised cost of pulp [€/ADt]	728.3	824.4
Levelised cost of newsprint [€/ADt]	374.5	411.1
Cost of CO_2 avoided [€/t_{CO_2}]	-	39.0

3.4.2 Sensitivity analysis

The techno-economic performance indicators were first evaluated for a range of relative make-up rates, varied between 0.01 and 0.06. As shown in Figure 3-3, increasing the relative make-up of fresh sorbent resulted in a nearly linear rise in *SPECCA*. The specific exported electricity to the grid reduced on an increase in the make-up rate, which is attributed to the fact that less heat is available in CaL for recovery. This can be explained by the increase of fresh limestone fed to the calciner and consequently, a higher sorbent conversion was achieved in the carbonator and less solids were recirculated. These results are in agreement with the previous study on CaL retrofit (Hanak and Manovic, 2017a). Once the retrofitted pulp and paper plant becomes an electricity exporter, the net power output reduction also has a negative impact on the *SPECCA*, increasing the equivalent fuel consumption and the equivalent CO_2 emissions. Namely, an increment of 0.02 from the initial value of F_0/F_R (0.04), led to a 44% reduction in the amount of electricity exported to the grid and a 6% raise in *SPECCA* (Figure 3-3).

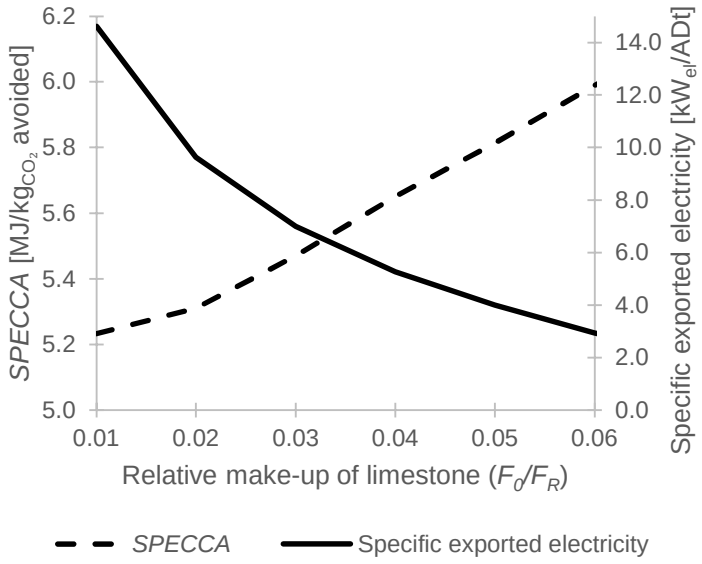

Figure 3-3: Impact of fresh limestone make-up rate on specific primary energy consumption for CO_2 avoided and specific exported electricity

Considering the economic performance (Figure 3-4), an increase of F_0/F_R translates into a rise in the cost of pulp, newsprint and the CO_2 capture. An increment of 0.02 from the initial value of F_0/F_R (0.04), resulted in a 1% increase in the levelised cost of pulp and newsprint (Figure 3-4a) and a 7% increase in the cost of CO_2 avoided (Figure 3-4b). However, for values below 0.02, the sorbent activity decay becomes more pronounced and limits the decrease of *SPECCA* (Figure 3-3) and the levelised costs (Figure 3-4). In practice, this is not a desirable situation as very low solid recirculation rate implies the need for larger reactors and, therefore, higher operational costs (Rodríguez, Alonso and Abanades, 2010).

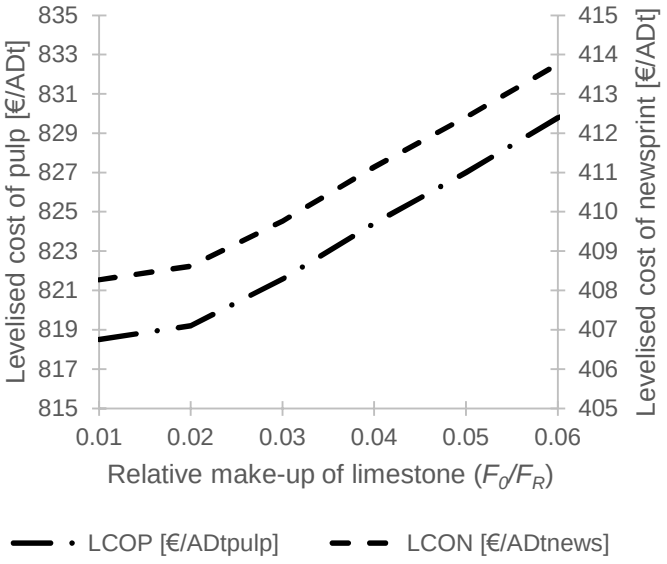

a)

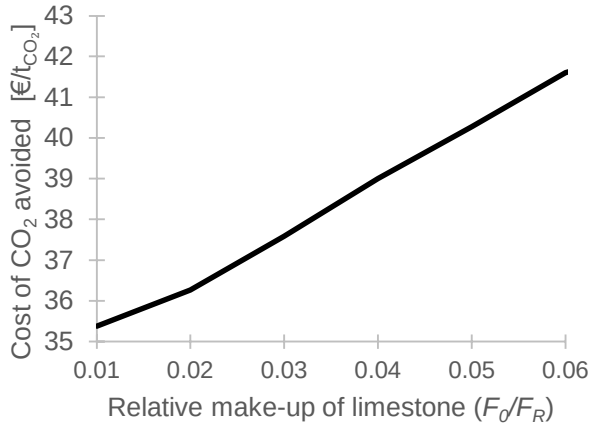

b)

Figure 3-4: Impact of fresh limestone make-up rate on (a) levelised cost of pulp and newsprint and (b) cost of CO_2 avoided

Furthermore, as the costs related to CaL are uncertain, a sensitivity analysis was performed by varying the main assumptions in the economic model (Figure 3-5). The CO_2 avoided cost was estimated by varying (±25%) the initial values of capital, fixed and variable costs of CaL as well as the CO_2 transport and storage, natural gas and limestone prices. It can be observed in Figure 3-5 that the natural gas price, which has been decreasing in the last year in North America (Business Inside, 2020b), and the CaL capital requirement are the two parameters with the highest impact on the CO_2 avoided cost. Importantly, a 25% reduction in these

parameters corresponded to a reduction in the CO_2 avoided cost of 16% and 11%, respectively. It was also found that CaL fixed and variable costs along with the sorbent price have a small impact (<2%) on the CO_2 avoided cost.

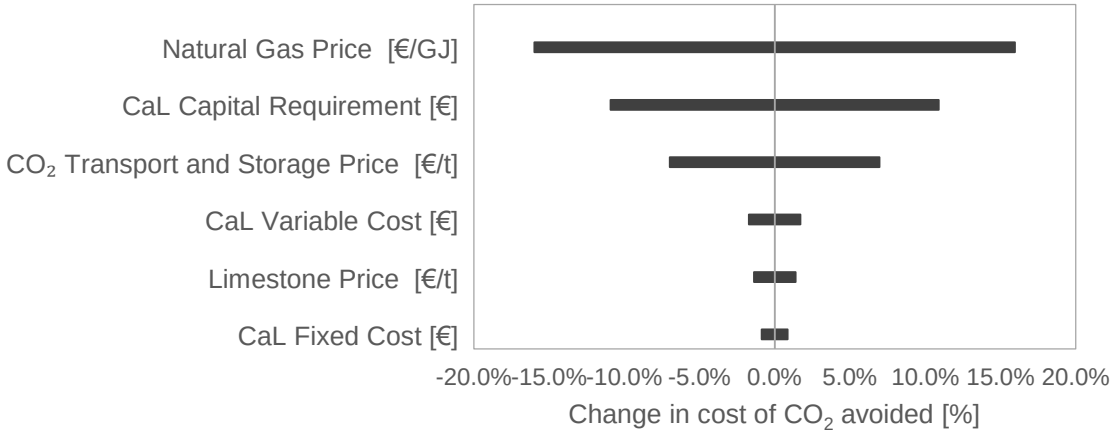

Figure 3-5: Effect of the key economic parameters on the economic performance of the retrofitted pulp and paper plant

Finally, the economic indicators were also assessed considering the following scenarios:

Scenario 1: No CO_2 emissions taxes and no credits for negative emissions (baseline scenario)

Scenario 2: Fossil CO_2 emissions tax and no credits for negative emissions (current situation)

Scenario 3: Fossil CO_2 emissions tax and credits for negative emissions

Before reporting the results obtained, it is worth mentioning that a negative CO_2 emissions credit of 23.74 €/t_{CO_2} was assumed, which is equal to the current price of CO_2 emission allowance under the EU ETS (Business Inside, 2020a). It should be noted that for a direct comparison, the economic indicators were also estimated for the pulp and paper plant with and without CO_2 capture.

As previously mentioned, CO_2 emissions are considered as carbon neutral under the current EU ETS biogenic. Therefore, only fossil CO_2 emissions are subject to the price of CO_2 emission allowances (Scenario 2). As shown in Figure 3-6, the

CO_2 emission allowance price levied on fossil emissions results in a marginal increase of the levelised costs for the reference plant and no change for the retrofitted plant. The CO_2 emission allowance price is also shown to have a minimal impact on CO_2 capture cost, as the CO_2 avoided cost changed from 39.0 €/t_{CO_2} (Scenario 1) to 38.0 €/t_{CO_2} (Scenario 2). This can be explained by the fact that around 96% of the total CO_2 emissions produced by the reference plant were biogenic. Nevertheless, it is clear from these figures that introduction of credits for negative emissions (Scenario 3) has the strongest effect on the levelised cost and CO_2 avoided cost. This can be attributed to the profit obtained from the negative CO_2 emissions. In this study, retrofit of CaL was characterised with an overall CO_2 capture rate of 94%, corresponding to 0.9 Mt_{CO_2}/y of negative CO_2 emissions. Consequently, the levelised costs in the retrofitted plant reduced by 6% (Figure 3-6a) and cost of CO_2 avoided (Figure 3-6b) decreased from 38.0 €/t_{CO_2} (Scenario 2) to 16.9 €/t_{CO_2} (Scenario 3). Thus, the CO_2 capture cost and pulp and newsprint prices are strongly affected by negative CO_2 emissions credits. For that reason, a parametric study was also carried out by varying the CO_2 emission allowance price between 0 and the value at which the cost of CO_2 avoided equals zero. This analysis was performed under Scenario 3, and the results are shown in Figure 3-7. The sensitivity analysis on electricity imported/exported price is also illustrated in Figure 3-7. The cost of CO_2 avoided was estimated for three electricity prices, 40 €/MW_{el}h (price electricity exported, base line), 87.3 €/MW_{el}h (price electricity imported, base line) and 120 €/MW_{el}h. Under the initial design assumptions (baseline), it was found that the negative CO_2 emissions credit must be 41.8 €/t_{CO_2}, which means there is no cost associated with CO_2 capture and, therefore, the levelised costs of the retrofitted plant equal the levelised costs of reference plant. The corresponding levelised costs of pulp and newsprint would be 732.6 €/ADt and 376.6 €/ADt, respectively. Because in this analysis the fossil fuel emissions were taxed, implying an additional cost, these values are slightly higher than the ones presented for the reference pulp and paper plant (Scenario 1). As also shown in Figure 3-7 the cost of CO_2 avoided depends strongly on the electricity price. As an example, an increase of 25% in the CO_2 emission allowance price initial value presented in

Table 3-6 (23.74 €/t_{CO_2}) results in cost of CO_2 avoided changing between 4.9 €/t_{CO_2} and 20.6 €/t_{CO_2}.

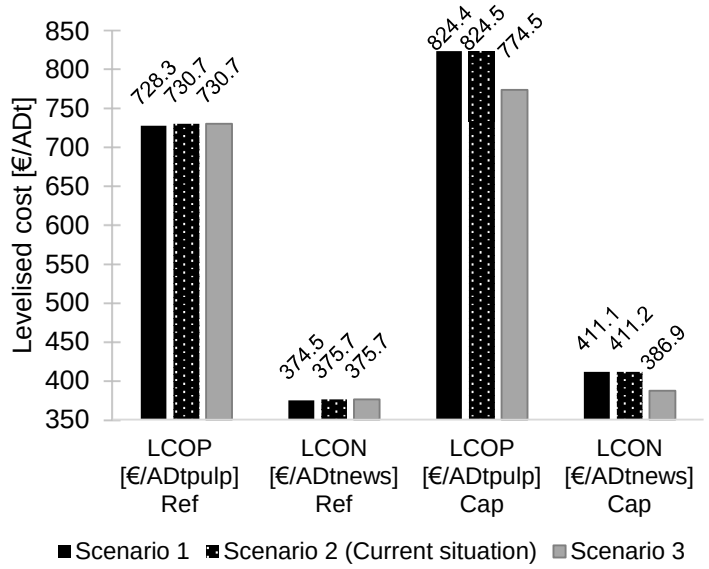

a)

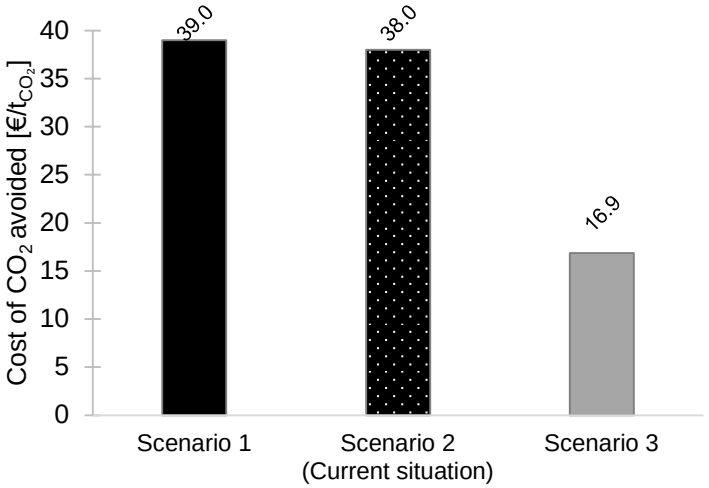

b)

Figure 3-6: Effect of different economic scenarios on (a) levelised cost of pulp newsprint and (b) cost of CO_2 avoided (Ref and Cap correspond to reference pulp and paper plant and retrofitted pulp and paper plant, respectively)

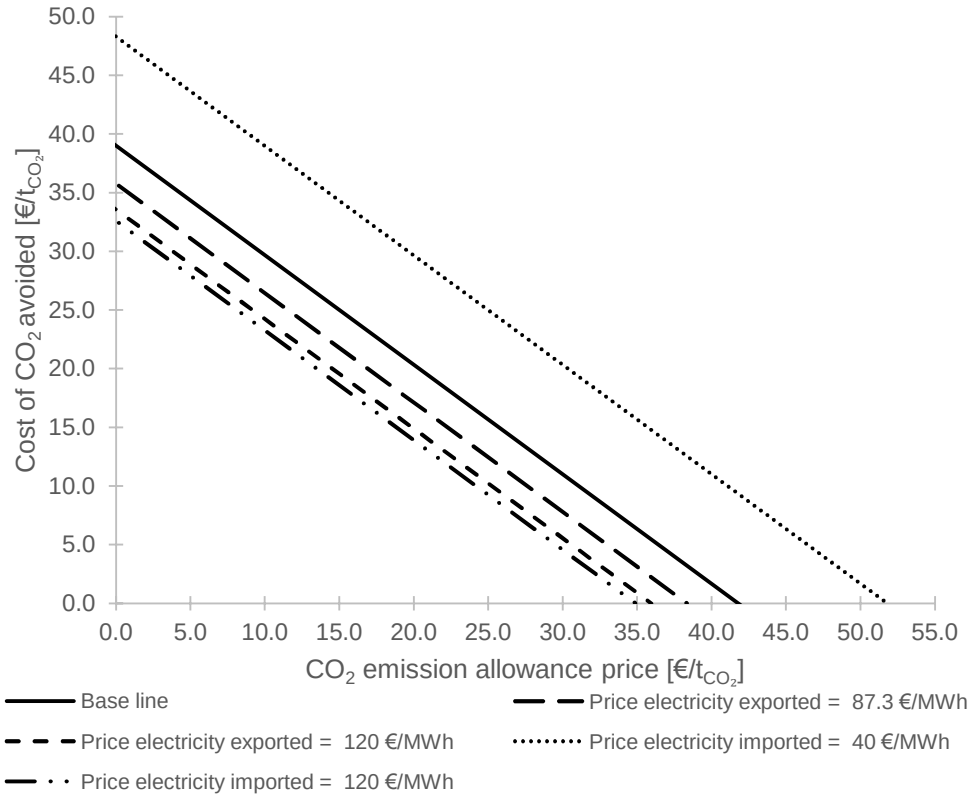

Figure 3-7: Impact of CO_2 emission allowance price and electricity price on the cost of CO_2 avoided under scenario 3

3.5 Conclusions

This study proposed a concept of the Kraft process with inherent CO_2 capture for a pulp and paper plant. Such a concept can be added to existing pulp and paper plants by integrating a CaL process in the existing lime cycle. The techno-economic feasibility of the proposed system was assessed. Under the initial design assumptions, it was found that the reference pulp and paper plant can turn from electricity importer to electricity exporter. Moreover, the cost of CO_2 avoided is estimated to be 39.0 €/t_{CO_2}. This figure is superior to that recently reported for pulp and paper plants retrofitted with amine scrubbing using MEA as a solvent. Such a superior performance can be associated with the fact that the energy input required for sorbent regeneration in CaL is recovered to generate additional electricity in the steam cycle. It is noteworthy that once the main purpose of this work was to show the potential of CaL integration in pulp and paper industry, the steam turbine island retrofit was considered outside of the boundary defined in the economic assessment. So, the costs associated with turbines and generator

modifications were not considered in the calculations as well as the full steam cycle optimisation. Therefore, CaL retrofitting to pulp and paper plant could still present more benefits.

A sensitivity analysis on techno-economic performance was also carried out by varying parameters, such as fresh limestone make-up rate, costs associated to CaL, and the sorbent and fuel prices. It was found that an increase in the make-up rate results in a linear rise of *SPECCA* and a reduction in electricity exported to the electric grid, corresponding to an increase in the pulp and newsprint prices as well as in the cost of CO_2 avoided. The latter was strongly affected by the natural gas price and CCS capital requirement.

This study showed that the pulp and paper industry has high potential to become carbon-negative, which with a change of policies would make CCS implementation feasible in this industry. Yet, the CCS feasibility depends strongly on the inclusion of biogenic emissions in the EU ETS and/or on the attribution of credits for them. Considering CaL as an emerging technology for CO_2 capture in the pulp and paper industry, its implementation would be viable with the recognition of negative CO_2 emissions and a negative CO_2 emission credit of 41.8 €/t_{CO_2} applied. Therefore, biogenic emissions should be considered in future policies and incentivised by the implementation of negative CO_2 emissions credits. So, further work is required to develop policies that will incentivise adoption of cleaner production technologies. Such policies should enable carbon-intensive industries to become carbon neutral or, as in case of the pulp and paper industry considered in this study, even carbon-negative.

3.6 References

Aminyavari, M., Mamaghani, A.H.A.H., Shirazi, A., Najafi, B. and Rinaldi, F. (2016) ‘Exergetic, economic, and environmental evaluations and multi-objective optimization of an internal-reforming SOFC-gas turbine cycle coupled with a Rankine cycle’, *Applied Thermal Engineering*, 108, pp. 833–846.

Atsonios, K., Koumanakos, A., Panopoulos, K.D., Doukelis, A. and Kakaras, E. (2013) ‘Techno-economic comparison of CO_2 capture technologies employed

with natural gas derived GTCC', *Proceedings of the ASME Turbo Expo*., Vol.2, p. V002T07A018.

Bank of England (2019) *Bank of England Statistical Interactive Database | Interest & Exchange Rates | Official Bank Rate History*. Available at: http://www.bankofengland.co.uk/boeapps/iadb/repo.asp (Accessed: 5 December 2019).

Barker, D.J., Turner, S.A., Napier-Moore, P.A., Clark, M. and Davison, J.E. (2009) 'CO_2 Capture in the Cement Industry', *Energy Procedia*, 1(1), pp. 87–94.

BEIS (2019) *Industrial electricity prices in the EU*. Business Energy & Industrial Strategy, United Kingdom.

Business Inside (2020a) *CO_2 European Emission Allowances*. https://markets.businessinsider.com/commodities/co2-european-emission-allowances. Available at: https://markets.businessinsider.com/commodities/co2-european-emission-allowances (Accessed: 31 January 2020).

Business Inside (2020b) *Natural Gas (Henry Hub) PRICE In USD - Historical Prices*. https://markets.businessinsider.com/commodities/natural-gas-price. Available at: https://markets.businessinsider.com/commodities/natural-gas-price (Accessed: 31 March 2020).

CEPCI (2020) *The Chemical Engineering Plant Cost Index*., *Chemical Engineering* Available at: https://www.chemengonline.com (Accessed: 5 December 2019).

Cormos, C.-C. (2015) 'Biomass direct chemical looping for hydrogen and power co-production: Process configuration, simulation, thermal integration and techno-economic assessment', *Fuel Processing Technology*, 137, pp. 16–23.

Dean, C.C., Blamey, J., Florin, N.H., Al-Jeboori, M.J. and Fennell, P.S. (2011) 'The calcium looping cycle for CO_2 capture from power generation, cement manufacture and hydrogen production', *Chemical Engineering Research and Design*, 89(6), pp. 836–855.

Dryden, I.G.C. (1982) *The Efficient Use of Energy*. 2nd edn. Elsevier.

Eurostat (2016) *Sankey diagrams for energy balance, November 2016.*

Fennell, P.S., Pacciani, R., Dennis, J.S., Davidson, J.F. and Hayhurst, A.N. (2007) 'The Effects of Repeated Cycles of Calcination and Carbonation on a Variety of Different Limestones, as Measured in a Hot Fluidized Bed of Sand', *Energy & Fuels*, 21(4), pp. 2072–2081.

Fernández-Dacosta, C., van der Spek, M., Hung, C.R., Oregionni, G.D., Skagestad, R., Parihar, P., Gokak, D.T., Strømman, A.H. and Ramirez, A. (2017) 'Prospective techno-economic and environmental assessment of carbon capture at a refinery and CO_2 utilisation in polyol synthesis', *Journal of CO_2 Utilization*, 21, pp. 405–422.

Garðarsdóttir, S.Ó., Normann, F., Skagestad, R. and Johnsson, F. (2018) 'Investment costs and CO_2 reduction potential of carbon capture from industrial plants – A Swedish case study', *International Journal of Greenhouse Gas Control*, 76, pp. 111–124.

Gerres, T., Chaves Ávila, J.P., Llamas, P.L. and San Román, T.G. (2019) 'A review of cross-sector decarbonisation potentials in the European energy intensive industry', *Journal of Cleaner Production*, 210, pp. 585–601.

Grasa, G.S. and Abanades, J.C. (2006) 'CO_2 capture capacity of CaO in long series of carbonation/calcination cycles', *Industrial and Engineering Chemistry Research*, 45(26), pp. 8846–8851.

Griffin, P.W., Hammond, G.P. and Norman, J.B. (2018) 'Industrial decarbonisation of the pulp and paper sector: A UK perspective', *Applied Thermal Engineering*, 134, pp. 152–162.

Hanak, D.P., Biliyok, C., Anthony, E.J. and Manovic, V. (2015) 'Modelling and comparison of calcium looping and chemical solvent scrubbing retrofits for CO_2 capture from coal-fired power plant', *International Journal of Greenhouse Gas Control*, 42, pp. 226–236.

Hanak, D.P. and Manovic, V. (2018) 'Combined heat and power generation with lime production for direct air capture', *Energy Conversion and Management*, 160,

pp. 455–466.

Hanak, D.P. and Manovic, V. (2017) ‘Calcium looping combustion for high-efficiency low-emission power generation’, *Journal of Cleaner Production*, 161, pp. 245–255.

Hektor, E. and Berntsson, T. (2009) ‘Reduction of greenhouse gases in integrated pulp and paper mills: Possibilities for CO_2 capture and storage’, *Clean Technologies and Environmental Policy*, 11(1), pp. 59–65.

Ho, M.T., Allinson, G.W. and Wiley, D.E. (2011) ‘Comparison of MEA capture cost for low CO_2 emissions sources in Australia’, *International Journal of Greenhouse Gas Control*, 5, pp. 49–60.

IPCC (2015) ‘Summary for Policymakers and Technical Summary’, in *Climate Change 2014 Mitigation of Climate Change*. Cambridge, United Kingdom and New York, NY, USA: Cambridge University Press, pp. 1–30.

Kreutz, T., Williams, R., Consonni, S., Chiesa, P., Consonni, S. and Kreutz, T. (2005) ‘Co-production of hydrogen, electricity and CO from coal with commercially ready technology. Part B: Economic analysis’, *International Journal of Hydrogen Energy*, 30(7), pp. 769–784.

Kuparinen, K. and Vakkilainen, E. (2017) ‘Green Pulp Mill: Renewable Alternatives to Fossil Fuels in Lime Kiln Operations’, *BioResources*, 12(2), pp. 4031–4048.

Kuparinen, K., Vakkilainen, E. and Hamaguchi, M. (2017) ‘Analysis on fossil fuel-free operation in a northern pulp and paper mill. Proceeding of International Chemical Recovery Conference’, *Proceeding of International Chemical Recovery Conference*.

Kuparinen, K., Vakkilainen, E. and Tynjälä, T. (2019) ‘Biomass-based carbon capture and utilization in kraft pulp mills’, *Mitigation and Adaptation Strategies for Global Change*, 24 Mitigation and Adaptation Strategies for Global Change, pp. 1213–1230.

Lee, Y.D., Ahn, K.Y., Morosuk, T. and Tsatsaronis, G. (2014) ‘Exergetic and

exergoeconomic evaluation of a solid-oxide fuel-cell-based combined heat and power generation system', *Energy Conversion and Management*, 85, pp. 154–164.

De Lena, E., Spinelli, M., Gatti, M., Scaccabarozzi, R., Campanari, S., Consonni, S., Cinti, G. and Romano, M.C. (2019) 'Techno-economic analysis of calcium looping processes for low CO_2 emission cement plants', *International Journal of Greenhouse Gas Control*, 82, pp. 244–260.

Lisbona, P., Martínez, A., Lara, Y. and Romeo, L.M. (2010) 'Integration of Carbonate CO_2 Capture Cycle and Coal-Fired Power Plants. A Comparative Study for Different Sorbents', *Energy & Fuels*, 24(1), pp. 728–736.

Martínez, A., Lara, Y., Lisbona, P. and Romeo, L.M. (2014) 'Operation of a mixing seal valve in calcium looping for CO_2 capture', *Energy and Fuels*, 28(3), pp. 2059–2068.

McGrail, B.P., Freeman, C.J., Brown, C.F., Sullivan, E.C., White, S.K., Reddy, S., Garber, R.D., Tobin, D., Gilmartin, J.J. and Steffensen, E.J. (2012) 'Overcoming business model uncertainty in a carbon dioxide capture and sequestration project: Case study at the Boise White Paper Mill', *International Journal of Greenhouse Gas Control*, 9, pp. 91–102.

Metz, B., Davidson, O., de Coninck, H., Loos, M. and Meyer, L. (2005) *Carbon Dioxide Capture and Storage*. Cambridge; New York; Melbourne; Madrid; Cape Town; Singapore; Sào Paulo: Cambridge University Press.

Michalski, S., Hanak, D.P. and Manovic, V. (2019) 'Techno-economic feasibility assessment of calcium looping combustion using commercial technology appraisal tools', *Journal of Cleaner Production*, 219, pp. 540–551.

Möllersten, K., Gao, L. and Yan, J. (2006) 'CO_2 capture in pulp and paper mills: CO_2 balances and preliminary cost assessment', *Mitigation and Adaptation Strategies for Global Change*, 11(5–6), pp. 1129–1150.

Möllersten, K., Gao, L., Yan, J. and Obersteiner, M. (2004) 'Efficient energy systems with CO_2 capture and storage from renewable biomass in pulp and paper

mills', *Renewable Energy*, 29(9), pp. 1583–1598.

Nwaoha, C. and Tontiwachwuthikul, P. (2019) 'Carbon dioxide capture from pulp mill using 2-amino-2-methyl-1-propanol and monoethanolamine blend: Techno-economic assessment of advanced process configuration', *Applied Energy*, 250, pp. 1202–1216.

Onarheim, K., Santos, S., Kangas, P. and Hankalin, V. (2017a) 'Performance and costs of CCS in the pulp and paper industry part 1: Performance of amine-based post-combustion CO_2 capture', *International Journal of Greenhouse Gas Control*, 59, pp. 58–73.

Onarheim, K., Santos, S., Kangas, P. and Hankalin, V. (2017b) 'Performance and cost of CCS in the pulp and paper industry part 2: Economic feasibility of amine-based post-combustion CO_2 capture', *International Journal of Greenhouse Gas Control*, 66, pp. 60–75.

Perry, R., Green, D. and Maloney, J. (2007) *Perry's chemical engineers' handbook*. USA: New York: McGraw-Hill.

Rao, A.B. and Rubin, E.S. (2002) 'A technical, economic, and environmental assessment of amine-based CO_2 capture technology for power plant greenhouse gas control', *Environmental Science and Technology*, 36(20), pp. 4467–4475.

Rodríguez, N., Alonso, M. and Abanades, J.C. (2010) 'Average activity of CaO particles in a calcium looping system', *Chemical Engineering Journal*, 156(2), pp. 388–394.

Rodríguez, N., Murillo, R. and Abanades, J.C. (2012) 'CO_2 capture from cement plants using oxyfired precalcination and/ or calcium looping', *Environmental Science and Technology*, 46(4), pp. 2460–2466.

Rolfe, A., Huang, Y., Haaf, M., Pita, A., Rezvani, S., Dave, A. and Hewitt, N.J. (2018) 'Technical and environmental study of calcium carbonate looping versus oxy-fuel options for low CO_2 emission cement plants', *International Journal of Greenhouse Gas Control*, 75, pp. 85–97.

Romano, M., Martínez, I., Murillo, R., Arstad, B., Bloom, R., Ozcan, D.C., H., A.

and Brandani, S. (2012) *11th International Conference on Greenhouse Gas Control Technologies, GHGT 2012*. Kyoto, Japan, pp. 18–22.

Romano, M.C. (2013) 'Ultra-high CO_2 capture efficiency in CFB oxyfuel power plants by calcium looping process for CO_2 recovery from purification units vent gas', *International Journal of Greenhouse Gas Control*, 18(0), pp. 57–67.

Sánchez-Biezma, A., Paniagua, J., Diaz, L., Lorenzo, M., Alvarez, J., Martínez, D., Arias, B., Diego, M.E. and Abanades, J.C. (2013) 'Testing postcombustion CO_2 capture with CaO in a 1.7 MW_{th} pilot facility', *Energy Procedia*, 37, pp. 1–8.

Schorcht, F., Kourti, I., Scalet, B.M., Roudier, S. and Sancho, L.D. (2013) *Best Available Techniques (BAT) Reference Document for the Production of Cement, Lime and Magnesium Oxide*. Publications Office of the European Union, Luxembourg.

Shao, R. and Stangeland, A. (2009) *Amines Used in CO_2 Capture - Health and Environmental Impacts*.

Shirazi, A., Aminyavari, M., Najafi, B., Rinaldi, F. and Razaghi, M. (2012) 'Thermal–economic–environmental analysis and multi-objective optimization of an internal-reforming solid oxide fuel cell–gas turbine hybrid system', *International Journal of Hydrogen Energy*, 37(24), pp. 19111–19124.

Sun, R., Li, Y., Liu, C., Xie, X. and Lu, C. (2013) 'Utilization of lime mud from paper mill as CO_2 sorbent in calcium looping process', *Chemical Engineering Journal*, 221, pp. 124–132.

Tian, S., Jiang, J., Zhang, Z. and Manovic, V. (2018) 'Inherent potential of steelmaking to contribute to decarbonisation targets via industrial carbon capture and storage', *Nature Communications*, 9(1), pp. 1–8.

Xu, G., Jin, H.G., Yang, Y.P., Xu, Y.J., Lin, H. and Duan, L. (2010) 'A comprehensive techno-economic analysis method for power generation systems with CO_2 capture', *International Journal of Energy Research*, 34(4), pp. 321–332.

Yang, Y., Zhai, R., Duan, L., Kavosh, M., Patchigolla, K. and Oakey, J. (2010) 'Integration and evaluation of a power plant with a CaO-based CO_2 capture

system', *International Journal of Greenhouse Gas Control*, 4(4), pp. 603–612.

Yao, Y., Marano, J., Morrow, W.R. and Masanet, E. (2018) 'Quantifying carbon capture potential and cost of carbon capture technology application in the U.S. refining industry', *International Journal of Greenhouse Gas Control*, 74, pp. 87–98.

4 BLACK LIQUOR GASIFICATION WITH CALCIUM LOOPING FOR CARBON-NEGATIVE PULP AND PAPER INDUSTRY*

Abstract

Although considered one of the major energy-intensive industries, the pulp and paper industry has also the potential for energy production from an industrial by-product, black liquor. This study proposes black liquor gasification coupled with calcium looping as a CO_2 capture route for the pulp and paper industry. Black liquor gasification with H_2 production (BLG-CaL-H_2), black liquor gasification with gas turbine combined cycle (BLG-CaL-GT) or with solid-oxide fuel cell (BLG-CaL-SOFC) were considered. The dependence of carbon capture and storage cost on the natural gas, limestone, electricity imported and H_2 sale prices aside the expenditures related with black liquor gasification coupled with calcium looping were evaluated. The carbon capture and storage route, based on calcium looping retrofitted to the pulp and paper plant, was found to have a lower cost of CO_2 avoided (39.0 €/t_{CO_2}) when compared with black liquor gasification coupled with calcium looping (48.8–57.1 €/t_{CO_2}). Between the black liquor gasification coupled with calcium looping scenarios, BLG-CaL-H_2 presented the lowest cost of CO_2 avoided (48.8 €/t_{CO_2}) but the highest energy penalty. Based on the thermodynamic performance, it was shown that calcium looping retrofit and BLG-CaL-SOFC presented the best overall performance, turning the electricity importer reference plant into electricity exporter. The economic sensitivity showed that the capital requirement of black liquor gasification coupled with calcium looping has a strong effect on the cost of CO_2 avoided for all alternatives. The H_2 production is also strongly affected by the H_2 sale price while BLG-CaL-SOFC and BLG-CaL-GT are strongly dependent on natural gas price.

Keywords: Black liquor gasification; calcium looping; carbon capture; techno-economic analysis; co-generation; hydrogen

---

*Santos, M.P.S., Manovic, V. and Hanak, D.P. (2021) 'Black liquor gasification with calcium looping for carbon-negative pulp and paper industry', *International Journal of Greenhouse Gas Control*, 110, p. 103436.

4.1 Introduction

To meet the ambitious targets set by the Paris Agreement, the net GHG emissions must be zero or even negative between 2055 and 2080 (Fuss et al., 2014; Millar et al., 2017; Rogelj et al., 2018). As a result, the EIIs need to improve material and energy efficiencies, implement CCS technologies and reduce their dependence on fossil fuels (Gerres et al., 2019; McGrail et al., 2012). The development of clean energy sources and vectors, such as hydrogen, is of paramount importance (Spallina et al., 2019; Vogl, Åhman and Nilsson, 2018). However, nearly all hydrogen is still produced from fossil fuel sources (International Energy Agency). Due to its abundance and carbon neutrality, biomass is considered to be an alternative feedstock in the energy sector (Sanna, 2014). The pulp and paper industry is one of the major consumers of biomass. Yet, this industry is still the fourth EII, contributing 4% of the total EU industry emissions in 2017 (Gerres et al., 2019). However, in contrast to other EIIs, the pulp and paper industry has the potential to become a carbon-negative industry on the integration of CCS (Santos, Manovic and Hanak, 2021).

Black liquor formed during the Kraft process is normally combusted in a recovery boiler to recover inorganic chemicals and produce process utilities (steam and electricity). Although the recovery boiler has been used for decades, this technology presents some drawbacks, such as low energy efficiency and health and safety issues such as smelt-water explosions and reduced-sulphur gas emissions (Larson et al., 2006; Whitty, 2005). Thus, technologies with improved efficiency and safety have been considered. Pressurised entrained flow gasification of black liquor, a technology developed by Chemrec AB, has been proven as a valid alternative to the recovery boiler. This technology has been demonstrated at the 3 MW_{th} LTU Green Fuels pilot plant in Piteå, Sweden (Jafri et al., 2016). As the alkali metals are present in black liquor, which have a catalytic effect, the produced syngas is characterised by low content of CH_4 and tars, even at short residence times and temperatures around 1000–1050 °C (Öhrman et al., 2012). As the smelt is dissolved in a quench bath at the bottom of the gasifier, the inorganic chemicals can be recovered as green liquor and recycled to the

Kraft process. The techno-economic feasibility of BLG for the production of biofuels (Andersson, Lundgren and Marklund, 2014; Carvalho et al., 2018) and bulk chemicals, such as ammonia (Akbari, Oyedun and Kumar, 2018), were reported. Andersson et al. (2014) assessed methanol production *via* BLG, Carvalho et al. (2018) studied methanol production *via* co-gasification with renewable feedstocks, such as pyrolysis liquid, crude glycerol and fermentation residues. The production of ammonia *via* BLG and co-gasification with pulp sludge or with waste sludge was evaluated by Akbari et al. (2018). However, the economic assessment of the integration of BLG with CO_2 capture (BLG-CCS) is still limited.

Zhang et al. (2011) have carried out a preliminary feasibility assessment of the integration of a BLG polygeneration system for the production of methanol, steam and electricity to a pulp and paper plant. This study also compared the BLG combined cycle with (BLG-CC-CCS) and without CO_2 capture (BLG-CC-NCC). The former considered both pre-combustion physical absorption (Selexol) from syngas and oxy-combustion of the unreacted gas from methanol synthesis. Their study concluded that the BLG polygeneration system achieved a higher first law efficiency (34.1%) than the reference pulp and paper plant (15.7%). Moreover, BLG-CC-CCS based on oxy-combustion showed a lower net energy penalty (4.0%) and CO_2 capture cost (26.3 €/t_{CO_2}) than that of the Selexol process (a net energy penalty of 6.5% and 40.9 €/t_{CO_2}). Pettersson and Harvey (2012) have assessed the techno-economic performance of the BLG polygeneration system for the production of dimethylether (DME) and electricity. This study compared the implementation of different BLG concepts and evaluated the economic performance based on the net annual profit and potential of CO_2 emission reduction under different energy market scenarios. The BLG with DME production was shown to be the most attractive option among the considered scenarios. The BLG with electricity generation in pulp plant was still attractive under policies that promoted biofuels and high-penetration of low-carbon electricity. The integration of CO_2 capture with BLG in pulp plants and pulp and paper plants was also studied. It was shown to have a high potential for CO_2 emissions reduction, but the process profitability was strongly dependent on the

CO_2 emission allowance price. Ferreira and Balestieri (2015) have compared the techno-economic performance of BLG-CC-CCS, which considered a conventional CO_2 absorption technology, and BLG-CC-NCC integrated to a pulp and paper plant. This study showed that the energy efficiency of the BLG-CC-NCC (34%) was higher than that for the BLG-CC-CCS (28%). The CO_2 avoided cost was shown to be around 20.5 €/t_{CO_2}, which was estimated without considering the costs associated with CO_2 transport and storage. Moreover, Ferreira and Balestieri (2015) considered a carbon credit of 5.3 €/t_{CO_2} captured which implies that the economic feasibility of BLG-CC-CCS depends on incentives.

To date, the economic feasibility of the BLG coupled with CO_2 capture has been assessed for amine scrubbing, physical absorption and oxy-fuel combustion. However, the current literature presents limited information on the application of high-temperature solid looping cycles for BLG. Darmawan et al. (2018) considered chemical looping for the co-production of H_2 and electricity from BLG. Although their work proved that this approach is feasible from the thermodynamic standpoint, the economic feasibility of such a process needs to be assessed. Moreover, CaL is an emerging high-temperature solid looping technology considered for thermochemical conversion of biomass. This technology can be either integrated with the thermochemical conversion process, so-called sorption-enhanced gasification (for solid biomass) or sorption-enhanced reforming (for gaseous or liquid biofuels) (Gil et al., 2015; Pfeifer, Puchner and Hofbauer, 2007; Wiranarongkorn and Arpornwichanop, 2017), in a single reactor, or can be integrated after the thermochemical conversion process in a secondary reactor (Armbrust et al., 2015; Connell et al., 2013; Müller et al., 2009). Although the pulp and paper process has an inherent CO_2 capture capability *via* CaL, as shown by Santos et al. (2021), no application of CaL for BLG has been considered.

For this reason, this work presents a comparative study between two different routes of CaL retrofit to the pulp and paper plant. The first route assumes that the existing Kraft process in the pulp and paper plant is retrofitted with CaL for CO_2 capture (Santos, Manovic and Hanak, 2021). The second route assumes that the

BLG is integrated with CaL for simultaneous CO_2 capture and H_2 production (BLG-CaL) in the same reference plant. Three co-production routes are evaluated within BLG-CaL, considering BLG with H_2 production (BLG-CaL-H_2), BLG with gas turbine combined cycle (BLG-CaL-GT) or with solid oxide fuel cell (BLG-CaL-SOFC) for electricity production. The feasibility of the BLG-CaL routes is assessed considering the process thermodynamic and economic performance. Finally, a sensitivity analysis is carried out to evaluate the influence of costs on the economic performance.

4.2 Process modelling and design

This study considered a retrofit of the reference pulp and paper plant with CO_2 capture and hydrogen. The process models were developed for the reference pulp and paper plant, CaL for CO_2 capture and BLG with CaL for simultaneous CO_2 capture and H_2 production. Overall, the techno-economic performance of the following cases was evaluated:

- Case 1 – reference pulp and paper plant
- Case 2 – calcium looping retrofit to the reference plant
- Case 3 – integrated black liquor gasification with calcium looping for H_2 production
- Case 4a – integrated black liquor gasification with calcium looping for power generation in gas turbine combined cycle
- Case 4b – integrated black liquor gasification with calcium looping for power generation in solid-oxide fuel cell

4.2.1 Reference pulp and paper plant

An integrated pulp and paper plant (Figure 4-1) considered by Santos et al. (2021) is considered as the reference case in this study. The energy and material balance essential to describe the reference plant was performed using CADSIM Plus®. The daily production capacity of this plant was assumed to be 1000 ADt (air-dried tonnes, containing 90% of dry solids), 375 ADt and 450 ADt of Kraft bleached pulp, thermochemical pulp and newsprint, respectively. Since the thermochemical pulp and part of bleached pulp are required in the newsprint

process production, the market products include the total newsprint production and 925 ADt of Kraft bleached pulp. This translates into about 1810 t/d of black liquor solids (dry). Table 4-1 presents the black liquor composition. The fibre line, the calcium or lime cycle and the sodium or recovery cycle are the main components of the reference plant. The steam required to drive the process is produced in the recovery boiler and, partially, in the biomass and power boilers. The remaining steam is used for electricity generation in the steam turbine island. However, the electrical demand is higher than the amount of electricity generated in the steam turbine island. Therefore, an additional amount of electricity is imported from the electrical grid to meet the auxiliary requirements of the process.

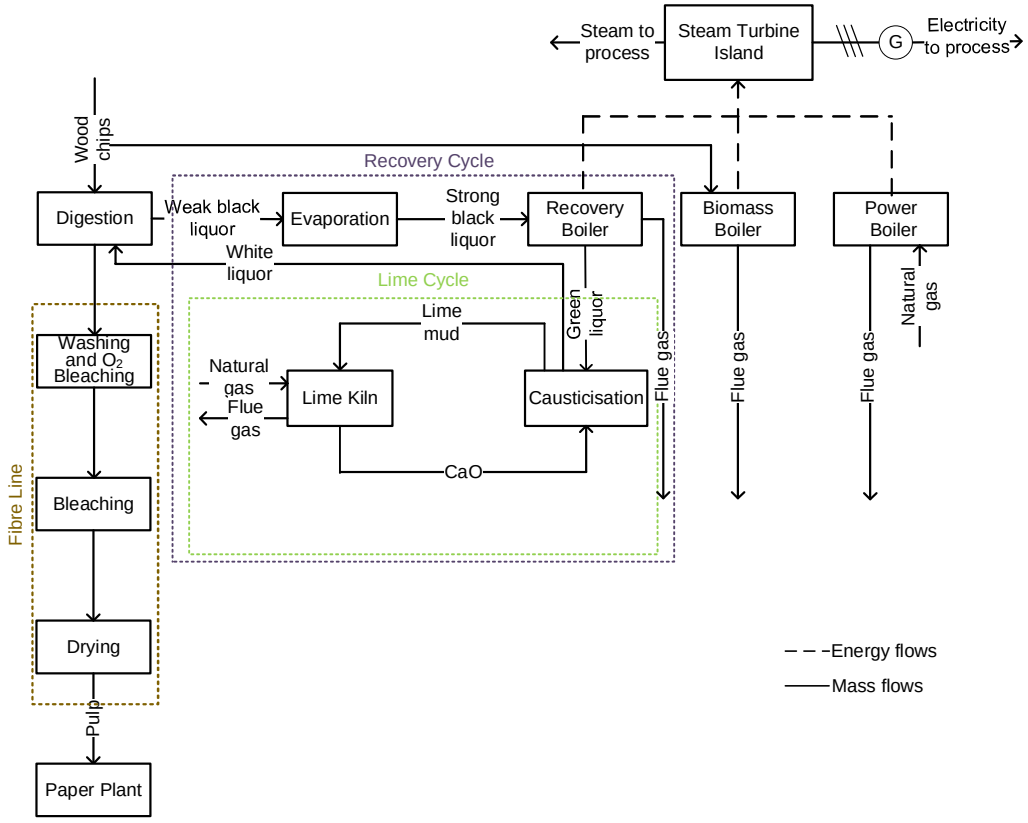

Figure 4-1: Simplified diagram of reference pulp and paper plant (Case 1)

Table 4-1: Black liquor composition

Properties	Value
Solids content [$\%_{wt}$]	74.0
Moisture content [$\%_{wt}$]	26.0
Elemental composition [$\%_{wt,db}$[5]]	C:36.1; H:3.5; O:34.2; Cl:0.4; Na:19.0; K:1.9; S:4.8
LHV[6] [MJ/kg, db]	12.37

4.2.2 Calcium looping retrofit to the reference plant

As CO_2 emissions originate mostly from the biomass conversion, the reference plant can become carbon-negative on CaL retrofit. Importantly, the lime mud from the Kraft process contains limestone and lime, the most commonly used sorbent in CaL. This implies an inherent CO_2 capture capability of the pulp and paper plants. Therefore, the CO_2 capture potential of the Kraft process was explored by retrofitting CaL in the lime cycle (Case 2). The approach to CaL retrofit in the existing Kraft process is shown in Figure 4-2. This concept has been described in detail by Santos et al. (2021) and the CaL model has previously been validated by Hanak et al. (2015). In such a concept, a larger kiln is used in place of the lime kiln in the reference plant. It is connected in parallel to the carbonator (*RStoich*). It is assumed that such a modification does not influence the other stages of the Kraft process. The lime (CaO) produced from the calcination of the limestone ($CaCO_3$) in the lime kiln (Eq. (4-1)) is used to capture CO_2 produced, in the recovery, power and biomass boilers, in the carbonator (Eq. (4-2)). The heat required for sorbent regeneration is supplied *via* oxy-fuel combustion of natural gas in the calciner (*RGibbs*). The properties and composition of flue gas streams are presented in Table 4-2.

Calcination: $CaCO_3(s) \rightarrow CaO(s) + CO_2(g)$ $\Delta H = 178$ kJ/mol **(4-1)**

Carbonation: $CaO(s) + CO_2(g) \rightarrow CaCO_3(s)$ $\Delta H = -178$ kJ/mol **(4-2)**

5 Dry basis

6 Lower heating value

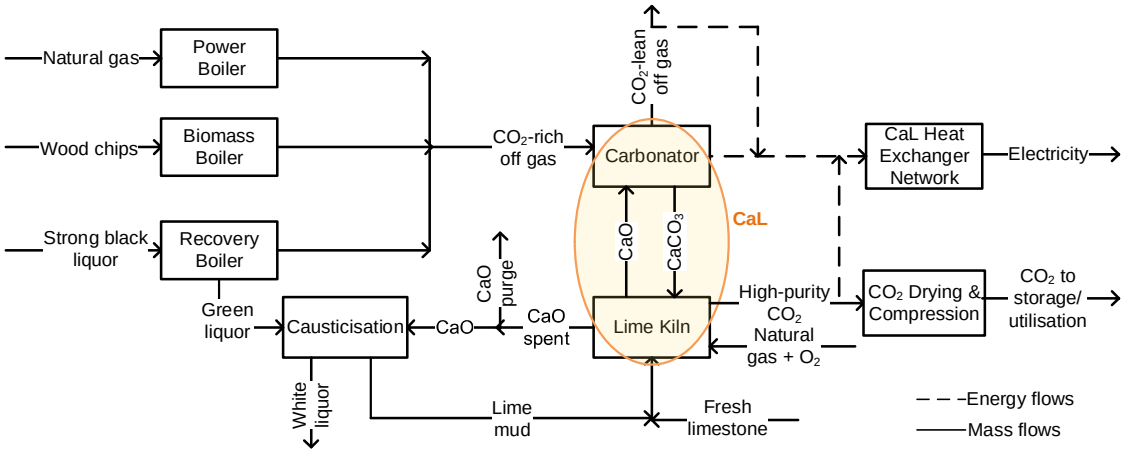

Figure 4-2: Simplified diagram of calcium looping retrofitted to the reference plant (Case 2)

Table 4-2: Summary of flue gas characteristic in reference pulp and paper plant (Santos, Manovic and Hanak, 2021)

Parameter	Power boiler	Recovery boiler	Hog boiler
Temperature [°C]	150.0	210.0	130.0
Mass flowrate [t/d]	330.3	11070.5	3957.0
N_2 [%vol]	71.7	63.5	56.6
O_2 [%vol]	0.7	1.7	0.8
H_2O [%vol]	18.4	21.4	29.8
CO_2 [%vol]	9.2	13.3	12.8
SO_x [ppm]	0.0	152.1	18.9

4.2.3 Integration of black liquor gasification with calcium looping (BLG-CaL)

To explore the feasibility of BLG, the model for BLG integrated with CaL for H_2 production was developed and retrofitted with the reference plant. It should be noted that CO_2 produced from the power and biomass boilers (Table 4-2) is also captured in CaL. BLG was modelled using a Gibbs reactor in Aspen Plus®. To match the syngas composition under gasification conditions presented in Table 4-3, the BLG model was optimised and validated (Figure 4-3) with experimental data (Carlsson et al., 2010). It can be seen that the model predictions were in good agreement with the experimental data reported in the literature. The main

design and operating conditions of the BLG-CaL process are presented in Table 4-3.

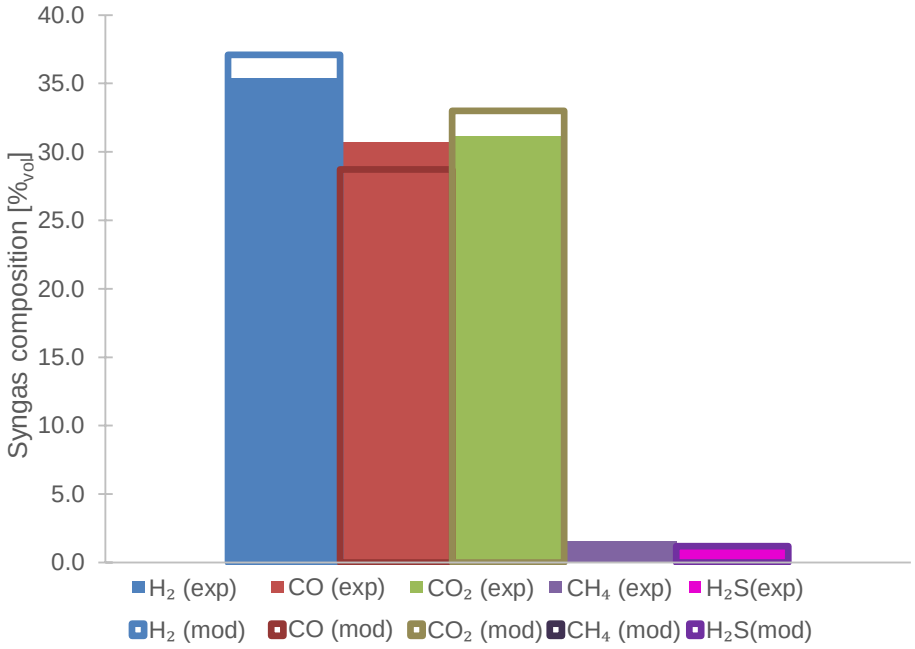

Figure 4-3: Black liquor gasification validation with literature data. Exp and mod correspond to experimental and simulated data, respectively

Table 4-3: Main modelling assumptions of the evaluated systems

Unit operation	Parameter	Value
Gasification	Temperature [°C]	1050
	Pressure [barg]	30
	Gasifier type	Entrained flow
Calcium looping (Santos, Manovic and Hanak, 2021)		
Carbonator	Temperature [°C]	650.0
	Carbonated sorbent fraction [-]	0.7
	CO_2 capture efficiency in carbonator [%]	90.0
Lime kiln (Calciner)	Temperature [°C]	900.0
	Calcined sorbent fraction [-]	0.95
	Excess oxygen [$\%_{vol,dry}$]	2.5
	Relative make-up [-]	0.04
Gas cleaning	H_2S removal [%]	99.9
Pressure swing adsorption	H_2 recovery [%]	52.11
	H_2 purity [$\%_{vol}$]	99.99
	Tail gas pressure [bar]	1
	Delivery pressure [bar]	700 or 60
Steam Cycle (Santos, Manovic and Hanak, 2021)		
Live Steam	Temperature [°C]	593.0
	Pressure [bar]	154.0
High-pressure turbine	Isentropic efficiency [%]	92.0
	Mechanical efficiency [%]	99.8
Intermediate-pressure turbine	Isentropic efficiency [%]	77.5
	Mechanical efficiency [%]	96.5
Low-pressure turbine	Isentropic efficiency [%]	59.0
	Mechanical efficiency [%]	96.5
Second low-pressure turbine	Isentropic efficiency [%]	60.0
	Mechanical efficiency [%]	98.0
Condenser	Feed water temperature [°C]	10.0
CO_2 compression		
Compressors	Polytropic efficiency [%]	80.0
	Mechanical efficiency [%]	99.6
	Intercooler temperature [°C]	40.0
Pump	Isentropic efficiency [%]	80.0
	Mechanical efficiency [%]	99.6
CO_2 final stream	Temperature [°C]	25.0
	Pressure [bar]	110.0
	CO_2 purity [$\%_{vol}$]	≥ 95.0
Gas turbine	Compressor outlet pressure [bar]	20
	Combustor pressure drop [%]	2
	Turbine inlet temperature [°C]	1268
	Turbine isentropic efficiency [%]	80
	Turbine mechanical efficiency [%]	99.6
Solid oxide fuel cell	Temperature [°C]	910
	Pressure [bar]	1.08
	Fuel utilisation [%]	85
Reference conditions (Zhang et al., 2005)	Fuel composition [$\%_{vol}$] (H_2:67.0; CO:22.0; H_2O:11.0)	
	Fuel utilisation, U_f [%]	85
	Air utilisation, U_a [%]	25
	Temperature, T_{ref} [°C]	1000
	Pressure, P_{ref} [bar]	1
	Ratio H_2 and H_2O partial pressures, $P_{\boldsymbol{H_2},ref}/P_{\boldsymbol{H_2O},ref}$	0.15
	O_2 partial pressure at cathode, $P_{O_2,ref}$	0.164
Fresh material (Hanak et al., 2017)	Limestone composition [$\%_{wt}$] ($CaCO_3$:95.0; $MgCO_3$:3.5; SiO_2:0.6; Fe_2O_3:0.4; Al_2O_3:0.5)	
Fuel (Hanak et al., 2017)	Natural gas composition [$\%_{vol}$] (CH_4:93.1; C_2H_6:3.2; C_3H_8:0.7, C_4H_{10}:0.4; CO_2:1.0; N_2 :1.6)	

As this study aims to compare the techno-economic performance of two different CCS implementation routes in a pulp and paper plant, the three BLG alternatives were evaluated using a common design basis. The integration of CaL with BLG is represented in detail in Figure 4-4. This study considers the entrained flow gasifier (*RGibbs*) that operates at elevated pressure and temperature, and uses oxygen as the gasifying agent. The concentrated black liquor is gasified at 30 barg and 1050 °C. At such conditions, the main components of the syngas are H_2, CO_2 and CO (Figure 4-3). This temperature is controlled by the flowrate of the gasifying agent, for example, the oxygen obtained from the ASU. The gasifier is equipped with a quench section that enables the separation of the hot gas from the inorganic smelt (Jafri et al., 2016), which leaves the gasifier as green liquor and is returned to the Kraft process. The hot and pressurised gas is then expanded in a turbo-expander that is coupled with a generator to produce electricity. The CO_2 capture takes place in a secondary carbonator called WGS carbonator (*RGibbs*). This layout presents some benefits over SEG. Since the system comprises the solids circulation between the interconnected carbonator and calciner, their operation at different pressures would not be desirable. Furthermore, if CaL is to operate at elevated pressure, the carbonator and the calciner will need to operate at higher temperatures. This will lead to enhanced sorbent degradation. Therefore, in the system comprising a separate gasifier and carbonator, the gasifier pressure and temperature can be increased as it is not restricted by the operating conditions of a carbonator (i.e. atmospheric pressure and 650 °C). This is particularly important in BLG because at a low temperature (600 °C), around 90% of the sulphur is gasified, producing H_2S in the gas phase. This affects the lime kiln balance since more Na is available as Na_2CO_3 (Larson, Consonni and Katofsky, 2003). In this study, the WGS carbonator is integrated in parallel with another carbonator that captures the CO_2 from the flue gas produced in power and biomass boilers. As can be seen in Figure 4-4, the carbonation reaction, represented by Eq. (4-2), occurs in both carbonators. The CaO stream is split to achieve a CO_2 capture rate of 90% in both carbonators. Because CO_2 is captured in the WGS carbonator, the water-gas shift reaction (WGSR), Eq. (4-3), is enhanced and a higher H_2 yield is achieved. Both $CaCO_3$ streams are

then fed to a single calciner, where $CaCO_3$ is decomposed to CaO and a high-purity stream of CO_2 on heating, Eq. (4-1).

Water Gas Shift: **(4-3)**

$$CO(g) + H_2O\ (g) \leftrightarrow CO_2(g) + H_2(g)\ \Delta H = \pm 40.9\ kJ/mol$$

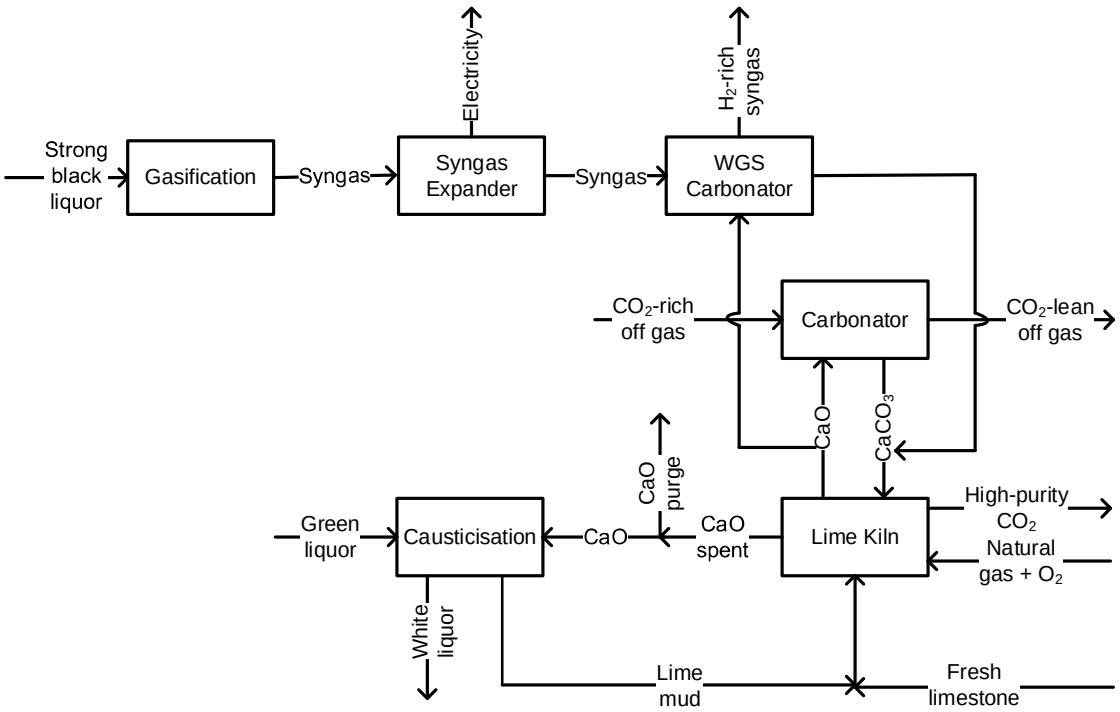

Figure 4-4: Detailed representation of calcium looping integration in the Kraft process for syngas upgrading

4.2.3.1 Retrofitted pulp and paper plant with calcium looping and BLG integrated with H_2 production

The H_2-rich syngas, along with the CO_2-lean off gas and high-purity CO_2 streams, are integrated in a heat exchanger network for steam production. The low-temperature H_2-rich syngas is then purified from H_2S (*Sep*), the sulphur is recovered in the Claus plant, and all the other minor contaminants in the PSA unit (*Sep*). Although the PSA unit was not modelled in detail, it was assumed that it is a multi-column process that achieves 99.99% purity of H_2 with a recovery of 52.11% (Ribeiro et al., 2008). In this case (Case 3), two scenarios were considered, H_2 compression (*MComp*) at 700 bar, transportation and storage (Case 3a) and H_2 available for immediate delivery at 60 bar (Case 3b). The latter

assumes integration of the pulp and paper plant in an industrial hub with H_2 used as feedstock in the nearby industries. The conceptual design of this case is presented in Figure 4-5 and the operating conditions are reported in Table 4-3. It should be noted that the carbonators and calciner are represented by CaL block in Figure 4-5.

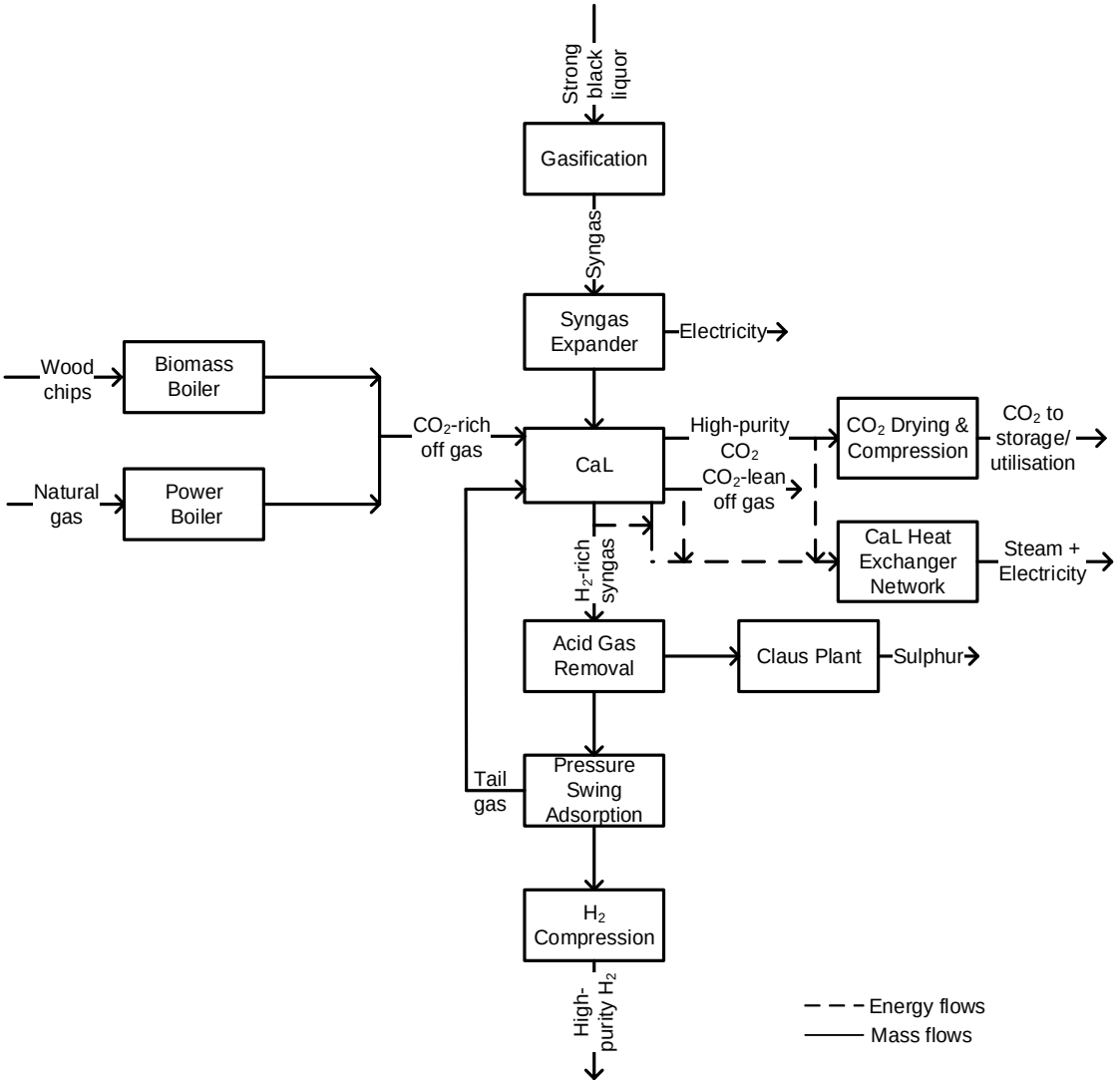

Figure 4-5: Simplified diagram of calcium looping and black liquor gasification integrated with H_2 production (Case 3)

4.2.3.2 Retrofitted pulp and paper plant with calcium looping and BLG integrated with GT combined cycle

In Case 4a, the H_2-rich syngas after H_2S removal is combusted in the gas turbine combustor (*RGibbs*). As a result of H_2 combustion in the air, the resulting

temperature of the flue gas is close to the adiabatic flame temperature (2229 °C). It should be mentioned that the remainder of the steam produced in the heat exchanger network of CaL is expanded in a small steam turbine and fed to the combustor to increase the mass flowrate of the stream entering the expander. The exhaust gas is then mixed with bleed air from the air compressor (*Comp*) to moderate the turbine inlet temperature to 1268 °C. In the expander, the exhaust gas is expanded from 20 to 1 bar, generating electricity. This stream is then cooled in a heat exchanger, preheating the water for the steam turbine and thus, further contributing to generation of electricity. The schematic representation of this case and the operating conditions are given in Figure 4-6 and Table 4-3, respectively.

4.2.3.3 Retrofitted pulp and paper plant with calcium looping and BLG integrated with SOFC

Another case assessed in this work considers that the chemical energy of the H_2-rich syngas is converted to electricity in a solid-oxide fuel cell (SOFC) (Case 4b). Figure 4-6 presents a simplified diagram of this case. The operating conditions are summarised in Table 4-3.The heat available in the exhaust gas leaving the SOFC is then used to preheat water for steam production. This steam, along with the remaining steam generated in the CaL heat exchanger network, is expanded in the steam turbine for electricity generation. The SOFC process model was modelled in Aspen Plus® based on the model developed by Zhang et al. (2005) and Doherty et al. (2010). This model is described in detail and validated in Matuszny et al. (2020).

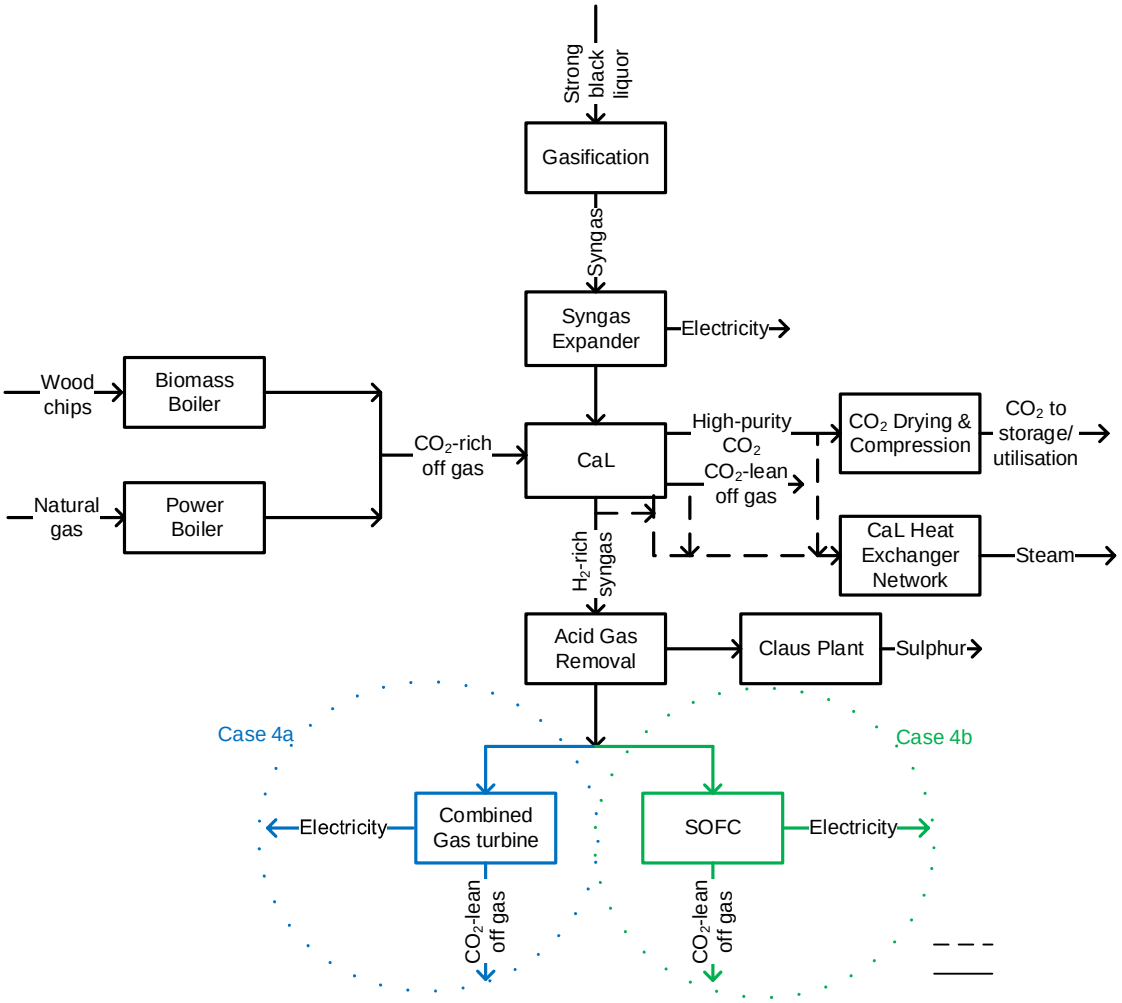

Figure 4-6: Simplified diagram of calcium looping and black liquor gasification integrated with gas turbine combined cycle (Case 4a) or integrated with solid-oxide fuel cell (Case 4b)

4.3 Techno-economic analysis

4.3.1 Parameters for thermodynamic assessment

The CCS and BLG cases presented above were compared with the reference case without carbon capture (Case 1), considering equivalent efficiency, gross power efficiency and net power efficiency as the key thermodynamic performance indicators.

The equivalent efficiency, Eq. (4-4), is defined as the ratio of the total useful energy outputs and the total energy inputs. The latter is defined as the total fuel consumed (natural gas, wood and black liquor) and, depending on the cases, the

electricity imported. An electric efficiency of 45.9% is assumed to represent the electricity imported in terms of the fuel chemical energy input (De Lena et al., 2019). In this study, the equivalent efficiency uses the lower heating value to represent the energy content of fuels. The total useful energy outputs is represented as the sum of process steam produced in the system, net power output and, in Case 3, the chemical energy of high-purity H_2. In order to achieve a fair comparison, it is assumed that H_2 fuel cell with an electric efficiency of 47.9% (80% utilisation of H_2 and operating fuel cell voltage of 0.75 V) is used to convert H_2 into electricity (Mitsushima, Gollas and Hacker, 2018). Moreover, the energy available in the produced process steam was converted to electricity by assuming an electric efficiency of 45.9% (De Lena et al., 2019).

$$Equivalent\ efficiency = \frac{Total\ useful\ energy\ outputs}{Total\ energy\ inputs} \quad \textbf{(4-4)}$$

The gross power efficiency, Eq. (4-5), is defined as the ratio of the gross power output and the total energy inputs. The former is defined as the total power output of the integrated pulp and paper plant, considering the electricity produced in the expanders and steam cycle.

$$Gross\ power\ efficiency = \frac{Gross\ power\ output}{Total\ energy\ inputs} \quad \textbf{(4-5)}$$

The net power efficiency, Eq. (4-6), is defined as the ratio of the net power output and the total energy inputs. The difference between the gross power output and the net power output is that the latter accounts for the power requirement by the auxiliary equipment in the integrated pulp and paper plant.

$$Net\ power\ efficiency = \frac{Net\ electric\ power\ output}{Total\ energy\ inputs} \quad \textbf{(4-6)}$$

4.3.2 Parameters for economic assessment

Similarly to the thermodynamic assessment, three economic performance indicators were selected to assess the economic performance. This study uses the levelised cost of pulp (*LCOP*), the levelised cost of newsprint (*LCON*) and the cost of CO_2 avoided (*AC*) to quantify the economic performance of the considered

cases (Santos, Manovic and Hanak, 2021). The levelised costs of products were estimated using the net present value method (*NPV*), presented in Eq. (4-7). The levelised costs correspond to the minimum prices for pulp and newsprint at which the NPV is zero. Under such condition, the project breaks even and the capital and operating costs associated with the specific case of the pulp and paper plant are equal to the revenues from the sales of the main products (pulp and newsprint) and by-products (electricity or hydrogen).

$$NPV = \sum_{t=1}^{n} \frac{CF_t}{(1+r)^t} - TCR \quad \textbf{(4-7)}$$

In Eq. (4-7), the discounted cash flow (CF_t) is estimated over the project lifetime (t), assuming a fixed project interest rate (r) and considering the total capital requirement (TCR). These parameters and other economic assumptions are presented in Table 4-4. Since inflation was not considered in this study, the material and feedstock prices, besides the market price of pulp and newsprint, were fixed during the project lifetime.

4.3.3 Cost estimation for the reference plant

The economic data reported by Onarheim et al. (2017b) was used to estimate the total capital investment and the operating costs of the reference plant. The capital cost was rescaled using the empirical correlation given by Eq. (4-8) where C represents the actual capital cost and S the scaling capacity factor. The reference value is denoted by the subscript 0. For capacity correction, a cost exponent (n) of 0.6 was assumed. The adopted economic methodology to estimate the capital and operating costs of the reference plant has been described in detail in Santos et al. (2021).

$$\frac{C}{C_0} = \left(\frac{S}{S_0}\right)^n \quad \textbf{(4-8)}$$

Table 4-4: Economic model assumptions

Parameter	Value
BLG-CaL	
CaL fixed operating costs [€] (Martínez et al., 2014a; Yang et al., 2010)	1.0% of TPC_{CaL}
CaL variable operating costs [€] (Martínez et al., 2014a; Yang et al., 2010)	2.0% of TPC_{CaL}
BLG fixed and variable operating costs [€] (Andersson et al., 2016)	4.0% of TPC_{BLGU}
Gas cleaning fixed operating costs [€]	1.0% of TPC_{GC}[7]
Gas cleaning variable operating costs [€]	2.0% of TPC_{GC}[7]
Unit cost of electricity exported to the grid [€/MW_{el}h] (Onarheim et al., 2017b)	40.0
Unit cost of electricity imported from the grid [€/MW_{el}h] (BEIS, 2019)	87.3
Natural gas unit cost [€/GJ] (Perry, Green and Maloney, 2007)	3.0
Limestone unit cost [€/t] (Lisbona et al., 2010; Martínez et al., 2014a; Yang et al., 2010)	6.0
CO_2 transport and storage cost [€/t_{CO_2}] (Romano et al., 2012)	7.0
Piping and integration costs indicator [%] (Michalski, Hanak and Manovic, 2019)	5.0
Others	
Expected lifetime [y] (Martínez et al., 2014a; Yang et al., 2010)	25.0
Project interest rate [%] (Martínez et al., 2014a; Yang et al., 2010)	8.8
Capacity factor [%] (Martínez et al., 2014a; Yang et al., 2010)	80.0
Average USD/EUR exchange rate 2017 (Bank of England, 2019)	0.8898
Average GBP/EUR exchange rate 2017 (Bank of England, 2019)	1.1418
H_2 sale price [€/kg_{H_2}] (Eichman, Townsend and Melaina, 2016)	2.0

4.3.4 Cost estimation for CCS retrofit to reference plant

This work assesses the techno-economic performance of four CCS cases based on CaL and compares it with that of the reference case (Case 1). The economic evaluation carried out for Case 2 has been described in detail in Santos et al. (2021). Table 4-4 details the economic assumptions and prices used to account for the operating costs, whose for CaL do not include limestone and natural gas costs or the CO_2 transport and storage cost. Nevertheless, these were accounted

7 In Case 3 this cost includes the costs associated with H_2 purification (PSA)

for in the economic assessment. The *CEPCI* was used to estimate the price level of 2017 (CEPCI, 2020). If a different currency was used, an exchange rate of 0.8898 USD/EUR and 1.1418 GBP/EUR was assumed. The following economic assessment procedure applies to Case 3 and Case 4. In addition to the costs of CaL (C_{CaL}) and the BLG unit (C_{BLGU}), the total capital requirement of the capture plant, Eq. (4-9), also comprises the ASU cost (C_{ASU}), the CO_2 compression unit cost (C_{CCU}), the costs associated to the steam production (C_{SC}), the cost of gas cleaning (C_{GC}) and depending on the case, the cost associated with H_2 production and electricity generation by GT or SOFC (C_{Case_i}).

$$TCR_{cap} = C_{CaL} + C_{BLGU} + C_{ASU} + C_{CCU} + C_{GC} + C_{SC} + C_{Case_i} \quad \textbf{(4-9)}$$

As shown in Table 4-5, the O_2 flowrate and the brake power requirement were used to scale the C_{ASU} and C_{CCU}, respectively. The capital cost of CaL, BLGU, GC, SC and the costs associated with the GT, SOFC and H_2 production were estimated based on the sum of the costs of each component, given by Eq. (4-10) to Eq. (4-16). Except for C_{SC}, all the other costs account for the costs associated with piping and integration by assuming a cost indicator ($i_{P\&C}$) of 5% (Michalski, Hanak and Manovic, 2019). As the BLG conditions and the CO_2 capture rate is the same for the three cases (Case 3-4), the CaL, BLGU and GC capital costs are the same.

$$C_{CaL} = (1 + i_{P\&C})(C_{calc} + C_{carb} + C_{FP} + C_{Fan} + C_{OXPH}) \quad \textbf{(4-10)}$$

$$C_{BLGU} = (1 + i_{P\&C})(C_{BLG} + C_{carb} + C_{SGE}) \quad \textbf{(4-11)}$$

$$C_{GC} = (1 + i_{P\&C})(C_{AGR} + C_{Claus}) \quad \textbf{(4-12)}$$

Besides the common capital costs, the H_2 production route also includes the costs associated with H_2 purification in PSA, C_{PSA}, and compression. To represent H_2 storage at 700 bar, the capital cost for compression to 700 bar, $C_{H_2StorComp}$, and storage, C_{H_2PV} were considered. To represent H_2 transportation at 60 bar, the capital cost for compression to 60 bar, C_{H_2Comp}, is accounted for, while the term C_{H_2PV} in Eq. (4-13) is eliminated.

$$C_{Case_3} = (1 + i_{P\&C})\left(C_{PSA} + C_{H_2StorComp} + C_{H_2PV}\right) \quad \textbf{(4-13)}$$

As shown in Eq. (4-14), the sum of a GT cost, C_{GT}, a steam turbine cost, C_{SST}, and a fuel compressor cost, C_{FC}, constitutes the capital cost associated with electricity generation in Case 4a.

$$C_{Case_{4a}} = (1 + i_{P\&C})(C_{GT} + C_{SST} + C_{FC}) \quad \textbf{(4-14)}$$

In Case 4b, the capital cost was estimated using Eq. (4-15) which, accounts for the individual cost of a SOFC stack, C_{SOFC}, and a DC/AC inverter, $C_{SOFC,DC/AC}$, an air compressor, C_{ArC}, and a fuel compressor, C_{FC}. In addition, 1% of the capital cost of the SOFC stack was also included for auxiliaries.

$$C_{Case_{4b}} = (1 + i_{P\&C})\left(C_{SOFC} + C_{SOFC,DC/AC} + C_{SOFC,aux} + C_{ArC} + C_{FC}\right) \quad \textbf{(4-15)}$$

The capital cost of the heat exchanger network, C_{SC}, is also estimated based on the individual cost of each component, as shown in Eq. (4-16). Because heat from the exhaust gas leaving the GT and SOFC is recovered to produce additional steam in the steam turbine island, the extra capital cost for two heat exchangers is accounted for. The correlations used to estimate these costs are summarised in Table 4-5.

$$C_{SC} = C_{HPW} + C_{ECON} + C_{LS} + C_{COND} + C_{HRSG} \quad \textbf{(4-16)}$$

The cost of CO_2 avoided (AC), represented by Eq. (4-17), depends on the levelised costs of pulp and newsprint, on the equivalent CO_2 emissions ($e_{CO_2,eq}$) of the reference and retrofitted plants and on the annual production rates, $\dot{m}_{Pulp}$ and $\dot{m}_{News}$.

$$AC = \frac{\left[\dot{m}_{Pulp}\frac{LCOP}{(\dot{m}_{Pulp}+\dot{m}_{News})} + \dot{m}_{News}\frac{LCON}{(\dot{m}_{Pulp}+\dot{m}_{News})}\right]_{cap} - \left[\dot{m}_{Pulp}\frac{LCOP}{(\dot{m}_{Pulp}+\dot{m}_{News})} + \dot{m}_{News}\frac{LCON}{(\dot{m}_{Pulp}+\dot{m}_{News})}\right]_{ref}}{e_{CO_2,eq,ref} - e_{CO_2,eq,cap}} \quad \textbf{(4-17)}$$

The equivalent CO_2 emissions ($e_{CO_2,eq}$), Eq. (4-18), accounts for the direct (e_{CO_2}) and indirect ($P_e \cdot e_{CO_2,e}$) CO_2 emissions. Since the indirect emissions are associated with the power generation of the imported electricity (P_e), they depend on the specific CO_2 emissions emitted by the power plant ($e_{CO_2,e}$). This figure was

estimated based on the average power generation, excluding the combined heat and power (CHP), in the UK and the 27 EU Member States in 2015 (η_e = 45.9% and $e_{CO_2,e}$ = 262 $kg_{CO_2}/MW_{el}h$) (De Lena et al., 2019). The direct and indirect CO_2 emissions considered in this study account only for the CO_2 released to the atmosphere as a result of the process operation and the CO_2 emissions associated with the energy carrier, respectively, following the approach by De Lena et al. (2019).

$$e_{CO_2,eq} = e_{CO_2} + Pe \cdot e_{CO_2,e} \quad \textbf{(4-18)}$$

If there is a surplus of electricity generated in the integrated pulp and paper plant, meaning that the retrofitted plant sells electricity to the electric grid, the indirect CO_2 emissions are deducted from the equivalent CO_2 emissions (De Lena et al., 2019).This has a favourable impact on the *AC.*

Table 4-5: Summary of cost correlations used for capital cost estimation

Unit operation	Cost Correlation
Gasification unit [BL flowrate, , $\dot{m}_{BL}$ (t/d)] (Ekbom et al., 2003)	$C_{BLG} = 63.1e6\left(\frac{\dot{m}_{BL}}{3420}\right)^{0.7}$
Syngas expander [Brake power output, $\dot{W}_{SGE,BRK}$ (kW_{el})] (Manzolini, Macchi and Gazzani, 2013)	$C_{SGE} = 33.7e6\left(\frac{\dot{W}_{SGE,BRK}}{200000}\right)^{0.67}$
Acid gas removal [Dry gas flowrate, $\dot{m}_{DG}$ (kg/s)] (Ekbom et al., 2003)	$C_{AGR} = 26.3e6\left(\frac{\dot{m}_{DG}}{37}\right)^{0.7}$
Claus sulphur plant [BL flowrate, $\dot{m}_{BL}$ (t/d)] (Ekbom et al., 2003)	$C_{Claus} = 6.6e6\left(\frac{\dot{m}_{BL}}{3420}\right)^{0.7}$
Air separation unit [O_2 production rate, $\dot{m}_{O2}$ (kg/s)] (Atsonios et al., 2013)	$C_{ASU} = 2.926e7\left(\frac{\dot{m}_{O2}}{28.9}\right)^{0.7}$
CO_2 compression unit [Brake power requirement, $\dot{W}_{CCU,BRK}$(kW_{el})] (Kreutz et al., 2005a)	$C_{CCU} = 1.22914e7\left(\frac{\dot{W}_{CCU,BRK}}{13000}\right)^{0.67}$
Heat exchanger high-pressure water [Heat exchange area, A_{HPW} (m^2)] (Lee et al., 2014)]	$C_{HPW} = 130\left(\frac{A_{HPW}}{0.093}\right)$
Economiser [Heat exchange area, A_{ECON} (m^2)] (Lee et al., 2014)	$C_{ECON} = 130\left(\frac{A_{ECON}}{0.093}\right)$
Heat exchanger live steam [Heat exchange area, A_{LS} (m^2)] (Shirazi et al., 2012)	$C_{LS} = 2290(A_{LS})^{0.6}$
Heat exchanger condensate [Heat exchange area, A_{COND} (m^2)] (Lee et al., 2014)	$C_{COND} = 130\left(\frac{A_{COND}}{0.093}\right)$
Heat recovery steam generator [Heat exchange area, A_{HRSG} (m^2)] (Lee et al., 2014)	$C_{HRSG} = 130\left(\frac{A_{HRSG}}{0.093}\right)$
Oxygen preheater [Heat exchange area, A_{OXPH} (m^2)] (Lee et al., 2014)	$C_{OXPH} = 130\left(\frac{A_{OXPH}}{0.093}\right)$
Calciner [Calciner heat flux, $\dot{Q}_{calc}$ (kW_{th})] (Michalski, Hanak and Manovic, 2019)	$C_{calc} = 13140\ (\dot{Q}_{cal})^{0.67}$
Carbonator [Carbonator heat flux, $\dot{Q}_{carb}$ (kW_{th})] (Michalski, Hanak and Manovic, 2019)	$C_{carb} = 16591\ (\dot{Q}_{carb})^{0.67}$
Fuel preparation system [Fuel flowrate $\dot{m}_F$ (kg/s)] (Michalski, Hanak and Manovic, 2019)	$C_{FP} = 14158479\ (\dot{m}_F)^{0.24}$
Fan [Brake power requirement, $\dot{W}_{Fan,BRK}$ (kW_{el})] (Michalski, Hanak and Manovic, 2019)	$C_{Fan} = 103193\left(\frac{\dot{W}_{Fan,BRK}}{445}\right)^{0.67}$
Pressure swing adsorption unit [Inlet gas molar flowrate, $\dot{n}_{PSA}$ (kmol/h)] (Spallina et al., 2016)	$C_{PSA} = 27.96e6\left(\frac{\dot{n}_{PSA}}{17069}\right)^{0.6}$
H_2 compressor [Brake power requirement, $\dot{W}_{H_2,BRK}$ (kW_{el})] (Spallina et al., 2016)	$C_{H_2Comp} = 1200\left(\frac{\dot{W}_{H_2,BRK}}{0.746}\right)^{0.82}$
H_2 storage compressor [Brake power requirement, $\dot{W}_{H_2Stor,BRK}$ (kW_{el})] (Ni, 2006)	$C_{H_2StorComp} = 80\ \dot{W}_{H_2Stor,BRK}$
H_2 pressure vessel [H_2 mass, m_{H_2Stor} (kg)] (Ni, 2006)	$C_{H_2PV} = 40\ m_{H_2Stor}$
Gas turbine [Inlet air flowrate, $\dot{m}_{Air}$ (kg/s)] (DOE/NETL, 2014)	$C_{GT} = 31.5e6\left(\frac{\dot{m}_{Air}}{209}\right)^{0.85}$
Small steam turbine [Brake power output, $\dot{W}_{SST,BRK}$ (kW_{el})] (DOE/NETL, 2010)	$C_{SST} = 1.71e6\left(\frac{\dot{W}_{SST,BRK}}{1.65}\right)^{0.67}$
Solid-oxide fuel cell stack [Active area, A_{SOFC} (m^2); Operating temperature, T_{SOFC} (K)] (Shirazi et al., 2012)	$C_{SOFC} = A_{SOFC}(2.96T_{SOFC} - 1907)$

Unit operation	Cost Correlation
DC-to-AC inverter [Rated power output, $\dot{W}_{SOCF,DC}$ (kW_{el})] (Shirazi et al., 2012)	$C_{SOFC,DC/AC} = 1e5\left(\frac{\dot{W}_{SOCF,DC}}{500}\right)^{0.7}$
Solid-oxide fuel cell auxiliaries [Stack cost, C_{SOFC} (USD)] (Shirazi et al., 2012)	$C_{SOFC,aux} = 0.1\ C_{SOFC}$
Fuel compressor [Brake power requirement, $\dot{W}_{FC,BRK}$ (kW_{el})] (Lee et al., 2014; Shirazi et al., 2012)	$C_{FC} = 91562\left(\frac{\dot{W}_{FC,BRK}}{445}\right)^{0.67}$
Air compressor [Brake power requirement, $\dot{W}_{ArC,BRK}$ (kW_{el})] (Lee et al., 2014; Shirazi et al., 2012)	$C_{ArC} = 91562\left(\frac{\dot{W}_{ArC,BRK}}{445}\right)^{0.67}$

4.4 Results and discussion

4.4.1 Thermodynamic assessment

The key outcomes from the thermodynamic analysis are presented in Figure 4-7. The steam demand of the reference plant, which remained constant for all the cases (132.6 kW_{th}/ADt), was met by a heat recovery steam generator (HRSG) that used the high-grade heat available in CaL. This shows the superior performance of CaL when compared with other CCS technologies, such as physical absorption that require an additional amount of steam to operate, resulting in a steam deficit if BLG is employed (Naqvi, Yan and Dahlquist, 2013). The steam generated in CaL is combined with the steam produced by the power and hog boilers. It is then used to meet the steam requirement of the pulp and paper plant and produce electricity. As shown in the energy balance (Figure 4-7), Case 2 and Case 4b were the only cases with positive net power efficiency. As a result, the pulp and paper plant turned from an electricity importer to an electricity exporter, exporting 5.2 kW_{el}/ADt and 5.7 kW_{el}/ADt, respectively. It is important to note that although Case 4a had the highest gross power efficiency, the power requirement of the retrofitted pulp and paper plant was not fully met, resulting in an electricity deficit. To compensate for this deficit, 6.3 kW_{el}/ADt were imported from the electric grid. This can be explained by the high-power consumption of the fuel gas and air compressors as these needed to be compressed to 20 bar to meet the operating requirements of the gas turbine. It was also found that the case with H_2 production, Case 3a and Case 3b, presented the lowest net power efficiency of around -7.0%. The negative value means that the electricity produced on-site did not meet the total power requirement, and thus, the pulp and paper plant needed to import electricity from the grid. This can be explained

by the power requirement for H_2-enriched syngas purification and H_2 compression for delivery. Besides, electricity generation was penalised. Compression of H_2 at 60 bar, instead of at 700 bar and storage, reduced the specific electricity imported by 3.7%. The reference plant (Case 1) showed the best performance in terms of equivalent efficiency. This can be explained by an additional fuel consumption in CaL that increased the total energy input of the system.

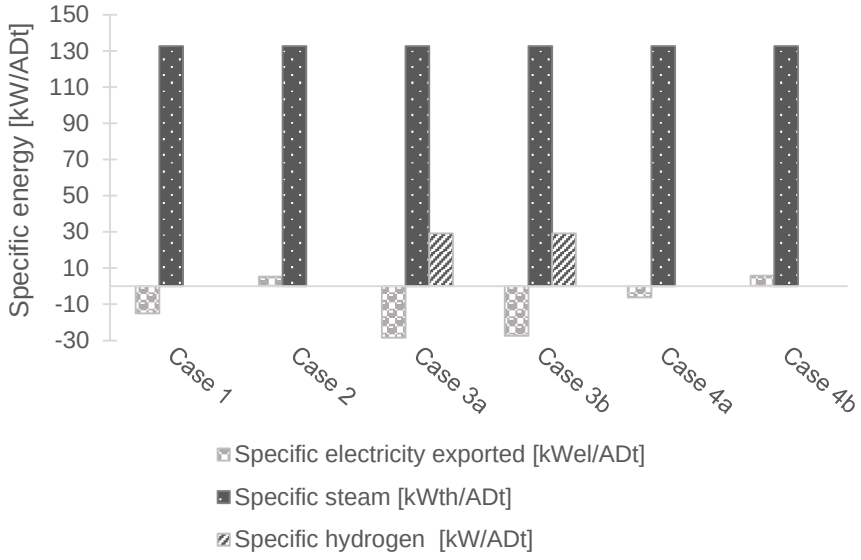

(a)

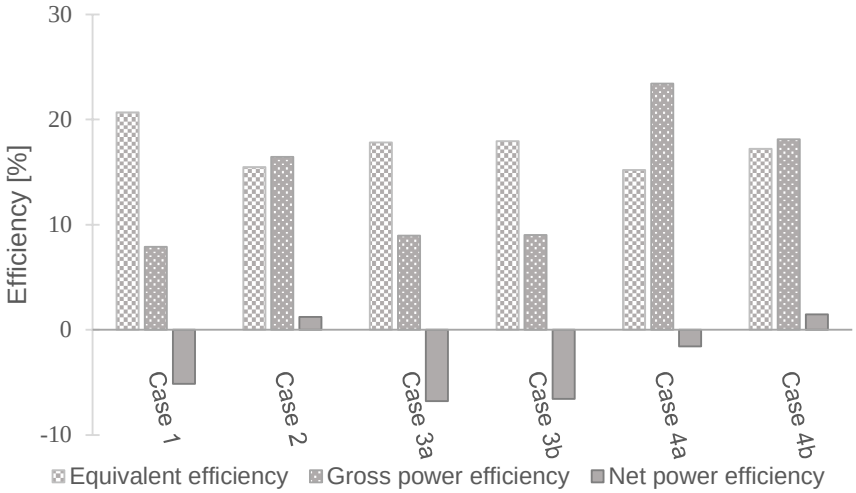

(b)

Figure 4-7: Comparative thermodynamic performance for (a) specific energy: electricity, steam and H_2 and (b) efficiency: equivalent, gross power and net power

4.4.2 Economic assessment

The economic performance assessment (Figure 4-8) has revealed that Case 2 presented the lowest capital cost requirement, resulting in the lowest CO_2 avoided cost (39.0 €/t_{CO_2}), followed by Case 3b (48.8 €/t_{CO_2}). Although Case 3a and Case 3b showed the highest operation and maintenance (O&M) costs, which was around 0.6% higher in Case 3a (413 €/ADt) than in Case 3b (410.6 €/ADt), these costs were compensated by the additional revenue obtained from the H_2 sales. An H_2 sale price of 2 €/kg_{H_2} was assumed, which is a conservative assumption considering the H_2 sale price adopted by Eichman et al. (2016) , (2.7–8.9 €/kg_{H_2}). The O&M costs included the fixed and variable operating costs, the natural gas and limestone costs and, only in Case 3 and Case 4a, the costs associated with electricity import.

Considering the BLG-CaL cases, Case 3 and Case 4b showed lower costs of CO_2 avoided (50.8 €/t_{CO_2}, 48.8 €/t_{CO_2} and 50.8 €/t_{CO_2}, respectively) than that for Case 4a (57.1 €/t_{CO_2}). This can be associated with the additional revenues obtained by the sales of H_2 (Case 3) and electricity (Case 4b). Importantly, the revenues from the pulp and newsprint sales are not represented in Figure 4-8 as these remained the same in all investigated cases. Though the cost of CO_2 avoided is higher in the BLG-CaL cases (Case 3 and Case 4) than that in the CaL retrofit case (Case 2, 39.0 €/t_{CO_2}), it is still comparable to the results reported by Ferreira and Balestieri (2015) and Zhang et al. (2011). Zhang et al. (2011) presented the CO_2 capture costs on the CO_2 captured basis (26.3 €/t_{CO_2} and 40.9 €/t_{CO_2} for oxy-fuel combustion and Selexol, respectively) that are lower than the cost per CO_2 avoided. It should also be noted that figures reported in that study were estimated based on the capital costs reported in 2000 and 2005. The estimated CO_2 avoided cost (20.5 €/t_{CO_2}) by Ferreira and Balestieri (2015) did not account for the cost of CO_2 transport and storage. It also considered a carbon credit for the CO_2 captured of 5.3 €/t_{CO_2}. The costs in their work were also estimated based on capital costs reported in 2005, and therefore, the final cost of CO_2 captured will be underestimated compared to the results presented in this

work. It also needs to be emphasised that in contrast to these studies, which only considered the CO_2 emissions from the BLG, this work considered CO_2 emitted by the entire pulp and paper plant.

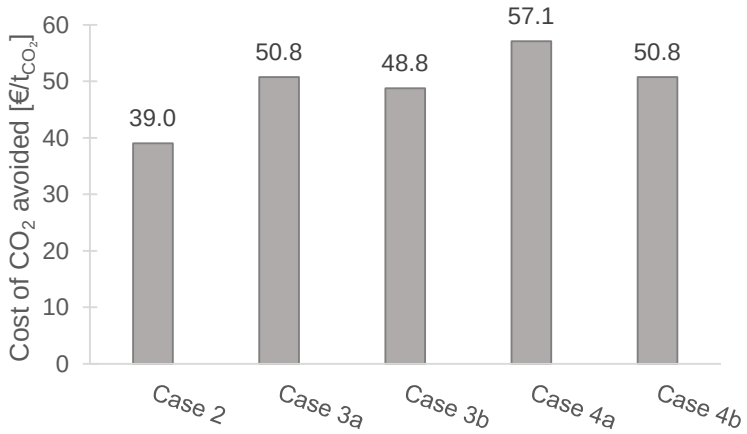

(a)

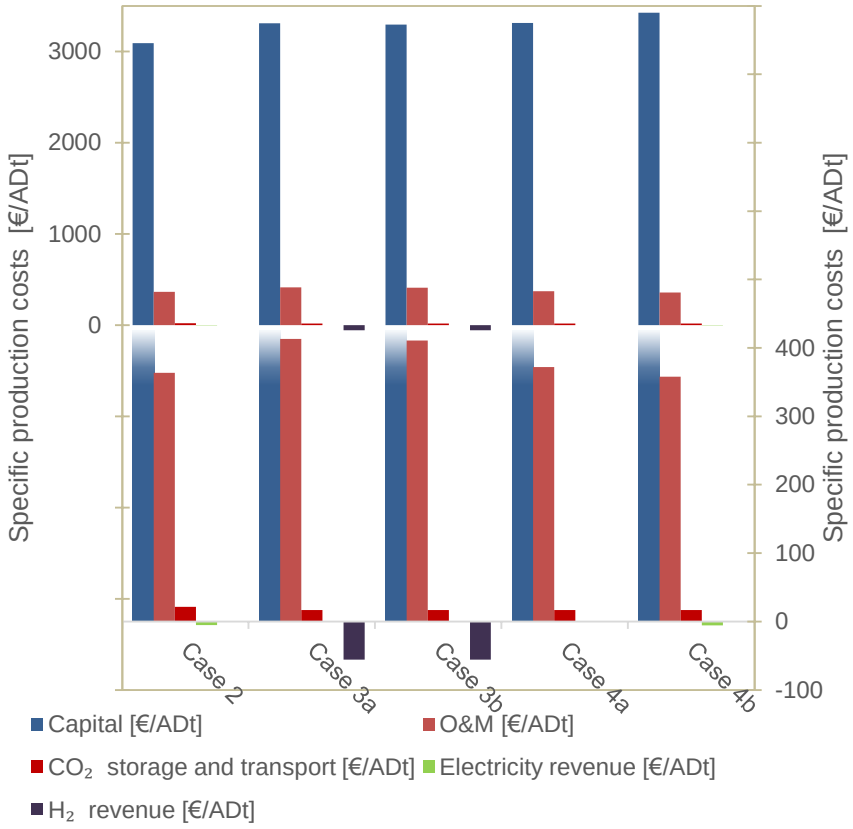

(b)

Figure 4-8: Economic case comparison of: (a) cost of CO_2 avoided and (b) specific production costs

4.4.3 Sensitivity analysis

To assess the dependence of CCS cost on various parameters and account for the uncertainty in the economic analysis, a sensitivity analysis was performed. The baseline figures for capital requirement, fixed and variable costs of BLG-CaL and the prices of H_2, natural gas, limestone, electricity imported, and CO_2 transport and storage were varied by ±25%. The subsequent change in the cost of CO_2 avoided is presented in Figure 4-9. It can be observed that the BLG-CaL capital requirement was the parameter that had a high impact in the investigated cases, changing from ±13.3% to ±17.2% in Case 4a and Case 4b, respectively. In Case 3, besides the BLG-CaL capital requirement, the CO_2 avoided cost is strongly dependent on the H_2 sale price, which in Case 3a had one percentage point higher impact on the CO_2 avoided cost than the BLG-CaL capital requirement. It was observed that a 25% increase of this parameter resulted in a reduction of around 15% in the cost of CO_2 avoided. On the other hand, a 25% reduction in the natural gas price, the second parameter with the highest influence on the CO_2 avoided cost in Case 4, caused a reduction in the cost of CO_2 avoided of 8.2% (Case 4a) and 8.9% (Case 4b), respectively. It should be noted that the reduction in the imported electricity price in Case 4b has a negative impact on the CO_2 avoided because only the reference plant imports electricity. Similarly to Case 2, the change in CO_2 avoided cost does not exceed 2% if the variable costs and limestone price rise 25%.

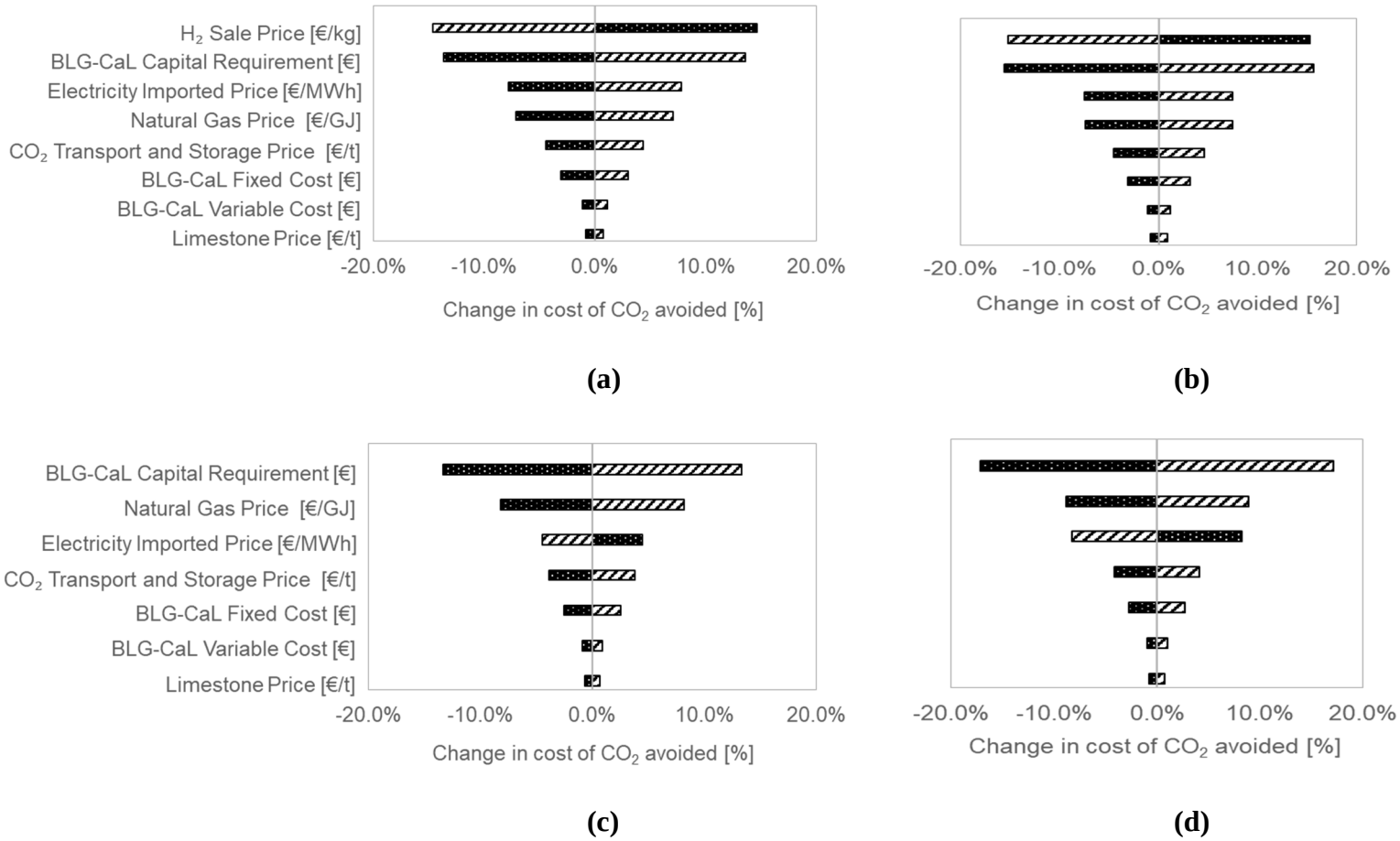

Figure 4-9: Effect of the main economic parameters on the cost of CO_2 avoided for (a) Case 3a, (b) Case 3b, (c) Case 4a and (d) Case 4b. Stripes: +25% of baseline parameter, Bubbles: -25% of baseline parameter

4.5 Conclusions

This study aimed to compare two CCS routes, CaL and BLG-CaL, retrofitted to a pulp and paper plant. Three O_2-blown BLG coupled with CaL were assessed: BLG with H_2 (BLG-CaL-H_2) production, BLG with gas turbine combined cycle (BLG-CaL-GT) or with solid-oxide fuel cell (BLG-CaL-SOFC). The proposed configurations were assessed from the thermodynamic and economic points of view. It was shown that pulp and paper integrated with CaL and integrated with BLG with SOFC showed the best overall performance based on the thermodynamic indicators. In these two cases, the electricity importer reference plant turns into an electricity exporter. From an economic standpoint, the integration of CaL in the reference plant is characterised by the lowest cost of CO_2 avoided, 39.0 €/t_{CO_2}. BLG-CaL was found to be a viable route for CCS; under the initial economic assumptions, BLG-CaL-H_2 presented the lowest cost of CO_2 avoided, 48.8 €/t_{CO_2}, but the highest energy penalty since additional electricity import was required. On the other hand, BLG-CaL-SOFC presented the best net power efficiency, although it also had the highest capital cost requirement, with an estimated cost of CO_2 avoided of 50.8 €/t_{CO_2}. Yet, the techno-economic results could be improved if the operating conditions of black liquor gasification are optimised. The impact of the uncertainty associated to the economic assumptions was also assessed, by varying the natural gas, limestone, electricity imported and H_2 sale prices as well as the costs associated to BLG-CaL. It was found that the capital requirement of BLG-CaL has a strong effect on the cost of CO_2 avoided for all alternatives. In Case 3, this is also strongly affected by the H_2 sale price while in Case 4, by the natural gas price.

4.6 References

Akbari, M., Oyedun, A.O. and Kumar, A. (2018) ‘Ammonia production from black liquor gasification and co-gasification with pulp and waste sludges: A techno-economic assessment’, *Energy*, 151, pp. 133–143.

Andersson, J., Furusjö, E., Wetterlund, E., Lundgren, J. and Landälv, I. (2016) ‘Co-gasification of black liquor and pyrolysis oil: Evaluation of blend ratios and

methanol production capacities', *Energy Conversion and Management*, 110, pp. 240–248.

Andersson, J., Lundgren, J. and Marklund, M. (2014) 'Methanol production via pressurized entrained flow biomass gasification – Techno-economic comparison of integrated vs. stand-alone production', *Biomass and Bioenergy*, 64, pp. 256–268.

Armbrust, N., Duelli, G., Dieter, H. and Scheffknecht, G. (2015) 'Calcium looping cycle for hydrogen production from biomass gasification syngas: Experimental investigation at a 20 kW_{th} dual fluidized-bed facility', *Industrial and Engineering Chemistry Research*, 54(21), pp. 5624–5634.

Atsonios, K., Koumanakos, A., Panopoulos, K.D., Doukelis, A. and Kakaras, E. (2013) 'Techno-economic comparison of CO_2 capture technologies employed with natural gas derived GTCC', *Proceedings of the ASME Turbo Expo*., Vol.2, p. V002T07A018.

Bank of England (2019) *Bank of England Statistical Interactive Database* | *Interest & Exchange Rates* | *Official Bank Rate History*. Available at: http://www.bankofengland.co.uk/boeapps/iadb/repo.asp (Accessed: 5 December 2019).

BEIS (2019) *Industrial electricity prices in the EU*. Business Energy & Industrial Strategy, United Kingdom.

Carlsson, P., Wiinikka, H., Marklund, M., Grönberg, C., Pettersson, E., Lidman, M. and Gebart, R. (2010) 'Experimental investigation of an industrial scale black liquor gasifier. 1. The effect of reactor operation parameters on product gas composition', *Fuel*, 89(12), pp. 4025–4034.

Carvalho, L., Lundgren, J., Wetterlund, E., Wolf, J. and Furusjö, E. (2018) 'Methanol production via black liquor co-gasification with expanded raw material base – Techno-economic assessment', *Applied Energy*, 225, pp. 570–584.

CEPCI (2020) *The Chemical Engineering Plant Cost Index*., *Chemical Engineering* Available at: https://www.chemengonline.com (Accessed: 5

December 2019).

Connell, D.P., Lewandowski, D.A., Ramkumar, S., Phalak, N., Statnick, R.M. and Fan, L.-S. (2013) 'Process simulation and economic analysis of the Calcium Looping Process (CLP) for hydrogen and electricity production from coal and natural gas', *Fuel*, 105, pp. 383–396.

Darmawan, A., Ajiwibowo, M.W., Yoshikawa, K., Aziz, M. and Tokimatsu, K. (2018) 'Energy-efficient recovery of black liquor through gasification and syngas chemical looping', *Applied Energy*, 219, pp. 290–298.

DOE/NETL (2014) *Baseline Analysis of Crude Methanol Production from Coal and Natural Gas*.

DOE/NETL (2010) *Assessment of hydrogen production with CO_2 capture volume 1: baseline state-of- the-art plants*.

Doherty, W., Reynolds, A. and Kennedy, D. (2010) 'Computer simulation of a biomass gasification-solid oxide fuel cell power system using Aspen Plus', *Energy*, 35(12), pp. 4545–4555.

Eichman, J., Townsend, A. and Melaina, M. (2016) *Economic Assessment of Hydrogen Technologies Participating in California Electricity Markets. NREL/TP-5400-65856*.

Ekbom, T., Lindblom, M., Berglin, N. and Ahlvik, P. (2003) *Technical and commercial feasibility study of black liquor gasification with methanol/DME production as motor fuels for automotive uses – BLGMF*. Stockholm, Sweden.

Ferreira, E.T.D.F. and Balestieri, J.A.P. (2015) 'Black liquor gasification combined cycle with CO_2 capture – Technical and economic analysis', *Applied Thermal Engineering*, 75, pp. 371–383.

Fuss, S., Canadell, J.G., Peters, G.P., Tavoni, M., Andrew, R.M., Ciais, P., Jackson, R.B., Jones, C.D., Kraxner, F., Nakicenovic, N., Le Quéré, C., Raupach, M.R., Sharifi, A., Smith, P. and Yamagata, Y. (2014) 'COMMENTARY: Betting on negative emissions', *Nature Climate Change*, 4(10), pp. 850–853.

Gerres, T., Chaves Ávila, J.P., Llamas, P.L. and San Román, T.G. (2019) ‘A review of cross-sector decarbonisation potentials in the European energy intensive industry’, *Journal of Cleaner Production*, 210, pp. 585–601.

Gil, M. V., Fermoso, J., Rubiera, F. and Chen, D. (2015) ‘H_2 production by sorption enhanced steam reforming of biomass-derived bio-oil in a fluidized bed reactor: An assessment of the effect of operation variables using response surface methodology’, *Catalysis Today*, 242, pp. 19–34.

Hanak, D.P., Biliyok, C., Anthony, E.J. and Manovic, V. (2015) ‘Modelling and comparison of calcium looping and chemical solvent scrubbing retrofits for CO_2 capture from coal-fired power plant’, *International Journal of Greenhouse Gas Control*, 42, pp. 226–236.

Hanak, D.P., Jenkins, B.G., Kruger, T. and Manovic, V. (2017) ‘High-efficiency negative-carbon emission power generation from integrated solid-oxide fuel cell and calciner’, *Applied Energy*, 205, pp. 1189–1201.

IEA (n.d.) *The Future of Hydrogen, IEA*. Available at: https://www.iea.org/reports/the-future-of-hydrogen (Accessed: 4 November 2020).

Jafri, Y., Furusjö, E., Kirtania, K. and Gebart, R. (2016) ‘Performance of a Pilot-Scale Entrained-Flow Black Liquor Gasifier’, *Energy & Fuels*, 30(4), pp. 3175–3185.

Kreutz, T., Williams, R., Consonni, S. and Chiesa, P. (2005) ‘Co-production of hydrogen, electricity and CO from coal with commercially ready technology. Part B: Economic analysis’, *International Journal of Hydrogen Energy*, 30(7), pp. 769–784.

Larson, E.D., Consonni, S. and Katofsky, R.E. (2003) *A Cost-Benefit Assessment of Biomass Gasification Power Generation in the Pulp and Paper Industry*. Princeton University, Politecnico Milano, Navigant consulting.

Larson, E.D., Consonni, S., Katofsky, R.E., Iisa, K. and Frederick, W.J. (2006) *A Cost-Benefit Assessment of Gasification-Based Biorefining in the Kraft Pulp and*

Paper Industry.

Lee, Y.D., Ahn, K.Y., Morosuk, T. and Tsatsaronis, G. (2014) 'Exergetic and exergoeconomic evaluation of a solid-oxide fuel-cell-based combined heat and power generation system', *Energy Conversion and Management*, 85, pp. 154–164.

De Lena, E., Spinelli, M., Gatti, M., Scaccabarozzi, R., Campanari, S., Consonni, S., Cinti, G. and Romano, M.C. (2019) 'Techno-economic analysis of calcium looping processes for low CO_2 emission cement plants', *International Journal of Greenhouse Gas Control*, 82, pp. 244–260.

Lisbona, P., Martínez, A., Lara, Y. and Romeo, L.M. (2010) 'Integration of Carbonate CO_2 Capture Cycle and Coal-Fired Power Plants. A Comparative Study for Different Sorbents', *Energy & Fuels*, 24(1), pp. 728–736.

Manzolini, G., Macchi, E. and Gazzani, M. (2013) 'CO_2 capture in natural gas combined cycle with SEWGS. Part B: Economic assessment', *International Journal of Greenhouse Gas Control*, 12, pp. 502–509.

Martínez, A., Lara, Y., Lisbona, P. and Romeo, L.M. (2014) 'Operation of a mixing seal valve in calcium looping for CO_2 capture', *Energy and Fuels*, 28(3), pp. 2059–2068.

Matuszny, K., Borhani, T.N., Nabavi, S.A. and Hanak, D.P. (2020) 'Integration of solid-oxide fuel cells and absorption refrigeration for efficient combined cooling, heat and power production', *Clean Energy*, 4(4), pp. 328–348.

McGrail, B.P., Freeman, C.J., Brown, C.F., Sullivan, E.C., White, S.K., Reddy, S., Garber, R.D., Tobin, D., Gilmartin, J.J. and Steffensen, E.J. (2012) 'Overcoming business model uncertainty in a carbon dioxide capture and sequestration project: Case study at the Boise White Paper Mill', *International Journal of Greenhouse Gas Control*, 9, pp. 91–102.

Michalski, S., Hanak, D.P. and Manovic, V. (2019) 'Techno-economic feasibility assessment of calcium looping combustion using commercial technology appraisal tools', *Journal of Cleaner Production*, 219, pp. 540–551.

Millar, R.J., Fuglestvedt, J.S., Friedlingstein, P., Rogelj, J., Grubb, M.J., Matthews, H.D., Skeie, R.B., Forster, P.M., Frame, D.J. and Allen, M.R. (2017) 'Emission budgets and pathways consistent with limiting warming to 1.5 °C', *Nature Geoscience*, 10(10), pp. 741–747.

Mitsushima, S., Gollas, B. and Hacker, V. (2018) 'Chapter 1 - Introduction', in Hacker, V. and Mitsushima, S. (eds.) *Fuel Cells and Hydrogen*. Elsevier, pp. 1–13.

Müller, C.R., Pacciani, R., Bohn, C.D., Scott, S.A. and Dennis, J.S. (2009) 'Investigation of the enhanced water gas shift reaction using natural and synthetic sorbents for the capture of CO_2', *Industrial and Engineering Chemistry Research*, 48(23), pp. 10284–10291.

Naqvi, M., Yan, J. and Dahlquist, E. (2013) 'System analysis of dry black liquor gasification based synthetic gas production comparing oxygen and air blown gasification systems', *Applied Energy*, 112, pp. 1275–1282.

Ni, M. (2006) 'An overview of hydrogen storage technologies', *Energy Exploration and Exploitation*, 24(3), pp. 197–209.

Öhrman, O., Häggström, C., Wiinikka, H., Hedlund, J. and Gebart, R. (2012) 'Analysis of trace components in synthesis gas generated by black liquor gasification', *Fuel*, 102, pp. 173–179.

Onarheim, K., Santos, S., Kangas, P. and Hankalin, V. (2017) 'Performance and cost of CCS in the pulp and paper industry part 2: Economic feasibility of amine-based post-combustion CO_2 capture', *International Journal of Greenhouse Gas Control*, 66, pp. 60–75.

Perry, R., Green, D. and Maloney, J. (2007) *Perry's chemical engineers' handbook*. USA: New York: McGraw-Hill.

Pettersson, K. and Harvey, S. (2012) 'Comparison of black liquor gasification with other pulping biorefinery concepts – Systems analysis of economic performance and CO_2 emissions', *Energy*, 37(1), pp. 136–153.

Pfeifer, C., Puchner, B. and Hofbauer, H. (2007) 'In-Situ CO_2-Absorption in a Dual Fluidized Bed Biomass Steam Gasifier to Produce a Hydrogen Rich Syngas', *International Journal of Chemical Reactor Engineering*, 5(1)

Ribeiro, A.M., Grande, C.A., Lopes, F.V.S., Loureiro, J.M. and Rodrigues, A.E. (2008) 'A parametric study of layered bed PSA for hydrogen purification', *Chemical Engineering Science*, 63(21), pp. 5258–5273.

Rogelj, J., Popp, A., Calvin, K. V., Luderer, G., Emmerling, J., Gernaat, D., Fujimori, S., Strefler, J., Hasegawa, T., Marangoni, G., Krey, V., Kriegler, E., Riahi, K., Van Vuuren, D.P., Doelman, J., Drouet, L., Edmonds, J., Fricko, O., Harmsen, M., Havlík, P., Humpenöder, F., Stehfest, E. and Tavoni, M. (2018) 'Scenarios towards limiting global mean temperature increase below 1.5 °C', *Nature Climate Change*, 8(4), pp. 325–332.

Romano, M., Martínez, I., Murillo, R., Arstad, B., Bloom, R., Ozcan, D.C., H., A. and Brandani, S. (2012) *11th International Conference on Greenhouse Gas Control Technologies, GHGT 2012*. Kyoto, Japan, pp. 18–22.

Sanna, A. (2014) 'Advanced Biofuels from Thermochemical Processing of Sustainable Biomass in Europe', *Bioenergy Research*, 7(1), pp. 36–47.

Santos, M.P.S., Manovic, V. and Hanak, D.P. (2021) 'Unlocking the potential of pulp and paper industry to achieve carbon-negative emissions via calcium looping retrofit', *Journal of Cleaner Production*, 280, p. 124431.

Shirazi, A., Aminyavari, M., Najafi, B., Rinaldi, F. and Razaghi, M. (2012) 'Thermal–economic–environmental analysis and multi-objective optimization of an internal-reforming solid oxide fuel cell–gas turbine hybrid system', *International Journal of Hydrogen Energy*, 37(24), pp. 19111–19124.

Spallina, V., Motamedi, G., Gallucci, F. and van Sint Annaland, M. (2019) 'Techno-economic assessment of an integrated high pressure chemical-looping process with packed-bed reactors in large scale hydrogen and methanol production', *International Journal of Greenhouse Gas Control*, 88, pp. 71–84.

Spallina, V., Pandolfo, D., Battistella, A., Romano, M.C., Van Sint Annaland, M.

and Gallucci, F. (2016) ‘Techno-economic assessment of membrane assisted fluidized bed reactors for pure H_2 production with CO_2 capture’, *Energy Conversion and Management*, 120, pp. 257–273.

Vogl, V., Åhman, M. and Nilsson, L.J. (2018) ‘Assessment of hydrogen direct reduction for fossil-free steelmaking’, *Journal of Cleaner Production*, 203, pp. 736–745.

Whitty, K. (2005) ‘Black Liquor Gasification: Development and Commercialization Update’, *ACERC Annual Conference*. Provo Utah.

Wiranarongkorn, K. and Arpornwichanop, A. (2017) ‘Analysis of the Ca-looping sorption-enhanced steam reforming and solid oxide fuel cell integrated process using bio-oil’, *Energy Conversion and Management*, 134, pp. 156–166.

Yang, Y., Zhai, R., Duan, L., Kavosh, M., Patchigolla, K. and Oakey, J. (2010) ‘Integration and evaluation of a power plant with a CaO-based CO_2 capture system’, *International Journal of Greenhouse Gas Control*, 4(4), pp. 603–612.

Zhang, G., Yan, J., Jin, H. and Dahlquist, E. (2011) ‘Integrated Black Liquor Gasification Polygeneration System with CO_2 Capture in Pulp and Paper Mills to Produce Methanol and Electricity’, *International Journal of Green Energy*, 8(2), pp. 275–293.

Zhang, W., Croiset, E., Douglas, P.L., Fowler, M.W. and Entchev, E. (2005) ‘Simulation of a tubular solid oxide fuel cell stack using AspenPlus^{TM} unit operation models’, *Energy Conversion and Management*, 46(2), pp. 181–196.

5 TECHNO-ECONOMIC FEASIBILITY ASSESSMENT OF SORPTION-ENHANCED GASIFICATION OF MUNICIPAL SOLID WASTE FOR HYDROGEN PRODUCTION*

Abstract

Waste-to-energy coupled with carbon capture and storage is forecasted to be an effective way to mitigate the greenhouse gas emissions, reduce the waste sent to landfill and, simultaneously, reduce the dependence of fossil fuels. The techno-economic feasibility of sorption-enhanced gasification was evaluated and benchmarked with the conventional gasification of municipal solid waste for H_2 production. The impact of a gate fee and tax levied on the fossil CO_2 emissions in economic feasibility was assessed. The results showed that the hydrogen production was enhanced in sorption-enhanced gasification, that achieved an optimum H_2 production efficiency of 48.7% (*T*=650 °C and *SBR*=1.8). This was 1.0% points higher than that of the conventional steam gasification (*T*=900 °C and *SBR*=1.2). The economic performance assessment showed that the sorption-enhanced gasification will result in a significantly higher levelised cost of hydrogen (5.0 €/kg_{H_2}) compared to that estimated for conventional gasification (2.7 €/kg_{H_2}). The levelised cost of hydrogen can be reduced to 4.5 €/kg_{H_2} on an introduction of the gate fee of 40.0 €/t_{MSW}. The cost of CO_2 avoided was estimated to be 114.9 €/t_{CO_2} (no gate fee and tax levied). However, this value can be reduced to 90.1 €/t_{CO_2} with the introduction of an emission allowance price of 39.6 €/t_{CO_2}. Despite better environmental performance, the capital cost of sorption-enhanced gasification needs to be reduced for this technology to become competitive with mature gasification technologies.

Keywords: Waste-to-energy; modelling; waste management; hydrogen production; CO_2 capture

---

*Santos, M.P.S. and Hanak, D.P. (2022) 'Techno-economic feasibility assessment of sorption-enhanced gasification of municipal solid waste for hydrogen production' *International Journal of Hydrogen Energy*, 47(10), pp. 6586–6604.

5.1 Introduction

Approximately two billion tonnes of MSW are generated worldwide every year. It is forecasted that this figure can reach 3.4 billion tonnes by 2050 (Kaza et al., 2018). The MSW composition varies with the country's economic development, with the developing countries being responsible for the MSW with higher contents of organic matter (Hameed et al., 2021). The UK has reduced the biodegradable municipal waste sent to landfill from 7.4 million tonnes in 2017 to 7.2 millions of tonnes in 2018 (Affairs, 2020). However, in terms of GHG emissions, these still corresponded to 14.4 million tonnes of CO_2 equivalent (Statista, 2021b). Therefore, WtE or waste-to-fuel conversion is a promising route to reduce the amount of waste landfilled. Such processes also have the potential to support a reduction in GHG emissions, reducing the dependence on fossil fuels *via* the production of biofuels, power and/or heat. Therefore, the adoption of clean processes is of paramount importance with economic, environmental and health benefits (Tursi, 2019).

Although H_2 production from different biomass feedstocks can be achieved *via* biological or thermochemical processes, the latter is most attractive as it offers faster process kinetics and leads to higher H_2 yields (Parthasarathy and Narayanan, 2014). Among the main thermochemical routes, biomass gasification offers better results in terms of H_2 yield when compared with pyrolysis (Kırtay, 2011). Biomass conversion into H_2 *via* gasification normally requires temperatures between 700 °C and 1200 °C and a gasifying agent, such as air (Chen et al., 2020a), oxygen (Meng, Meng and Zhang, 2018), steam (Fremaux et al., 2015) or CO_2 (Zheng et al., 2018). The use of pure oxygen rather than air leads to higher H_2 content and higher calorific value of the final product because there is no nitrogen dilution (Udomsirichakorn and Salam, 2014). Steam gasification leads to even higher H_2 yields when compared with O_2 gasification. This can be attributed to the decomposition of water and the WGS and methane reforming reactions (Udomsirichakorn and Salam, 2014). The addition of steam also moves the equilibrium to the right enhancing the H_2 formation.

The products of biomass gasification are tars, chars and syngas. The typical syngas composition includes 30–50%$_{vol}$ of H_2, 25–40%$_{vol}$ of CO, 8–20%$_{vol}$ of CO_2 and 6–15%$_{vol}$ of CH_4, (Arregi et al., 2018). The composition and the H_2 yield depend on the biomass characteristics, gasification operating conditions, use of catalysts and reactor design configurations (Parthasarathy and Narayanan, 2014). It needs to be emphasised that the formation of undesired by-products, such tars and inorganic impurities (H_2S, NH_3 and HCL), is the key drawback of biomass gasification. However, the content of tars, which increase the risk of fouling and blockage in the pipelines and equipment, can be reduced by introducing a catalyst such as Ni nanoparticles embedded carbon nanofiber/porous carbon (Zhang et al., 2021), perovskite (Umar, Neagu and Irvine, 2021) or CaO (Jordan and Akay, 2013). Zhang et al., (2021) have found that the use Ni nanoparticles embedded carbon nanofiber/porous carbon enhanced the tar conversion efficiency to 94.78% at 700 °C. Umar, Neagu and Irvine (2021) have shown that perovskite dopped with nanoparticles alkaline metals can be an effective catalyst on steam reforming of glycerol for H_2 production. Besides, this catalyst has proven to contribute to the fouling reduction. Jordan and Akay (2013) have compared the syngas composition for the process with and without CaO and concluded that H_2 concentration increased from 12.1%$_{vol}$ to 16.5%$_{vol}$ without and with 6%$_{wt}$ CaO, respectively. Furthermore, the carbon nanotubes supported Pt-bimetallic catalysts with CaO have proven to be an effective catalyst for H_2 production from sorption-enhanced aqueous phase reforming of glycerol (He et al., 2015). Since the WGS reaction is favoured in detriment to methanation reaction, the H_2 yield increases and the CH_4 yield reduces.

Importantly, calcium oxide (CaO) is regarded as a promising catalyst and CO_2 sorbent due to its low cost and abundance, and is commonly considered as the sorbent in a carbonate looping technology. The integration of H_2 production and *in-situ* CO_2 capture, called SEG, presents the following benefits: the heat required in endothermic gasification reactions is provided by the exothermic $CaCO_3$ formation reaction and the gasification equilibrium is favourably affected by CaO presence, leading to higher H_2 yields (Perejón et al., 2016).

The concept of SEG for H_2-rich syngas production has been extensively studied and its feasibility proved for different types of biomass, including corn stalk (Li et al., 2017, 2020), palm kernel shell (Khan et al., 2014), sawdust (Acharya, Dutta and Basu, 2010, 2017), sewage sludge (Chen et al., 2020b), wood (Detchusananard et al., 2020; Pitkäoja et al., 2020) and by-product/waste of wine production process (Martínez et al., 2020b). However, only a few publications have studied the feasibility of this technology using MSW as feedstock. He et al. (2009) have evaluated steam MSW SEG for H_2-rich gas production using calcined dolomite as sorbent. The effect of steam/MSW and weight hourly space velocity on gas production and composition were assessed. The experiments were carried out in a laboratory-scale fixed bed reactor at the gasification temperature of 900 °C. Their study found that the catalytic activity of dolomite was enhanced by the steam presence. At steam/MSW of 1.04, the H_2 yield and H_2 mole fraction reached the maximum, 42.98 mol H_2/kg_{MSW} and 53.22%, respectively. Zhou et al. (2014) have studied the steam MSW SEG with CaO as CO_2 sorbent in a batch-type fixed bed. They studied the impact of the gasification temperature and sorbent/ MSW ratio on the H_2 yield. They showed that the H_2 mole fraction was improved on the addition of CaO. At the gasification temperature of 700 °C and with CaO:MSW mass ratio of 1:1, the H_2 mole fraction in the syngas raised from around 35%, without sorbent, to around 50% with CaO. The CaO sorbent has also been shown to have a catalytic effect on the MSW devolatilisation and char gasification. Hu et al. (2015) studied the effect of the moisture content in MSW on H_2 yield using a laboratory-scale fixed bed reactor. Their study showed that the H_2 mole fraction in the syngas achieved a maximum value of 49.4% at the gasification temperature of 750 °C, a molar ratio of CaO to carbon in MSW of 0.7 and a 40% moisture content in MSW. Irfan et al. (2019) have studied the potential of using waste marble powder, whose main component is $CaCO_3$, as a catalyst and CO_2 capture sorbent in the MSW gasification. The effect of temperature, steam/MSW and sorbent/MSW on the gas composition, dry gas yield, tar content and carbon conversion efficiency were investigated in a laboratory-scale batch-type fixed bed reactor. They found the rise of the four variables analysed have a positive effect on the production of H_2-rich gas

resulting in an increase in the H_2 mole fraction, the dry gas yield and the carbon conversion efficiency. On the other hand, the tar content was reduced. Martínez et al. (2020a) have studied the feasibility of MSW SEG for the production of synthetic fuel in a 30 kW_{th} BFB pilot plant. The effect of the gasification temperature, sorbent/MSW ratio and steam excess were also analysed. The gasification temperature was shown to have the most significant influence on the syngas composition. Importantly, for temperatures higher than 680 °C the CaO carbonation is inhibited and the amount of CO_2 captured is limited. As a result, the mole fraction of H_2 decreased and the mole fraction of CO_2 increased at temperatures above 680 °C. Their study also showed that higher contents of tar (mainly benzene and toluene) were produced than that reported in the other studies using a dual fluidised bed (DFB) (Hawthorne et al., 2012; Müller et al., 2017). They concluded that such enhanced tar formation could be associated with the limited low amount of sorbent present in the freeboard zone of BFB and therefore, the tar formation was promoted. However, this drawback would be overcome by a cyclic operation, where the BFB is connected to the calciner as this set-up operates at higher sorbent/MSW ratios, reducing the tar formation (Martínez et al., 2020a).

The feasibility assessments of SEG presented in the literature focused mainly on characterising the CO_2 capture rate and syngas composition associated with this type of gasification technology (Table 5-1). However, a comprehensive energy analysis, which would determine the heat required for the regeneration of CaO sorbent for the cyclic operation of MSW SEG, was not performed. Though SEG has to be shown a technically feasible option for converting MSW into valuable products, such as H_2, its commercialisation depends on the H_2 production costs. The H_2 production costs based on SEG of biomass were assessed for the first time by Schweitzer et al. (2018), which reported values between 6 €/kg_{H_2} and 10 €/kg_{H_2}. However, to date no techno-economic assessment was performed for the SEG of MSW.

Therefore, this study aimed to evaluate the techno-economic feasibility of H_2 production through SEG of MSW using steam as a gasifying agent. To

understand the benefits of SEG, this study benchmarked the techno-economic performance of SEG with conventional steam gasification of MSW. A parametric study was also performed to understand the impact of the steam-to-biomass ratio (*SBR*; both technologies) and the gasification temperature (conventional steam gasification only) on the thermodynamic performance. The impact of the economic assumptions on the economic performance was also assessed.

Table 5-1: Literature cases on sorption-enhanced gasification of municipal solid waste

Literature Case	This work	He et al. (2009)	Zhou et al. (2014)	Hu et al. (2015)	Irfan et al. (2019)	Martínez et al. (2020a)
Feedstock	MSW	MSW	MSW (refused-derived fuels)	MSW	MSW	MSW-derived
Catalyst/sorbent	Limestone	Dolomite	CaO	CaO	Waste marble power	Limestone
Agent gasifying	Steam	Steam	Steam	Steam[8]	Steam	Steam
Reactor type	Dual Fluidised bed	Laboratory-scale fixed bed	Laboratory-scale batch-type fixed bed	Laboratory-scale fixed bed	Laboratory-scale batch-type fixed bed	30 kW_{th} bubbling fluidised bed
Production	H_2	Syngas	Syngas	Syngas	Syngas	Syngas
Work type	Theoretical	Experimental	Experimental	Experimental	Experimental	Experimental
Sorbent regeneration	Yes	N/A	N/A	N/A[9]	N/A	N/A
Thermodynamic analysis	Yes	N/A	N/A	N/A	N/A	N/A
Economic analysis	Yes	N/A	N/A	N/A	N/A	N/A

8 Auto generated steam from MSW moisture

9 Not assessed but a new cyclic process for direct gasification of wet MSW was proposed

5.2 Process and model description

This study benchmarked the techno-economic performance of two WtE conversion processes, conventional steam gasification without CO_2 capture and SEG with CO_2 capture. The MSW properties were taken from Wang et al. (2012), and the main properties, such as lower heating value (LHV), moisture content, ultimate and proximate analysis are presented in Table 5-2. The considered processes were assumed to have a processing capacity of 500 t/d of MSW, which translates to around 100 MW_{th} fuel input. The process models for the considered WtE conversion processes were modelled in Aspen Plus®. The following assumptions were considered in both models:

- the process is steady state, isothermal with temperature and pressure uniformity;
- all the gases are ideal;
- char consists only of carbon;
- ash is inert and does not take part in any reactions; and
- tar and higher hydrocarbon formation is not considered.

Table 5-2: Ultimate and proximate analysis of municipal solid waste (Wang et al., 2012)

Properties	Value
LHV[10] [MJ/kg]	19.99
Moisture content [$\%_{wt}$]	9.34
Ultimate Analysis [$\%_{wt,db}$[11]]	
Elemental composition	C:49.51; H:6.42; O:35.69; N:0.78; S:0.48
Proximate Analysis [$\%_{wt,db}$[11]]	
Volatile matter	77.52
Fixed carbon	15.36
Ash	7.12

10 Lower heating value

11 Dry basis

The Peng-Robinson equation of state with Boston-Mathias modifications was selected to estimate the physical properties of the components. The syngas composition was determined using the minimisation of the total Gibbs free energy (*RGibbs*). The considered gasification processes usually do not achieve chemical equilibrium, leading to an overestimation of H_2 and CO production and underestimation of CO_2 and CH_4 production (Russo, de Oliveira and Desideri, 2018). For this reason, the equilibrium temperatures for the WGS and methane reforming reactions were restricted. This method has previously been successfully employed to accurately represent the gasification process of different feedstocks (Arteaga-Pérez et al., 2013).

5.2.1 Conventional steam gasification of municipal solid waste (Case 1)

The MSW steam gasification plant consists mainly of a gasification unit, the syngas clean-up and upgrading units, a heat exchanger network and a gas turbine. The conceptual design of the H_2 production *via* steam gasification of MSW is presented in Figure 5-1 and the operating conditions are summarised in Table 5-3.

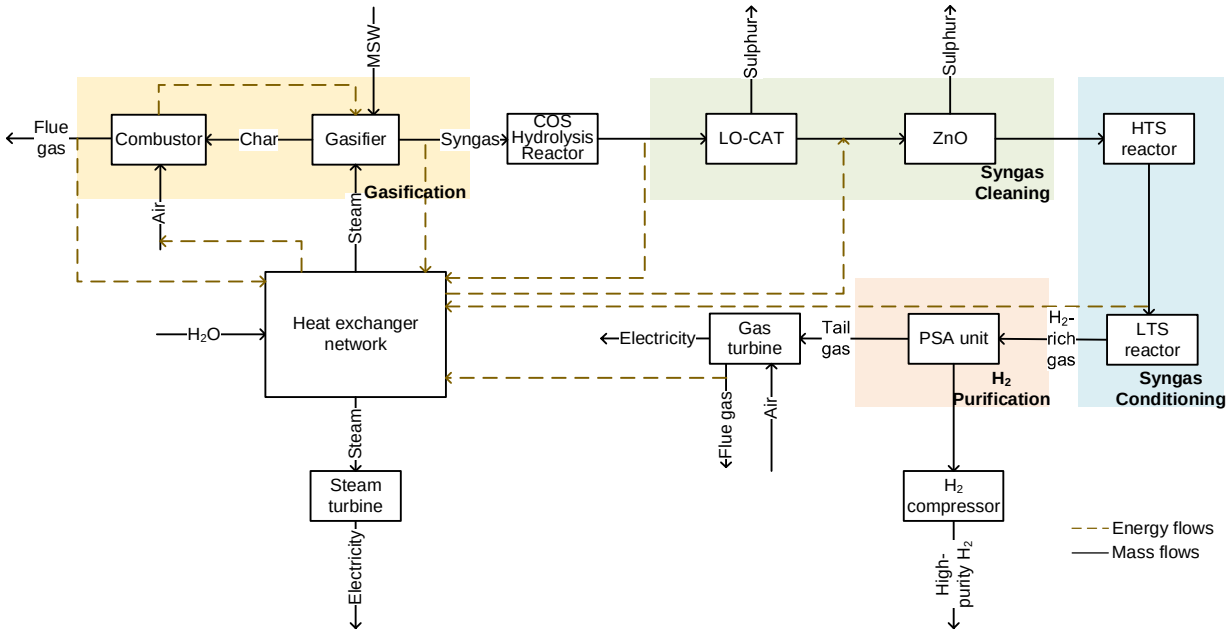

Figure 5-1: Simplified diagram of municipal solid waste gasification for H_2 production

Although not presented in Figure 5-1, it was assumed that MSW was subject to a pre-treatment before being fed to the gasifier. This is completed in two stages, a primary separation of the recyclables and a mechanical treatment to produce briquettes (Luz et al., 2015). It is noteworthy that the power requirement of these stages was accounted for and estimated based on the data reported based on the literature data (Luz et al., 2015). A DFB was selected as a gasifier that comprises two distinctive zones, gasification zone and combustion zone. The gasification unit was modelled using a Gibbs reactor (*RGibbs*) and a stoichiometric reactor (*RStoich*). The process model was developed based on the study by Doherty, Reynolds and Kennedy (2013). In the combustor, the unconverted char is burnt in the excess amount of air (λ=1.12), providing the heat necessary to maintain a constant temperature in the gasifier. This heat is transferred to the gasifier by circulating the bed material between the two reactors. The temperature of the combustor was set to be 55 °C higher than the gasification temperature. Moreover, steam at 350 °C and 1 bar was used as the gasifying agent. The gasification process was validated with the experimental data reported by Fremaux et al. (2015), considering the gas composition (Figure 5-2a) and H_2 yield (Figure 5-2b) for different temperatures (700 °C, 800 °C and 900 °C) and steam-to-biomass ratios (0.5, 0.7 and 1.0). The results presented in Figure 5-2 show a good agreement between the experimental results and the model predictions, indicating that the model developed in this study accurately represents the MSW steam gasification process.

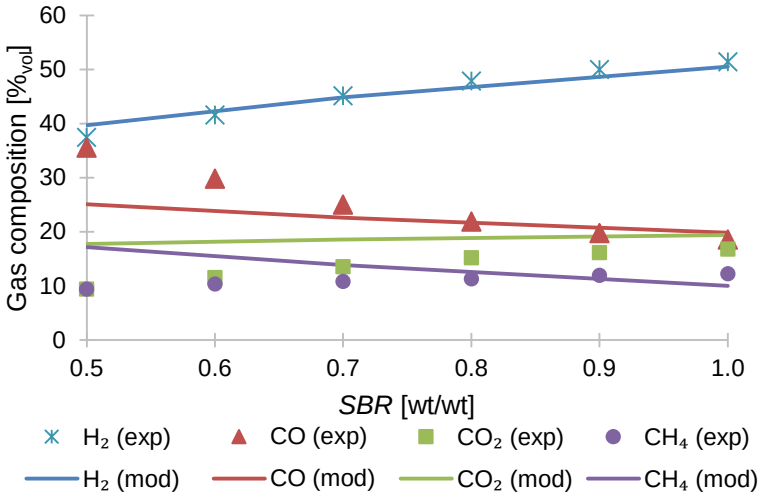

a)

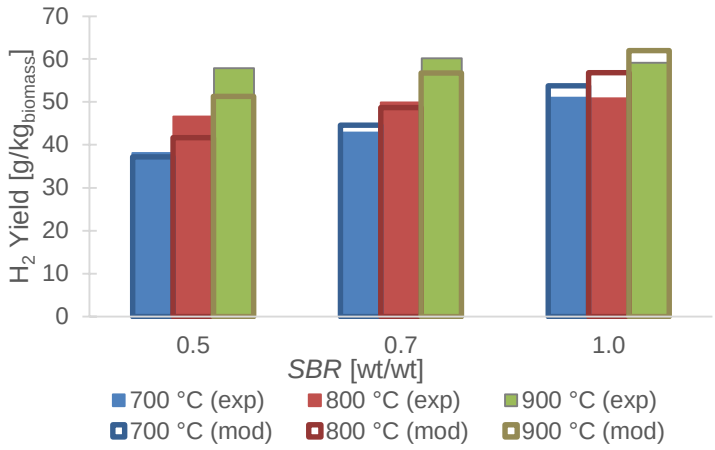

b)

Figure 5-2: Validation of the municipal solid waste steam gasification model with experimental data, obtained at three different temperatures and steam-to-biomass ratios, in terms of a) gas composition and b) hydrogen yield. Exp and mod correspond to experimental and simulated data, respectively (Fremaux et al., 2015)

Since the activity of the reforming catalysts is negatively affected by the presence of sulphur compounds, the raw syngas leaving the gasifier is then directed to the syngas clean-up unit to reduce the H_2S concentration to around 1ppm (NREL, 2005). Before the sulphur removal, the carbonyl sulphide (COS) present in the raw syngas is converted to H_2S in the COS reactor (NETL, 2019). This was modelled as stoichiometric reactor (*RStoich*) with the assumption that 99.5% of COS is converted to CO_2 and H_2S. In the first stage of the syngas clean-up unit,

the H_2S concentration is reduced to 11 ppm using a liquid oxidation catalyst (LO-CAT process). In a second step, a zinc oxide (ZnO) bed is used to remove the remaining sulphur to achieve the desired level of H_2S in syngas. To promote the H_2 yield, high-temperature (HTS) and low-temperature (LTS) shift reactors are employed. These reactors were modelled as equilibrium reactors (*REquil*) with the WGS reaction, Eq. (5-1) (Marcantonio et al., 2019). The performance of the WGS reactors was compared with the experimental data obtained in a pilot plant by Materazzi, Taylor and Cairns-Terry (2019). Considering the same gas composition and operating conditions, the CO global conversion was 96.7%. Such performance is comparable with the conversion of 92.1% reported by Materazzi, Taylor and Cairns-Terry (2019). After this stage, the H_2-rich syngas is further purified in a PSA unit. It is assumed that 99.9% H_2 purity can be achieved with a H_2 recovery rate of 85% (NREL, 2005). Although this unit is not modelled in detail in this study, its energy requirement and associated costs were accounted for. The H_2 stream is then compressed to 60 bar and the tail gas is routed to the gas turbine where is burnt in the combustor. The flue gas is then mixed with bleed compressed air to reduce the turbine inlet temperature below 1250 °C. The heated and compressed gas is then expanded in the turbine generating mechanical work required to generate electricity. Additionally, a heat exchanger network and steam cycle are also considered for heat recovery and electricity production. The considered steam cycle is based on a superheated Rankine cycle, which has already been validated and described in detail in Santos, Manovic and Hanak (2021).

5.2.2 Sorption-enhanced gasification of municipal solid waste (Case 2)

Similarly to the conventional steam gasification considered in Case 1, SEG also uses the dual fluidised bed layout. However, the material circulated between the interconnected fluidised beds acts simultaneously as the heat and CO_2 carrier. Since the CO_2 is removed by the sorbent in the sorption-enhanced gasifier, the equilibrium of the WGS, Eq. (5-1), shifts to the right, leading to an enhanced H_2 yield. A simplified diagram of the MSW SEG plant is depicted in Figure 5-3. As can be seen, the WGS reactors and the syngas clean-up unit (LO-CAT and ZnO

beds) are not present in the SEG process. This is because these are replaced by the sorption-enhanced gasifier where the CO_2 capture also takes place. The calciner, PSA unit, CO_2 compression unit, heat exchanger network and gas turbine are the remaining main components of the SEG process. Similarly to conventional steam gasification, it was assumed that a pre-treatment comprising primary separation and mechanical treatment is required to obtain a feedstock suitable for gasification. Therefore, the power requirement of this treatment was also taken into account.

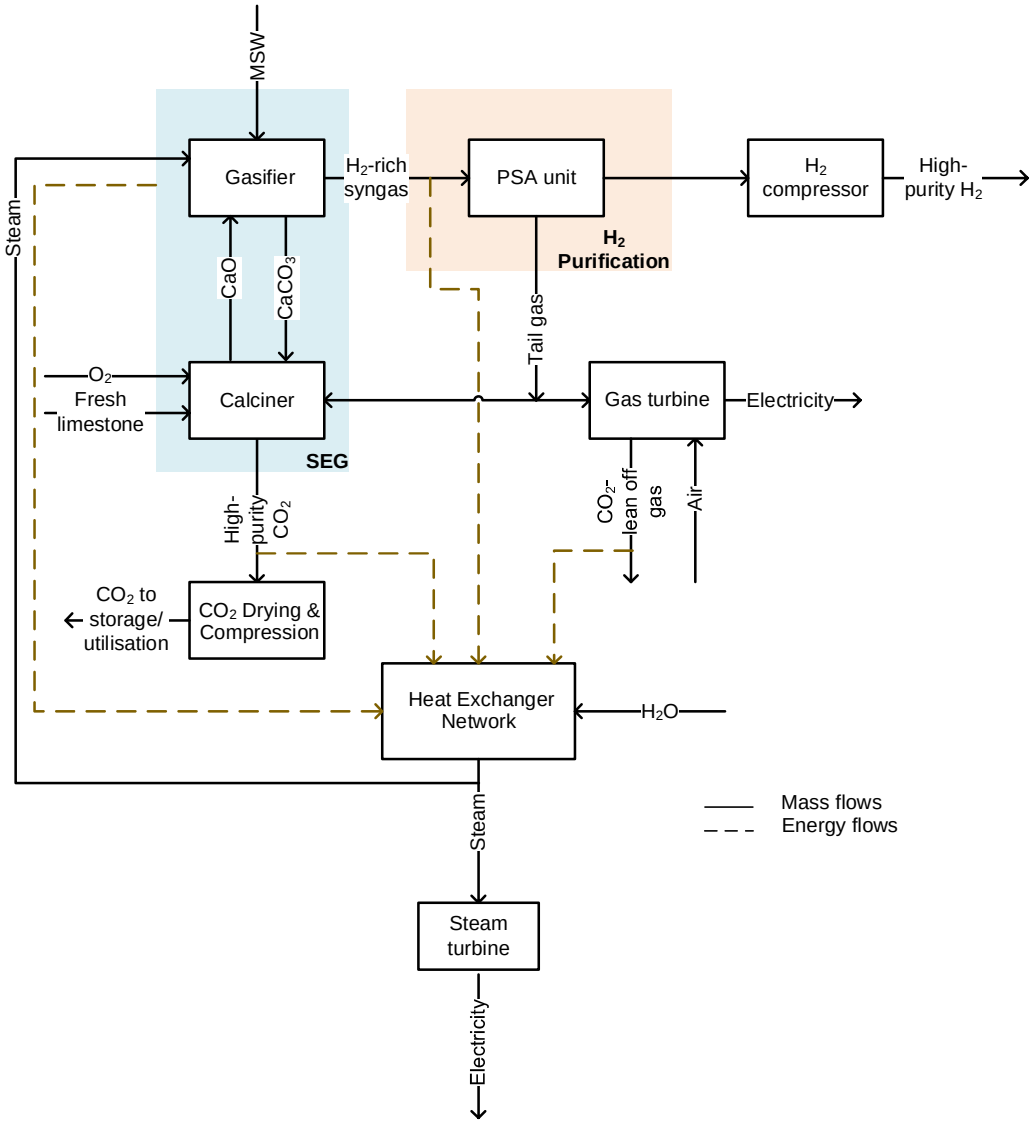

Figure 5-3: Simplified diagram of municipal solid waste sorption-enhanced gasification for hydrogen production

To model the sorption-enhanced gasifier in Aspen Plus®, two reactors (a Gibbs reactor and a stoichiometric reactor) are connected with a heat stream. The raw syngas produced during the steam gasification (steam at 350 °C and 1 bar), which occurs in the first reactor, is directed to the second reactor where the CO_2 produced during the gasification is captured by the CaO, Eq. (5-2). As a result, the energy demand for the gasification reaction is met by the sensible heat carried by the sorbent and the heat released during the carbonation reaction. The WGS reaction occurs simultaneously during the CO_2 capture process, leading to the production of H_2-rich syngas. The decomposition of $CaCO_3$, formed in the sorption-enhanced gasifier, into CaO and CO_2 occurs in the calciner, Eq. (5-3). Because the calcination reaction is endothermic, the unconverted char transported from the sorption-enhanced gasifier and part of the tail gas from the PSA unit are combusted directly in the calciner. To achieve a high-purity CO_2 stream, pure O_2 is used for combustion in the calciner. The O_2 is produced in a cryogenic ASU, the energy requirement of which was assumed to be 200 $kW_{el}h/t_{O_2}$ (Romano, 2013). The high-purity stream of CO_2 is then cooled to 25°C and compressed to 110 bar (Metz et al., 2005). The H_2-rich stream is fed to the PSA unit where H_2 is separated from other gaseous impurities. Because SEG includes both gasification and CO_2 capture, the composition of H_2-rich syngas is different (H_2:79.9%$_{vol}$; CO:5.6%$_{vol}$; CO_2:2.7%$_{vol}$; CH_4:11.1%$_{vol}$) than that received in the conventional steam gasification (H_2:68.7%$_{vol}$; CO:0.1%$_{vol}$; CO_2:29.0%$_{vol}$; CH_4:1.6%$_{vol}$) processes. Therefore, it was assumed that a high-purity H_2 stream (99.9%) is produced with an H_2 recovery rate of 93% (Hu, 2015; Luberti et al., 2014). The tail gas from the PSA unit is used as fuel in the process. A part of the tail gas is used in the calciner, providing heat for calcination, whereas the remaining amount is used in a gas turbine to produce electricity. A heat exchanger network is also considered to recover the high-grade heat of H_2-rich syngas, CO_2-lean off gas and high-purity CO_2 streams that, along with the heat from SEG, are used for steam production. The approach to gas turbine and steam cycle modelling was described in detail in the previous section. The main input parameters and operating conditions for SEG are described in Table 5-3.

Table 5-3: Main model assumptions used for gasification and sorption-enhanced gasification

Unit operation	Parameter	Value
Gasification	Temperature [°C]	650-1000
	Pressure [bar]	1
	Gasifier type	Dual fluidised bed
	Steam-to-biomass ratio [wt/wt]	0.5-1.3
Syngas clean-up		
COS hydrolysis	Temperature [°C]	200
LO-CAT	Temperature [°C]	50
	Outlet H_2S [ppm]	11
ZnO	Temperature [°C]	375
	Outlet H_2S [ppm]	1
Syngas upgrading		
HTS	Temperature [°C]	350
LTS	Temperature [°C]	200
PSA	H_2 recovery [%]	85.0
	H_2 purity [$\%_{vol}$]	99.9
	Temperature [°C]	30
	Feed pressure [bar]	25
	Tail gas pressure [bar]	1
	Delivery pressure [bar]	60
Sorption-enhanced gasification		
Sorption-enhanced gasifier	Temperature [°C]	650
	Steam-to-biomass ratio [mass basis]	0.5-2
	Carbonated sorbent fraction [-]	0.7
	CO_2 capture efficiency in carbonator [%]	90.0
Calciner	Temperature [°C]	900
	Calcined sorbent fraction [-]	0.95
	Excess oxygen [$\%_{vol,dry}$]	2.5
	Relative make-up [-]	0.02
H_2-rich syngas upgrading		
PSA	H_2 recovery [%]	93.0
	H_2 purity [$\%_{vol}$]	99.9
	Temperature [°C]	30
	Feed pressure [bar]	34
	Tail gas pressure [bar]	1
	Delivery pressure [bar]	60
CO_2 compression		
Compressors	Polytropic efficiency [%]	80.0
	Mechanical efficiency [%]	99.6
Pump	Isentropic efficiency [%]	80.0
	Mechanical efficiency [%]	99.6
CO_2 final stream	Temperature [°C]	25.0
	Pressure [bar]	110.0
Steam Cycle		
Live Steam	Temperature [°C]	593.0
	Pressure [bar]	154.0
High-pressure turbine	Isentropic efficiency [%]	92.0
	Mechanical efficiency [%]	99.8
Intermediate-pressure turbine	Isentropic efficiency [%]	94
	Mechanical efficiency [%]	99.8
Low-pressure turbine	Isentropic efficiency [%]	88
	Mechanical efficiency [%]	98
Condenser	Feed water temperature [°C]	10.0
Gas turbine	Compressor outlet pressure [bar]	20
	Combustor pressure drop [%]	2
	Turbine inlet temperature [°C]	1268
	Turbine isentropic efficiency [%]	80
	Turbine mechanical efficiency [%]	99.6
Fresh material (Hanak and Manovic, 2018)	Limestone (95.0%$_{wt}$ $CaCO_3$, 3.5%$_{wt}$ $MgCO_3$, 0.6%$_{wt}$ SiO_2, 0.4%$_{wt}$ Fe_2O_3, 0.5%$_{wt}$ Al_2O_3)	

Water Gas Shift:

$CO(g) + H_2O(g) \leftrightarrow CO_2(g) + H_2(g)$ $\Delta H = \pm 40.9$ kJ/mol **(5-1)**

Carbonation:

$CaO(s) + CO_2(g) \rightarrow CaCO_3(s)$ $\Delta H = -178$ kJ/mol **(5-2)**

Calcination:

$CaCO_3(s) \rightarrow CaO(s) + CO_2(g)$ $\Delta H = 178$ kJ/mol **(5-3)**

The developed SEG model was validated as two separated processes, the steam gasification process described in the previous section (Figure 5-2) and CaL. The experimental results obtained at a 20 kW_{th} dual fluidised bed by Armbrust et al. (2015) were used to validate the CaL process. The simulated results were compared with the experimental data obtained at different operating conditions, such as syngas composition, carbonator temperature and looping ratio ($mol_{Ca}/(mol_{CO}+mol_{CO_2})$). The operating conditions of each run are presented in Table 5-4. This comparison, depicted in Figure 5-4, shows that the model can well describe the experimental results.

Table 5-4: Operating conditions of each run used to validate the calcium looping model (Armbrust et al., 2015)

Run	Parameter	Value
1	Syngas mole fraction [$\%_{vol,dry}$]	H_2:51.4; CO:20.9; CO_2:23.4; CH_4+C_xH_y: 4.3
	Carbonator temperature [°C]	637
	Looping ratio	7
2	Syngas mole fraction [$\%_{vol,dry}$]	H_2:55.9; CO:12.9; CO_2:23.2; CH_4+C_xH_y:8.0
	Carbonator temperature [°C]	643
	Looping ratio	8.6

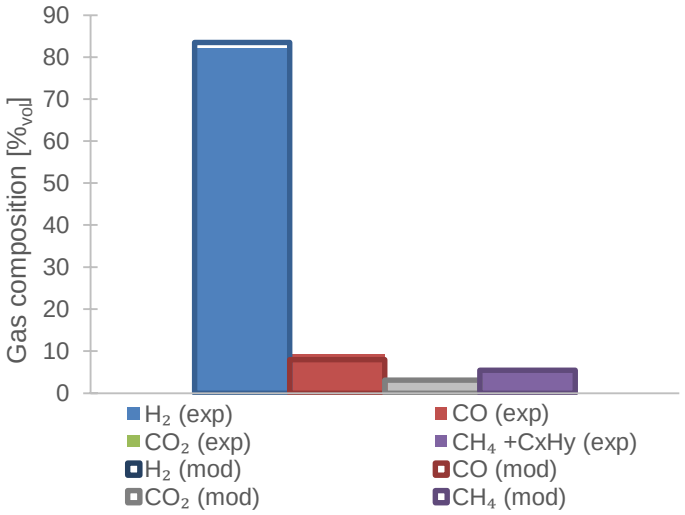

a)

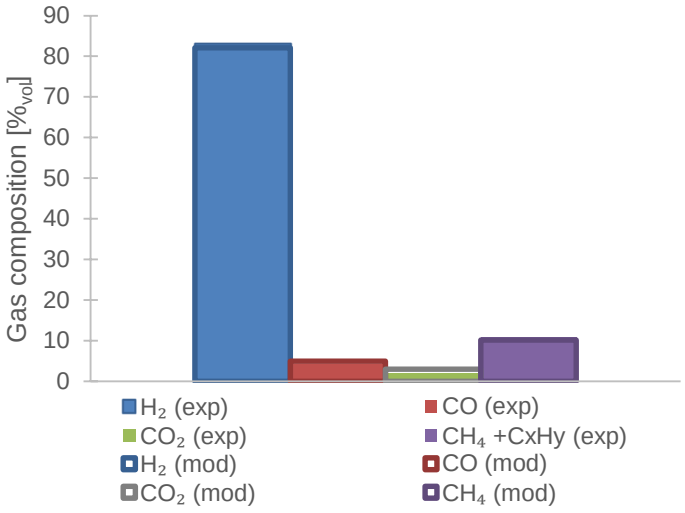

b)

Figure 5-4: Sorption-enhanced gasification validation with literature data for different operating conditions: a) Run 1 and b) Run 2 presented in Table 5-4. Exp and mod correspond to experimental and simulated data, respectively (Armbrust et al., 2015)

5.3 Techno-economic feasibility assessment

To understand the benefits of SEG, the process models described in Section 5.2 were used to assess the techno-economic performance of conventional steam gasification and SEG.

5.3.1 Thermodynamic performance indicators

Four parameters were used to assess and compare the thermodynamic performance of the considered cases, including H_2 production efficiency, gross power efficiency, net power efficiency and total efficiency were the indicators selected for comparison. The H_2 production efficiency (η_{H_2}), Eq. (5-4), is defined as the ratio of the H_2 chemical energy and the chemical energy of MSW. It is noteworthy that all the indicators are calculated based on the lower heating value of H_2 (LHV_{H_2}) and MSW (LHV_{MSW}). In Eq. (5-4), $\dot{m}_{H_2}$ and $\dot{m}_{MSW}$ are the H_2 and MSW mass flowrates, respectively.

$$\eta_{H_2} = \frac{\dot{m}_{H_2} \cdot LHV_{H_2}}{\dot{m}_{MSW} \cdot LHV_{MSW}} \quad \textbf{(5-4)}$$

The gross power efficiency ($\eta_{el,gross}$), given by Eq. (5-5), is defined as the ratio of the gross electric power output ($W_{el,gross}$) and the chemical energy of MSW. The former accounts the electricity generated in the steam cycle and the gas turbine.

$$\eta_{el,gross} = \frac{W_{el,gross}}{\dot{m}_{MSW} \cdot LHV_{MSW}} \quad \textbf{(5-5)}$$

The ratio between the net electric power output and the total chemical energy of MSW, calculated by Eq. (5-6), defines the net power efficiency ($\eta_{el,net}$). The net electric power output ($W_{el,net}$) is the gross electric power output minus the electric power required to run the auxiliary equipment.

$$\eta_{el,net} = \frac{W_{el,net}}{\dot{m}_{MSW} \cdot LHV_{MSW}} \quad \textbf{(5-6)}$$

Finally, the total efficiency (η_{tot}), defined in Eq. (5-7), is the sum of H_2 production efficiency and the net power efficiency.

$$\eta_{tot} = \frac{\left(\dot{m}_{H_2} \cdot LHV_{H_2}\right) + W_{el,net}}{\dot{m}_{MSW} \cdot LHV_{MSW}} \quad \textbf{(5-7)}$$

5.3.2 Economic performance indicators

The economic performance of the considered cases was assessed in terms of the levelised cost of hydrogen (*LCOH*), and the cost of CO_2 avoided (*AC*). The levelised cost corresponds to the minimum hydrogen sale price at which the net present value (*NPV*), given by Eq. (5-8), reaches zero.

$$NPV = \sum_{t=1}^{n} \frac{CF_t}{(1+r)^t} - TCR \quad \textbf{(5-8)}$$

The NPV method estimates the discounted cash flow (CF_t) throughout the project lifetime (*t*), accounting for the total capital requirement (*TCR*), which was estimated following the approach described in Table 5-5, and the project discount rate (*r*). Since the inflation was not considered, the material and feedstock prices considered in the beginning of the project were valid for the project lifetime. These costs and other economic parameters are presented in Table 5-6. The cost correlations used on the estimation of capital cost of each unit are shown in Table 5-7. For the conventional steam gasification case, the annual operating and maintenance costs, the sum of variable and fixed costs, were calculated assuming a fraction of the *TCR*. It was assumed 6.6% of *TCR* to cover the variable operating costs (raw materials and utilities) and 6.7% of *TCR* to account the fixed costs (NREL, 2005). In the SEG case, the variable costs account the costs of raw materials, utilities along with the cost associated with CO_2 transport and storage. Since the economic assessment of this technology is very scarce in the literature, the fixed costs were estimated based on the figures reported by Schweitzer et al. (2018). It was assumed that 10%, 4%, 2% and 1.8% of *TCR* covered the costs relating to the working capital, maintenance (labour & material), insurances & taxes and the plant overhead costs, respectively.

Table 5-5: Economic approach used for total capital requirement estimation (Spallina et al., 2019)

	Correlation
Actual capital cost of j-component (*Cj*)	$C_j = C_{j,0}\left(\frac{CEPCI_{2017}}{CEPCI_0}\right)$
Total installed cost (*TIC*)	$TIC = \sum C_j$
Engineering procurement and construction (*EPC*)	*EPC = 10% TIC*
Contingency plan (*PC*)	*PC = 20% (TIC + EPC)*
Total plant cost (*TPC*)	*TPC = TIC + EPC + PC*
Other capital costs (*OCAPEX*)	*OCAPEX = 20% TPC*
Total capital requirement (*TCR*)	*TCR = 18% (TPC + OCAPEX)*

Table 5-6: Main economic parameters and assumptions

Parameter	Value
Unit cost of electricity exported to the grid [€/$MW_{el}h$] (Onarheim et al., 2017b)	40.0
Limestone unit cost [€/t] (Schweitzer et al., 2018)	11.6
Clean water unit cost [€/m^3] (Schweitzer et al., 2018)	2.4
CO_2 transport and storage cost [€/t_{CO_2}] (Maas, n.d.)	20.0
Others	
Expected lifetime [y] (Martínez et al., 2014b; Yang et al., 2010)	25.0
Project interest rate [%] (Martínez et al., 2014b; Yang et al., 2010)	8.8
Capacity factor [%] (Martínez et al., 2014b; Yang et al., 2010)	80.0
Average USD/EUR exchange rate 2017 (Bank of England, 2019)	0.8898
Average GBP/EUR exchange rate 2017 (Bank of England, 2019)	1.1418
CO_2 emission allowance price [€/t_{CO_2}] (Ember, 2022)	39.6
Gate fee [€/t_{MSW}] (Haaf et al., 2020)	40.0

The cost CO_2 avoided (*AC*), represented by Eq. (5-9), is calculated based on the *LCOH* and the CO_2 emission intensity determined for both plants.

$$AC = \frac{LCOH_{SEG} - LCOH_{Gasf}}{e_{CO_2,eq,Gasf} - e_{CO_2,eq,SEG}} \quad \textbf{(5-9)}$$

The CO_2 emission intensity accounts the direct $\left(e_{CO_2}\right)$ and indirect $\left(P_e \cdot e_{CO_2,e}\right)$ CO_2 emissions, which is defined by the equivalent CO_2 emissions $(e_{CO_2,eq})$, Eq. (5-10). The indirect emissions are associated with the surplus or deficit of electricity generated (P_e) and therefore, depend on the power

plant characteristics. In that case, it was assumed the power plant emits 262 kg_{CO_2} per 1 $MW_{el}h$ of electricity generated with an efficiency of 45.9%, which were determined take into account the power generation of the 27 EU Member States and UK in 2015 (De Lena et al., 2019).

$$e_{CO_2,eq} = e_{CO_2} + P_e \cdot e_{CO_2,e} \quad \textbf{(5-10)}$$

Table 5-7: List of cost correlations used on the estimation of capital cost of each unit (*Cj*)

Unit operation	Cost Correlation
Gasifier [Inlet steam flowrate, $\dot{m}_{Steam}$(kg/h)] (NREL, 2011)	$C_{Gasf} = 6.5e6 \left(\frac{\dot{m}_{Steam}}{226.8}\right)^{0.6}$
LO-CAT oxidiser vessel [Sulphur removed flowrate, $\dot{m}_S$ (kg/h)] (NREL, 2005)	$C_{LO\text{-}CAT} = 1.0e6 \left(\frac{\dot{m}_S}{234.5}\right)^{0.65}$
ZnO bed [Inlet syngas flowrate, $\dot{m}_{Syngas}$(kg/h)] (NREL, 2005)	$C_{ZnO} = 3.7e4 \left(\frac{\dot{m}_{Syngas}}{81371.7}\right)^{0.56}$
HTS reactor [Inlet syngas flowrate, $\dot{m}_{Syngas}$ (kg/h)] (NREL, 2005)	$C_{HTS} = 4.65907e5 \left(\frac{\dot{m}_{Syngas}}{160763.9}\right)^{0.56}$
LTS reactor [Inlet syngas flowrate, $\dot{m}_{Syngas}$ (kg/h)] (NREL, 2005)	$C_{LTS} = 3.23464e5 \left(\frac{\dot{m}_{Syngas}}{160763.9}\right)^{0.56}$
Pressure swing adsorption unit [Inlet gas molar flowrate, $\dot{n}_{PSA}$ (kmol/h)] (Spallina et al., 2016)	$C_{PSA} = 27.96e6 \left(\frac{\dot{n}_{PSA}}{17069}\right)^{0.60}$
H_2 compressor [Brake power requirement, $\dot{W}_{H_2,BRK}$ (kW_{el})] (Spallina et al., 2016)	$C_{H_2Comp} = 1200 \left(\frac{\dot{W}_{H_2,BRK}}{0.746}\right)^{0.82}$
Sorption-enhanced gasifier [Installed capacity LHV, P_{inst} (MW)] (Schweitzer et al., 2018)	$C_{SEG} = 22.1e6 \left(\frac{P_{inst}}{10}\right)^{0.80}$
Calciner [Calciner heat flux, $\dot{Q}_{calc}$ (kW_{th})] (Michalski, Hanak and Manovic, 2019)	$C_{calc} = 13140\ (\dot{Q}_{cal})^{0.67}$
Air separation unit [O_2 production rate, $\dot{m}_{O_2}$(kg/s)] (Atsonios et al., 2013)	$C_{ASU} = 2.926e7 \left(\frac{\dot{m}_{O_2}}{28.9}\right)^{0.70}$
CO_2 compression unit [Brake power requirement, $\dot{W}_{CCU,BRK}$ (kW_{el})] (Kreutz et al., 2005a)	$C_{CCU} = 1.22914e7 \left(\frac{\dot{W}_{CCU,BRK}}{13000}\right)^{0.67}$
Gas turbine [Inlet air flowrate, $\dot{m}_{Air}$ (kg/s)] (Spallina et al., 2016)	$C_{GT} = 31.5e6 \left(\frac{\dot{m}_{Air}}{209}\right)^{0.85}$
Fuel compressor [Brake power requirement, $\dot{W}_{FC,BRK}$ (kW_{el})] (Lee et al., 2014; Shirazi et al., 2012)	$C_{FC} = 91562 \left(\frac{\dot{W}_{FC,BRK}}{445}\right)^{0.67}$
Steam Cycle	
High-pressure steam turbine [Brake power output, $\dot{W}_{HPST,BRK}$ (kW_{el})] (Manzolini, Macchi and Gazzani, 2013)	$C_{HPST} = 33.7e6 \left(\frac{\dot{W}_{HPST,BRK}}{200000}\right)^{0.67}$
Intermediate-pressure steam turbine [Brake power output, $\dot{W}_{IPST,BRK}$ (kW_{el})] (Manzolini, Macchi and Gazzani, 2013)	$C_{IPST} = 33.7e6 \left(\frac{\dot{W}_{IPST,BRK}}{200000}\right)^{0.67}$
Low-pressure steam turbine [Brake power output, $\dot{W}_{LPST,BRK}$ (kW_{el})] (Manzolini, Macchi and Gazzani, 2013)	$C_{LPST} = 33.7e6 \left(\frac{\dot{W}_{LPST,BRK}}{200000}\right)^{0.67}$
Deaerator [Inlet flowrate, $\dot{m}_{Dea}$ (kg/h)] (NREL, 2005)	$C_{Dea} = 1.30721e5 \left(\frac{\dot{m}_{Dea}}{157970.7}\right)^{0.72}$
Deaerator feed pump [Condensate flowrate, $\dot{m}_{COND}$ (kg/h)] (NREL, 2005)	$C_{P\_Dea} = 8679 \left(\frac{\dot{m}_{COND}}{158425.2}\right)^{0.33}$
Low-pressure water pump [Feed water flowrate, $\dot{m}_{LPW}$ (kg/h)] (NREL, 2005)	$C_{P\_LPW} = 95660 \left(\frac{\dot{m}_{LPW}}{158425.2}\right)^{0.33}$

Unit operation	Cost Correlation
Fresh water pump [Fresh water flowrate, $\dot{m}_{CW}$ (kg/h)] (NREL, 2005)	$C_{P\_CW} = 5437\left(\frac{\dot{m}_{CW}}{42625.9}\right)^{0.33}$
Heat exchanger GT flue gas cooler/Steam generator [PINCH, $\dot{Q}_{GT\text{-}SG}$ (kW_{th})] (NREL, 2005)	$C_{GT\text{-}SG} = 26143\left(\frac{\dot{Q}_{GT\text{-}SG}}{401.5}\right)^{0.60}$
Heat exchanger Syngas cooler/Steam generator [PINCH, $\dot{Q}_{Syngas\text{-}SG}$ (kW_{th})] (NREL, 2005)	$C_{\boldsymbol{Syngas}\text{-}SG} = 26143\left(\frac{\dot{Q}_{Syngas\text{-}SG}}{401.5}\right)^{0.60}$
Condenser [Heat exchange area, A_{COND} (m^2)] (Sayyaadi and Mehrabipour, 2012)	$C_{COND} = 8500+490(A_{COND})^{0.85}$
Heat exchanger live steam [Heat exchange area, A_{LS} (m^2)] (Shirazi et al., 2012)	$C_{LS} = 2290(A_{LS})^{0.60}$
Heat exchanger condensate [Heat exchange area, A_{COND} (m^2)] (Lee et al., 2014)	$C_{COND} = 130\left(\frac{A_{COND}}{0.093}\right)$
Heat recovery steam generator [Steam flowrate, Q_{HRSG} (kg/h)] (NETL, 2019)	$C_{\mathrm{HRSG}} = 42427\left(\frac{AQ_{HRSG}}{277458}\right)^{0.7}$
Air preheater [Heat exchange area, A_{AXPH} (m^2)] (Lee et al., 2014)	$C_{AXPH} = 130\left(\frac{A_{AXPH}}{0.093}\right)$
Syngas preheater [Heat exchange area, $A_{SyngasPH}$ (m^2)] (Lee et al., 2014)	$C_{SyngasPH} = 130\left(\frac{A_{SyngasPH}}{0.093}\right)$
Heat exchanger high-pressure water [Heat exchange area, A_{HPW} (m^2)] (Lee et al., 2014)	$C_{HPW} = 130\left(\frac{A_{HPW}}{0.093}\right)$
Economiser [Heat exchange area, A_{ECON} (m^2)] (Lee et al., 2014)	$C_{ECON} = 130\left(\frac{A_{ECON}}{0.093}\right)$
Pre-treatment [Processing capacity, $\dot{m}_{MSW}$ (t/h)] (Luz et al., 2015)	$C_{Pre\text{-}t} = (9.0e4\dot{m}_{MSW}+6.6e4) + (7.1e4\dot{m}_{MSW}+8.0e4)$

5.4 Results and discussion

The parameters and design specifications presented in Section 5.3 were used to evaluate the techno-economic feasibility of SEG, which was benchmarked with the techno-economic performance of conventional steam gasification. A sensitivity analysis was also carried out to study the impact of the main economic parameters on the cost of CO_2 avoided.

5.4.1 Thermodynamic performance

To set the baseline for techno-economic assessment, the performance of the conventional steam gasification was first assessed.

5.4.1.1 Conventional steam gasification

First, the effect of the gasification temperature on the H_2 yield and on the overall system performance was investigated by varying the gasification temperature between 650 °C and 1000 °C under constant *SBR* of 1.0. It can be seen from Figure 5-5 that H_2 yield increased from 60 g/$kg_{dry\ MSW}$ to 78.8 g/$kg_{dry\ MSW}$ with the

temperature rise from 650 °C to 900 °C, at which the H_2 production reached the maximum. At higher temperatures, a slightly decrease in H_2 yield was observed. This can be attributed to the reverse WGS reaction that shifts the equilibrium and favours the reactants, consuming the H_2 and CO_2 (Li et al., 2014). As expected, the temperature increase favours the endothermic reaction, steam methane reforming, enhancing the H_2 and CO formation and the CH_4 consumption. The increase of the temperature from 600 °C to 1000 °C resulted in a reduction of the gross power output from 36.4 MW to 19.4 MW. However, the net power output remained almost constant (between 6 MW and 7 MW). This can be explained by the reduced amount of the tail gas available from PSA at higher gasification temperatures, resulting in a reduced electricity production in the gas turbine, but also reduced compression energy requirement. It should be noted the energy requirement for MSW pre-treatment was accounted for and was assumed to be constant since the MSW flowrate was kept constant in all considered cases (Luz et al., 2015). While the H_2 production efficiency (47.3%) reached the maximum at 900 °C, the net power efficiency had varied slightly, changing between 6.8% at 650 °C and 7.0% at 1000 °C. On the contrary, the gross power efficiency decreased from 34.7% to 18.5% within the same temperature range. Although the maximum total efficiency (53.0%) was obtained at 950 °C, further assessment will consider the gasification temperature of 900 °C as it maximises the efficiency of H_2 production that is the main product of the considered cases.

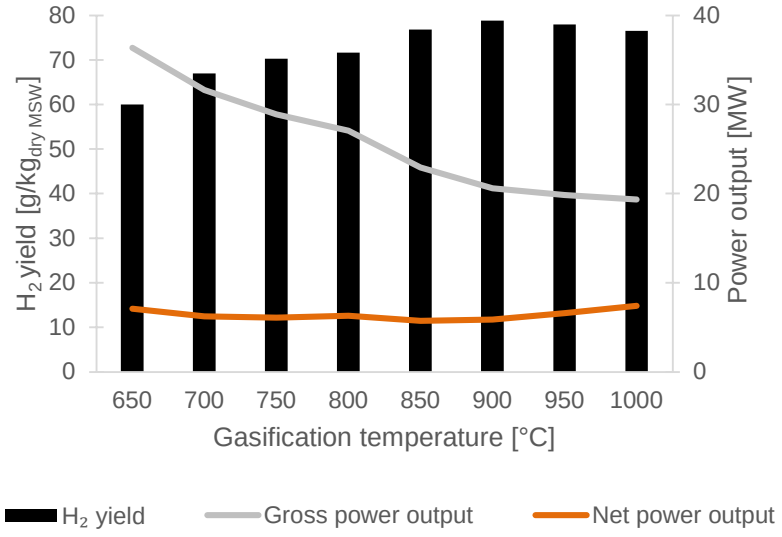

a)

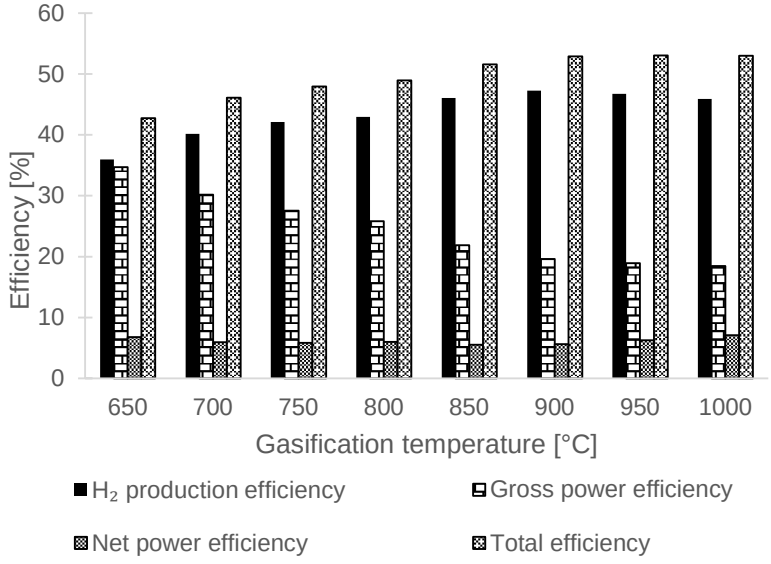

b)

Figure 5-5: Effect of gasification temperature on (a) hydrogen yield, gross and net power outputs, and (b) hydrogen production, gross power, net power and total efficiencies for conventional steam gasification at steam-to-biomass ratio of 1.0

The influence of *SBR* on the H_2 yield and the thermodynamic performance was assessed by varying the *SBR* between 0.5 and 1.3 at 900 °C. Figure 5-6 revealed that an increase in *SBR* led to an increase in the H_2 yield. However, the effect of *SBR* on H_2 yield was observed to be less pronounced than that of the gasification

temperature. This behaviour is in agreement with the experimental results reported by Rapagnà et al. (2000). The effect of *SBR* can be explained by the enhancement of the WGS and steam-methane reforming reactions that shift the equilibrium to the right, enhancing the H_2 formation. The increase of the *SBR* from 1.1 to 1.3 caused a marginal increase (0.4%) in the H_2 yield, from 79.3 $g/kg_{dry\ MSW}$ to 79.6 $g/kg_{dry\ MSW}$. This corresponded to a H_2 production efficiency between 47.6% and 47.8%, respectively. In the considered *SBR* range, the gross power output decreased from 26.0 MW to 19.6 MW and the net power output increased from 6.0 MW to 6.6 MW. Therefore, the gross power efficiency decreased from 24.8% to 18.7% and the net power efficiency increased slightly from 5.7% to 6.3%. The maximum total efficiency obtained was 54.0% at the *SBR* of 1.3. As can be seen in Figure 5-6, the difference between the two last points (*SBR* of 1.2 and 1.3), for all the considered indicators, was less than 1%. Therefore, it was concluded that the *SBR* of 1.2 resulted in the optimal operating conditions for the conventional steam gasification.

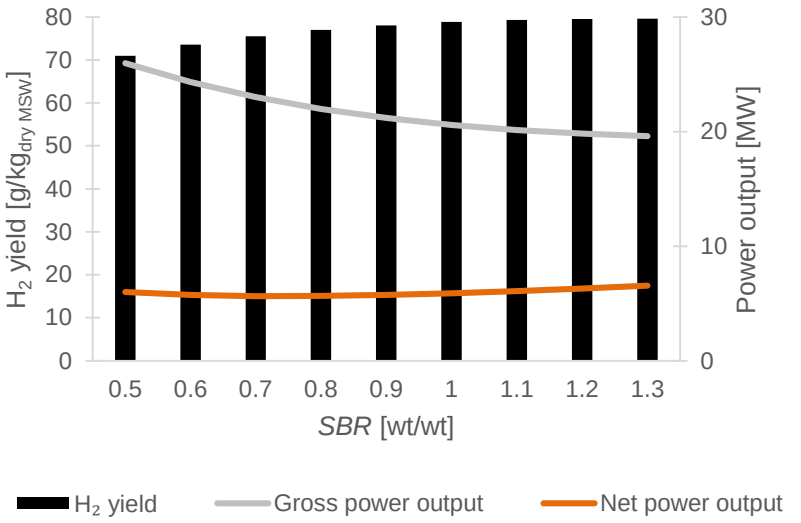

a)

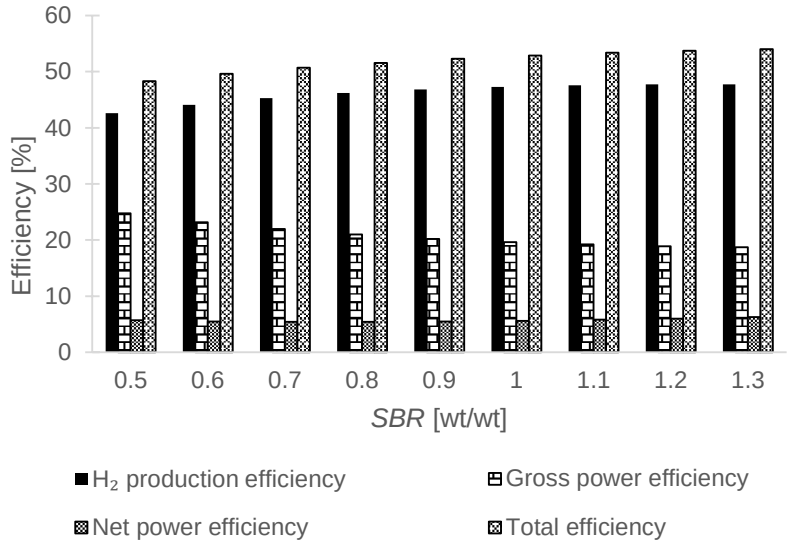

b)

Figure 5-6: Effect of steam-to-biomass ratio on (a) hydrogen yield, gross and net power outputs, and (b) hydrogen production, gross power, net power and total efficiencies for conventional steam gasification at gasification temperature of 900 °C

5.4.1.2 Sorption-enhanced gasification

Similarly to the conventional steam gasification, a parametric analysis was performed to evaluate the effect of SEG operating conditions on the H_2 yield and

the thermodynamic performance. However, in case of SEG, the gasification temperature was assumed to be 650 °C. This was because the carbonation reaction becomes the limiting factor at temperatures higher than 680 °C (Martínez et al., 2020a). Moreover, Armbrust et al. (2015) studied three carbonator temperatures (606 °C, 637 °C and 697 °C) in CaL for H_2 production from syngas and concluded that the maximum CO conversion and CO_2 capture rate were achieved at 637 °C. Although the SEG temperature was fixed at 650 °C in this study, the *SBR* was varied from 0.5 to 2, which corresponded to a molar steam-to-carbon (*S/C*) of 0.6–2.4. Figure 5-7 presents the effect of the *SBR* on the thermodynamic performance of SEG. It can be observed that the H_2 yield increased gradually on an increase in the *SBR*, while the gross and net power output reduced. This can be explained by the fact that less tail gas from the PSA was available to be burnt in the gas turbine, more energy was required for steam production and CO_2 compression, and less heat excess was available for power generation by the steam cycle. Thus, the maximum H_2 production efficiency maximum (51.2%) was achieved at *SBR* of 2.0. However, at such *SBR*, the gross and net efficiencies were 13.6% and -1.2%, respectively. The negative value for the net efficiency means that the available power output of the system was insufficient to meet its power requirement. Therefore, further assessment of SEG assumes the *SBR* of 1.8, as at this *SBR* the SEG process self-sufficient and there is no need to use electricity from the grid to support its operation (Figure 5-7b).

Comparing the considered gasification technologies, the H_2 production efficiency is almost 4% points higher for the SEG than the optimum value obtained for conventional steam gasification (47.7%). However, a trade-off between H_2 yield and power efficiency should also be considered. For the optimal operating conditions of SEG (*SBR*=1.8; *S/C*=2.2), a H_2 production efficiency of 48.7% and a total efficiency of 49.3% were obtained. Yet, the latter was lower than that obtained for conventional steam gasification (53.7%). This can be attributed to the higher power demand by SEG which translated into a net power efficiency of 0.6% that is around 5% points lower than the figure obtained for conventional steam gasification. The H_2 production efficiency is comparable with the SEG performance obtained by Detchusananard et al. (2020), who reported the H_2

production efficiency of around 56% for a sorption-enhanced chemical looping process operating with a *S/C* of 3.0.

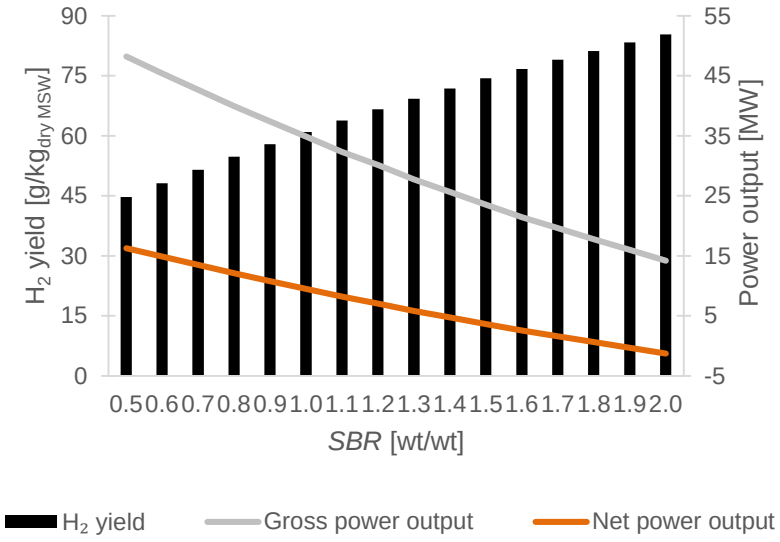

a)

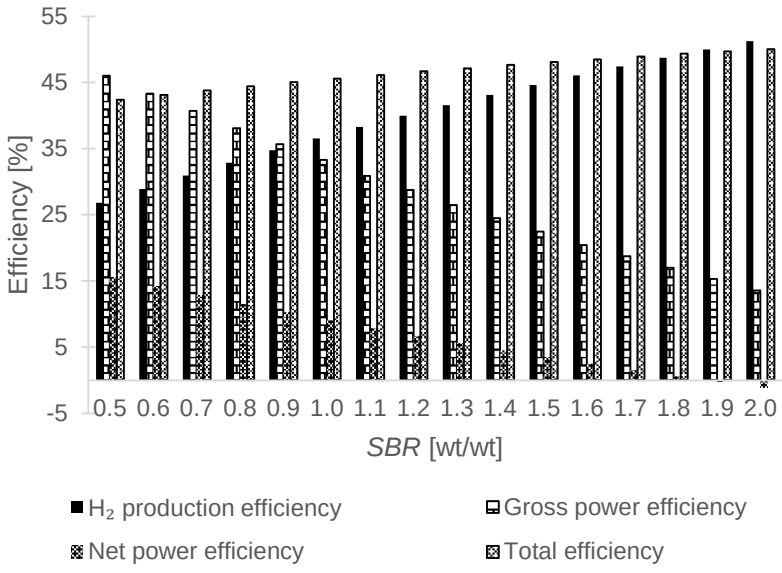

b)

Figure 5-7: Effect of steam-to-biomass ratio on (a) hydrogen yield, gross and net power outputs, and (b) hydrogen production, gross power, net power and total efficiencies for sorption-enhanced gasification at gasification temperature of 650 °C

5.4.2 Economic performance

The breakdown of total capital costs for the conventional steam gasification and SEG are shown in Figure 5-8. It can be observed that the gasification units in both cases were the most expensive pieces of equipment, accounting for 74% and 77% of the total capital cost, respectively. It should also be noted that the data to estimate the cost of SEG is scarce in the current literature. For this reason, the capital cost estimate of the SEG bears significant uncertainty and is subject to sensitivity analysis later in this study. For the remaining costs, the heat network (13%) and H_2 purification and upgrading (8%) accounted for 21% of the total capital cost of the conventional steam gasification unit. For SEG, these units accounted for 10% of the total capital, with a share of 5% of each. This was due to the higher share of SEG unit and the additional units required for SEG. These units, ASU (5%) and CO_2 compression unit (4%), accounted for 9% of the total capital cost of SEG.

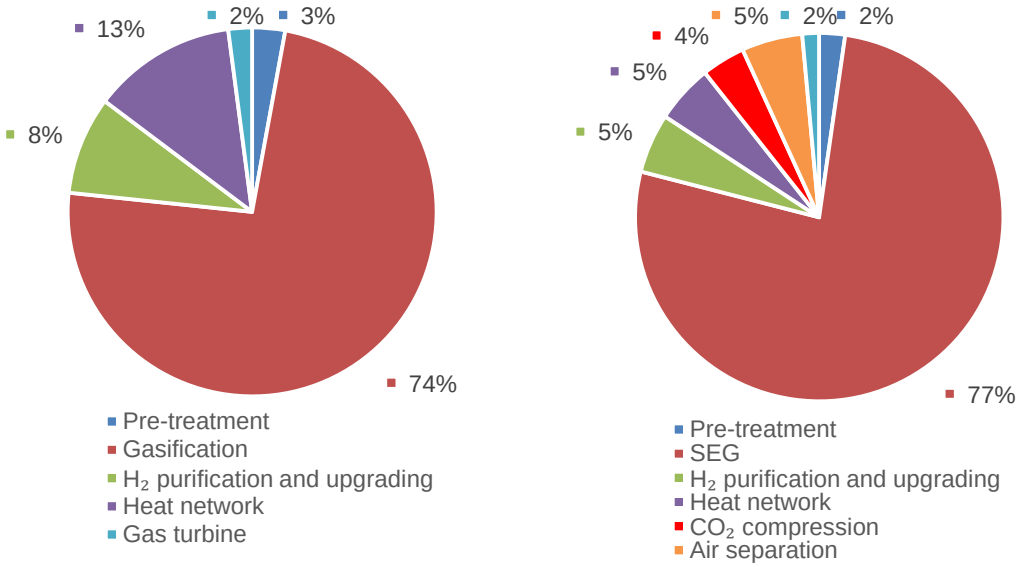

a) **b)**

Figure 5-8: Split of total capital costs for (a): gasification and (b): sorption-enhanced gasification

As there is still a high degree of uncertainty associated with the CCS technologies and the CO_2 allowances, the economic indicators considered in this study were evaluated under different scenarios.

Scenario 1: No gate fee and no fossil CO_2 emissions tax (baseline scenario)

Scenario 2: Gate fee and no fossil CO_2 emissions tax

Scenario 3: No gate fee and fossil CO_2 emissions tax

Scenario 4: Gate fee and fossil CO_2 emissions tax

A gate fee, which is a tax levied by the waste management facility, of 40.0 €/t_{MSW} was assumed (Haaf et al., 2020). Although the MSW composition may vary depending on the location or the time of the year, it was assumed that 40% of the carbon present in the MSW was of biogenic origin (Haaf et al., 2020). It should be noted that the CO_2 released during the calcination of fresh limestone make-up in SEG is of fossil origin (Santos, Manovic and Hanak, 2021). This was accounted for in the economic assessment of Scenario 3 and Scenario 4. Under the current EU ETS, the biogenic CO_2 emissions are considered carbon neutral. Therefore, only the CO_2 emissions of fossil origin are subject to the CO_2 emission allowance (EUA) price. The EUA price has been increasing since the end of 2020, reaching 50.0 €/t_{CO_2} for the first time in 2021. Therefore, an average value for the first 3 months of 2021 was taken, 39.6 €/t_{CO_2} (Ember, 2022).

Figure 5-9 presents the *LCOH*, which was estimated for both considered gasification technologies, and the cost of CO_2 avoided estimated under different scenarios. The economic evaluation showed that consideration of the CO_2 capture in SEG increased the *LCOH*. While for conventional steam gasification the *LCOH* varied between 2.1 €/kg_{H_2} and 3.2 €/kg_{H_2}, for SEG the *LCOH* almost doubled (4.5–5.1 €/kg_{H_2}) under the considered scenarios. This translated into a cost of CO_2 avoided between 90.1 €/t_{CO_2} and 115.5 €/t_{CO_2}.

As shown in Figure 5-9a, the introduction of a gate fee of 40 €/t_{MSW} (Scenario 2) reduced the *LCOH* by 20.5% and 11% in case of conventional steam gasification and SEG, respectively. However, as the gate fee was introduced for both technologies, the cost of CO_2 avoided remained the same, around 115 €/t_{CO_2}. This implies that consideration of the gate fee will not incentivise investment in SEG over the conventional steam gasification. On the contrary, introduction of

the CO_2 emission allowance price (Scenario 3) has increased the *LCOH* of conventional steam gasification by 20.1% (from 2.7 €/kg_{H_2} to 3.2 €/kg_{H_2}), whereas the *LCOH* of SEG did increase by less than 0.8% (from 5.0 €/kg_{H_2} to 5.1 €/kg_{H_2}). This can be attributed to the lower CO_2 emitted in the latter case, since 90% of CO_2 emissions were captured in the carbonator. It is clear from Figure 5-9b that the introduction of the CO_2 emission allowance price had a large impact on the CO_2 avoided cost, reducing it by 21.5% with respect to Scenario 1.

Finally, the simultaneous introduction of the gate fee and the tax levied on fossil CO_2 emissions (Scenario 4) did not influence the *LCOH* for the conventional steam gasification, which remained at 2.7 €/kg_{H_2}. This implies that the reduction in the *LCOH* as a result of the introduction of the gate fee is balanced by the increase in the *LCOH* due to the tax levied on the fossil CO_2 emissions. For SEG, however, the *LCOH* reduced by 10.2% under Scenario 4. The CO_2 avoided cost estimated for Scenario 4 was 90.7 €/t_{CO_2}, which corresponds to a decrease of 21% with respect to baseline Scenario 1. Although SEG is not yet economically competitive with the conventional steam gasification, the results presented in this study demonstrated that SEG can become the preferred option when the EUA price exceeds 183 €/t_{CO_2}. Even though the costs of CO_2 avoided associated with MSW gasification with CO_2 capture and SEG are not available, the figures estimated in this study are comparable with that reported for the steam-methane reforming (15.3–127.0 €/t_{CO_2}), but almost the double of that reported for coal gasification (16.1–61.4 €/t_{CO_2}). This can be explained by the large scale of plants considered in these studies as well as the low costs of feedstock (Parkinson et al., 2019).

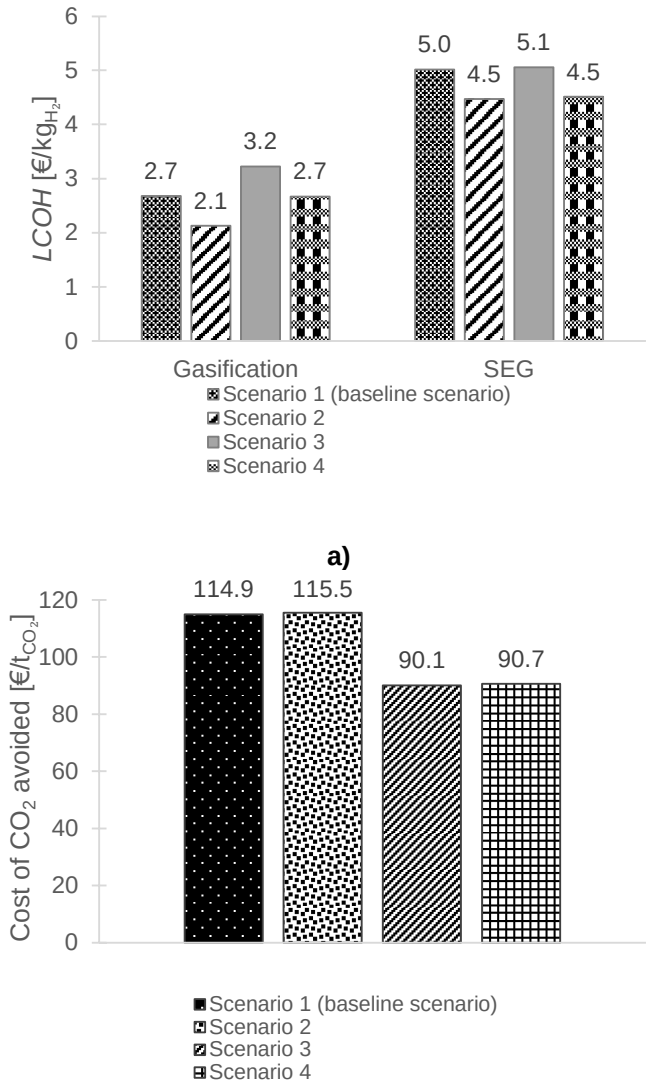

Figure 5-9: Comparison of a) levelised cost of hydrogen for gasification and sorption-enhanced gasification plant and b) cost of CO_2 avoided, with and without a gate fee and CO_2 allowance price of 40 €/t_{MSW} and 39.6 €/t_{CO_2}, respectively

5.4.3 Sensitivity study

As shown above, the technical and economic assumptions, such as the plant capacity, fuel price, capital cost or a gate fee, are associated with uncertainty that can influence the economic results. Therefore, a sensitivity analysis was carried out to understand the effect of the main input variables in the economic model on the cost of CO_2 avoided. The capital costs of conventional steam gasification and

SEG, as well as the price of limestone, electricity and CO_2 transport and storage were varied by ±25%.

The results presented in Figure 5-10 show that the uncertainty in the capital cost had the highest impact on the CO_2 avoided cost. Namely, a 25% reduction in the capital cost of SEG was shown to result in a 47% reduction in the cost of CO_2 avoided, assuming that the capital cost of conventional steam gasification remained fixed. On the contrary, if the capital cost of the conventional steam gasification increased 25% while the SEG cost remained unchanged, the CO_2 avoided cost would reduce by 30.5%. This indicates that even small reduction in the capital cost of SEG can significantly improve its economic viability. Furthermore, the variation in the electricity and limestone prices had shown a marginal impact on cost of CO_2 avoided. The ±25% variation in these parameters resulted only in ±1.6% and ±0.6% change in the cost of CO_2 avoided, respectively. Finally, a 25% increase in the cost associated with the CO_2 transport and storage was shown to result in a 5% increase in the cost of CO_2 avoided. Therefore, further work should focus on reducing the capital cost of SEG.

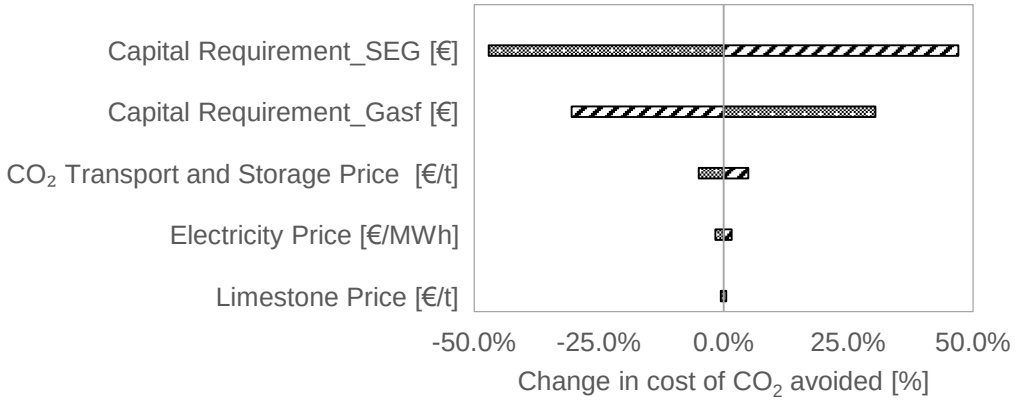

Figure 5-10: Effect of the main economic parameters on the cost of CO_2 avoided. Stripes: +25% of baseline parameter, Bubbles: -25% of baseline parameter

5.5 Technology benchmarks

The techno-economic performance of SEG was benchmarked against the conventional steam gasification, the comparison is shown in Table 5-8. The equivalent CO_2 emissions, estimated by Eq. (5-10), were used as an

environmental indicator to compare the environmental performance of SEG and conventional steam gasification (Table 5-8). As can be seen, the equivalent CO_2 emissions were reduced from 21.7 kg_{CO_2}/kg_{H_2} (conventional steam gasification) to 1.4 kg_{CO_2}/kg_{H_2} (SEG). In future works, this analysis should be carried out using advanced sustainability assessment tools such as life cycle assessment, exergy analysis and the combination of the latter with economic and environmental analysis, exergoenvironmental and exergoeconomic analyses (Rosen, 2018).

Table 5-8: Summary of techno-economic performance for both technologies

Parameter	Conventional steam gasification	Sorption-enhanced gasification
Thermodynamic assessment		
H_2 production efficiency [%]	47.7	48.7
Gross power efficiency [%]	18.9	17.0
Net power efficiency [%]	6.0	0.6
Total efficiency [%]	53.3	49.3
Environmental assessment		
Equivalent CO_2 emissions [kg_{CO_2}/kg_{H_2}]	21.7	1.4
Economic assessment		
Levelised cost of H_2 [€/kg_{H_2}]	2.7	5.0
Cost of CO_2 avoided [€/t_{CO_2}]	-	114.9

A comparison between the *LCOH* estimated in this study and the *LCOH* reported in the literature for different technologies is shown in Figure 5-11.

Currently, steam methane reforming (SMR) is the most commonly used and the cheapest technology for hydrogen production at scale, although its economic viability is very sensitive to the natural gas price. For this technology, the *LCOH* falls in the range between 1.0–1.5 €/kg_{H_2} without CO_2 capture and between 1.1 €/kg_{H_2} and 2.6 €/kg_{H_2} with CO_2 capture (Parkinson et al., 2019). It can be seen in Figure 5-11 that coal gasification is also a competitive route for hydrogen production. While the *LCOH* for the processes without CO_2 capture varies between 0.9 €/kg_{H_2} and 1.8 €/kg_{H_2}, the integration of CO_2 capture results in a 33–94% increase in the *LCOH* (1.2–3.4 €/kg_{H_2}) (Parkinson et al., 2019). Another

route to produce hydrogen using renewable energy is biomass gasification. Yet, it is not a competitive technology at the current stage of development. The *LCOH* reported in the literature falls between 1.4 €/kg_{H_2} and 3.2 €/kg_{H_2} without CO_2 capture and between 2.1 €/kg_{H_2} and 3.3 €/kg_{H_2} with CO_2 capture (Parkinson et al., 2019; Salkuyeh, Saville and MacLean, 2018). It should be noted that there is a limited number of economic assessments for this technology in the current literature and, therefore, the latter figures are based only on the studies by Parkinson et al. (2019) and Salkuyeh, Saville and MacLean (2018). Shahabuddin et al. (2020) were the first to estimate the *LCOH* for the MSW gasification without CO_2 capture. In their preliminary study, they found that the *LCOH* depended on the plant capacity and the consideration of a gate fee of around 45 €/t_{MSW}. The *LCOH* ranged from 2.4 €/kg_{H_2} (with gate fee) to 4.5 €/kg_{H_2} (without gate fee) for a plant of 75 MW_{th}. An increase of the plant capacity to 150 MW_{th} was shown to reduce the *LCOH* to between 1.3–3.5 €/kg_{H_2}. The economic feasibility of biomass SEG, at the plant capacity of 70 MW_{th}, was studied as a hydrogen production alternative by Schweitzer et al. (2018). They estimated the *LCOH* of between 6.1 €/kg_{H_2} and 10.1 €/kg_{H_2}, which were assessed for a capital cost between 1000 €/kW_{th} and 2000 €/kW_{th}.

The *LCOH* estimated in this study for a 100 MW_{th} MSW gasification plant without CO_2 capture (2.0–3.4 €/kg_{H_2}) is comparable with the figures reported above. Regarding the MSW SEG, the *LCOH* found in this work (3.9–6.1 €/kg_{H_2}) is lower than the values reported for biomass SEG by Schweitzer et al. (2018). This which can be primarily explained by no fuel cost associated with the use of MSW and the higher capacity of the SEG assumed in this work (100 MW_{th}).

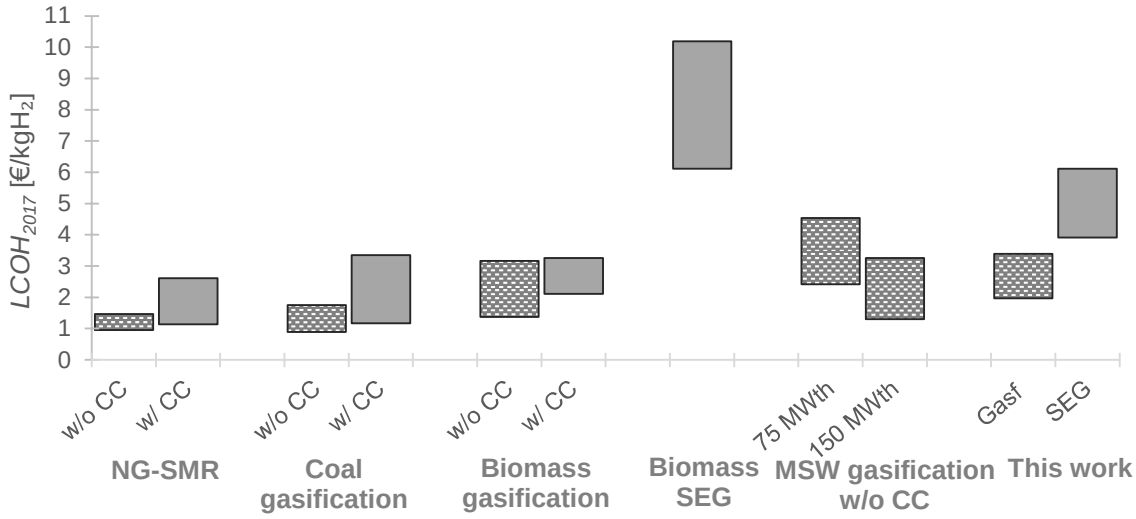

Figure 5-11: Levelised cost of hydrogen estimated for different technologies. Data from (Parkinson et al., 2019; Salkuyeh, Saville and MacLean, 2018; Schweitzer et al., 2018; Shahabuddin et al., 2020). Values for biomass sorption-enhanced gasification based on the sensitivity analysis of capital cost. Values for municipal solid waste based on application of gate fee for different size plant

5.6 Conclusions

WtE conversion is a promising technology to simultaneously tackle the climate change and reduce the waste landfilling. In this work, the techno-economic performance of the MSW steam gasification without CO_2 capture and SEG, which comprises *in-situ* CO_2 capture, was compared. The *LCOH* was one of the key economic indicators to assess the economic performance of the considered gasification technologies. The cost associated with CO_2 capture, defined by the cost of CO_2 avoided, was also determined. It was shown that SEG can deliver a higher H_2 production efficiency than the conventional steam gasification. Depending on the operating conditions, the improvement in H_2 production efficiency can reach almost 4 percentual points. However, considering the optimal conditions of both technologies, the total efficiency delivered by SEG was 49.3% compared to 53.3% for the conventional steam gasification. This can be explained by the energy penalty associated with the CO_2 capture. Under the baseline scenario, the *LCOH* of 2.7 €/kg_{H_2} and 5.0 €/kg_{H_2} was estimated for MSW steam gasification and SEG, respectively. This corresponded to a cost of CO_2

avoided of 114.9 €/t_{CO_2}. Although the integration of CO_2 capture resulted in an economic penalty, the cost of CO_2 avoided can be lowered by around 20% (90.1 €/t_{CO_2}) if a CO_2 emission allowance price of 39.6 €/t_{CO_2} is levied to the fossil CO_2 emissions. Overall, the *LCOH* estimated for the MSW SEG was lower than the figures reported for biomass SEG and the cost of CO_2 avoided was in the range for steam-methane reforming, indicating the potential of SEG to produce low-carbon H_2. As the economic analysis was associated with a high uncertainty, a sensitivity analysis was carried out. The results indicated the capital cost of both technologies had the highest impact on the cost of CO_2 avoided. The sensitivity study showed that the cost of CO_2 avoided can be reduced by 47% and 30.5% if the capital cost of SEG decreased by 25% and the capital cost of gasification increased by 25%, respectively.

Although the *LCOH* was shown to be lower for more technologies, such as natural gas SMR or coal gasification, SEG can become a competitive technology in the future. This can be primarily achieved by considering advanced reactors to reduce the capital cost. Moreover, the recent forecasts of the EUA prices indicate that it will increase in the next decades, promoting application of low-carbon technologies such as SEG.

It is noteworthy this study research presents some limitations that need to be address in future research. A quasi-equilibrium approach was adopted to model the gasification. This model does not account the tar formation and the reaction kinetics. However, this limitation can be overcome in future work by adopting a kinetic based model and considering the bed hydrodynamics. The performance of the system was evaluated only from a thermodynamic and economic point of view. Besides, the energy analysis was based on the first law of thermodynamics, which does not consider the irreversibility of system. Therefore, the future work on the H_2 production systems should be simultaneously assessed under a thermodynamic, economic and environmental perspective.

5.7 References

Acharya, B., Dutta, A. and Basu, P. (2017) ‘Gasification of biomass in a circulating fluidized bed based calcium looping gasifier for hydrogen-enriched gas

production: experimental studies', *Biofuels*, 8(6), pp. 643–650.

Acharya, B., Dutta, A. and Basu, P. (2010) 'An investigation into steam gasification of biomass for hydrogen enriched gas production in presence of CaO', *International Journal of Hydrogen Energy*, 35(4), pp. 1582–1589.

Affairs, D. for E.F.& R. (2020) *Uk Statistics on Waste*.

Armbrust, N., Duelli, G., Dieter, H. and Scheffknecht, G. (2015) 'Calcium looping cycle for hydrogen production from biomass gasification syngas: Experimental investigation at a 20 kW_{th} dual fluidized-bed facility', *Industrial and Engineering Chemistry Research*, 54(21), pp. 5624–5634.

Arregi, A., Amutio, M., Lopez, G., Bilbao, J. and Olazar, M. (2018) 'Evaluation of thermochemical routes for hydrogen production from biomass: A review', *Energy Conversion and Management*, 165, pp. 696–719.

Arteaga-Pérez, L.E., Casas-Ledón, Y., Pérez-Bermúdez, R., Peralta, L.M., Dewulf, J. and Prins, W. (2013) 'Energy and exergy analysis of a sugar cane bagasse gasifier integrated to a solid oxide fuel cell based on a quasi-equilibrium approach', *Chemical Engineering Journal*, 228, pp. 1121–1132.

Atsonios, K., Koumanakos, A., Panopoulos, K.D., Doukelis, A. and Kakaras, E. (2013) 'Techno-economic comparison of CO_2 capture technologies employed with natural gas derived GTCC', *Proceedings of the ASME Turbo Expo*., Vol.2, p. V002T07A018.

Bank of England (2019) *Bank of England Statistical Interactive Database | Interest & Exchange Rates | Official Bank Rate History*. Available at: http://www.bankofengland.co.uk/boeapps/iadb/repo.asp (Accessed: 5 December 2019).

Chen, G., Jamro, I.A., Samo, S.R., Wenga, T., Baloch, H.A., Yan, B. and Ma, W. (2020a) 'Hydrogen-rich syngas production from municipal solid waste gasification through the application of central composite design: An optimization study', *International Journal of Hydrogen Energy*, 45(58), pp. 33260–33273.

Chen, S., Zhao, Z., Soomro, A., Ma, S., Wu, M., Sun, Z. and Xiang, W. (2020b)

‘Hydrogen-rich syngas production via sorption-enhanced steam gasification of sewage sludge’, *Biomass and Bioenergy*, 138, p. 105607.

Detchusananard, T., Im-orb, K., Maréchal, F. and Arpornwichanop, A. (2020) ‘Analysis of the sorption-enhanced chemical looping biomass gasification process: Performance assessment and optimization through design of experiment approach’, *Energy*, 207, p. 118190.

Doherty, W., Reynolds, A. and Kennedy, D. (2013) ‘Aspen plus simulation of biomass gasification in a steam blown dual fluidised bed’, *Materials and Process for Energy*, , pp. 212–220.

Ember (2022) *Daily Carbon Prices*. Available at: https://ember-climate.org/data/carbon-price-viewer/ (Accessed: 24 March 2022).

Fremaux, S., Beheshti, S.-M., Ghassemi, H. and Shahsavan-Markadeh, R. (2015) ‘An experimental study on hydrogen-rich gas production via steam gasification of biomass in a research-scale fluidized bed’, *Energy Conversion and Management*, 91, pp. 427–432.

Haaf, M., Ohlemüller, P., Ströhle, J. and Epple, B. (2020) ‘Techno-economic assessment of alternative fuels in second-generation carbon capture and storage processes’, *Mitigation and Adaptation Strategies for Global Change*, 25(2), pp. 149–164.

Hameed, Z., Aslam, M., Khan, Z., Maqsood, K., Atabani, A.E., Ghauri, M., Khurram, M.S., Rehan, M. and Nizami, A.S. (2021) ‘Gasification of municipal solid waste blends with biomass for energy production and resources recovery: Current status, hybrid technologies and innovative prospects’, *Renewable and Sustainable Energy Reviews*, 136, p. 110375.

Hanak, D.P. and Manovic, V. (2018) ‘Combined heat and power generation with lime production for direct air capture’, *Energy Conversion and Management*, 160, pp. 455–466.

Hawthorne, C., Poboss, N., Dieter, H., Gredinger, A., Zieba, M. and Scheffknecht, G. (2012) ‘Operation and results of a 200-kW_{th} dual fluidized bed pilot plant

gasifier with adsorption-enhanced reforming', *Biomass Conversion and Biorefinery*, 2(3), pp. 217–227.

He, C., Zheng, J., Wang, K., Lin, H., Wang, J.Y. and Yang, Y. (2015) 'Sorption enhanced aqueous phase reforming of glycerol for hydrogen production over Pt-Ni supported on multi-walled carbon nanotubes', *Applied Catalysis B: Environmental*, 162, pp. 401–411.

He, M., Xiao, B., Liu, S., Guo, X., Luo, S., Xu, Z., Feng, Y. and Hu, Z. (2009) 'Hydrogen-rich gas from catalytic steam gasification of municipal solid waste (MSW): Influence of steam to MSW ratios and weight hourly space velocity on gas production and composition', *International Journal of Hydrogen Energy*, 34, pp. 2174–2183.

Hu, M. (2015) 'The New SeparALLTM Process and PolybedTM PSA for IGCC and CTL Application', *7th International Freiberg Conference Hohhot, China, June 7th-11th*.

Hu, M., Guo, D., Ma, C., Hu, Z., Zhang, B., Xiao, B., Luo, S. and Wang, J. (2015) 'Hydrogen-rich gas production by the gasification of wet MSW (municipal solid waste) coupled with carbon dioxide capture', *Energy*, 90, pp. 857–863.

Irfan, M., Li, A., Zhang, L., Wang, M., Chen, C. and Khushk, S. (2019) 'Production of hydrogen enriched syngas from municipal solid waste gasification with waste marble powder as a catalyst', *International Journal of Hydrogen Energy*, 44, pp. 8051–8061.

Jordan, C.A. and Akay, G. (2013) 'Effect of CaO on tar production and dew point depression during gasification of fuel cane bagasse in a novel downdraft gasifier', *Fuel Processing Technology*, 106, pp. 654–660.

Jordan, C.A. and Akay, G. (2012) 'Occurrence, composition and dew point of tars produced during gasification of fuel cane bagasse in a downdraft gasifier', *Biomass and Bioenergy*, 42, pp. 51–58.

Kaza, S., Yao, L.C.., Bhada-Tata, P. and Van Woerden, F. (2018) *What a Waste 2.0 : A Global Snapshot of Solid Waste Management to 2050.* Washington, DC:

Urban Development;. Washington, DC: World Bank.

Khan, Z., Yusup, S., Ahmad, M.M. and Chin, B.L.F. (2014) ‘Hydrogen production from palm kernel shell via integrated catalytic adsorption (ICA) steam gasification’, *Energy Conversion and Management*, 87, pp. 1224–1230.

Kırtay, E. (2011) ‘Recent advances in production of hydrogen from biomass’, *Energy Conversion and Management*, 52, pp. 1778–1789.

Kreutz, T., Williams, R., Consonni, S. and Chiesa, P. (2005) ‘Co-production of hydrogen, electricity and CO from coal with commercially ready technology. Part B: Economic analysis’, *International Journal of Hydrogen Energy*, 30(7), pp. 769–784.

Lee, Y.D., Ahn, K.Y., Morosuk, T. and Tsatsaronis, G. (2014) ‘Exergetic and exergoeconomic evaluation of a solid-oxide fuel-cell-based combined heat and power generation system’, *Energy Conversion and Management*, 85, pp. 154–164.

De Lena, E., Spinelli, M., Gatti, M., Scaccabarozzi, R., Campanari, S., Consonni, S., Cinti, G. and Romano, M.C. (2019) ‘Techno-economic analysis of calcium looping processes for low CO_2 emission cement plants’, *International Journal of Greenhouse Gas Control*, 82, pp. 244–260.

Li, B., Fabrice Magoua Mbeugang, C., Liu, D., Zhang, S., Wang, S., Wang, Q., Xu, Z. and Hu, X. (2020) ‘Simulation of sorption enhanced staged gasification of biomass for hydrogen production in the presence of calcium oxide’, *International Journal of Hydrogen Energy*, 45(51), pp. 26855–26864.

Li, B., Yang, H., Wei, L., Shao, J., Wang, X. and Chen, H. (2017) ‘Absorption-enhanced steam gasification of biomass for hydrogen production: Effects of calcium-based absorbents and NiO-based catalysts on corn stalk pyrolysis-gasification’, *International Journal of Hydrogen Energy*, 42(9), pp. 5840–5848.

Li, W., Li, Q., Chen, R., Wu, Y. and Zhang, Y. (2014) ‘Investigation of hydrogen production using wood pellets gasification with steam at high temperature over 800 °C to 1435 °C’, *International Journal of Hydrogen Energy*, 39(11), pp. 5580–

5588.

Luberti, M., Friedrich, D., Brandani, S. and Ahn, H. (2014) ‘Design of a H_2 PSA for cogeneration of ultrapure hydrogen and power at an advanced integrated gasification combined cycle with pre-combustion capture’, *Adsorption*, 20(2–3), pp. 511–524.

Luz, F.C., Rocha, M.H., Lora, E.E.S., Venturini, O.J., Andrade, R.V., Leme, M.M.V., Del Olmo, O.A., Codignole, F., Henrique, M., Eduardo, E., Lora, S. and José, O. (2015) ‘Techno-economic analysis of municipal solid waste gasification for electricity generation in Brazil’, *Energy Conversion and Management*, 103, pp. 321–337.

Maas, W. (n.d.) *The post-2020 Cost-Competitiveness of CCS Cost of Storage*.

Manzolini, G., Macchi, E. and Gazzani, M. (2013) ‘CO_2 capture in natural gas combined cycle with SEWGS. Part B: Economic assessment’, *International Journal of Greenhouse Gas Control*, 12, pp. 502–509.

Marcantonio, V., De Falco, M., Capocelli, M., Bocci, E., Colantoni, A. and Villarini, M. (2019) ‘Process analysis of hydrogen production from biomass gasification in fluidized bed reactor with different separation systems’, *International Journal of Hydrogen Energy*, 44(21), pp. 10350–10360.

Martínez, A., Lara, Y., Lisbona, P. and Romeo, L.M. (2014) ‘Operation of a mixing seal valve in calcium looping for CO_2 capture’, *Energy and Fuels*, 28(3), pp. 2059–2068.

Martínez, I., Grasa, G., Callén, M.S., López, J.M. and Murillo, R. (2020a) ‘Optimised production of tailored syngas from municipal solid waste (MSW) by sorption-enhanced gasification’, *Chemical Engineering Journal*, 401, p. 126067.

Martínez, I., Kulakova, V., Grasa, G. and Murillo, R. (2020b) ‘Experimental investigation on sorption enhanced gasification (SEG) of biomass in a fluidized bed reactor for producing a tailored syngas’, *Fuel*, 259, p. 116252.

Materazzi, M., Taylor, R. and Cairns-Terry, M. (2019) ‘Production of biohydrogen from gasification of waste fuels: Pilot plant results and deployment prospects’,

Waste Management, 94, pp. 95–106.

Meng, F., Meng, J. and Zhang, D. (2018) 'Influence of higher equivalence ratio on the biomass oxygen gasification in a pilot scale fixed bed gasifier', *Journal of Renewable and Sustainable Energy*, 10, p. 053101.

Metz, B., Davidson, O., de Coninck, H., Loos, M. and Meyer, L. (2005) *Carbon Dioxide Capture and Storage*. Cambridge; New York; Melbourne; Madrid; Cape Town; Singapore; Sào Paulo: Cambridge University Press.

Michalski, S., Hanak, D.P. and Manovic, V. (2019) 'Techno-economic feasibility assessment of calcium looping combustion using commercial technology appraisal tools', *Journal of Cleaner Production*, 219, pp. 540–551.

Müller, S., Fuchs, J., Schmid, J.C., Benedikt, F. and Hofbauer, H. (2017) 'Experimental development of sorption enhanced reforming by the use of an advanced gasification test plant', *International Journal of Hydrogen Energy*, 42(50), pp. 29694–29707.

NETL (2019) *Cost and performance baseline for fossil energy plants. Volume 1: Bituminous coal and natural gas to electricity.*

NREL (2005) *Biomass to Hydrogen Production Detailed Design and Economics Utilizing the Battelle Columbus Laboratory Indirectly-Heated Gasifier*.

NREL (2011) *Process Design and Economics for Conversion of Lignocellulosic Biomass to Ethanol: Thermochemical Pathway by Indirect Gasification and Mixed Alcohol Synthesis*.

Onarheim, K., Santos, S., Kangas, P. and Hankalin, V. (2017) 'Performance and cost of CCS in the pulp and paper industry part 2: Economic feasibility of amine-based post-combustion CO_2 capture', *International Journal of Greenhouse Gas Control*, 66, pp. 60–75.

Parkinson, B., Balcombe, P., Speirs, J.F., Hawkes, A.D. and Hellgardt, K. (2019) 'Levelized cost of CO_2 mitigation from hydrogen production routes', *Energy & Environmental Science*, 12(1), pp. 19–40.

Parthasarathy, P. and Narayanan, K.S. (2014) ‘Hydrogen production from steam gasification of biomass: Influence of process parameters on hydrogen yield – A review’, *Renewable Energy*, 66, pp. 570–579.

Perejón, A., Romeo, L.M., Lara, Y., Lisbona, P., Martínez, A. and Valverde, J.M. (2016) ‘The Calcium-Looping technology for CO_2 capture: On the important roles of energy integration and sorbent behavior’, *Applied Energy*, 162, pp. 787–807.

Pitkäoja, A., Ritvanen, J., Hafner, S., Hyppänen, T. and Scheffknecht, G. (2020) ‘Simulation of a sorbent enhanced gasification pilot reactor and validation of reactor model’, *Energy Conversion and Management*, 204, p. 112318.

Rapagnà, S., Jand, N., Kiennemann, A. and Foscolo, P.U. (2000) ‘Steam-gasification of biomass in a fluidised-bed of olivine particles’, *Biomass and Bioenergy*, 19(3), pp. 187–197.

Romano, M.C. (2013) ‘Ultra-high CO_2 capture efficiency in CFB oxyfuel power plants by calcium looping process for CO_2 recovery from purification units vent gas’, *International Journal of Greenhouse Gas Control*, 18(0), pp. 57–67.

Rosen, M.A. (2018) ‘Environmental sustainability tools in the biofuel industry’, *Biofuel Research Journal*, 5(1), pp. 751–752.

Russo, S., de Oliveira, S. and Desideri, U. (2018) ‘Thermo-economic evaluation of cogeneration plants based on municipal solid waste gasification in the Brazilian scenario’, *ECOS 2018 - Proceedings of the 31st International Conference on Efficiency, Cost, Optimization, Simulation and Environmental Impact of Energy Systems*, (August)

Salkuyeh, Y.K., Saville, B.A. and MacLean, H.L. (2018) ‘Techno-economic analysis and life cycle assessment of hydrogen production from different biomass gasification processes’, *International Journal of Hydrogen Energy*, 43(20), pp. 9514–9528.

Santos, M.P.S., Manovic, V. and Hanak, D.P. (2021) ‘Unlocking the potential of pulp and paper industry to achieve carbon-negative emissions via calcium looping retrofit’, *Journal of Cleaner Production*, 280, p. 124431.

Sayyaadi, H. and Mehrabipour, R. (2012) ‘Efficiency enhancement of a gas turbine cycle using an optimized tubular recuperative heat exchanger’, *Energy*, 38(1), pp. 362–375.

Schweitzer, D., Albrecht, F.G., Schmid, M., Beirow, M., Spörl, R., Dietrich, R.-U. and Seitz, A. (2018) ‘Process simulation and techno-economic assessment of SER steam gasification for hydrogen production’, *International Journal of Hydrogen Energy*, 43(2), pp. 569–579.

Shahabuddin, M., Krishna, B.B., Bhaskar, T. and Perkins, G. (2020) ‘Advances in the thermo-chemical production of hydrogen from biomass and residual wastes: Summary of recent techno-economic analyses’, *Bioresource Technology*, 299, p. 122557.

Shirazi, A., Aminyavari, M., Najafi, B., Rinaldi, F. and Razaghi, M. (2012) ‘Thermal–economic–environmental analysis and multi-objective optimization of an internal-reforming solid oxide fuel cell–gas turbine hybrid system’, *International Journal of Hydrogen Energy*, 37(24), pp. 19111–19124.

Spallina, V., Motamedi, G., Gallucci, F. and van Sint Annaland, M. (2019) ‘Techno-economic assessment of an integrated high pressure chemical-looping process with packed-bed reactors in large scale hydrogen and methanol production’, *International Journal of Greenhouse Gas Control*, 88, pp. 71–84.

Spallina, V., Pandolfo, D., Battistella, A., Romano, M.C., Van Sint Annaland, M. and Gallucci, F. (2016) ‘Techno-economic assessment of membrane assisted fluidized bed reactors for pure H_2 production with CO_2 capture’, *Energy Conversion and Management*, 120, pp. 257–273.

Statista (2021) *Greenhouse gas emissions from landfill in the UK 2010-2019*. Available at: https://www.statista.com/statistics/509129/greenhouse-gas-emissions-landfill-in-the-united-kingdom-uk/ (Accessed: 27 January 2021).

Tursi, A. (2019) ‘A review on biomass: Importance, chemistry, classification, and conversion’, *Biofuel Research Journal*, 6(2), pp. 962–979.

Udomsirichakorn, J. and Salam, P.A. (2014) ‘Review of hydrogen-enriched gas

production from steam gasification of biomass: The prospect of CaO-based chemical looping gasification', *Renewable and Sustainable Energy Reviews*, 30, pp. 565–579.

Umar, A., Neagu, D. and Irvine, J.T.S. (2021) 'Alkaline modified A-site deficient perovskite catalyst surface with exsolved nanoparticles and functionality in biomass valorisation', *Biofuel Research Journal*, 8(1), pp. 1342–1350.

Wang, J., Cheng, G., You, Y., Xiao, B., Liu, S., He, P., Guo, D., Guo, X. and Zhang, G. (2012) 'Hydrogen-rich gas production by steam gasification of municipal solid waste (MSW) using NiO supported on modified dolomite', *International Journal of Hydrogen Energy*, 37(8), pp. 6503–6510.

Yang, Y., Zhai, R., Duan, L., Kavosh, M., Patchigolla, K. and Oakey, J. (2010) 'Integration and evaluation of a power plant with a CaO-based CO_2 capture system', *International Journal of Greenhouse Gas Control*, 4(4), pp. 603–612.

Zhang, S., Yin, H., Wang, J., Zhu, S. and Xiong, Y. (2021) 'Catalytic cracking of biomass tar using Ni nanoparticles embedded carbon nanofiber/porous carbon catalysts', *Energy*, 216, p. 119285.

Zheng, X., Ying, Z., Wang, B. and Chen, C. (2018) 'Hydrogen and syngas production from municipal solid waste (MSW) gasification via reusing CO_2', *Applied Thermal Engineering*, 144, pp. 242–247.

Zhou, C., Stuermer, T., Gunarathne, R., Yang, W. and Blasiak, W. (2014) 'Effect of calcium oxide on high-temperature steam gasification of municipal solid waste', *Fuel*, 122, pp. 36–46.

6 SORPTION-ENHANCED GASIFICATION OF MUNICIPAL SOLID WASTE FOR HYDROGEN PRODUCTION: A COMPARATIVE TECHNO-ECONOMIC ANALYSIS USING LIMESTONE, DOLOMITE AND DOPED LIMESTONE*

Abstract

Sorption-enhanced gasification has been shown as a viable low-carbon alternative to conventional gasification, as it enables simultaneous gasification with *in-situ* CO_2 capture to enhance the production of H_2. CaO-based sorbents have been a preferred choice due to their low cost and wide availability. This work assessed the technical and economic viability of sorption-enhanced gasification using natural limestone, doped limestone with seawater and dolomite. The techno-economic performance of the sorption-enhanced gasification using different sorbents was compared with that of conventional gasification. Regarding the thermodynamic performance, dolomite presented the worst performance (46.0% of H_2 production efficiency), whereas doped limestone presented the highest H_2 production efficiency (50.0%). The use of dolomite also resulted in the highest levelised cost of hydrogen (5.4 €/kg_{H_2} against 5.0 €/kg_{H_2} when limestone is used as sorbent), which translates into a CO_2 avoided cost ranging between 114.9 €/t_{CO_2} (natural limestone) and 130.4 €/t_{CO_2} (dolomite). Although doped limestone has shown a CO_2 avoided cost of 117.7 €/t_{CO_2}, this can be reduced if the production cost of doped limestone is lower than 42.6 €/t. The production costs of new sorbents for CO_2 capture and H_2 production need to be similar to that of natural limestone to become an attractive alternative to natural limestone.

Keywords: Sorption-enhanced gasification, waste-to-energy, hydrogen production, dolomite, doped limestone

---

⁎Santos, M.P.S. and Hanak, D.P. (2022) 'Sorption-enhanced gasification of municipal solid waste for hydrogen production: a comparative techno-economic analysis using limestone, dolomite and doped limestone', *Biomass Conversion and Biorefinery*.

6.1 Introduction

Global CO_2 emissions have been rising for over a century now (Statista, 2021c). Although a significant emission reduction was recorded in 2020, mostly due to reduced economic activity caused by Covid-19, the global energy-related CO_2 emissions bounced back to the pre-pandemic levels in 2021 (IEA, 2021a). Thus unless the CO_2 and other greenhouse emissions are significantly reduced, the 1.5°C and 2°C global warming scenarios will be overcome until the end of this century (Intergovernmental Panel on Climate Change, 2021). CCS, as well as the reduction of fossil fuel dependency, have been identified as routes to tackle CO_2 emissions. The latter can be achieved by expanding the production of cleaner fuels and energy carriers, including hydrogen.

H_2 or H_2-rich syngas production has been thoroughly investigated from different types of biomass and wastes feedstocks such as sawdust (Yan et al., 2020), sewage sludge (Chen et al., 2020b; Yang et al., 2019), hazelnut shells (Marcantonio et al., 2019), wood chips (Schweitzer et al., 2018), wood pellets (Li et al., 2014), palm kernel shell (Hussain et al., 2021), plastics (Lazzarotto et al., 2020), food waste (Raizada et al., 2021) and MSW (Irfan et al., 2019). Although biomass is a renewable source and accessible at a reduced price, the generalised use of biomass for bioenergy production can start competing with food and crops production. Thus, wastes from agriculture, landfills, food, biomass residues, sewage sludge and manure, are regarded as sustainable feedstocks and should play a role in decarbonisation (Foster et al., 2021).

Considering the current state of solid waste management, there are significant differences between developed and developing countries, with the latter relying on open waste dumping (Kaza et al., 2018). Such practice, on top of open burning and unsanitary landfills, raises several environmental issues comprising global warming, ozone and resources depletion, damage of ecosystems and human health hazards (Laurent et al., 2014). Furthermore, it is forecasted that the annual $CO_{2,eq}$ emissions associated with solid wastes can reach 2.6 billion tonnes by 2050 if no improvements in waste management are deployed. It is because the

amount of solid waste generated by developing countries is forecasted to triple by that year (Kaza et al., 2018).

A range of technologies for thermochemical conversion of MSW have been considered, including plasma gasification (Mazzoni and Janajreh, 2017; Mehrpooya et al., 2022), chemical looping combustion (Yaqub, Oboirien and Akintola, 2021), gasification (Janajreh, Adeyemi and Elagroudy, 2020; Zheng et al., 2018), gasification integrated with simultaneous chemical and CaL (Lv, Zhang and Li, 2019), and SEG (He et al., 2009; Hu et al., 2015; Irfan et al., 2019; Martínez et al., 2020; Santos and Hanak, 2022; Zhou et al., 2014). MSW SEG was assessed by He et al. (2009) in a lab-scale fixed bed reactor at the gasification temperature of 900 °C. They have investigated the catalytic effect of calcined dolomite on the gasification performance, as well as the effect of the steam/MSW ratio on the gas composition and H_2 yield. They found that the increase in a steam/MSW ratio increased the H_2 mole fraction and the H_2 yield, which peaked (53% and 43 mol H_2/kg MSW, respectively) for a steam/MSW ratio of 1.04. Hu et al. (2015) used CaO as a CO_2 sorbent to study the effect of parameters such as gasification temperature, Ca/C molar ratio and moisture content on the H_2 yield and syngas composition. The experiments were carried out in a lab-scale fixed bed reactor. They found that a maximum H_2 mole fraction in syngas (49.4%) could be achieved at the gasification temperature of 750 °C, a CaO/MSW molar ratio of 0.7 and moisture content in MSW of 40%. Similarly, Zhou et al. (2014) selected a fixed bed to study the effect of CaO sorbent on the performance of MSW steam SEG. In that case, a lab-scale batch type reactor was used. The H_2 mole fraction in the syngas has been shown to increase by 15% points with the addition of CaO sorbent, from around 35% when no sorbent was present in the reactor. This result was achieved for a CaO/MSW mass ratio of 1 and at the gasification temperature of 700 °C. They have also shown that CaO acts as a CO_2 sorbent and catalyst, being responsible for enhancing the MSW devolatilization and char gasification. The use of waste marble powder as a CaO-based sorbent and simultaneously a catalyst was investigated by Irfan et al. (2019) in a lab-scale batch-type reactor. The performance of MSW SEG, including syngas yield and composition, tar content and carbon conversion

efficiency, were evaluated at different gasification temperatures, steam/MSW and sorbent/MSW ratios. They found that the increase in gasification temperature, steam/MSW and sorbent/MSW ratios promoted the H_2 mole fraction in the syngas. Consequently, the syngas yield and the carbon conversion efficiency have increased. However, it is important to notice that an increase in the considered operating conditions also resulted in a decrease in the tar formation. The concept of MSW SEG has also been proven to be a feasible technology for H_2-rich gas production at a 30 kW_{th} BFB plant (Martínez et al., 2020). This study considered limestone as a CO_2 sorbent, mostly because of its availability and low cost. Yet, this study did not consider the deterioration of the sorbent performance, which is a known challenge of using limestone as a sorbent (Rodríguez, Alonso and Abanades, 2010), because the set-up was operated in a semi-batch mode. Finally, Santos and Hanak (2022) have compared the techno-economic performance of MSW steam SEG with that of conventional steam gasification for H_2 production. The authors have shown that MSW SEG could deliver a higher H_2 production efficiency (48.7%) than conventional gasification (47.7%). Yet, such improvement is obtained at the expense of higher H_2 production costs, the *LCOH* increased from 2.1–3.2 €/kg H_2 (conventional gasification) to 4.5–5.1 €/kg H_2 (SEG).

Natural materials such as the shells from mollusc, scallop, oyster and mussel as well as eggshells have been shown viable as a CO_2 sorbent. However, the calcined sorbent also presented deactivation along with the carbonation/calcination cycles (Salaudeen, Acharya and Dutta, 2018). Moreover, it would be challenging to convert such waste to sorbent for large-scale applications. Thus, alternative sorbents for SEG need to be considered. These sorbents, besides the high CO_2 sorption capacity, should also present fast sorption kinetics, good mechanical properties, good cyclic stability and be economically viable (Chen, Duan and Sun, 2020). If the properties of synthetic sorbents are easier to be manipulated, the high cost of the chemical precursors results in a higher cost of sorbent production (Shokrollahi Yancheshmeh, Radfarnia and Iliuta, 2016).

Therefore, several approaches have been considered to enhance the performance of natural CaO-based sorbents, including the incorporation of inert materials with high Tammann temperatures, doping of sorbent and additional treatments including hydration or chemical pre-treatment.

Several inert materials have been studied as potential support materials to improve the sorbent stability, including aluminium oxide (Al_2O_3) (Radfarnia and Iliuta, 2013; Zhang et al., 2013), magnesium oxide (MgO) (Radfarnia and Iliuta, 2013), zirconium oxide (ZrO_2) (Radfarnia and Iliuta, 2013; Zhao et al., 2014), titanium oxide (TiO_2) (Sun et al., 2019), yttrium oxide (Y_2O_3) (Radfarnia and Iliuta, 2013), silica (SiO_2) (Sedghkerdar et al., 2014). Because these materials modify the sorbent skeleton, the sorbent granulation is improved and the sintering phenomenon is prevented. However, these sorbents are more expensive than natural CaO-based sorbents.

Hydration is another technique investigated in the current literature to increase the sorption capacity of the CaO-based sorbents. Water hydration (Yin et al., 2012) or steam hydration (Rong et al., 2013) can be used to improve the CO_2 sorption capacity of the fresh sorbent. This technique has also been applied for reactivation of the spent sorbent (Sun et al., 2020). In the latter case, the enhancement of sorption capacity is attributed to the formation of $Ca(OH)_2$. Since the molecule $Ca(OH)_2$ presents a higher molar volume than CaO, this contributes to the formation of cracks and then paths. This morphology alteration increases the surface area and pore volume, enhancing the CO_2 sorption (Wu et al., 2010).

The chemical treatment is another approach considered in the current literature to improve the CO_2 sorption capacity of the sorbent. In this approach, an enhancement of sorption capacity is achieved by treating the sorbent with chemicals such as acetic acid and pyroligneous acid (Chen, Duan and Sun, 2020). Li et al. (2009) have found that after 20 cycles of carbonation/calcination, the conversion of limestone pre-treated with acetic acid increased by more than a factor of 3 when compared with that of natural limestone (0.5 against 0.15). This can be attributed to the higher surface area and higher pore volume of treated limestone, which prevents the sintering phenomenon.

The CO_2 sorption capacity of sorbent has been shown to be enhanced by doping the CaO-based sorbents with sodium chloride (NaCl) (Salvador et al., 2003), hydrogen bromide (HBr) (González et al., 2016) and seawater (González, Kokot-Blamey and Fennell, 2020; Xu et al., 2017). Salvador et al. (2003) have studied the effect of doping limestone with 0.5%$_{wt}$ NaCl in a TGA and fluidised bed reactor. While in the tests performed in the fluidised bed reactor, there was no positive effect on the CO_2 sorption capacity. In the TGA experiments, this figure was higher than that for natural limestone after 14 cycles. It should be noted that in the first cycles the natural limestone presented a better performance than the doped one. The addition of 0.167 %$_{mol}$ HBr to limestone was studied by González et al. (2016) in a fluidised bed reactor. The authors found that the CO_2 sorption capacity of limestone, after 13 cycles, doubled when compared with the natural limestone. Xu et al. (2017) have investigated the possibility of using an abundant and cheap material, seawater, as a dopant to improve the CO_2 sorption capacity of limestone. They have carried out 20 cycles of carbonation/calcination in a fixed bed reactor. The authors concluded the CO_2 sorption capacity was maximum for 0.25%$_{wt}$ of dopant. Morona, Erans and Hanak (2019) have also studied the doping of limestone with different concentrations of seawater. After the sorbent had undergone 20 cycles of carbonation/calcination, the carbonation conversion was evaluated in a TGA. Unlike the previous work, the authors observed a deleterious effect on sorbent performance when dopped with seawater, which can be associated with an excessive addition of dopant (Armutlulu et al., 2017). The use of seawater as a dopant was also studied by González, Kokot-Blamey and Fennell (2020), although in this work the experiments were performed in a fluidised bed reactor. Similarly, to previous work, the authors have investigated different concentrations of dopant. They concluded that the addition of seawater to the four limestones tested improved the sorbent performance.

Similar to limestone, dolomite is another inexpensive natural CaO-based sorbent available worldwide. De La Calle Martos et al. (2016) have compared the limestone and dolomite CO_2 capture performance in a TGA, undergoing 20 cycles of carbonation/calcination. They concluded that dolomite compared with limestone presented the following advantages: lower regeneration temperature,

lower deactivation along with the cycles, superior CaO conversion, and thus, a higher CO_2 capture capacity. Although dolomite and doped limestone have been extensively assessed, the mentioned studies were carried out from a CO_2 capture performance standpoint of view. Moreover, the majority of studies that assessed SEG to date have solely focused on syngas production through MSW gasification with *in-situ* CO_2 capture, disregarding the sorbent regeneration step that is essential for the continuous operation of the SEG process. Santos and Hanak (2022) have reported for the first time the techno-economic feasibility of a cyclic SEG of MSW for H_2 production. However, that study only assessed the H_2 production costs for SEG of MSW using natural limestone as sorbent and, therefore, no comparative study has been carried out for other sorbents. Martínez et al. (2020) and Santos and Hanak (2022) have shown that SEG using limestone is a feasible technology to convert waste-to-fuel, despite the fact that the economic assessment performed by Santos and Hanak (2022) has shown it is still not competitive. Yet, dolomite and doped limestone may be an attractive alternative to limestone sorbent, promoting the deployment of SEG of MSW. Dolomite presents higher CO_2 desorption kinetics, which implies lower calcination temperature and, thus, a lower energy penalty. Doped limestone has shown to have a lower reactivity decaying over the cycles, improving CO_2 sorption capacity and, therefore, leading to an enhancement of H_2 production. Thus, it is crucial to evaluate these alternative sorbents for H_2 production with *in-situ* CO_2 capture.

This work aims to examine whether alternative sorbents can improve the techno-economic viability of MSW SEG for H_2 production. The techno-economic assessment of the MSW SEG was performed for three different CaO-based sorbents, including natural limestone, doped limestone with seawater and dolomite. Furthermore, an assessment of the MSW SEG design specifications and economic assumptions on the process energy, economic and environmental performance was assessed *via* a sensitivity analysis.

6.2 Process and model description

MSW, whose characteristics are shown in Table 6-1, was selected as feedstock for hydrogen production through SEG. The MSW SEG process is presented in

the simplified block flow diagram in Figure 6-1. The operating conditions are listed in Table 6-2. The MSW processing rate was assumed to be 500 t of MSW per day, corresponding to approximately 100 MW_{th}. The SEG process model, based on a set of mass and energy balances, was developed in Aspen Plus®. The model was based on the Gibbs free energy minimisation approach. The physical properties of the components were assessed using the Peng-Robinson equation of state with Boston-Mathias modifications. To simplify the model, it was considered that: (1) the process is isothermal, (2) the process operates under steady-state conditions, (3) the heat losses and the pressure drops are negligible, (4) graphitic carbon is the only compound of char, (5) ash is inert and (6) the formation of tar and higher hydrocarbon is negligible. The SEG process was validated with the experimental data reported by Fremaux et al. (2015) and Armbrust et al. (2015). The syngas composition was obtained at 700 °C, 800 °C and 900 °C for a range of *SBR* between 0.5 and 1.0, besides the H_2 yield obtained at the same temperatures and for the *SBR* 0.5, 0.7 and 1.0 were compared with that obtained by the model. The experiments carried out by Armbrust et al. (2015) at two different syngas compositions were used to validate the carbonation reaction and thus, the H_2-rich gas composition. Besides the syngas composition, the carbonation temperature (637 °C and 643 °C) and sorbent looping ratio (7.0 and 8.6) were used to validate the process. The SEG process validation is described in detail by Santos and Hanak (2022).

Since the raw MSW is not suitable for gasification, this is subjected to a pre-treatment (Luz et al., 2015). In the first stage, the recyclables and non-recyclables are separated (primary separation). In the second stage, mechanical treatment is carried out to produce briquettes suitable to be gasified. Therefore, the energy requirement and the costs of pre-treatment have been accounted for in the techno-economic evaluation. The data detailed by Luz et al. (2015) was used to appraise both.

Table 6-1: Municipal solid waste properties (Wang et al., 2012)

Properties	Value
LHV[12] [MJ/kg]	19.99
Moisture content [$\%_{wt}$]	9.34
Ultimate Analysis [$\%_{wt,db}$[13]]	
Elemental composition	C:49.51; H:6.42; O:35.69; N:0.78; S:0.48
Proximate Analysis [$\%_{wt,db}$[13]]	
Volatile matter	77.52
Fixed carbon	15.36
Ash	7.12

As shown in Figure 6-1, the MSW SEG plant comprises a gasifier operating in parallel with a calciner. In this work, three CaO precursor sorbents were selected, natural limestone, dolomite and doped limestone with seawater. In the SEG process, sorbent acts as a heat and CO_2 carrier, and circulates between the two interconnected fluidised beds. The CO_2 removal by the sorbent takes place in a gasifier (Eq. (6-1)), whereas the sorbent regeneration, represented by Eq. (6-2) and Eq. (6-3), takes place in a calciner. It should be noted that Eq. (6-3) corresponds to the first stage of dolomite decomposition, which occurs at around 700 °C and is not dependent on the CO_2 content in the gas phase present in the calciner (De La Calle Martos et al., 2016).

Carbonation:

$$CaO(s) + CO_2(g) \rightarrow CaCO_3(s) \qquad \Delta H = -178\ kJ/mol \qquad \textbf{(6-1)}$$

Calcination:

$$CaCO_3(s) \rightarrow CaO(s) + CO_2(g) \qquad \Delta H = 178\ kJ/mol \qquad \textbf{(6-2)}$$

Dolomite decomposition:

$$MgCa(CO_3)_2(s) \rightarrow CaCO_3(s) + MgO(s) + CO_2(g) \qquad \Delta H = 127\ kJ/mol \qquad \textbf{(6-3)}$$

12 Lower heating value

13 Dry basis

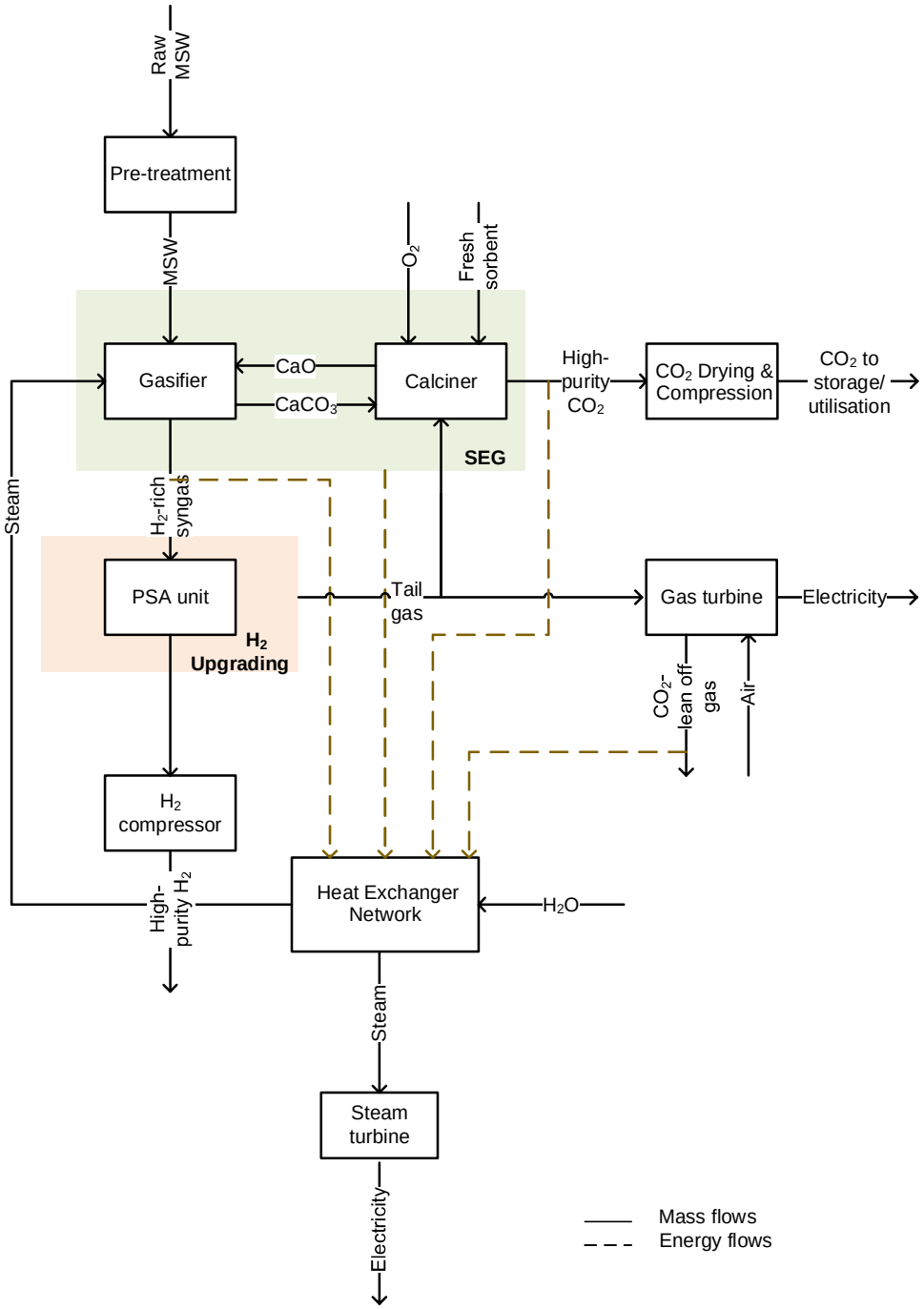

Figure 6-1: Simplified block diagram representation of sorption-enhanced gasification of municipal solid waste for hydrogen production

To compensate for the sorbent deactivation and corresponding decrease in the CaO conversion, a fresh stream of sorbent, called make-up (F_0), is fed to the calciner. Eq. (6-4) represents the maximum average conversion (X_{ave}) that can be accomplished by the sorbent over the cycles of carbonation/calcination and is

based on the model presented by Rodríguez, Alonso and Abanades (2010). The maximum average conversion depends on the properties of sorbent (a_1, a_2, f_1, f_2 and b), the carbonated (f_{carb}) and calcined sorbent fraction (f_{calc}), the fresh make-up sorbent rate (F_0) and the sorbent circulation rate (F_R). The sorbent properties were determined by the curve-fitting procedure. The experimental data detailed by Zhen-Shan et al. (2008) and González, Kokot-Blamey and Fennell (2020) were used to determine the sorbent characteristics for dolomite and doped limestone, respectively. It is noteworthy that since the gasification and CO_2 capture take place in the gasifier, the solid stream leaving the gasifier comprises the sorbent and the ash. Part of the ash is purged with the deactivated sorbent after the calcination.

$$X_{ave}=(F_0+F_R r_0)f_{calc}\left[\frac{a_1 f_1^2}{F_0+F_R f_{carb} f_{calc}(1-f_1)}+\frac{a_2 f_2^2}{F_0+F_R f_{carb} f_{calc}(1-f_2)}+\frac{b}{F_0}\right] \quad \textbf{(6-4)}$$

The heat required by the endothermic calcination reaction is met by the oxy-combustion of the unconverted char and a fraction of the tail gas from the H_2 upgrading unit. It was assumed that the O_2 is delivered by a cryogenic ASU, which corresponds to energy consumption of 200 $kW_{el}h/t_{O_2}$ (Romano, 2013). Since the gasification and CO_2 capture take place simultaneously in the same reactor, the equilibrium of water gas shift reaction, Eq. (6-5), is altered and the forward reaction is favoured, enhancing the H_2 formation. Moreover, this kind of integration is beneficial because the heat released by the exothermic carbonation reaction and the sensible heat of sorbent sustains the endothermic gasification process.

Water Gas Shift:

$$CO(g) + H_2O(g) \leftrightarrow CO_2(g) + H_2(g) \qquad \Delta H = \pm 40.9\ kJ/mol \quad \textbf{(6-5)}$$

Two reactors, Gibbs reactor and stoichiometric reactor, were used to represent the gasification and carbonation processes, respectively. As these processes occur in the same reactor, a heat stream is connected between the Gibbs and stoichiometric reactors. A Gibbs reactor was also used to model the calcination process. It should be noted that besides the reactor units of SEG, a PSA unit, an ASU, a gas turbine, a heat exchanger network and a CO_2 compression unit are

also components of the plant. Because the temperature of flue gas leaving the combustor chamber is close to the adiabatic flame temperature, this is mixed with compressed air at 20 bar to lower the turbine inlet temperature to 1268 °C. Then, the flue gas is expanded in the turbine that is coupled with the generator to produce electricity. It was assumed that the H_2-rich stream produced in the sorption-enhanced gasifier is upgraded in a PSA unit, which was modelled as a black box. According to Luberti et al. (2014) and Hu (2015), an H_2 stream with 99.9% of purity and 93% of recovery rate is achievable at 34 bar. Consequently, the H_2-rich syngas produced in the sorption-enhanced gasifier is compressed from 1 bar to 34 bar in a 9-stage compressor. It should be noted the H_2-rich stream upgrading is preceded by cooling the gas to 30 °C and water removal stages. The heat recovered during these stages is integrated into the heat exchanger network to produce steam that is used as the gasifying agent in the SEG process. Then, the high-purity H_2 stream is subjected to compression until 60 bar. Part of the tail gas from the PSA unit is used to meet the calciner energy requirement and the remaining part is burnt in the gas turbine to generate electricity. In the CO_2 compression unit, the pressure of the high-purity CO_2 stream produced in the calciner is increased to 110 bar and the temperature is reduced to 25 °C (Metz et al., 2005). The high-grade heat of the high-purity CO_2 stream along with the one from the CO_2-lean off-gas and the H_2-rich syngas, is recovered in the heat exchanger network and used in the steam cycle to produce electricity. The SEG model, as well as the steam cycle, have been described in detail and validated elsewhere (Santos, Manovic and Hanak, 2021; Santos and Hanak, 2022)

Table 6-2: Summary of the key sorption-enhanced gasification model assumptions

Unit operation	Parameter	Value
Sorption-enhanced gasification		
Sorption-enhanced gasifier	Temperature [°C]	650
	Steam-to-biomass ratio [wt/wt]	0.5-1.7 (Dolomite) 0.5-2.0 (Limestone and doped limestone)
	Carbonattion extent [-]	0.7
	CO_2 capture efficiency in carbonator [%]	90.0
Calciner	Temperature [°C]	850 (Dolomite) 900 (Limestone and doped limestone)
	Calcination extent [-]	0.95
	Excess oxygen [$\%_{vol,dry}$]	2.5
	Ratio between fresh make-up sorbent rate and sorbent circulation rate [-]	0.02
H_2-rich syngas upgrading		
Compression		
Compressor	Polytropic efficiency [%]	80.0
	Mechanical efficiency [%]	99.6
H_2-rich syngas final stream	Temperature [°C]	30
	Pressure [bar]	34
PSA	H_2 recovery [%]	93.0
	H_2 purity [$\%_{vol}$]	99.9
	Temperature [°C]	30
	Feed pressure [bar]	34
	Tail gas pressure [bar]	1
	Delivery pressure [bar]	60
CO_2 compression		
Compressors	Polytropic efficiency [%]	80.0
	Mechanical efficiency [%]	99.6
Pump	Isentropic efficiency [%]	80.0
	Mechanical efficiency [%]	99.6
CO_2 final stream	Temperature [°C]	25.0
	Pressure [bar]	110.0
Steam Cycle		
Condenser	Fresh water temperature [°C]	10.0
Low-pressure turbine	Isentropic efficiency [%]	88
	Mechanical efficiency [%]	98
Intermediate-pressure turbine	Isentropic efficiency [%]	94
	Mechanical efficiency [%]	99.8
High-pressure turbine	Isentropic efficiency [%]	92.0
	Mechanical efficiency [%]	99.8
Live Steam	Temperature [°C]	593.0
	Pressure [bar]	154.0
Gas turbine		
	Turbine inlet temperature [°C]	1268
	Turbine isentropic efficiency [%]	80
	Turbine mechanical efficiency [%]	99.6
	Compressor outlet pressure [bar]	20
	Combustor pressure drop [%]	2
Fresh material (Hanak et al., 2017)	Dolomite (57.5%$_{wt}$ $CaCO_3$, 42.44%$_{wt}$ $MgCO_3$, 0.01%$_{wt}$ SiO_2, 0.02%$_{wt}$ Fe_2O_3, 0.03%$_{wt}$ Al_2O_3) Limestone (95.0%$_{wt}$ $CaCO_3$, 3.5%$_{wt}$ $MgCO_3$, 0.6%$_{wt}$ SiO_2, 0.4%$_{wt}$ Fe_2O_3, 0.5%$_{wt}$ Al_2O_3)	

6.3 Techno-economic feasibility assessment

In this work, the techno-economic analysis of MSW SEG for dolomite and doped limestone was evaluated at its best performance to ensure a fair comparison. As

explained in Section 6.4, it was assumed that the best performance of each sorbent is achieved for the highest value of *SBR* at which the plant is energy self-sufficient. These figures were benchmarked with that obtained for SEG using limestone as sorbent and conventional gasification (Santos and Hanak, 2022).

6.3.1 Thermodynamic performance indicators

H_2 production efficiency, gross power efficiency, net power efficiency, and total efficiency were the indicators chosen to appraise and compare the thermodynamic performance of SEG and conventional gasification. The H_2 production efficiency, described by Eq. (6-6), is the coefficient between the heat content of the product, H_2 and the fuel heat content, MSW. LHV_{H_2} and $\dot{m}_{H_2}$ represent the lower heating value and mass flow rate of H_2, respectively, and LHV_{MSW} and $\dot{m}_{MSW}$ correspond to the same variables for MSW.

$$\eta_{H_2} = \frac{\dot{m}_{H_2} \cdot LHV_{H_2}}{\dot{m}_{MSW} \cdot LHV_{MSW}} \quad \textbf{(6-6)}$$

The ratio between the sum of electric power output from the gas turbine and the steam cycle ($W_{el,gross}$) and the fuel heat content, MSW, defines the gross power efficiency ($\eta_{el,gross}$) defined by Eq. (6-7).

$$\eta_{el,gross} = \frac{W_{el,gross}}{\dot{m}_{MSW} \cdot LHV_{MSW}} \quad \textbf{(6-7)}$$

The Eq. (6-8) represents the net power efficiency ($W_{el,net}$) that is defined as the ratio between the net electric power output ($W_{el,net}$) and the fuel heat content, MSW. The former is the difference between the gross electric power output and the electric power demand by the auxiliary equipment.

$$\eta_{el,net} = \frac{W_{el,net}}{\dot{m}_{MSW} \cdot LHV_{MSW}} \quad \textbf{(6-8)}$$

The sum of H_2 production and net power efficiencies, defines the total efficiency (η_{tot}) represented by Eq. (6-9).

$$\eta_{tot} = \frac{\left(\dot{m}_{H_2} \cdot LHV_{H_2}\right) + W_{el,net}}{\dot{m}_{MSW} \cdot LHV_{MSW}} \quad \textbf{(6-9)}$$

6.3.2 Economic performance indicators

The levelised cost of H_2 (*LCOH*) and the cost of CO_2 avoided (*AC*) were selected as indicators to assess the economic performance of SEG. These were used to benchmark the performance of MSW SEG with that of conventional gasification. The *LCOH*, minimum H_2 selling price at which the profits offset the total costs over the project lifetime, was estimated based on the net present value (*NPV*). The capital costs of each piece of equipment were scaled up using a scaling size factor. All the correlations are listed as supplementary information. The approach used to assess the total capital requirement is detailed in Santos and Hanak (Santos and Hanak, 2022). Although the inflation was not considered over the project lifetime, the capital costs were updated to the year 2017 using *CEPCI* (CEPCI, 2020).

Since in this work all the costs are presented in Euro (€), if the costs reported in the literature were in a different currency, an average conversion rate for the year 2017 was used (Bank of England, 2019). The average conversion rate for the year 2017 and the other economic parameters and assumptions are summarised in Table 6-3. The operating and maintenance costs account for the variable and the fixed costs. The former was calculated based on the production output, including the costs associated with raw materials, utilities and CO_2 transport and storage. To estimate the latter, it was assumed 17.8% of the total capital requirement is spent to cover the costs associated with salaries, insurance & tax payments, mortgage payments and indirect expenses of running a business (Schweitzer et al., 2018).

Table 6-3: Parameters used to assess the economic performance

Parameter	Value
Unit cost of electricity exported to the grid [€/$MW_{el}h$] (Onarheim et al., 2017b)	40.0
Limestone unit cost [€/t] (Schweitzer et al., 2018)	11.6
Dolomite unit cost [€/t]	11.6
Doped limestone unit cost [€/t]	58.0[14]
Fresh water unit cost [€/m^3] (Schweitzer et al., 2018)	2.4
CO_2 transport and storage cost [€/t_{CO_2}] (Maas, n.d.)	20.0
Others	
Project interest rate [%] (Martínez et al., 2014b; Yang et al., 2010)	8.8
Project lifetime [y] (Martínez et al., 2014b; Yang et al., 2010)	25.0
Capacity factor [%] (Martínez et al., 2014b; Yang et al., 2010)	80.0
Average GBP/EUR exchange rate 2017 (Bank of England, 2019)	1.1418
Average USD/EUR exchange rate 2017 (Bank of England, 2019)	0.8898
CO_2 emission allowance price [€/t_{CO_2}] (Ember, 2022)	39.6
Gate fee [€/t_{MSW}] (Haaf et al., 2020)	40.0

The cost of CO_2 avoided, given by Eq. (6-10), is the ratio between the difference of *LCOH* and the difference of equivalent CO_2 emissions ($e_{CO_2,eq}$) of conventional gasification and of sorption-enhanced gasification plants. The equivalent CO_2 emission accounts for the direct and indirect CO_2 emissions. The latter is associated with the electric power imported or exported by the plant. The subscripts Gasf and SEG refer to conventional gasification and sorption-enhanced gasification, respectively.

$$AC = \frac{LCOH_{SEG} - LCOH_{Gasf}}{e_{CO_2,eq,Gasf} - e_{CO_2,eq,SEG}} \quad \textbf{(6-10)}$$

6.4 Results and discussion

The techno-economic performance of SEG using dolomite and doped limestone with seawater as sorbent was assessed based on the indicators defined in the previous section. These sorbents' performance was compared with that obtained for SEG using natural limestone. The SEG performance was benchmarked with the conventional gasification.

6.4.1 Thermodynamic performance

A parametric study was carried out varying the *SBR* between 0.5 and 1.7 and between 0.5 and 2.0 for SEG using dolomite and doped limestone, respectively.

14 The price of doped limestone was assumed to be 5 times the price of natural limestone (11.6 €/t) to account the doping and drying of sorbent

The *SBR* ranges are different because it was assumed that the plant is energetic self-sufficient, which after the last point of the interval (*SBR*=1.7 and *SBR*=2.0, for dolomite and doped limestone, respectively) is no more valid. The gasification temperature was kept constant at 650 °C because for temperatures behind 680 °C the CO_2 capture is controlled by the equilibrium of carbonation reaction (Martínez et al., 2020a). The effect of *SBR* on the H_2 yield and gross and net power outputs is shown in Figure 6-2. This analysis revealed a trade-off between H_2 production and the net power output. It can be seen the profiles of the analysed variables are similar for both sorbents. The H_2 yield increased gradually with the *SBR* increase, which is due to the equilibrium shift of steam-methane reforming and water gas shift reactions. As the H_2O content increases, the equilibrium changes and the forward reaction is favoured, thus, boosting the H_2 production. On the other hand, the gross and net power outputs decreased which can be attributed to the higher power consumption for the H_2 final product compression and CO_2 compression, as well as higher energy consumption for steam production. Moreover, the power generation by the gas turbine and the steam cycle was penalised. This is due to the reduced availability of the tail gas, from the H_2 upgrading unit, to be burnt in the gas turbine and the heat excess to be recovered. These trends were observed for both sorbents with some particularities. In the case of dolomite, the lower electric power generated by the gas turbine was compensated by the higher electric power generated by the steam cycle. It was because there was less tail gas available to be burnt in the gas turbine and there was more heat excess recovered in the steam cycle. The latter can be attributed to the fact that more solids were recirculated. Therefore, more heat was released at the carbonator, which is in agreement with the study carried out by Ortiz, Valverde and Chacartegui (2016) for CaL process. In the case of doped limestone, since less tail gas was needed to meet the energy requirement of the calciner, the electric power generated by the gas turbine compensated the lower one generated by the steam cycle.

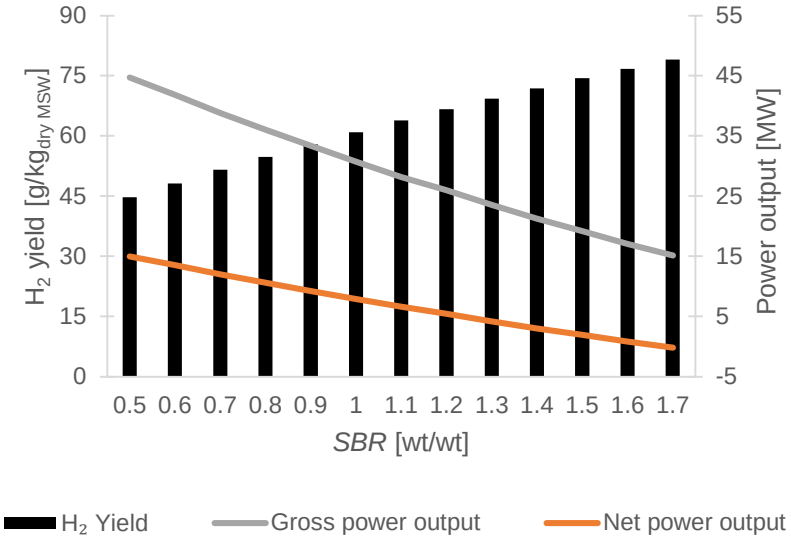

a)

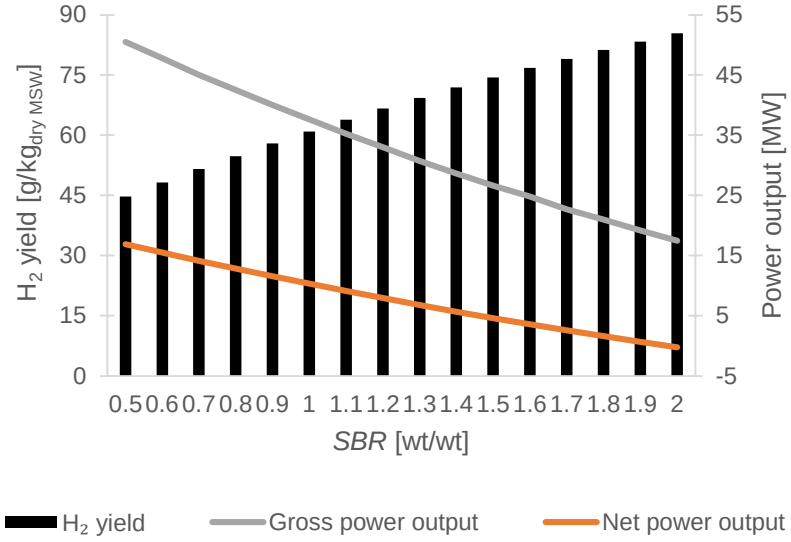

b)

Figure 6-2: Effect of steam-to-biomass ratio, at gasification temperature of 650 °C, on hydrogen yield, gross and net power outputs for sorption-enhanced gasification using (a) dolomite and (b) doped limestone with seawater as sorbent

The effect of *SBR* on the thermodynamic performance indicators, described in Section 6.3.1, is presented in Figure 6-3. As would be expected, the H_2 production, gross power and net power efficiencies follow the trends seen for H_2 yield, gross and net power outputs (Figure 6-2). The total efficiency increased

marginally in the *SBR* range investigated. Because this work intends to compare the H_2 production from MSW SEG using different sorbents, to perform a fair comparison, the optimum *SBR* was determined as the value at which there was a change from positive to negative sign on the net power output. This means the plant is self-sufficient from an energy standpoint and the H_2 production is maximised. Thus, the optimum *SBR* was 1.6 and 1.9 for dolomite and doped limestone, respectively. For higher *SBR* values, the electricity generated by the system was insufficient to meet the auxiliary power requirement of the SEG process. Consequently, the SEG plant would need to draw electricity from the grid. At the optimum *SBR,* the SEG process was found to result in an H_2 yield of 76.7 $g/kg_{dry\ MSW}$ and 83.3 $g/kg_{dry\ MSW}$ (Figure 6-2) for dolomite and doped limestone, respectively. This translated into an H_2 production efficiency of 46.0% and 50.0% (Figure 6-3). Similar to the H_2 production efficiency, the use of dolomite resulted in a lower total efficiency by 4 percentage points, 46.8% (dolomite) compared to that of the SEG process using doped limestone (50.6%). Although the calciner temperature can be reduced from 900 °C to 850 °C when dolomite was used as sorbent, a higher sorbent make-up was fed to the calciner due to the presence of inert material. This result is in agreement with the reported for the CaL process (Ortiz, Valverde and Chacartegui, 2016). Consequently, more tail gas from the H_2 upgrading unit was consumed as fuel in the calciner and less was available for power generation in the gas turbine. Besides, more power was required by the ASU and the CO_2 compression unit. The latter can be explained by the fact that more fresh material was calcined. At the carbonator operating conditions (650 °C), the MgO content in the dolomite is not carbonated and more fresh sorbent is needed. Therefore, the SEG process using dolomite has shown to have the highest heat requirement in the calciner (4.9 GJ/t_{CO_2}), on the other hand, the SEG process using doped limestone presents the lowest figure (4.6 GJ/t_{CO_2}).

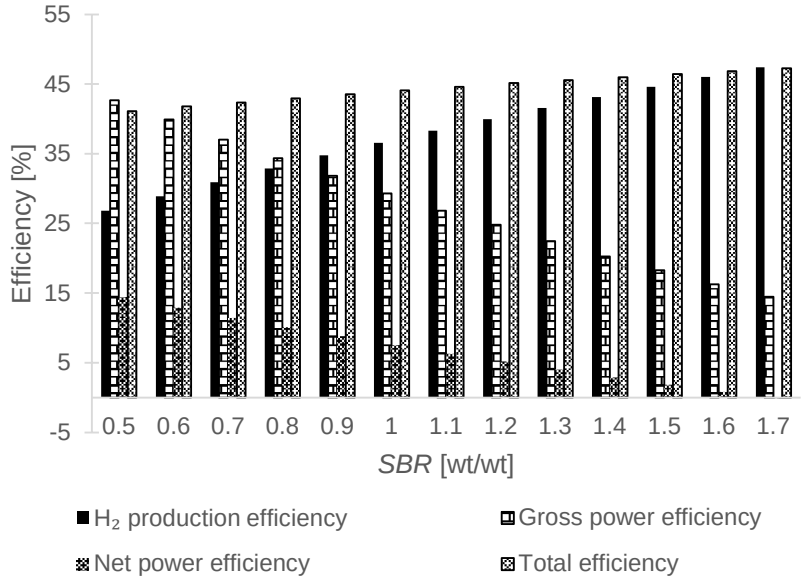

a)

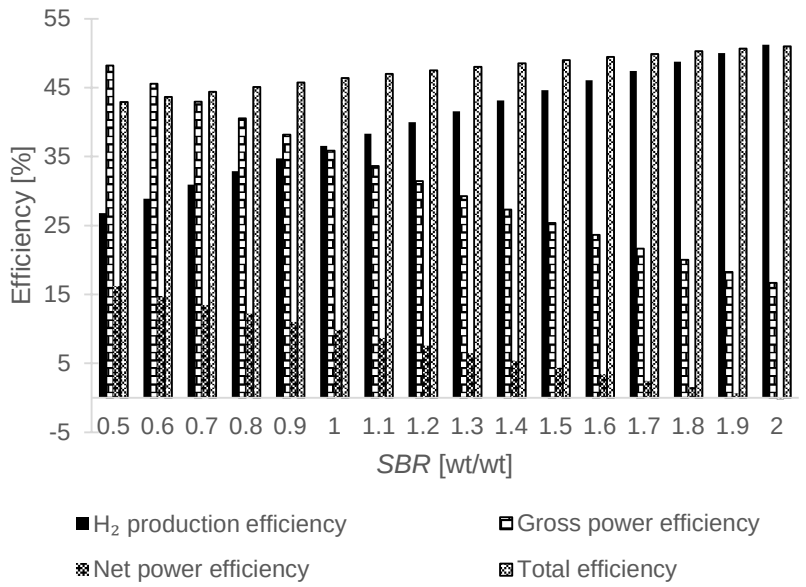

b)

Figure 6-3: Effect of steam-to-biomass ratio, at gasification temperature of 650 °C, on hydrogen production, gross power, net power and total efficiencies for sorption-enhanced gasification using (a) dolomite and (b) doped limestone with seawater as sorbent

6.4.2 Economic performance

Because there is still some discrepancy between the economic data reported in the literature, the economic assessment was performed for different scenarios. In Scenario 1, considered as the baseline scenario, there was no gate fee or fossil CO_2 emissions tax considered; Scenario 2 accounted for a gate fee but no tax on fossil CO_2 emissions; in Scenario 3, the levy of fossil CO_2 emissions but without a gate fee was considered; and in Scenario 4, the application of both, gate fee and fossil CO_2 emissions tax, were considered.

In the techno-economic evaluation of Scenario 2 and Scenario 4, it was assumed that the SEG plant charges a fee of 40.0 €/t_{MSW}, gate fee, to the waste disposers (Haaf et al., 2020). In Scenario 3 and Scenario 4, to estimate the fossil CO_2 emissions, it was assumed there were no fluctuations in MSW composition over the year and 40% of the carbon present was of biogenic origin (Haaf et al., 2020). It is worth noting that the CO_2 emissions from fresh sorbent calcination were also accounted for in the calculation of fossil CO_2 emissions (Santos, Manovic and Hanak, 2021). These CO_2 emissions are the only ones levied with the CO_2 EUA, which was estimated taking into account the average value for the first trimester of 2021, 39.6 €/t_{CO_2} (Ember, 2022). This is a conservative figure since the value in the current year of 2022 is close to 90.0 €/t_{CO_2}.

The estimated *LCOH* and CO_2 avoided cost of SEG using dolomite and doped limestone for each scenario are depicted in Figure 6-4 and Figure 6-5, respectively. The *LCOH* of SEG is also compared with conventional gasification in Figure 6-4. It can be seen from this figure that there is no difference in the trend observed for each sorbent over the scenarios. For both sorbents, the selection of SEG technology over gasification technology led to an increase in the *LCOH*. However, this rise ranged between 79.5% and 100.0% in the case of dolomite and for doped limestone felt between 67.9% and 89.2%. This can be attributed to the higher conversion in the carbonator obtained in the case of doped limestone and thus, a higher H_2 production was achieved.

Regarding the baseline scenario (Scenario 1) the *LCOH* increased from 2.7 (conventional gasification) to 5.4 €/kg_{H_2} or 5.0 €/kg_{H_2} of SEG using dolomite or SEG using doped limestone, respectively. These figures corresponded to a CO_2 avoided cost of 130.4 €/t_{CO_2} and 117.7 €/t_{CO_2} in the case of dolomite and doped limestone, respectively.

The application of a gate fee (Scenario 2) decreased the *LCOH* of conventional gasification and SEG due to an additional revenue obtained by the waste management plant. While this reduction was more pronounced for conventional gasification, about 20.5%, in the case of SEG was about half of this figure for both sorbents, around 10.5%. Because both technologies benefited from this additional revenue, this difference was not reproduced on the cost of CO_2 avoided (Figure 6-5), which varied just about 1.0%.

On the other hand, in Scenario 3, as more than 90.0% of the CO_2 emissions were captured in the case of SEG, the levy of fossil CO_2 emissions reduced the cost of CO_2 avoided by around 20.0% (from 130.4 €/t_{CO_2} to 105.6 €/t_{CO_2}, in the case of dolomite and 177.7 €/t_{CO_2} to 92.9 €/t_{CO_2}, in the case of doped limestone) compared to baseline Scenario 1. While the *LCOH* increased by 20.0% in the conventional gasification, the *LCOH* of SEG just increased by 0.6% and 0.8% in the case of dolomite and doped limestone, respectively (Figure 6-4).

It can be observed in Figure 6-4 that the application of both gate fee and fossil CO_2 emissions tax (Scenario 4) did not impact the *LCOH* of conventional gasification. This happened because the additional revenue obtained from the gate fee compensated the additional cost regarding the tax on fossil CO_2 emissions. Nevertheless, the *LCOH* of SEG was reduced by 10.0% (from 5.4 and 5.0 €/kg_{H_2} to 4.8 €/kg_{H_2} and 4.5 €/kg_{H_2}, for dolomite and doped limestone, respectively). This corresponded to a decrease in the cost of CO_2 avoided of around 20.0% when compared with the baseline Scenario 1 (130.4 €/t_{CO_2} against 104.7 €/t_{CO_2} and 117.7 €/t_{CO_2} against 94.1 €/t_{CO_2}, in the case of dolomite and doped limestone, respectively).

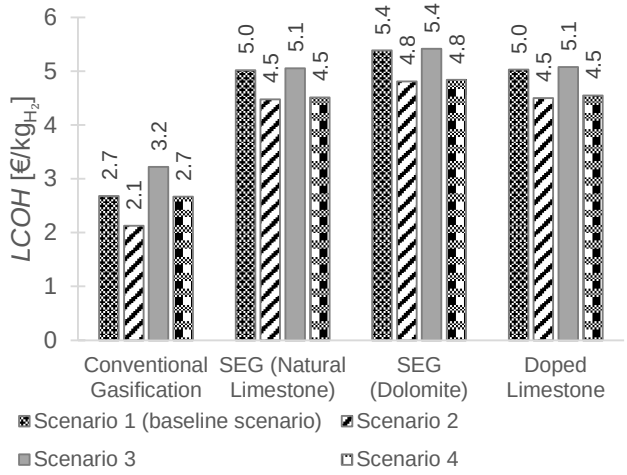

Figure 6-4: Comparison of levelised cost of hydrogen of conventional gasification and of sorption-enhanced gasification using natural limestone, dolomite and doped limestone with seawater as sorbent, for the different scenarios

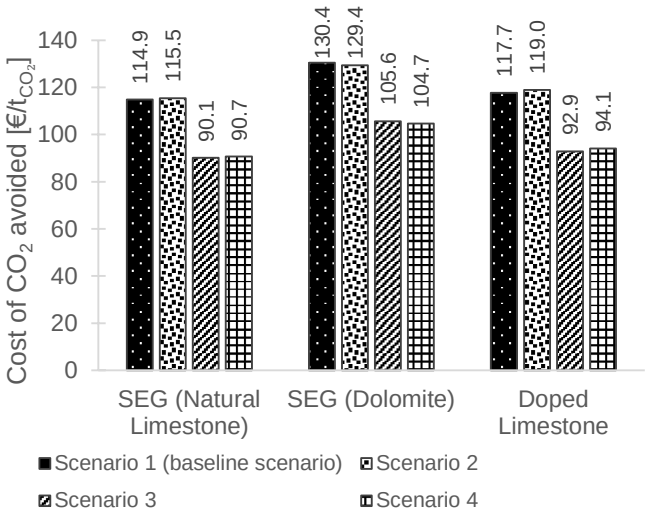

Figure 6-5: Comparison of cost of CO_2 avoided for sorption-enhanced gasification using natural limestone, dolomite and doped limestone with seawater as sorbent, for the different scenarios

6.4.3 Sensitivity analysis

Since there is still some uncertainty associated with the economic assessment and in particular to the capital cost of SEG, which is very scarce, a sensitivity analysis on the main economic parameters was performed. The effect of these parameters on the cost of CO_2 avoided was investigated by varying their values by ±25% for the baseline Scenario 1 (Figure 6-6). The conventional gasification and SEG capital requirements, in addition to the prices of CO_2 transport and storage, electricity and sorbent were the parameters considered in the sensitivity analysis.

As can be seen in Figure 6-6, the results are quite similar for both sorbents, with the capital requirement playing the main role in the cost of CO_2 avoided. An increase of 25% in the capital cost of SEG led to a 43.3% and 45.6% increase in the cost of CO_2 avoided for dolomite and doped limestone, respectively. On the other hand, the cost of CO_2 avoided can be lowered by 26.3% and 30.3% for dolomite and doped limestone, respectively, if the capital required by conventional gasification rises by 25%. The only difference observed between the two sorbents stems from the difference in the sorbent cost. While the variation of ±25% on dolomite price changed the cost of CO_2 avoided by no more than ±0.8%, the cost associated with the doped dolomite can influence the cost of CO_2 avoided by ±2.2%. This can be explained by the fact that it was assumed that the price of doped limestone (58.0 €/t) was 5 times the price of natural limestone (11.6 €/t), the latter was assumed to be the price of dolomite. For that reason, and since there is no precise cost associated with doping limestone, a further sensitivity for the baseline scenario (no gate fee or fossil CO_2 emissions tax) was carried out.

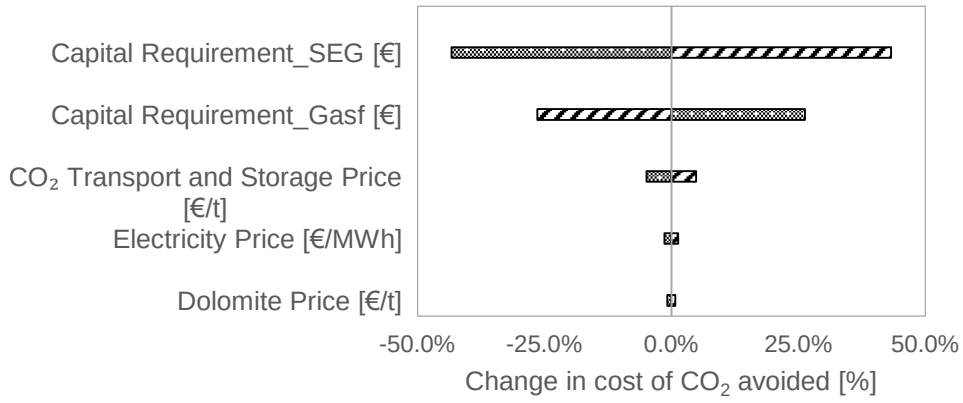

a)

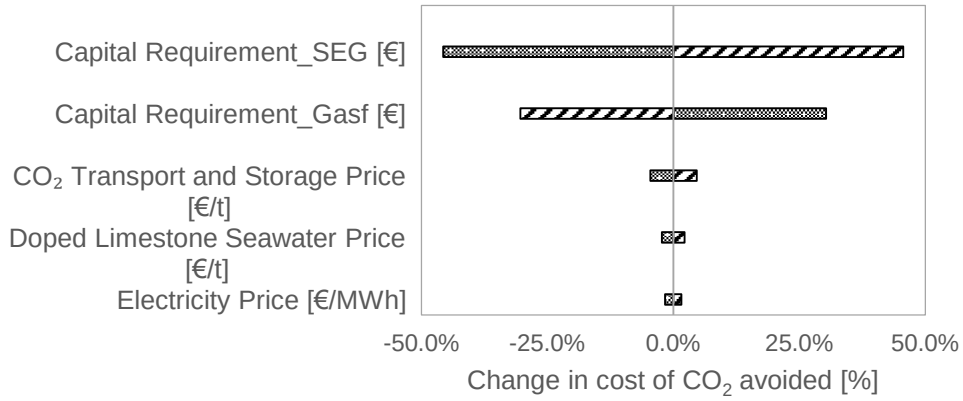

b)

Figure 6-6: Effect of the main economic parameters on the cost of CO_2 avoided: a) using dolomite as sorbent and b) using doped limestone with seawater as sorbent. Bubbles: -25% of baseline parameter, Stripes: +25% of baseline parameter

To understand how the cost of doped limestone influences the SEG MSW viability, the effect of the doped limestone price on the *LCOH* and the cost of CO_2 avoided was assessed. The price of the doped limestone was varied from 11.6 €/t (limestone price) to 116 €/t (10x limestone price). The results are shown in Figure 6-7. It can be observed that the *LCOH* can vary from 4.9 €/kg_{H_2} to 5.2 €/kg_{H_2}, which corresponds to a cost of CO_2 avoided between 109.3 €/t_{CO_2} and 128.4 €/t_{CO_2}. Thus, if the doping process did not impose any cost penalty on sorbent price, the use of doped limestone would slightly reduce the *LCOH* from

5.0 €/kg_{H_2} (natural limestone) to 4.9 €/kg_{H_2}, followed by a reduction of 5% on the cost of CO_2 avoided.

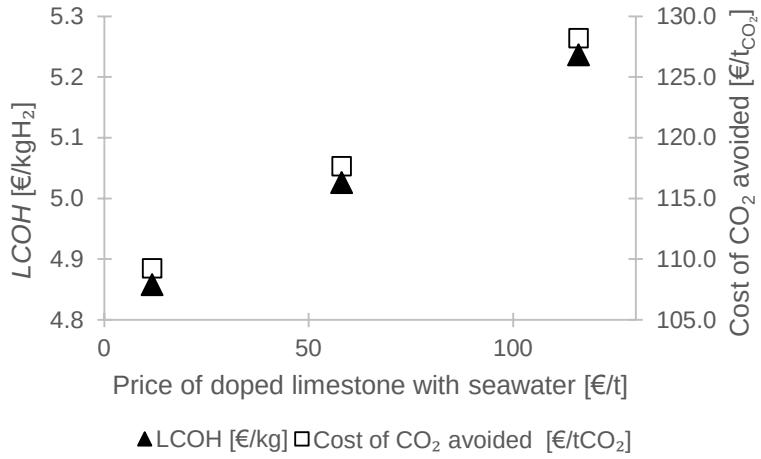

Figure 6-7: Effect of doped limestone price on the levelised cost of hydrogen and cost of CO_2 avoided

The comparison of SEG performance using dolomite and doped limestone with that of SEG using natural limestone and conventional gasification is presented in Table 6-4. It should be mentioned that the optimum conditions for each case were a trade-off between H_2 productivity and net power efficiency. Thus, in all cases, it was considered an energetic self-sufficient plant.

Regarding the thermodynamic performance, the technology SEG using doped limestone presented a higher H_2 production efficiency, 50.0%. This can be attributed to the enhanced CO_2 sorption capacity of doped limestone. When compared with conventional gasification, this higher H_2 productivity was obtained at the expense of electrical power production. The net power efficiency of conventional gasification (6.0%) was more from 5 percentage points than that of SEG using doped limestone (0.6%).

As can be seen from Table 6-4, the integration of CO_2 capture, SEG, led to a reduction of more than 90% of equivalent CO_2 emissions. These decreased from 21.7 kg_{CO_2}/kg_{H_2} (conventional gasification) to the range between 1.0–1.8 kg_{CO_2}/kg_{H_2}.

The economic assessment has shown that the introduction of CO_2 capture doubles the *LCOH* when dolomite was used as a sorbent. Between the natural and doped limestone, the former presented a lower cost of CO_2 avoided (114.9 €/t_{CO_2}) than the latter (117.7 €/t_{CO_2}). It is noteworthy that in the analysis of doped limestone, the energy penalty associated with sorbent drying was associated with the higher sorbent price. However, it is clear from Figure 6-7 that if the cost of doped limestone is reduced to below 42.6 €/t, this sorbent would present the lowest cost of CO_2 avoided. Thus, the doped limestone seems to be a route that should be explored to replace natural limestone, whose one of the main drawbacks is the deactivation over the cycles.

Table 6-4: Summary of techno-economic performance of conventional gasification and sorption-enhanced gasification. The latter was carried out for three sorbents: natural limestone, dolomite and doped limestone with seawater

Parameter	Conventional gasification	Sorption-enhanced gasification		
		Natural limestone	Dolomite	Doped limestone
Thermodynamic assessment				
H_2 production efficiency [%]	47.7	48.7	46.0	50.0
Gross power efficiency [%]	18.9	17.0	16.2	18.3
Net power efficiency [%]	6.0	0.6	0.8	0.6
Total efficiency [%]	53.3	49.3	46.8	50.6
Environmental assessment				
Equivalent CO_2 emissions [kg_{CO_2}/kg_{H_2}]	21.7	1.4	1.0	1.8
Economic assessment				
Levelised cost of H_2 [€/kg_{H_2}]	2.7	5.0	5.4	5.0
Cost of CO_2 avoided [€/t_{CO_2}]		114.9	130.4	117.7

6.5 Conclusions

In this work, the techno-economic performance of MSW SEG using three CaO-based sorbents, natural limestone, dolomite and doped limestone, was compared. While the H_2 production was one of the key thermodynamic performance indicators selected, the *LCOH* and cost of CO_2 avoided were the key economic performance indicators. The use of limestone as sorbent has

shown to have the best techno-economic performance. The *LCOH* of SEG using dolomite is 5.4 €/kg_{H_2} against 5.0 €/kg_{H_2} when the limestone is used as sorbent. The natural limestone has shown to have the lowest cost of CO_2 avoided (114.9 €/t_{CO_2}), whereas the doped limestone had the highest H_2 production efficiency (50.0%).

In this work, the heat requirement in the calciner falls between 4.6 GJ/t_{CO_2} (doped limestone) and 4.9 GJ/t_{CO_2} (dolomite). These results revealed a link between the heat requirement in the calciner and the H_2 production costs, however, detailed work on the effect of calcination temperature on energy requirement and overall costs should be carried out.

A sensitivity analysis on the cost of CO_2 avoided was also performed by varying the main economic parameters by ± 25%. The capital requirement of conventional gasification and SEG, the CO_2 transport and storage price, the electricity and sorbent prices were the selected parameters in the sensitivity analysis. From these parameters, the capital requirement has the greatest influence on the CO_2 avoided cost, a reduction of 25% of SEG capital cost reduced the cost of CO_2 avoided by more than 40%.

Although there is no data available for doped limestone price, it was found that a reduction on its price to below 42.6 €/t would reduce the cost of CO_2 avoided to a value lower than that for natural limestone. Furthermore, new sorbents for CO_2 capture and H_2 production would be an attractive alternative to natural limestone if produced with similar costs to that of natural limestone.

6.6 References

Armbrust, N., Duelli, G., Dieter, H. and Scheffknecht, G. (2015) ‘Calcium looping cycle for hydrogen production from biomass gasification syngas: Experimental investigation at a 20 kW_{th} dual fluidized-bed facility’, *Industrial and Engineering Chemistry Research*, 54(21), pp. 5624–5634.

Armutlulu, A., Naeem, M.A., Liu, H.J., Kim, S.M., Kierzkowska, A., Fedorov, A. and Müller, C.R. (2017) ‘Multishelled CaO Microspheres Stabilized by Atomic Layer Deposition of Al_2O_3 for Enhanced CO_2 Capture Performance’, *Advanced*

Materials, 29(41), pp. 1–9.

Atsonios, K., Koumanakos, A., Panopoulos, K.D., Doukelis, A. and Kakaras, E. (2013) 'Techno-economic comparison of CO_2 capture technologies employed with natural gas derived GTCC', *Proceedings of the ASME Turbo Expo*., Vol.2, p. V002T07A018.

Bank of England (2019) *Bank of England Statistical Interactive Database | Interest & Exchange Rates | Official Bank Rate History*. Available at: http://www.bankofengland.co.uk/boeapps/iadb/repo.asp (Accessed: 5 December 2019).

CEPCI (2020) *The Chemical Engineering Plant Cost Index*., *Chemical Engineering* Available at: https://www.chemengonline.com (Accessed: 5 December 2019).

Chen, J., Duan, L. and Sun, Z. (2020) 'Review on the Development of Sorbents for Calcium Looping', *Energy & Fuels*, 34(7), pp. 7806–7836.

Chen, S., Zhao, Z., Soomro, A., Ma, S., Wu, M., Sun, Z. and Xiang, W. (2020) 'Hydrogen-rich syngas production via sorption-enhanced steam gasification of sewage sludge', *Biomass and Bioenergy*, 138, p. 105607.

Ember (2022) *Daily Carbon Prices*. Available at: https://ember-climate.org/data/carbon-price-viewer/ (Accessed: 24 March 2022).

Foster, W., Azimov, U., Gauthier-Maradei, P., Molano, L.C., Combrinck, M., Munoz, J., Esteves, J.J. and Patino, L. (2021) 'Waste-to-energy conversion technologies in the UK: Processes and barriers – A review', *Renewable and Sustainable Energy Reviews*, 135, p. 110226.

Fremaux, S., Beheshti, S.-M., Ghassemi, H. and Shahsavan-Markadeh, R. (2015) 'An experimental study on hydrogen-rich gas production via steam gasification of biomass in a research-scale fluidized bed', *Energy Conversion and Management*, 91, pp. 427–432.

González, B., Blamey, J., Al-Jeboori, M.J., Florin, N.H., Clough, P.T. and Fennell,

P.S. (2016) ‘Additive effects of steam addition and HBr doping for CaO-based sorbents for CO_2 capture’, *Chemical Engineering and Processing: Process Intensification*, 103, pp. 21–26.

González, B., Kokot-Blamey, J. and Fennell, P. (2020) ‘Enhancement of CaO-based sorbent for CO_2 capture through doping with seawater’, *Greenhouse Gases: Science and Technology*, 10(5), pp. 878–883.

Haaf, M., Ohlemüller, P., Ströhle, J. and Epple, B. (2020) ‘Techno-economic assessment of alternative fuels in second-generation carbon capture and storage processes’, *Mitigation and Adaptation Strategies for Global Change*, 25(2), pp. 149–164.

Hanak, D.P., Jenkins, B.G., Kruger, T. and Manovic, V. (2017) ‘High-efficiency negative-carbon emission power generation from integrated solid-oxide fuel cell and calciner’, *Applied Energy*, 205, pp. 1189–1201.

He, M., Xiao, B., Liu, S., Guo, X., Luo, S., Xu, Z., Feng, Y. and Hu, Z. (2009) ‘Hydrogen-rich gas from catalytic steam gasification of municipal solid waste (MSW): Influence of steam to MSW ratios and weight hourly space velocity on gas production and composition’, *International Journal of Hydrogen Energy*, 34, pp. 2174–2183.

Hu, M. (2015) ‘The New SeparALLTM Process and PolybedTM PSA for IGCC and CTL Application’, *7th International Freiberg Conference Hohhot, China, June 7th-11th*.

Hu, M., Guo, D., Ma, C., Hu, Z., Zhang, B., Xiao, B., Luo, S. and Wang, J. (2015) ‘Hydrogen-rich gas production by the gasification of wet MSW (municipal solid waste) coupled with carbon dioxide capture’, *Energy*, 90, pp. 857–863.

Hussain, M., Zabiri, H., Uddin, F., Yusup, S. and Tufa, L.D. (2021) ‘Pilot-scale biomass gasification system for hydrogen production from palm kernel shell (part B): dynamic and control studies’, *Biomass Conversion and Biorefinery*

IEA (2021) *Global energy-related CO_2 emissions, 1990-2021, IEA, Paris*. Available at: https://www.iea.org/data-and-statistics/charts/global-energy-

related-co2-emissions-1990-2021 (Accessed: 27 October 2021).

Intergovernmental Panel on Climate Change (2021) *Headline Statements from the Summary for Policymakers*.

Irfan, M., Li, A., Zhang, L., Wang, M., Chen, C. and Khushk, S. (2019) 'Production of hydrogen enriched syngas from municipal solid waste gasification with waste marble powder as a catalyst', *International Journal of Hydrogen Energy*, 44, pp. 8051–8061.

Janajreh, I., Adeyemi, I. and Elagroudy, S. (2020) 'Gasification feasibility of polyethylene, polypropylene, polystyrene waste and their mixture: Experimental studies and modeling', *Sustainable Energy Technologies and Assessments*, 39, p. 100684.

Kaza, S., Yao, L.C.., Bhada-Tata, P. and Van Woerden, F. (2018) *What a Waste 2.0 : A Global Snapshot of Solid Waste Management to 2050.* Washington, DC: Urban Development;. Washington, DC: World Bank.

Kreutz, T., Williams, R., Consonni, S. and Chiesa, P. (2005) 'Co-production of hydrogen, electricity and CO from coal with commercially ready technology. Part B: Economic analysis', *International Journal of Hydrogen Energy*, 30(7), pp. 769–784.

De La Calle Martos, A., Valverde, J.M., Sanchez-Jimenez, P.E., Perejón, A., García-Garrido, C. and Perez-Maqueda, L.A. (2016) 'Effect of dolomite decomposition under CO_2 on its multicycle CO_2 capture behaviour under calcium looping conditions', *Physical Chemistry Chemical Physics*, 18(24), pp. 16325–16336.

Laurent, A., Bakas, I., Clavreul, J., Bernstad, A., Niero, M., Gentil, E., Hauschild, M.Z. and Christensen, T.H. (2014) 'Review of LCA studies of solid waste management systems - Part I: Lessons learned and perspectives', *Waste Management*, 34(3), pp. 573–588.

Lazzarotto, I.P., Ferreira, S.D., Junges, J., Bassanesi, G.R., Manera, C., Perondi, D. and Godinho, M. (2020) 'The role of CaO in the steam gasification of plastic

wastes recovered from the municipal solid waste in a fluidized bed reactor', *Process Safety and Environmental Protection*, 140, pp. 60–67.

Lee, Y.D., Ahn, K.Y., Morosuk, T. and Tsatsaronis, G. (2014) 'Exergetic and exergoeconomic evaluation of a solid-oxide fuel-cell-based combined heat and power generation system', *Energy Conversion and Management*, 85, pp. 154–164.

Li, W., Li, Q., Chen, R., Wu, Y. and Zhang, Y. (2014) 'Investigation of hydrogen production using wood pellets gasification with steam at high temperature over 800 °C to 1435 °C', *International Journal of Hydrogen Energy*, 39(11), pp. 5580–5588.

Li, Y., Zhao, C., Chen, H., Liang, C., Duan, L. and Zhou, W. (2009) 'Modified CaO-based sorbent looping cycle for CO_2 mitigation', *Fuel*, 88(4), pp. 697–704.

Luberti, M., Friedrich, D., Brandani, S. and Ahn, H. (2014) 'Design of a H_2 PSA for cogeneration of ultrapure hydrogen and power at an advanced integrated gasification combined cycle with pre-combustion capture', *Adsorption*, 20(2–3), pp. 511–524.

Luz, F.C., Rocha, M.H., Lora, E.E.S., Venturini, O.J., Andrade, R.V., Leme, M.M.V., Del Olmo, O.A., Codignole, F., Henrique, M., Eduardo, E., Lora, S. and José, O. (2015) 'Techno-economic analysis of municipal solid waste gasification for electricity generation in Brazil', *Energy Conversion and Management*, 103, pp. 321–337.

Lv, L., Zhang, Z. and Li, H. (2019) 'SNG-electricity cogeneration through MSW gasification integrated with a dual chemical looping process', *Chemical Engineering and Processing - Process Intensification*, 145, p. 107665.

Maas, W. (n.d.) *The post-2020 Cost-Competitiveness of CCS Cost of Storage*.

Manzolini, G., Macchi, E. and Gazzani, M. (2013) 'CO_2 capture in natural gas combined cycle with SEWGS. Part B: Economic assessment', *International Journal of Greenhouse Gas Control*, 12, pp. 502–509.

Marcantonio, V., De Falco, M., Capocelli, M., Bocci, E., Colantoni, A. and Villarini, M. (2019) ‘Process analysis of hydrogen production from biomass gasification in fluidized bed reactor with different separation systems’, *International Journal of Hydrogen Energy*, 44(21), pp. 10350–10360.

Martínez, A., Lara, Y., Lisbona, P. and Romeo, L.M. (2014) ‘Operation of a mixing seal valve in calcium looping for CO_2 capture’, *Energy and Fuels*, 28(3), pp. 2059–2068.

Martínez, I., Grasa, G., Callén, M.S., López, J.M. and Murillo, R. (2020) ‘Optimised production of tailored syngas from municipal solid waste (MSW) by sorption-enhanced gasification’, *Chemical Engineering Journal*, 401, p. 126067.

Mazzoni, L. and Janajreh, I. (2017) ‘Plasma gasification of municipal solid waste with variable content of plastic solid waste for enhanced energy recovery’, *International Journal of Hydrogen Energy*, 42(30), pp. 19446–19457.

Mehrpooya, M., Ghorbani, A., Ali Moosavian, S.M. and Amirhaeri, Y. (2022) ‘Optimal design and economic analysis of a hybrid process of municipal solid waste plasma gasification, thermophotovoltaic power generation and hydrogen/liquid fuel production’, *Sustainable Energy Technologies and Assessments*, 49, p. 101717.

Metz, B., Davidson, O., de Coninck, H., Loos, M. and Meyer, L. (2005) *Carbon Dioxide Capture and Storage*. Cambridge; New York; Melbourne; Madrid; Cape Town; Singapore; Sào Paulo: Cambridge University Press.

Michalski, S., Hanak, D.P. and Manovic, V. (2019) ‘Techno-economic feasibility assessment of calcium looping combustion using commercial technology appraisal tools’, *Journal of Cleaner Production*, 219, pp. 540–551.

Morona, L., Erans, M. and Hanak, D.P. (2019) ‘Effect of Seawater, Aluminate Cement, and Alumina-Rich Spinel on Pelletized CaO-Based Sorbents for Calcium Looping’, *Industrial & Engineering Chemistry Research*, 58(27), pp. 11910–11919.

NETL (2019) *Cost and performance baseline for fossil energy plants. Volume 1:*

Bituminous coal and natural gas to electricity.

NREL (2005) *Biomass to Hydrogen Production Detailed Design and Economics Utilizing the Battelle Columbus Laboratory Indirectly-Heated Gasifier*.

Onarheim, K., Santos, S., Kangas, P. and Hankalin, V. (2017) 'Performance and cost of CCS in the pulp and paper industry part 2: Economic feasibility of amine-based post-combustion CO_2 capture', *International Journal of Greenhouse Gas Control*, 66, pp. 60–75.

Ortiz, C., Valverde, J.M. and Chacartegui, R. (2016) 'Energy Consumption for CO_2 Capture by means of the Calcium Looping Process: A Comparative Analysis using Limestone, Dolomite, and Steel Slag', *Energy Technology*, 4(10), pp. 1317–1327.

Radfarnia, H.R. and Iliuta, M.C. (2013) 'Metal oxide-stabilized calcium oxide CO_2 sorbent for multicycle operation', *Chemical Engineering Journal*, 232, pp. 280–289.

Raizada, A., Yadav, S., Tripathi, M., Misra, S. and Mohanty, P. (2021) 'Food waste treatment using in situ gasification after pyrolysis to produce hydrogen-rich syngas', *Biomass Conversion and Biorefinery*

Rodríguez, N., Alonso, M. and Abanades, J.C. (2010) 'Average activity of CaO particles in a calcium looping system', *Chemical Engineering Journal*, 156(2), pp. 388–394.

Romano, M.C. (2013) 'Ultra-high CO_2 capture efficiency in CFB oxyfuel power plants by calcium looping process for CO_2 recovery from purification units vent gas', *International Journal of Greenhouse Gas Control*, 18(0), pp. 57–67.

Rong, N., Wang, Q., Fang, M., Cheng, L., Luo, Z. and Cen, K. (2013) 'Steam hydration reactivation of cao-based sorbent in cyclic carbonation/calcination for CO_2 capture', *Energy and Fuels*, 27(9), pp. 5332–5340.

Salaudeen, S.A., Acharya, B. and Dutta, A. (2018) 'CaO-based CO_2 sorbents: A review on screening, enhancement, cyclic stability, regeneration and kinetics

modelling', *Journal of CO_2 Utilization*, 23, pp. 179–199.

Salvador, C., Lu, D., Anthony, E.J. and Abanades, J.C. (2003) 'Enhancement of CaO for CO_2 capture in an FBC environment', *Chemical Engineering Journal*, 96(1–3), pp. 187–195.

Santos, M.P.S. and Hanak, D.P. (2022) 'Techno-economic feasibility assessment of sorption enhanced gasification of municipal solid waste for hydrogen production', *International Journal of Hydrogen Energy*, 47(10), pp. 6586–6604.

Santos, M.P.S., Manovic, V. and Hanak, D.P. (2021) 'Unlocking the potential of pulp and paper industry to achieve carbon-negative emissions via calcium looping retrofit', *Journal of Cleaner Production*, 280, p. 124431.

Sayyaadi, H. and Mehrabipour, R. (2012) 'Efficiency enhancement of a gas turbine cycle using an optimized tubular recuperative heat exchanger', *Energy*, 38(1), pp. 362–375.

Schweitzer, D., Albrecht, F.G., Schmid, M., Beirow, M., Spörl, R., Dietrich, R.-U. and Seitz, A. (2018) 'Process simulation and techno-economic assessment of SER steam gasification for hydrogen production', *International Journal of Hydrogen Energy*, 43(2), pp. 569–579.

Sedghkerdar, M.H., Mahinpey, N., Sun, Z. and Kaliaguine, S. (2014) 'Novel synthetic sol-gel CaO based pellets using porous mesostructured silica in cyclic CO_2 capture process', *Fuel*, 127, pp. 101–108.

Shirazi, A., Aminyavari, M., Najafi, B., Rinaldi, F. and Razaghi, M. (2012) 'Thermal–economic–environmental analysis and multi-objective optimization of an internal-reforming solid oxide fuel cell–gas turbine hybrid system', *International Journal of Hydrogen Energy*, 37(24), pp. 19111–19124.

Shokrollahi Yancheshmeh, M., Radfarnia, H.R. and Iliuta, M.C. (2016) 'High temperature CO_2 sorbents and their application for hydrogen production by sorption enhanced steam reforming process', *Chemical Engineering Journal*, 283, pp. 420–444.

Spallina, V., Pandolfo, D., Battistella, A., Romano, M.C., Van Sint Annaland, M. and Gallucci, F. (2016) 'Techno-economic assessment of membrane assisted fluidized bed reactors for pure H_2 production with CO_2 capture', *Energy Conversion and Management*, 120, pp. 257–273.

Statista (2021) *Global historical CO_2 emissions from fossil fuels and industry 1750-2020*. Available at: https://www.statista.com/statistics/264699/worldwide-co2-emissions/ (Accessed: 27 October 2021).

Sun, J., Guo, Y., Yang, Y., Li, W., Zhou, Y., Zhang, J., Liu, W. and Zhao, C. (2019) 'Mode investigation of CO_2 sorption enhancement for titanium dioxide-decorated CaO-based pellets', *Fuel*, 256, p. 116009.

Sun, J., Wang, W., Yang, Y., Cheng, S., Guo, Y., Zhao, C., Liu, W. and Lu, P. (2020) 'Reactivation mode investigation of spent CaO-based sorbent subjected to CO_2 looping cycles or sulfation', *Fuel*, 266, p. 117056.

Wang, J., Cheng, G., You, Y., Xiao, B., Liu, S., He, P., Guo, D., Guo, X. and Zhang, G. (2012) 'Hydrogen-rich gas production by steam gasification of municipal solid waste (MSW) using NiO supported on modified dolomite', *International Journal of Hydrogen Energy*, 37(8), pp. 6503–6510.

Wu, Y., Blamey, J., Anthony, E.J. and Fennell, P.S. (2010) 'Morphological changes of limestone sorbent particles during carbonation/calcination looping cycles in a thermogravimetric analyzer (TGA) and reactivation with steam', *Energy and Fuels*, 24(4), pp. 2768–2776.

Xu, Y., Luo, C., Zheng, Y., Ding, H., Zhou, D. and Zhang, L. (2017) 'Natural Calcium-Based Sorbents Doped with Sea Salt for Cyclic CO_2 Capture', *Chemical Engineering and Technology*, 40(3), pp. 522–528.

Yan, J., Sun, R., Shen, L., Bai, H., Jiang, S., Xiao, Y. and Song, T. (2020) 'Hydrogen-rich syngas production with tar elimination via biomass chemical looping gasification (BCLG) using $BaFe_2O_4/Al_2O_3$ as oxygen carrier', *Chemical Engineering Journal*, 387, p. 124107.

Yang, X., Tian, S., Kan, T., Zhu, Y., Xu, H., Strezov, V., Nelson, P. and Jiang, Y.

(2019) ‘Sorption-enhanced thermochemical conversion of sewage sludge to syngas with intensified carbon utilization’, *Applied Energy*, 254, p. 113663.

Yang, Y., Zhai, R., Duan, L., Kavosh, M., Patchigolla, K. and Oakey, J. (2010) ‘Integration and evaluation of a power plant with a CaO-based CO_2 capture system’, *International Journal of Greenhouse Gas Control*, 4(4), pp. 603–612.

Yaqub, Z.T., Oboirien, B.O. and Akintola, A.T. (2021) ‘Process modeling of chemical looping combustion (CLC) of municipal solid waste’, *Journal of Material Cycles and Waste Management*

Yin, J., Zhang, C., Qin, C., Liu, W., An, H., Chen, G. and Feng, B. (2012) ‘Reactivation of calcium-based sorbent by water hydration for CO_2 capture’, *Chemical Engineering Journal*, 198–199, pp. 38–44.

Zhang, M., Peng, Y., Sun, Y., Li, P. and Yu, J. (2013) ‘Preparation of CaO-Al_2O_3 sorbent and CO_2 capture performance at high temperature’, *Fuel*, 111, pp. 636–642.

Zhao, M., Bilton, M., Brown, A.P., Cunliffe, A.M., Dvininov, E., Dupont, V., Comyn, T.P. and Milne, S.J. (2014) ‘Durability of CaO-$CaZrO_3$ sorbents for high-temperature CO_2 capture prepared by a wet chemical method’, *Energy and Fuels*, 28(2), pp. 1275–1283.

Zhen-Shan, L., Ning-Sheng, C., Li, Z., Cai, N. and Croiset, E. (2008) ‘Process Analysis of CO_2 Capture from Flue Gas Using Carbonation/Calcination Cycles’, *AIChE Journal*, 54(7), pp. 1912–1925.

Zheng, X., Ying, Z., Wang, B. and Chen, C. (2018) ‘Hydrogen and syngas production from municipal solid waste (MSW) gasification via reusing CO_2’, *Applied Thermal Engineering*, 144, pp. 242–247.

Zhou, C., Stuermer, T., Gunarathne, R., Yang, W. and Blasiak, W. (2014) ‘Effect of calcium oxide on high-temperature steam gasification of municipal solid waste’, *Fuel*, 122, pp. 36–46.

7 GENERAL DISCUSSION

7.1 Discussion

CCS has been identified as one of the main pathways for industrial decarbonisation. However, just CCS is not enough to meet the targets of the Paris Agreement and deep decarbonisation is required.

Across several industrial sectors, such as iron and steel, cement, petroleum refining and pulp and paper, amine scrubbing has been extensively studied as a carbon capture technology. However, the energy penalty associated with this technology and, thus, the high cost is one of the main drawbacks of amine scrubbing use. The use of a conventional amine, 30%$_{wt}$ MEA, requires regeneration energy in the range between 3.2 GJ/t_{CO_2} and 5.5 GJ/t_{CO_2} (Luis, 2016).

Conversely, CaL has been shown to reduce the energy penalty in the power sector. Due to the high-heat grade available and associated with sorbents of improved performance, the efficiency penalty can be reduced by less than 5% points (Hanak, Michalski and Manovic, 2018). Nevertheless, the superior performance of CaL is not limited to the power sector. In the cement industry, Voldsund et al. (2019) showed that the specific primary energy consumption of CaL was around half (3.2–4.1 GJ/t_{CO_2}) of that for MEA (7.1 GJ/t_{CO_2}).

CaL is an attractive technology for industrial decarbonisation, simultaneously contributing to reducing CO_2 emissions and fossil fuel dependence. The latter can be achieved by the generation of power (Hanak and Manovic, 2017b), H_2 production (Schweitzer et al., 2018) or syngas production (Martínez et al., 2020a). Therefore, the CaL implementation in retrofit (Chapter 3 and Chapter 4) and greenfield scenarios (Chapter 5 and Chapter 6) has been investigated. In the former scenario, CaL was explored as a process for simultaneous CO_2 capture and heat, power and/or H_2 production, whose main objective was reducing the carbon intensity of the pulp and paper plant. In the latter scenario, CaL was investigated for H_2 production from MSW.

Nevertheless, from the concept stage to the commercialisation, the development of technology is costly and also time-consuming. Modelling and simulation tools are a valuable resource for evaluating a process and understand its overall viability, including size, utilities and costs.

CADSIM Plus® and Aspen Plus® were the software packages selected to assess the reference pulp and paper plant and the CaL process, respectively. The process models developed in this project were compared and validated against the data published in the literature.

In the case of the retrofit scenario, the techno-economic assessment was compared for an integrated pulp and paper plant without CO_2 capture (reference) and the same plant with CO_2 capture and, in some cases, coupled with BLG. In the greenfield scenario, the SEG plant was benchmarked with a conventional gasification plant without CO_2 capture.

The implementation of CaL as a CO_2 capture route in the pulp and paper industry has shown to be a viable option to decarbonise and, at the same time, become a carbon-negative industry (Chapter 3). Since most of the CO_2 emissions are from biomass origin, considered neutral, the capture of these leads to negative net carbon emission. Moreover, it was also shown that the integration of CaL led to an increase in the net power output. Consequently, the reference plant turned from an electricity importer to an electricity exporter. Previous studies (Kuparinen, Vakkilainen and Tynjälä, 2019; Möllersten, Gao and Yan, 2006; Onarheim et al., 2017b) had reported an energy penalty in the net power output when post-combustion amine scrubbing was selected as CO_2 capture technology. Therefore, this work demonstrated the CaL superiority to post-combustion amine scrubbing. It also demonstrated that the reduction of CO_2 emissions could be achieved with a cost of CO_2 avoided of 39.0 €/t_{CO_2}. This cost is comparable with studies performed more than one decade ago where amine scrubbing (Hektor and Berntsson, 2009; McGrail et al., 2012) or physical absorption (Möllersten, Gao and Yan, 2006) were selected to capture the CO_2 emissions. Compared with more recent studies (Nwaoha and Tontiwachwuthikul, 2019; Onarheim et al., 2017b), such cost is lower by between 50% and 65% than that reported for post-

combustion amine scrubbing. This work also showed that an EII, pulp and paper, has a high potential to become a carbon-negative industry. It was shown that the simultaneous levy of fossil CO_2 emissions and introduction of credit for negative emissions could reduce the cost of CO_2 avoided by more than 50% (16.9 €/t_{CO_2}). Nevertheless, with the actual policies, which means no recognition of negative CO_2 emissions, there are no incentives to implement CCS. In the future, the inclusion of biogenic emissions in the EU ETS and/or the attribution of credits to them would incentivise the decarbonisation of the pulp and paper industry.

Still, in the pulp and paper industry, the evaluation of CaL coupled with BLG for simultaneous CO_2 capture and H_2 or power production was revealed to be a viable route for both (Chapter 4). Unlike other CO_2 capture technologies, such as physical absorption (Naqvi, Yan and Dahlquist, 2013), which require an additional amount of steam to operate, the high-grade heat available in CaL can be recovered to meet the energy demand of the pulp and paper plant. Yet, this route showed a higher cost of CO_2 avoided (around 50.0 €/t_{CO_2}), still comparable with the figures estimated in the literature. Oxy-fuel combustion and Selexol presented costs of 26.3 €/t_{CO_2} and 40.9 €/t_{CO_2}, respectively (Zhang et al., 2011). It should be noted that these costs correspond to the cost of CO_2 captured instead of the cost of CO_2 avoided. The cost of CO_2 avoided of 20.5 €/t_{CO_2} was found for a conventional CO_2 absorption technology (Ferreira and Balestieri, 2015). Although these figures are lower than the costs reported in this work, it is noteworthy that:

- the cost of CO_2 captured is lower than the cost of CO_2 avoided;
- the capital costs of the mentioned works were estimated based on costs reported in 2000 and 2005; and
- the latter work referent conventional CO_2 absorption technology, considered a carbon credit for the CO_2 captured of 5.3 €/t_{CO_2} and did not account for the cost of CO_2 transport and storage.

Furthermore, in contrast to the abovementioned studies that only considered the CO_2 emissions from the BLG, this work considered the capture of the CO_2 emitted by the entire pulp and paper plant. The implementation of CaL coupled with BLG for H_2 production showed to be the least expensive option compared with BLG

with BLG-CaL-GT or BLG-CaL-SOFC for electricity production. Therefore, the reduction of fossil fuel dependence by producing an energy carrier, such as H_2, was shown to be a promising route to reduce CO_2 emissions.

Another alternative to reduce the dependence on fossil fuels and simultaneously reduce the waste sent to landfills is the waste-to-fuel or waste-to-energy conversion. Besides, if the conversion of waste into fuel is coupled with CO_2 capture, it also plays an important role in tackling climate change. This is because waste usually comprises a substantial biogenic fraction. Thus, the resulting fuels and energy carriers would have a lower carbon footprint than the corresponding fossil fuels. This work has shown that MSW gasification coupled with *in-situ* CO_2 capture (SEG) could deliver a higher H_2 production efficiency (48.7%) than conventional gasification (47.7%) (Chapter 5). Nevertheless, such an increase in thermodynamic performance resulted in an increase in H_2 production costs. This, in turn, translated into an increase in the *LCOH* from 2.1–3.2 €/kg_{H_2} (conventional gasification) to 4.5–5.1 €/kg_{H_2} (SEG). The first figure was found to be in good agreement with the first work published to date for economic appraisal of MSW gasification (Shahabuddin et al., 2020). The authors found that the *LCOH* depended on the plant capacity and the introduction of a gate fee. The *LCOH* ranged from 2.4 €/kg_{H_2} (with gate fee) to 4.5 €/kg_{H_2} (without gate fee) for a plant of 75 MW_{th}. An increase of the plant capacity to 150 MW_{th} was shown to reduce the *LCOH* to the range of 1.3–3.5 €/kg_{H_2}. Although this work also demonstrated that the CO_2 capture implies a cost penalty, the *LCOH* of SEG was lower than that reported for SEG of biomass, 6.1–10.1 €/kg_{H_2}(Schweitzer et al., 2018). This can be explained by the fact there are no fuel costs associated with the use of MSW and the higher plant capacity (100 MW_{th} in this work against 70 MW_{th} in the literature). Yet, SEG is still not competitive at the current stage of development when compared with more mature technologies such as steam methane reforming (SMR) and coal gasification. For the former, *LCOH* falls in the range between 1.0 €/kg_{H_2} and 1.5 €/kg_{H_2} without CO_2 capture and between 1.1 €/kg_{H_2} and 2.6 €/$kg_{H_2}$with CO_2 capture (Parkinson et al., 2019). For the latter, *LCOH* for

the processes without CO_2 capture varies between 0.9 €/kg_{H_2} and 1.8 €/kg_{H_2}, while the integration of CO_2 capture results in a 33–94% increase in the *LCOH* (1.2–3.4 €/kg_{H_2}) (Parkinson et al., 2019). Unlike the SMR and coal gasification, biomass gasification is still not competitive. The *LCOH* reported in the literature falls between 1.4 €/kg_{H_2} and 3.2 €/kg_{H_2} without CO_2 capture and between 2.1 €/kg_{H_2} and 3.3 €/kg_{H_2} with CO_2 capture (Parkinson et al., 2019; Salkuyeh, Saville and MacLean, 2018). Moreover, it should be mentioned that the economic feasibility of H_2 production using renewable energy is still not competitive. Depending on the price of the renewable electricity, water electrolysis has shown the *LCOH* between 4.0 €/kg_{H_2} and 8.0 €/kg_{H_2} for the electricity cost of 50 €/MWh, or even higher than 10.0 €/kg_{H_2} for the electricity cost of >100 €/MWh. The implementation of CO_2 capture entails a cost, cost of CO_2 avoided, that in this work was revealed to be between 90.1 €/t_{CO_2} and 115.5 €/t_{CO_2}. These figures are comparable with that reported for the steam-methane reforming (15.3–127.0 €/t_{CO_2}), but almost the double of that reported for coal gasification (16.1–61.4 €/t_{CO_2}). This can be explained by the large scale of plants considered in these studies as well as the low costs of feedstock (Parkinson et al., 2019).

Although the cost of H_2 production through SEG of MSW has shown to be lower than that of SEG of biomass, this technology is still not competitive. One route to improve the economic performance of this technology is the enhancement of H_2 production, which can be achieved by using sorbents with better CO_2 capture capacity and higher stability after several cycles (Chapter 6). The replacement of limestone with another natural CaO based sorbent, dolomite, has shown no improvement in the thermodynamic performance. This can be attributed to the assumption that the process is energy self-sufficient. Thus, negative net power output was assumed as the cut-off in the thermodynamic appraisal. Since part of the dolomite sorbent ($MgO/MgCO_3$) is inert at the process operation conditions, a higher sorbent make-up was fed to the calciner and, therefore, more energy was consumed to meet the calcination requirements. The use of doped limestone with seawater has been shown to increase the H_2 production efficiency from

48.7% to 50.0%. Still, the thermodynamic performance superiority of doped limestone is not so clear in the economic assessment. This work has revealed that the *LCOH* would be 5.0 €/kg_{H_2} when doped limestone was used, which was the same figure obtained for the process using natural limestone as a sorbent. However, the former figure is associated with higher uncertainty since the price of doped limestone is not available. Depending on this price, the *LCOH* ranged from 4.9 €/kg_{H_2} to 5.2 €/kg_{H_2}, which translated into a cost of CO_2 avoided between 109.3 €/t_{CO_2} and 128.4 €/t_{CO_2}. Furthermore, it was found that a reduction in its price to below 42.6 €/t would reduce the cost of CO_2 avoided (117.7 €/t_{CO_2}) to a value lower than that for natural limestone (114.9 €/t_{CO_2}). A summary of economic performance of the two analysed scenarios, retrofit and greenfield, is presented in Table 7-1.

Table 7-1: Summary of economic performance of the two analysed scenarios, retrofit and greenfield. Case 1: reference pulp and paper plant; Case 2: calcium looping retrofit to the reference plant; Case 3a and Case 3b: integrated black liquor gasification with calcium looping for H_2 production, H_2 compressed at 700 bar and 60 bar, respectively; Case 4a: integrated black liquor gasification with calcium looping for power generation in gas turbine combined cycle; Case 4b: integrated black liquor gasification with calcium looping for power generation in solid-oxide fuel cell

Scenario		Levelised cost of pulp [€/ADt]	Levelised cost of newsprint [€/ADt]	Levelised cost of hydrogen [€/kg_{H_2}]	Cost of CO_2 avoided [€/t_{CO_2}]
Retrofit: Calcium looping for pulp and paper decarbonisation	Case 1	728.3	374.5	N/A	N/A
	Case 2	824.4	411.1	N/A	39.0
	Case 3a	846.6	421.9	N/A	50.8
	Case 3b	842.1	419.8	N/A	48.8
	Case 4a	865.4	431.1	N/A	57.1
	Case 4b	855.1	426.1	N/A	50.8
Greenfield: Calcium looping for H_2 production from sorption-enhanced gasification of municipal solid waste	Conventional gasification	N/A	N/A	2.7	N/A
	Sorption-enhanced gasification (natural limestone)	N/A	N/A	5.0	114.9
	Sorption-enhanced gasification (dolomite)	N/A	N/A	5.4	130.4
	Sorption-enhanced gasification (doped limestone)	N/A	N/A	5.0	117.7

These results show the importance of carrying out an economic assessment besides the thermodynamic assessment. CaL has shown to be a promising technology for the decarbonisation of EIIs and waste-to-energy conversion. Regarding the decarbonisation of EIIs, CaL has presented a superior techno-economic performance to that of mature CO_2 technology, amine scrubbing. Regarding the WtE conversion, CaL has been shown to result in enhanced H_2 production when compared with conventional gasification. However, mature technologies, such as natural gas SMR and coal gasification, present lower costs of H_2 production. Yet, in the future, CaL for H_2 production can become a competitive technology as new sorbents, process layouts and regeneration methods are being developed. Moreover, low-carbon technologies are expected to gain a competitive advantage over fossil fuel options. Such promotion of low-carbon technologies will be achievable by a change in energy policies, attribution of credits to negative emissions, since part of the carbon in the MSW is biogenic, an increase in the CO_2 EUA and funding of R&D. Although the CO_2 EUA has dropped almost 40% at the beginning of the war Ukraine-Russia, it has been gradually recovering in the last two weeks of March to around 80 €/t_{CO_2} (Ember, 2022). Besides, it is forecasted that it will bounce back in the next decades, which will stimulate the adoption of clean technologies.

7.2 References

Ember (2022) *Daily Carbon Prices*. Available at: https://ember-climate.org/data/carbon-price-viewer/ (Accessed: 24 March 2022).

Ferreira, E.T.D.F. and Balestieri, J.A.P. (2015) 'Black liquor gasification combined cycle with CO_2 capture – Technical and economic analysis', *Applied Thermal Engineering*, 75, pp. 371–383.

Hanak, D.P. and Manovic, V. (2017) 'Calcium looping combustion for high-efficiency low-emission power generation', *Journal of Cleaner Production*, 161, pp. 245–255.

Hanak, D.P., Michalski, S. and Manovic, V. (2018) 'From post-combustion carbon capture to sorption-enhanced hydrogen production: A state-of-the-art review of

carbonate looping process feasibility', *Energy Conversion and Management*, 177, pp. 428–452.

Hektor, E. and Berntsson, T. (2009) 'Reduction of greenhouse gases in integrated pulp and paper mills: Possibilities for CO_2 capture and storage', *Clean Technologies and Environmental Policy*, 11(1), pp. 59–65.

Kuparinen, K., Vakkilainen, E. and Tynjälä, T. (2019) 'Biomass-based carbon capture and utilization in kraft pulp mills', *Mitigation and Adaptation Strategies for Global Change*, 24 Mitigation and Adaptation Strategies for Global Change, pp. 1213–1230.

Luis, P. (2016) 'Use of monoethanolamine (MEA) for CO_2 capture in a global scenario: Consequences and alternatives', *Desalination*, 380, pp. 93–99.

Martínez, I., Grasa, G., Callén, M.S., López, J.M. and Murillo, R. (2020) 'Optimised production of tailored syngas from municipal solid waste (MSW) by sorption-enhanced gasification', *Chemical Engineering Journal*, 401, p. 126067.

McGrail, B.P., Freeman, C.J., Brown, C.F., Sullivan, E.C., White, S.K., Reddy, S., Garber, R.D., Tobin, D., Gilmartin, J.J. and Steffensen, E.J. (2012) 'Overcoming business model uncertainty in a carbon dioxide capture and sequestration project: Case study at the Boise White Paper Mill', *International Journal of Greenhouse Gas Control*, 9, pp. 91–102.

Möllersten, K., Gao, L. and Yan, J. (2006) 'CO_2 capture in pulp and paper mills: CO_2 balances and preliminary cost assessment', *Mitigation and Adaptation Strategies for Global Change*, 11(5–6), pp. 1129–1150.

Naqvi, M., Yan, J. and Dahlquist, E. (2013) 'System analysis of dry black liquor gasification based synthetic gas production comparing oxygen and air blown gasification systems', *Applied Energy*, 112, pp. 1275–1282.

Nwaoha, C. and Tontiwachwuthikul, P. (2019) 'Carbon dioxide capture from pulp mill using 2-amino-2-methyl-1-propanol and monoethanolamine blend: Techno-economic assessment of advanced process configuration', *Applied Energy*, 250, pp. 1202–1216.

Onarheim, K., Santos, S., Kangas, P. and Hankalin, V. (2017) ‘Performance and cost of CCS in the pulp and paper industry part 2: Economic feasibility of amine-based post-combustion CO_2 capture’, *International Journal of Greenhouse Gas Control*, 66, pp. 60–75.

Parkinson, B., Balcombe, P., Speirs, J.F., Hawkes, A.D. and Hellgardt, K. (2019) ‘Levelized cost of CO_2 mitigation from hydrogen production routes’, *Energy & Environmental Science*, 12(1), pp. 19–40.

Salkuyeh, Y.K., Saville, B.A. and MacLean, H.L. (2018) ‘Techno-economic analysis and life cycle assessment of hydrogen production from different biomass gasification processes’, *International Journal of Hydrogen Energy*, 43(20), pp. 9514–9528.

Schweitzer, D., Albrecht, F.G., Schmid, M., Beirow, M., Spörl, R., Dietrich, R.-U. and Seitz, A. (2018) ‘Process simulation and techno-economic assessment of SER steam gasification for hydrogen production’, *International Journal of Hydrogen Energy*, 43(2), pp. 569–579.

Shahabuddin, M., Krishna, B.B., Bhaskar, T. and Perkins, G. (2020) ‘Advances in the thermo-chemical production of hydrogen from biomass and residual wastes: Summary of recent techno-economic analyses’, *Bioresource Technology*, 299, p. 122557.

Voldsund, M., Gardarsdottir, S., De Lena, E., Pérez-Calvo, J.-F., Jamali, A., Berstad, D., Fu, C., Romano, M., Roussanaly, S., Anantharaman, R., Hoppe, H., Sutter, D., Mazzotti, M., Gazzani, M., Cinti, G. and Jordal, K. (2019) ‘Comparison of Technologies for CO_2 Capture from Cement Production—Part 1: Technical Evaluation’, *Energies*, 12(3), p. 559.

Zhang, G., Yan, J., Jin, H. and Dahlquist, E. (2011) ‘Integrated Black Liquor Gasification Polygeneration System with CO_2 Capture in Pulp and Paper Mills to Produce Methanol and Electricity’, *International Journal of Green Energy*, 8(2), pp. 275–293.

8 CONCLUSIONS AND RECOMMENDATIONS

8.1 General conclusion

This PhD project aimed to examine the techno-economic feasibility of CaL as a carbon capture technology for combined heat, power and hydrogen production from biomass and/or waste. This aim was accomplished by fulfilling the objectives defined in Section 1.2 and listed as follows:

1. Conduct a comprehensive review of carbon capture technologies across the EIIs, focusing on solid looping cycle technology.
2. Develop a model in Aspen Plus®/CADSIM Plus® to represent a retrofit of a pulp and paper plant with CCS and validate it against the literature data.
3. Develop and validate the process model of hydrogen production from black liquor (by-product from pulp and paper industry) gasification with CO_2 capture.
4. Evaluate the techno-economic feasibility of CaL retrofit to the pulp and paper industry, as a carbon capture route or as a hydrogen production route.
5. Assess the applicability of CaL for hydrogen production with CO_2 capture from another feedstock, MSW.
6. Examine the effect of sorbent selection on the techno-economic performance of the hydrogen production route.

To accomplish the aim and objectives, commercial software (CADSIM Plus® and Aspen Plus®) and deterministic methods were employed for the process modelling and simulation and techno-economic analysis, respectively. As a result of this PhD project, the overall conclusion is that CaL is a feasible technology that can be employed for carbon capture in the pulp and paper industry, turning it into a carbon-negative industry and a net electricity exporter. CaL is also a viable technology for hydrogen production from MSW. Due to its characteristics, CaL can also be used for heat and power production. Although CaL is more cost-efficient for carbon capture in a retrofitted scenario, this technology can become a competitive technology for hydrogen production in a greenfield scenario.

The state-of-the-art in CCS for decarbonisation of the main four EIIs, including iron and steel, cement, petroleum refining and pulp and paper industries, was reviewed over the last decade (Objective 1). It has revealed that of the four EIIs, the pulp and paper industry has been the one with less attention being paid by the researchers. It was also identified that the lack of methodology and assumptions standardisation results in some thermodynamic and economic analysis discrepancies. These discrepancies cause uncertainty and, therefore, a delay in the technology deployment at a commercial scale. To date, there is no dominant CO_2 capture technology. However, high-temperature solid looping cycles seem to be an emerging technology with the potential to be implemented across the EIIs studied.

As identified in the comprehensive literature review, the use of CCS for decarbonisation of the pulp and paper industry has not been thoroughly evaluated and solid looping cycles have not been considered to date. To address this research gap, the techno-economic feasibility of CaL retrofitted to a pulp and paper plant was assessed for the first time (Objective 2 and Objective 4). A new concept of the Kraft process with inherent CO_2 capture was proposed. Such a concept means the integration of CaL in the existing lime cycle, where part of the fresh sorbent of CaL is comprised of the lime mud from the Kraft process. The thermodynamic analysis has shown that the reference plant can turn from electricity importer to electricity exporter. Regarding the economic analysis, the cost of CO_2 avoided was estimated to be 39.0 €/t_{CO_2}. This figure is lower than that recently reported for pulp and paper plants retrofitted with amine scrubbing using MEA as a solvent. It was also identified that the pulp and paper industry has a high potential to become carbon-negative, which with a change of policies would make CCS implementation feasible in this industry. Yet, the CCS feasibility depends strongly on the inclusion of biogenic emissions in the EU ETS and/or on the attribution of credits for them. Carbon capture implementation in this industry would be viable if the negative CO_2 emissions were recognised and a CO_2 emission credit of 41.8 €/t_{CO_2} was applied.

Since the implementation of CaL in the pulp and paper industry promised to be energy and cost-efficient for its decarbonisation, the feasibility of CaL for simultaneous CO_2 capture and H_2 production was assessed. Furthermore, the application of high-temperature solid looping cycles in pulp and paper industry had been limited to the work carried out in this PhD project, mentioned above, and CL for BLG. Although the latter proved that this approach is feasible from the thermodynamic standpoint, the economic feasibility of such a process was not assessed. Therefore, the comparison of CaL implemented in the Kraft process with BLG integrated with CaL for simultaneous CO_2 capture and H_2 production was carried out for the first time (Objective 3 and Objective 4). In the latter case, three configurations were assessed: BLG-CaL-H_2 production, BLG-CaL-GT or BLG-CaL-SOFC. It was found that BLG-CaL is a viable route for CCS, although the CaL route has been shown to be the best option in terms of thermodynamic and economic performance. The CCS route, based on CaL retrofitted to the pulp and paper plant, was found to have a lower cost of CO_2 avoided (39.0 €/t_{CO_2}) when compared with BLG-CaL (48.8–57.1 €/t_{CO_2}). Based on the thermodynamic performance, it was shown that CaL retrofit and BLG-CaL-SOFC presented the best overall performance, turning the electricity importer reference plant into an electricity exporter. Between the BLG-CaL scenarios, BLG-CaL-H_2 presented the lowest cost of CO_2 avoided (48.8 €/t_{CO_2}) but the highest energy penalty. Yet, the techno-economic results could be improved if the operating conditions of BLG are optimised. This implies that the BLG-CaL route is also a promising route for pulp and paper decarbonisation.

In a retrofit scenario, gasification coupled with CO_2 capture seems to be a feasible option for pulp and paper decarbonisation. Moreover, the SEG, gasification with CO_2 capture *in-situ*, presents some advantages relative to the previous option. The gasification and CO_2 capture occur simultaneously in a single reactor and the heat of exothermic carbonation and WGS reactions can meet the energy requirement of endothermic gasification reactions. Although MSW SEG feasibility was already proved and reported in the literature, these works focused on characterising the CO_2 capture rate and syngas composition associated with this type of gasification technology. To date, a comprehensive energy analysis, which

would determine the heat required for the regeneration of CaO sorbent for the cyclic operation of MSW SEG, was not performed. So, the techno-economic viability of H_2 production through SEG of MSW was assessed for the first time (Objective 5). It was shown that SEG can deliver a higher H_2 production efficiency than conventional steam gasification. Depending on the operating conditions, the improvement in H_2 production efficiency can reach almost 4% points. The economic performance assessment showed that the SEG will result in a significantly higher levelised cost of hydrogen (*LCOH*) (5.0 €/kg_{H_2}) compared to that estimated for conventional steam gasification (2.7 €/kg_{H_2}). However, the *LCOH* can be reduced to 4.5 €/kg_{H_2}on an introduction of the gate fee of 40.0 €/t_{MSW}. This translates into a reduction of the cost of CO_2 avoided from 114.9 €/t_{CO_2} to 90.1 €/t_{CO_2}. It should be noted that the *LCOH* found in this work is lower than the values reported for biomass SEG (6.1–10.1 €/kg_{H_2}). Furthermore, the figures reported for the cost of CO_2 avoided are comparable with that reported for the steam methane reforming (15.3–127.0 €/t_{CO_2}). And take into account that the CO_2 emission allowance price has been increasing in recent months and the recent forecasts indicate that it will keep rising, the application of low-carbon technologies such as SEG of MSW will be a feasible option.

MSW SEG has shown to be a valid decarbonisation option in the greenfield scenario, but it is still not a competitive technology. Although the sorbent employed is a low-cost sorbent, it is known that its poor performance over the cyclic process is one of the main drawbacks. For the first time, the effect of sorbent on the performance of H_2 production from MSW through SEG was performed (Objective 6). The dolomite, another natural CaO-based sorbent, and doped limestone with seawater were selected. The techno-economic performance was benchmarked with that of natural limestone. This work revealed that limestone presented the best techno-economic performance with a *LCOH* of around 5.0 €/kg_{H_2}, which translated into a cost of CO_2 avoided of 114.9 €/t_{CO_2} (natural limestone) and 117.7 €/t_{CO_2} (doped limestone). However, it was found that a reduction in doped limestone price to below 42.6 €/t would reduce the cost of CO_2 avoided to a value lower than that for natural limestone.

In summary, CaL has shown to be a promising technology for the decarbonisation of EIIs and waste-to-energy conversion.

- CaL can be integrated into the pulp and paper industry, using the inherent potential of the Kraft process for CO_2 capture. Since part of the sorbent used is composed by lime mud (by-product) there is a reduction in the material cost.
- The integration of CaL in the pulp and paper industry has resulted in a higher overall energy efficiency when compared with other carbon capture technologies such as amine scrubbing. This can be attributed to the fact that CaL operates a higher temperature and therefore, the heat recovery potential is also higher.
- Furthermore, CaL retrofit to the pulp and paper plant has revealed to convert an EII into a carbon-negative industry at lower cost than amine scrubbing retrofit.
- In a greenfield scenario, the H_2 production can be enhanced by the implementation of CaL, delivering a higher H_2 production efficiency higher than that obtained by conventional gasification.

As mentioned above, CaL technology has revealed some advantages when compared with more mature technologies such as amine scrubbing or conventional gasification in case of CO_2 capture or H_2 production routes, respectively. However, there are some hurdles that need to be overcome.

- Although CaL has been attracted more attention in the last decade, the sorbent degradation along the cycles continues being the main drawback of this technology. Natural CaO-based sorbents are characterised with lower sorbent cost but have a high rate of degradation compared to synthetic sorbents. At the time being, given the low price and widely availability of natural limestone, there is no sorbent that could replace this CaO-natural sorbent. So, it is imperative to develop new sorbents for CO_2 capture and H_2 production at similar cost.
- In case of H_2 production route, even though SEG has presented a better environmental performance, this technology it is still not competitive. The

capital cost of SEG needs to be reduced which could be achieved by considering advanced reactors.

- Furthermore, there is a wide range on the techno-economic data in case of CCS and for MSW SEG is still very scarce which cause uncertainty and consequently, delays in the technology implementation.

8.2 Limitations and recommendations for future work

The contribution of this PhD thesis to the current state of knowledge of CaL and CO_2 capture technologies is demonstrated by the publication of five high-impact factor peer-reviewed publications. In addition, this PhD project comprises a comprehensive analysis of the viability of CaL across a wide spectrum of industries, including the pulp and paper industry and WtE industry, and this research presents some limitations that need to be addressed in future research.

Process model design:

- The integration of CaL in the Kraft process was assumed to be achieved by replacing the existing lime kiln with a larger capacity interconnected with the add-on carbonator without affecting the process. However, in practice, the integration of CaL in the pulp and paper process needs to be carefully designed. The process requirements such as the causticisation specifications and the make-up specifications to meet the CO_2 capture requirement of the carbonator need to be taken into account.
- It was also assumed that the make-up composed of fresh limestone and lime mud from the pulp and paper process presents the same behaviour as fresh limestone. In future work, the effect of limestone hydration on the calcination and carbonation reactions and, thus, the effect on CO_2 sorption capacity over the cycles should be studied.
- The BLG model was performed as a black box, which means this model can only be applied to the black liquor composition considered in this work. Likewise, in the MSW gasification or SEG, it was assumed that MSW composition is constant over the year that also limits the flexibility of the model. A quasi-equilibrium approach was adopted to model the MSW gasification, which does not account for the tar formation and the reaction

kinetics. Still, these limitations can be overcome in future work by adopting a kinetic-based model and considering the fluidised bed hydrodynamics.

- The model did not consider the $Ca(OH)_2$ formation, which is not relevant at atmospheric pressure but is enhanced at higher pressures, for example, when high-pressure steam is used in gasification. Thus, the CO_2 capture rate could be reduced. In the case of hydrogen production *via* SEG, the hydrogen yield can also be affected. In future work, the model should account for $Ca(OH)_2$ formation to understand its impact on hydrogen production.

Process analysis:

- The performance of the H_2 production system was evaluated only from a thermodynamic and economic perspective. Besides, the energy analysis was based on the first law of thermodynamics that does not consider the irreversibility of the system. In future work, the performance of the system should be simultaneously assessed from a thermodynamic, economic and environmental perspective. The latter can be achieved by using advanced sustainability assessment tools such as life cycle assessment, exergy analysis and the combination of the latter with economic and environmental analysis, exergoenvironmental and exergoeconomic analyses.

General:

- Further work should focus on standardising the techno-economic assessment of technologies for industrial decarbonisation to support industry and policy decision-makers in deriving reliable decarbonisation pathways.

Appendix A SUPPLEMENTARY INFORMATION TO SUPPORT THE PRESENTED PUBLICATIONS

A.1 Carbon capture for decarbonisation of energy-intensive industries: a comparative review of techno-economic feasibility of solid looping cycles

Table_Apx 1: Input data for calculation of equivalent energy consumption: thermal energy of fuel (Q_{LHV}), thermal energy of steam (Q_{th}) and electrical energy (P_e). The values are presented as the difference between the plant with CO_2 capture and the reference plant, respectively

Reference			Thermal energy of fuel /($MJ_{th}/kgCO_2$)	Thermal energy of steam /($MJ_{th}/kgCO_2$)	Electrical energy[15]/($MJ_{el}/kgCO_2$)
	Iron and Steel				
Ho, Allinson and Wiley (2011)	Amine scrubbing (Monoethanolamine): Blast furnace flue gas				1.51
	Amine scrubbing (Monoethanolamine): Corex iron production flue gas				1.41
	Physical absorption: Shifted blast furnace flue gas				1.08
	Physical absorption: Shifted corex flue gas				0.55
Ho, Bustamante and Wiley (2013)	VPSA: Blast furnace flue gas				1.04
	Amine scrubbing (Monoethanolamine): TGRBF				1.44
	VPSA: TGRBF				0.93
	Amine scrubbing (Monoethanolamine): Hismelt				1.50
	VPSA: Hismelt				1.08
	VPSA: Corex				0.82
Tsupari et al. (2013)	Amine scrubbing (Monoethanolamine)	Layout 1			0.23
		Layout 2			1.27
		Layout 3			1.20

15 Minus sign represents an output compared with the reference

		Layout 4			1.96
		Layout 5			1.88
	Amine scrubbing (Advanced amine)	Layout 1			0.26
		Layout 2			1.09
		Layout 3			1.04
		Layout 4			1.86
		Layout 5			1.86
	Amine scrubbing (Low-temperature regeneration amine, “Low-T”)	Layout 1			0.32
		Layout 2			1.07
		Layout 3			1.01
		Layout 4			1.86
		Layout 5			1.86
Garðarsdóttir et al. (2018)	Amine scrubbing (Monoethanolamine)			3.60	0.37
Cormos et al. (2020)	Amine scrubbing (Monoethanolamine)		-0.60		-0.44
	Calcium looping		2.52		0.57
Tian et al. (2018)	Calcium looping		2.80		
		Cement			
Barker et al. (2009)	Amine scrubbing (Monoethanolamine)		6.01		-0.38
	Oxy-fuel combustion		0.07		0.79
Ho, Allinson and Wiley (2011)	Amine scrubbing (Monoethanolamine)				1.50
Atsonios et al. (2015)	Amine scrubbing (Monoethanolamine)		3.57		0.38
	Calcium looping		6.18		-1.46
Zhou et al. (2016)	Amine scrubbing (Monoethanolamine) + CHP		9.47		-0.62
	Amine scrubbing (Monoethanolamine) + imported utilities			3.7	0.54
	Oxy-fuel combustion		0.80		0.54
Gardarsdottir et al. (2019)	Amine scrubbing (Monoethanolamine)			3.65	0.54
	Oxy-fuel combustion		0.15		0.70
Markewitz et al. (2019)	Amine scrubbing (Monoethanolamine) + imported utilities			3.60	0.41
	Amine scrubbing (Monoethanolamine) + imported utilities			3.50	0.41
	Amine scrubbing (Monoethanolamine) + steam produced on-site			3.80	0.44
	Amine scrubbing (Monoethanolamine) + CHP			3.80	0.44
Cormos et al. (2020)	Amine scrubbing (Monoethanolamine)		5.97		-0.52
	Calcium looping		4.97		-0.51

Romeo et al. (2011)	Calcium looping		0.71		
Rodríguez, Murillo and Abanades (2012)	Calcium looping		1.51		-0.11
	Oxy-fuel combustion		1.20		-0.01
Diego, Arias and Abanades (2016)	Calcium looping (94 % capture rate)		3.09		-0.69
	Calcium looping (58 % capture rate)		0.19		0.44
De Lena et al. (2019)	Calcium looping (100% integration)		2.19		0.15
	Calcium looping (50% integration)		3.34		-0.23
	Calcium looping (20% integration)		4.37		-0.69
		Petroleum refining			
van Straelen et al. (2010)	Amine scrubbing (Monoethanolamine)		4.86		-0.51
Ho, Allinson and Wiley (2011)	Amine scrubbing (Monoethanolamine)				1.59
Berghout, van den Broek and Faaij (2013)[16]	Refinery 1	Amine scrubbing (Monoethanolamine)		2.40(ST)/1.60(LT)	0.35(ST)/0.37(LT)
		Post-Amine scrubbing (Monoethanolamine)			0.54
		Pre-Oxy-fuel combustion			1.31(ST)/1.00(LT)
	Refinery 2	Amine scrubbing (Monoethanolamine)		2.74(ST)/2.05(LT)	0.43(ST)/0.47(LT)
		Post-Amine scrubbing (Monoethanolamine)			0.50
		Pre-Oxy-fuel combustion			1.19 (ST)/0.88(LT)
	Chemical Plant 1	Amine scrubbing (Monoethanolamine)		3.25(ST)/2.00(LT)	0.50(ST)/0.50(LT)
		Post-Amine scrubbing (Monoethanolamine)			0.50
		Pre-Oxy-fuel combustion			1.25(ST)/1.00(LT)
	Chemical Plant 2	Amine scrubbing (Monoethanolamine)		3.60(ST)/1.89(LT)	
		Post-Oxy-fuel combustion			1.79 (ST)/2.38(LT)

16 ST: short-term; LT: long-term

	Steam Reforming H2 plant	Amine scrubbing (Monoethanolamine) Post-		3.0(ST)/2.13(LT)	1.13(ST)/1.13(LT)
		Amine scrubbing (Monoethanolamine) Pre-		2.00	0.40
Fernández-Dacosta et al. (2017)	Amine scrubbing (Mixture of methyl diethanolamine and piperazine)			3.00	0.31
		Pulp and Paper			
Hektor and Berntsson (2009)	Amine scrubbing (Monoethanolamine): configuration 1		4.02		-0.27
	Amine scrubbing (Monoethanolamine): configuration 2		4.50		-2.48
	Amine scrubbing (Monoethanolamine): configuration 3				1.09
	Amine scrubbing (Monoethanolamine): configuration 4		3.09		-0.09
	Amine scrubbing (Monoethanolamine): configuration 5		1.30		-1.42
McGrail et al. (2012)	Amine scrubbing (Monoethanolamine):		2.18		
Onarheim et al. (2017a)	Pulp plant	Amine scrubbing (Monoethanolamine): configuration 1			1.12
		Amine scrubbing (Monoethanolamine): configuration 2			1.06
		Amine scrubbing (Monoethanolamine): configuration 3			0.94
		Amine scrubbing (Monoethanolamine): configuration 4			1.17
		Amine scrubbing (Monoethanolamine): configuration 5			1.12
		Amine scrubbing (Monoethanolamine): configuration 6			1.37
	Pulp and paper plant	Amine scrubbing (Monoethanolamine): configuration 1		3.07	0.90
		Amine scrubbing (Monoethanolamine): configuration 2			1.11
		Amine scrubbing (Monoethanolamine): configuration 3			1.01
		Amine scrubbing (Monoethanolamine): configuration 4		3.07	0.80
		Amine scrubbing (Monoethanolamine): configuration 5		3.05	0.83

		Amine scrubbing (Monoethanolamine): configuration 6	3.05	0.72
Garðarsdóttir et al. (2018)	Amine scrubbing (Monoethanolamine)		3.75	0.39
Santos, Manovic and Hanak (2021)	Calcium looping	5.09		-0.63

A.2 Unlocking the potential of pulp and paper industry to achieve carbon-negative emissions *via* calcium looping retrofit

Table_Apx 2: Capital cost of reference pulp and paper plant and each unit of the retrofitted pulp and paper plant, for the baseline scenario

Installation cost		**Cost M€$_{2017}$**	
		Reference pulp and paper plant	Retrofitted pulp and paper plant
		819.4	819.4
Air separation unit			31.6
CO_2 compression unit			20.1
Calcium looping	Calciner		64.2
	Carbonator		38.9
	Fuel preparation system		22.4
	Fan		0.5
Steam cycle	Steam turbine		4.5
	HRSG & heat exchangers		10.2

Table_Apx 3: Main thermodynamic parameters of the retrofitted pulp and paper plant, for the baseline scenario

Parameter	**Retrofitted pulp and paper plant**
HP steam turbine [MW_{el}]	29.2
IP steam turbine [MW_{el}]	31.4
First LP steam turbine [MW_{el}]	8.9
Second LP steam turbine [MW_{el}]	16.5
ASU consumption [MW_{el}]	19.2
CCU consumption [MW_{el}]	22.6
Flue gas compression [MW_{el}]	4.6
Auxiliary power consumption [MW_{el}]	2.2
Heat available carbonator [MW_{th}]	107.1
Heat available high-purity CO_2 stream [MW_{th}]	65.6
Heat available CO_2-lean off gas [MW_{th}]	101

Table_Apx 4: Main parameters and components of gas streams (molar composition) presented in Figure 3-1, for the baseline scenario

Parameter	CO_2-lean off gas	CO_2 storage
Temperature [°C]	100	25
Pressure [bar]	1	110
Flowrate [t/d]	12498.4	5248.5
Molar composition [-]		
N_2	0.7012	0.0149
O_2	0.0165	0.0143
H_2O	0.2670	0.0025
CO_2	0.0148	0.9657
CO	0.0004	0.0000
H_2S	1 ppm	0.0000
Ar	0.0000	0.0026

A.3 Black liquor gasification with calcium looping for carbon-negative pulp and paper industry

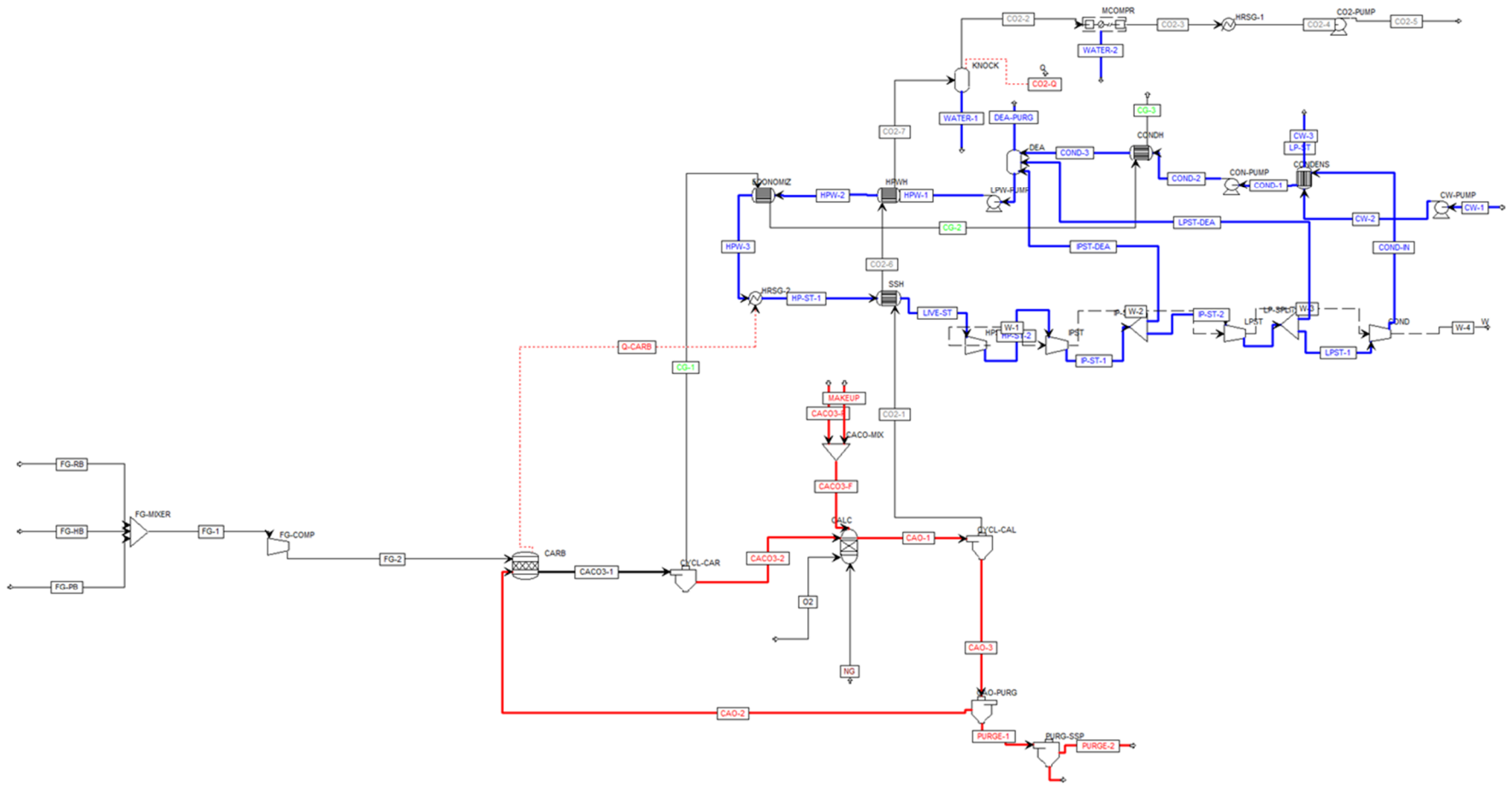

Figure_Apx 1: Flowsheet of CaL retrofitted to the reference plant (Case 2)

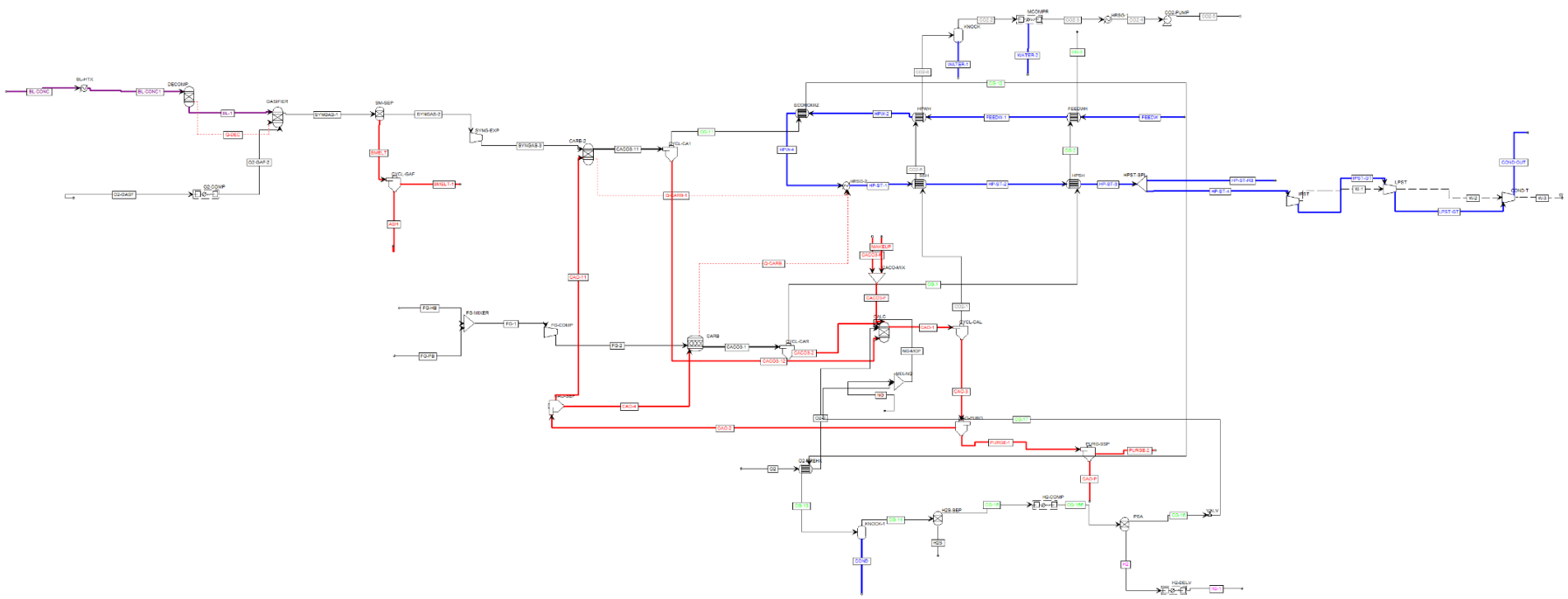

Figure_Apx 2: Flowsheet of CaL and BLG integrated with H_2 production (Case 3)

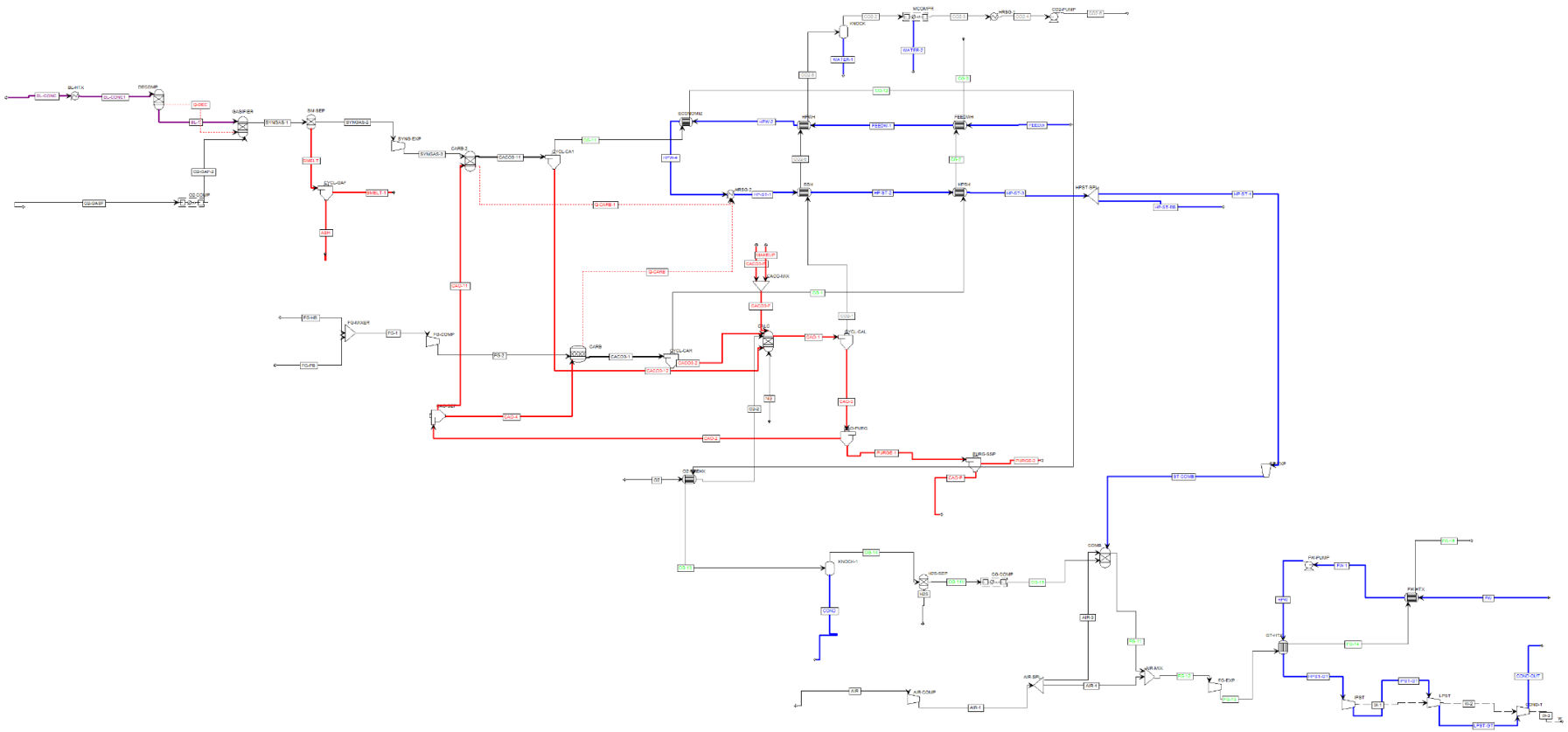

Figure_Apx 3: Flowsheet of CaL and BLG integrated with GT combined cycle (Case 4a)

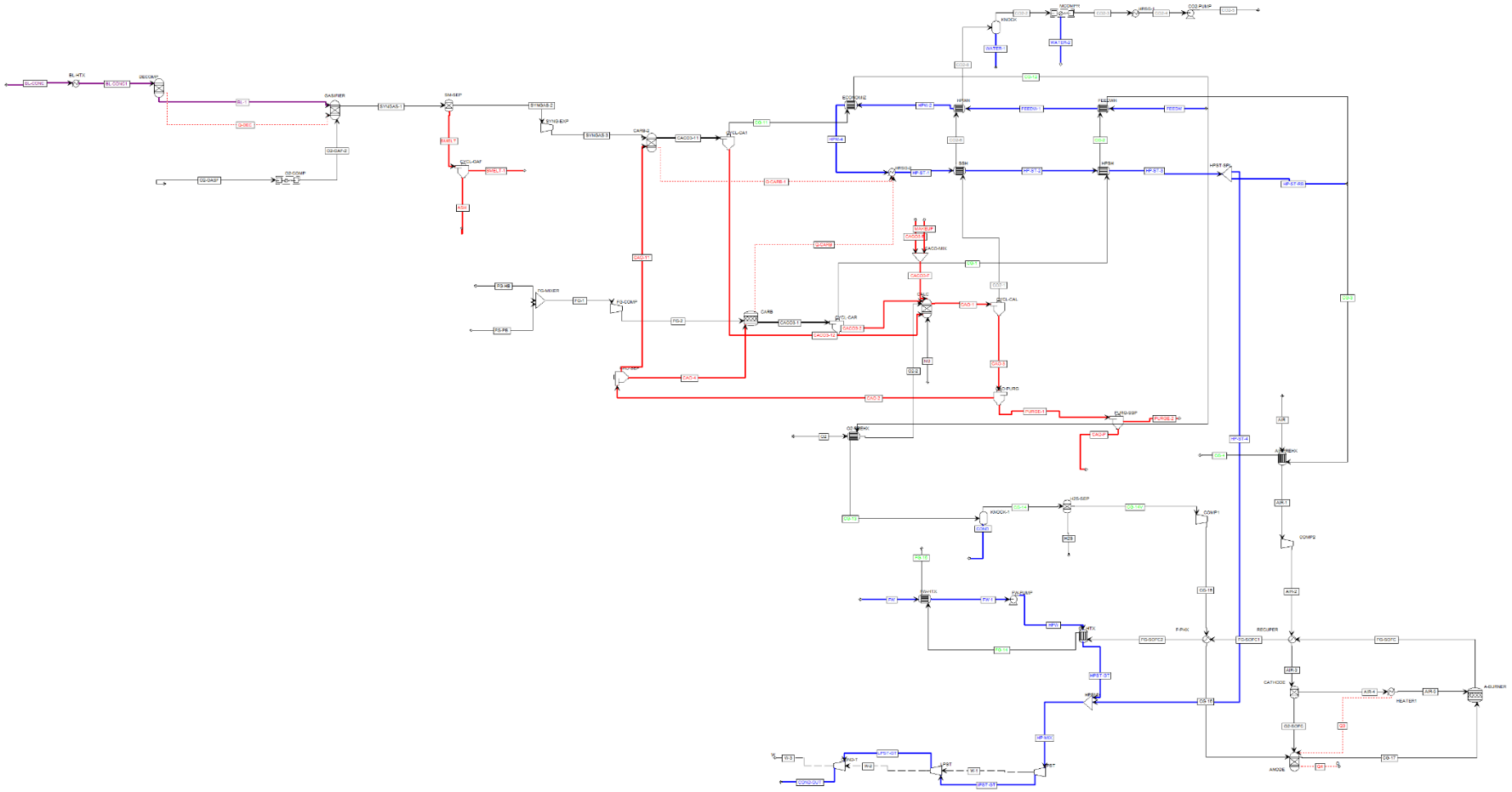

Figure_Apx 4: Flowsheet of CaL and BLG integrated with SOFC combined cycle (Case 4)

Table_Apx 5: Capital cost of reference pulp and paper plant and each unit of the retrofitted pulp and paper plant, for the baseline scenario. Case 3a and Case 3b: integrated black liquor gasification with calcium looping for H_2 production, H_2 compressed at 700 bar and 60 bar, respectively; Case 4a: integrated black liquor gasification with calcium looping for power generation in gas turbine combined cycle; Case 4b: integrated black liquor gasification with calcium looping for power generation in solid-oxide fuel cell

Installation cost		**Cost M€$_{2017}$**				
		Reference pulp and paper plant	Retrofitted pulp and paper plant			
Pulp and paper plant		819.4	819.4			
			Case 3a	Case 3b	Case 4a	Case 4b
Air separation unit		0.0	33.8	33.8	34.3	34.3
CO_2 compression unit		0.0	16.9	16.9	17.0	17.0
Calcium looping	Calciner	0.0	54.2	54.2	53.9	53.9
	Carbonator	0.0	14.3	14.3	14.3	14.3
	Fuel preparation system	0.0	22.1	22.1	21.1	21.1
	Fan	0.0	0.2	0.2	0.2	0.2
	Heat exchanger	0.0	3.9	3.9	4.0	4.0
Black liquor gasification unit	Gasifier	0.0	57.1	57.1	57.1	57.1
	Carbonator	0.0	39.2	39.2	39.2	39.2
	Syngas expander	0.0	9.1	9.1	9.1	9.1
Gas cleaning	Acid gas removal	0.0	6.4	6.4	6.4	6.4
	Claus sulphur plant	0.0	6.0	6.0	6.0	6.0
Pressure swing adsorption		0.0	7.6	7.6	0.0	0.0
H_2 compressor		0.0	5.4	1.1	0.0	0.0
H_2 pressure vessel		0.0	2.0	0.0	0.0	0.0
Gas turbine	Gas turbine	0.0	0.0	0.0	16.9	0.0
	Small steam turbine	0.0	0.0	0.0	0.6	0.0
	Fuel compressor	0.0	0.0	0.0	0.8	0.0
SOFC	SOFC	0.0	0.0	0.0	0.0	63.2
	SOFC auxiliaries	0.0	0.0	0.0	0.0	6.3
	DC/AC inverter	0.0	0.0	0.0	0.0	3.4
	Air compressor	0.0	0.0	0.0	0.0	0.2
	Fuel compressor	0.0	0.0	0.0	0.0	0.4
Steam cycle	HRSG & heat exchangers	0.0	1.5	1.5	3.8	2.6

Table_Apx 6: Main thermodynamic parameters of the retrofitted pulp and paper plant, for the baseline scenario. Case 3a and Case 3b: integrated black liquor gasification with calcium looping for H_2 production, H_2 compressed at 700 bar and 60 bar, respectively; Case 4a: integrated black liquor gasification with calcium looping for power generation in gas turbine combined cycle; Case 4b: integrated black liquor gasification with calcium looping for power generation in solid-oxide fuel cell

Parameter	Retrofitted pulp and paper plant			
	Case 3a	Case 3b	Case 4a	Case 4b
HP steam turbine [MW_{el}]	0.0	0.0	0.0	0.0
IP steam turbine [MW_{el}]	0.6	0.6	7.4	4.8
First LP steam turbine [MW_{el}]	0.2	0.2	2.5	1.7
Second LP steam turbine [MW_{el}]	0.4	0.4	4.7	3.1
Small steam turbine [MW_{el}]	0.0	0.0	0.4	0.0
Syngas expander [MW_{el}]	25.1	25.1	25.1	25.1
Gas turbine [MW_{el}]	0.0	0.0	88.6	0.0
SOFC [MW_{el}]	0.0	0.0	0.0	50.9
ASU consumption [MW_{el}]	21.2	21.2	21.6	21.6
CCU consumption [MW_{el}]	17.4	17.4	17.6	17.6
Flue gas compression [MW_{el}]	1.1	1.1	1.1	1.1
PSA consumption [MW_{el}]	3.8	3.8	0.0	0.0
H_2 compression [MW_{el}]	3.5	1.5	0.0	0.0
Air compression [MW_{el}]	0.0	0.0	60.0	0.9
Fuel compression [MW_{el}]	0.0	0.0	8.4	2.5
Auxiliary power consumption [MW_{el}]	3.7	3.7	3.9	3.9
Heat available carbonators [MW_{th}]		132.2	132.2	132.2
Heat available High-purity CO_2 stream [MW_{th}]		60.9	59.6	59.6
Heat available CO_2-lean off gas [MW_{th}]		26.5	26.5	26.5
Heat available H_2-rich syngas [MW_{th}]		14.7	14.8	14.8
Auxiliary heat produced[17] [MW_{th}]		0.0	77.0	45.0

17 From flue gas from gas turbine or SOFC for Case 4a and Case 4b, respectively.

Table_Apx 7: Main parameters and components of gas streams (molar composition) presented in Figure 4-5 (CASE 3a and CASE 3b) , for the baseline scenario

Parameter	Syngas	H_2-rich syngas	CO_2-lean off gas	CO_2 storage	Tail gas	High-purity H_2
Temperature [°C]	1050	650	157	25	29.4	30
Pressure [bar]	31	1	1	110	1	700/60
Flowrate [t/d]	2162.7	690.5	3502.9	4096.0	194.2	38.2
Molar composition [-]						
N_2	0.0096	0.0146	0.6506	0.0371	0.0438	0.0000
O_2	0.0000	0.0000	0.0093	0.0000	0.0000	0.0000
H_2O	0.4002	0.3826	0.3257	0.0024	0.0000	0.0000
CO_2	0.1863	0.0282	0.0141	0.9405	0.0848	0.0000
CO	0.1821	0.0196	0.0002	0.0031	0.0590	0.0000
H_2	0.2126	0.5482	0.0000	0.0019	0.7924	0.9999
CH_4	0.0002	0.0030	0.0000	0.0000	0.0091	0.0000
H_2S	0.0065	0.0003	0.0000	14 ppm	0.0000	0.0000
SO_2	0.0000	0.0000	0.0000	0.0065	0.0000	0.0000
Ar	0.0024	0.0036	0.0000	0.0084	0.0109	0.0000

Table_Apx 8: Main parameters and components of gas streams (molar composition) presented in Figure 4-6 (CASE 4a) , for the baseline scenario

Parameter	Syngas	H_2-rich syngas	CO_2-lean off gas	CO_2 storage	CO_2-lean off gas (GT)
Temperature [°C]	1050	650	157	25	54.4
Pressure [bar]	31	1	1	110	1
Flowrate [t/d]	2162.7	690.5	3503.1	4171.7	9538.4
Molar composition [-]					
N_2	0.0096	0.0146	0.6506	0.0269	0.7031
O_2	0.0000	0.0000	0.0093	0.0000	0.1340
H_2O	0.4002	0.3826	0.3257	0.0025	0.1421
CO_2	0.1863	0.0282	0.0141	0.9535	0.0092
CO	0.1821	0.0196	0.0002	0.0032	0.0007
H_2	0.2126	0.5482	0.0000	0.0017	0.0018
CH_4	0.0002	0.0030	0.0000	0.0000	0.0000
H_2S	0.0065	0.0003	0.0000	14 ppm	0.0000
SO_2	0.0000	0.0000	0.0000	0.0064	0.0000
Ar	0.0024	0.0036	0.0000	0.0056	0.0090

Table_Apx 9: Main parameters and components of gas streams (molar composition) presented in Figure 4-6 (CASE 4b) , for the baseline scenario

Parameter	Syngas	H_2-rich syngas	CO_2-lean off gas	CO_2 storage	CO_2-lean off gas (SOFC)
Temperature [°C]	1050	650	80	25	144.3
Pressure [bar]	31	1	1	110	1.1
Flowrate [t/d]	2162.7	690.5	3503.1	4171.7	9239.5
Molar composition [-]					
N_2	0.0096	0.0146	0.6506	0.0269	0.7209
O_2	0.0000	0.0000	0.0093	0.0000	0.1351
H_2O	0.4002	0.3826	0.3257	0.0025	0.1242
CO_2	0.1863	0.0282	0.0141	0.9535	0.0103
CO	0.1821	0.0196	0.0002	0.0032	0.0000
H_2	0.2126	0.5482	0.0000	0.0017	0.0000
CH_4	0.0002	0.0030	0.0000	0.0000	0.0000
H_2S	0.0065	0.0003	0.0000	14 ppm	0.0000
SO_2	0.0000	0.0000	0.0000	0.0064	0.0000
Ar	0.0024	0.0036	0.0000	0.0056	0.0093

A.4 Sorption-enhanced gasification of municipal solid waste for hydrogen production: a comparative techno-economic analysis using limestone, dolomite and doped limestone

Table_Apx 10: Cost correlations used on the estimation of the capital cost of each unit

Unit operation	Cost Correlation
Sorption-enhanced gasification	
Sorption-enhanced gasifier [Installed capacity LHV, P_{inst} (MW)] (Schweitzer et al., 2018)	$C_{SEG} = 22.1e6 \left(\frac{P_{inst}}{10}\right)^{0.80}$
Calciner [Calciner heat flux, $\dot{Q}_{calc}$ (kW_{th})] (Michalski, Hanak and Manovic, 2019)	$C_{calc} = 13140\ (\dot{Q}_{cal})^{0.67}$
Air separation unit [O_2 production rate, $\dot{m}_{O_2}$(kg/s)] (Atsonios et al., 2013)	$C_{ASU} = 2.926e7 \left(\frac{\dot{m}_{O_2}}{28.9}\right)^{0.70}$
H_2-rich syngas upgrading	
Pressure swing adsorption unit [Inlet gas molar flowrate, $\dot{n}_{PSA}$ (kmol/h)] (Spallina et al., 2016)	$C_{PSA} = 27.96e6 \left(\frac{\dot{n}_{PSA}}{17069}\right)^{0.60}$
H_2 compressor [Brake power requirement, $\dot{W}_{H_2,BRK}$ (kW_{el})] (Spallina et al., 2016)	$C_{H_2Comp} = 1200 \left(\frac{\dot{W}_{H_2,BRK}}{0.746}\right)^{0.82}$
CO_2 compression	
CO_2 compression unit [Brake power requirement, $\dot{W}_{CCU,BRK}$ (kW_{el})] (Kreutz et al., 2005a)	$C_{CCU} = 1.22914e7 \left(\frac{\dot{W}_{CCU,BRK}}{13000}\right)^{0.67}$
Fuel compressor [Brake power requirement, $\dot{W}_{FC,BRK}$ (kW_{el})] (Lee et al., 2014; Shirazi et al., 2012)	$C_{FC} = 91562 \left(\frac{\dot{W}_{FC,BRK}}{445}\right)^{0.67}$
Steam Cycle	
High-pressure steam turbine [Brake power output, $\dot{W}_{HPST,BRK}$ (kW_{el})] (Manzolini, Macchi and Gazzani, 2013)	$C_{HPST} = 33.7e6 \left(\frac{\dot{W}_{HPST,BRK}}{200000}\right)^{0.67}$
Intermediate-pressure steam turbine [Brake power output, $\dot{W}_{IPST,BRK}$ (kW_{el})] (Manzolini, Macchi and Gazzani, 2013)	$C_{IPST} = 33.7e6 \left(\frac{\dot{W}_{IPST,BRK}}{200000}\right)^{0.67}$
Low-pressure steam turbine [Brake power output, $\dot{W}_{LPST,BRK}$ (kW_{el})] (Manzolini, Macchi and Gazzani, 2013)	$C_{LPST} = 33.7e6 \left(\frac{\dot{W}_{LPST,BRK}}{200000}\right)^{0.67}$
Deaerator [Inlet flowrate, $\dot{m}_{DEA}$ (kg/h)] (NREL, 2005)	$C_{DEA} = 1.30721e5 \left(\frac{\dot{m}_{DEA}}{157970.7}\right)^{0.72}$

Deaerator feed pump [Condensate flowrate, $\dot{m}_{COND}$ (kg/h)] (NREL, 2005)	$C_{P\_DEA} = 8679\left(\frac{\dot{m}_{COND}}{158425.2}\right)^{0.33}$
Low-pressure water pump [Feed water flowrate, $\dot{m}_{LPW}$ (kg/h)] (NREL, 2005)	$C_{P\_LPW} = 95660\left(\frac{\dot{m}_{LPW}}{158425.2}\right)^{0.33}$
Fresh water pump [Fresh water flowrate, $\dot{m}_{CW}$ (kg/h)] (NREL, 2005)	$C_{P\_CW} = 5437\left(\frac{\dot{m}_{CW}}{42625.9}\right)^{0.33}$
Heat exchanger H_2-rich syngas cooler/Steam generator [PINCH, $\dot{Q}_{Syngas\text{-}SG}$ (kW_{th})] (NREL, 2005)	$C_{Syngas\text{-}SG} = 26143\left(\frac{\dot{Q}_{Syngas-SG}}{401.5}\right)^{0.60}$
Condenser [Heat exchange area, A_{COND} (m^2)] (Sayyaadi and Mehrabipour, 2012)	$C_{COND} = 8500+490(A_{COND})^{0.85}$
Heat exchanger live steam [Heat exchange area, A_{LS} (m^2)] (Shirazi et al., 2012)	$C_{LS} = 2290(A_{LS})^{0.60}$
Heat exchanger condensate [Heat exchange area, A_{COND} (m^2)] (Lee et al., 2014)	$C_{COND} = 130\left(\frac{A_{COND}}{0.093}\right)$
Heat recovery steam generator [Steam flowrate, $\dot{Q}_{HRSG}$ (kg/h)] (NETL, 2019)	$C_{HRSG} = 42427\left(\frac{\dot{Q}_{HRSG}}{277458}\right)^{0.7}$
Heat exchanger high-pressure water [Heat exchange area, A_{HPW} (m^2)] (Lee et al., 2014)	$C_{HPW} = 130\left(\frac{A_{HPW}}{0.093}\right)$
Economiser [Heat exchange area, A_{ECON} (m^2)] (Lee et al., 2014)	$C_{ECON} = 130\left(\frac{A_{ECON}}{0.093}\right)$
Gas turbine	
Gas turbine [Inlet air flowrate, $\dot{m}_{Air}$ (kg/s)] (Spallina et al., 2016)	$C_{GT} = 31.5e6\left(\frac{\dot{m}_{Air}}{209}\right)^{0.85}$
Pre-treatment	
Pre-treatment [Processing capacity, $\dot{m}_{MSW}$ (t/h)] (Luz et al., 2015)	$C_{Pre\text{-}t} = (9.0e4\dot{m}_{MSW}+6.6e4) + (7.1e4\dot{m}_{MSW}+8.0e4)$

Table_Apx 11: Capital cost of each unit for the conventional gasification and sorption-enhanced gasification, for the baseline scenario

Installation cost		**Cost M€$_{2017}$**	
		Conventional Gasification	Sorption-enhanced gasification
MSW pre-treatment		3.5	3.5
Gasifier		89.0	0.0
Syngas cleaning	LO-CAT oxidiser vessel	0.7	0.0
	ZnO bed	0.03	0.0
Syngas conditioning	HTS reactor	0.3	0.0
	LTS reactor	0.2	0.0
H_2 purification	Pressure swing adsorption	6.4	5.6
	H_2 compressor	0.5	0.4
Gas turbine	Gas turbine	2.2	2.2
	Fuel compressor	0.4	0.1
Steam cycle	HP Steam turbine	1.8	1.9
	IP Steam turbine	2.2	2.2
	LP Steam turbine	3.0	3.0
	HRSG, heat exchangers & pumps	7.0	0.8
Air separation unit		0.0	8.2
CO_2 compression unit		0.0	5.9
Sorption-enhanced gasifier		0.0	106.5
Calciner		0.0	11.1

Table_Apx 12: Main thermodynamic parameters of conventional gasification and sorption-enhanced gasification, for the baseline scenario

Parameter	Conventional Gasification	Sorption-enhanced gasification
HP steam turbine [MW_{el}]	2.2	2.3
IP steam turbine [MW_{el}]	3.0	3.1
LP steam turbine [MW_{el}]	4.8	4.8
Gas turbine [MW_{el}]	9.8	7.6
ASU consumption [MW_{el}]	0.0	2.8
CCU consumption [MW_{el}]	0.0	3.6
PSA consumption [MW_{el}]	3.9	3.4
H_2 compression [MW_{el}]	0.6	0.4
Air compression [MW_{el}]	5.2	5.3
Fuel compression [MW_{el}]	2.4	0.3
Auxiliary power consumption [MW_{el}]	0.2	0.2
Heat available carbonator [MW_{th}]	0.0	8.2
Heat available high-purity CO_2 stream [MW_{th}]	0.0	9.6
Heat available CO_2-lean off gas [MW_{th}]	0.0	6.6
H_2-rich syngas [MW_{th}]	0.0	28.4
Heat exchanger network [MW_{th}]	103.8	0.0

Table_Apx 13: Main parameters and components of gas streams (molar composition) presented in Figure 5-1, for the baseline scenario

Parameter	Syngas	H_2-rich syngas	Tail gas	High-purity H_2	Flue gas (GT)
Temperature [°C]	900	200	30	30	284
Pressure [bar]	1	1	1	60	1
Flowrate [t/d]	853.9	851.6	411.2	36.1	1221.7
Molar composition [-]					
H_2O	0.5226	0.4236	0.0041	0.0000	0.1150
CO	0.1002	0.0007	0.0027	0.0000	0.0000
CO_2	0.0676	0.1674	0.6960	0.0000	0.2404
CH_4	0.0096	0.0096	0.0400	0.0000	0.0000
H_2	0.2963	0.3963	0.2472	0.9999	0.0000
O_2	0.0000	0.0000	0.0000	0.0000	0.0816
N_2	0.0024	0.0024	0.0099	0.0000	0.5560
H_2S	0.0013	1 ppm	5 ppm	0.0000	0.0000
NH_3	2 ppm	2 ppm	4 ppm	0.0000	0.0000
COS	10 ppm	0.0000	0.0000	0.0000	0.0000
NO	0.0000	0.0000	0.0000	0.0000	0.0002
Ar	0.0000	0.0000	0.0000	0.0000	0.0066

Table_Apx 14: Main parameters and components of gas streams (molar composition) presented in Figure 5-3, for the baseline scenario

Parameter	H_2-rich syngas	Tail gas	CO_2-lean off gas	CO_2 storage	High-purity H_2
Temperature [°C]	650	30	49.1	25	30
Pressure [bar]	1	1	1	110	60
Flowrate [t/d]	778.8	118.7	851.2	856.1	36.8
Molar composition [-]					
H_2O	0.5853	0.0050	0.0740	0.0025	0.0000
CO	0.0231	0.2169	0.0034	0.0000	0.0000
CO_2	0.0114	0.1069	0.0423	0.9632	0.0000
CH_4	0.0461	0.4324	0.0000	0.0000	0.0000
H_2	0.3319	0.2181	0.0009	0.0000	0.9999
O_2	0.0000	0.0000	0.1334	0.0058	0.0000
N_2	0.0021	0.0200	0.7352	0.0237	0.0000
S	0.0000	0.0000	28 ppm	0.0000	0.0000
H_2S	57 ppm	0.0005	6 ppm	0.0000	0.0000
NH_3	6 ppm	24 ppm	0.0000	0.0000	0.0000
COS	5 ppm	46 ppm	1 ppm	0.0000	0.0000
Ar	0.0000	0.0000	0.0087	0.0048	0.0000
NO	0.0000	0.0000	0.0020	5 ppm	0.0000
NO_2	0.0000	0.0000	2 ppm	0.0000	0.0000

A.5 Sorption-enhanced gasification of municipal solid waste for hydrogen production: a comparative techno-economic analysis using limestone, dolomite and doped limestone

Table_Apx 15: Capital cost of each unit for the sorption-enhanced gasification carried out for the two sorbents: dolomite and doped limestone with seawater, for the baseline scenario

Installation cost		**Cost M€$_{2017}$**	
		Sorption-enhanced gasification	
		Dolomite	Doped limestone with seawater
MSW pre-treatment		3.5	3.5
Air separation unit		8.8	7.7
CO_2 compression unit		6.2	5.7
Sorption-enhanced gasifier		106.5	106.5
Calciner		12.1	10.0
H_2 purification	Pressure swing adsorption	5.5	5.6
	H_2 compressor	0.3	0.4
Gas turbine	Gas turbine	1.7	2.7
	Fuel compressor	0.1	0.1
Steam cycle	HP Steam turbine	2.0	1.7
	IP Steam turbine	2.4	2.1
	LP Steam turbine	3.2	2.9
	HRSG, heat exchangers & pumps	0.7	1.0

Table_Apx 16: Main thermodynamic parameters of sorption-enhanced gasification carried out for the two sorbents: dolomite and doped limestone with seawater, for the baseline scenario

Parameter	Sorption-enhanced gasification	
	Dolomite	Doped limestone with seawater
HP steam turbine [MW_{el}]	2.6	2.1
IP steam turbine [MW_{el}]	3.5	2.8
LP steam turbine [MW_{el}]	5.2	4.5
Gas turbine [MW_{el}]	5.6	9.7
ASU consumption [MW_{el}]	3.1	2.6
CCU consumption [MW_{el}]	3.9	3.5
PSA consumption [MW_{el}]	3.3	3.5
H_2 compression [MW_{el}]	0.4	0.4
Air compression [MW_{el}]	4.0	6.8
Fuel compression [MW_{el}]	0.2	0.5
Auxiliary power consumption [MW_{el}]	0.2	0.2
Heat available carbonator [MW_{th}]	12.2	5.3
Heat available High-purity CO_2 stream [MW_{th}]	9.6	9.0
Heat available CO_2-lean off gas [MW_{th}]	4.9	8.4
Heat available H_2-rich syngas [MW_{th}]	25.0	30.1

Table_Apx 17: Main parameters and components of gas streams (molar composition) presented in Figure 6-1 for sorption-enhanced gasification using dolomite as sorbent, for the baseline scenario

Parameter	H_2-rich syngas	Tail gas	CO_2-lean off gas	CO_2 storage	High-purity H_2
Temperature [°C]	650	30	49.1	25	30
Pressure [bar]	1	1	1	110	60
Flowrate [t/d]	697.6	120.2	633.7	921.2	34.8
Molar composition [-]					
H_2O	0.5602	0.0047	0.0739	0.0025	0.0000
CO	0.0256	0.2140	0.0034	0.0000	0.0000
CO_2	0.0113	0.0943	0.0412	0.9600	0.0000
CH_4	0.0556	0.4650	0.0000	0.0000	0.0000
H_2	0.3448	0.2017	0.0009	0.0000	0.9999
O_2	0.0000	0.0000	0.1334	0.0065	0.0000
N_2	0.0023	0.0196	0.7363	0.0260	0.0000
S	0.0000	0.0000	26 ppm	0.0000	0.0000
H_2S	63 ppm	0.0005	5 ppm	0.0000	0.0000
NH_3	7 ppm	24 ppm	0.0000	0.0000	0.0000
COS	6 ppm	48 ppm	0.0000	0.0000	0.0000
Ar	0.0000	0.0000	0.0088	0.0053	0.0000
NO	0.0000	0.0000	0.0021	0.0000	0.0000
NO_2	0.0000	0.0000	2 ppm	0.0000	0.0000

Table_Apx 18: Main parameters and components of gas streams (molar composition) presented in Figure 6-1 for sorption-enhanced gasification using doped limestone with seawater as sorbent, for the baseline scenario

Parameter	H_2-rich syngas	Tail gas	CO_2-lean off gas	CO_2 storage	High-purity H_2
Temperature [°C]	650	30	49.1	25	30
Pressure [bar]	1	1	1	110	60
Flowrate [t/d]	818.4	116.6	1094.7	823.9	37.8
Molar composition [-]					
H_2O	0.5968	0.0051	0.0741	0.0025	0.0000
CO	0.0220	0.2193	0.0034	0.0000	0.0000
CO_2	0.0109	0.1087	0.0425	0.9636	0.0000
CH_4	0.0420	0.4187	0.0000	0.0000	0.0000
H_2	0.3260	0.2272	0.0009	0.0000	0.9999
O_2	0.0000	0.0000	0.1334	0.0050	0.0000
N_2	0.0023	0.0203	0.7349	0.0240	0.0000
S	0.0000	0.0000	29 ppm	0.0000	0.0000
H_2S	55 ppm	0.0005	6 ppm	0.0000	0.0000
NH_3	6 ppm	24 ppm	0.0000	0.0000	0.0000
COS	5 ppm	45 ppm	1 ppm	0.0000	0.0000
Ar	0.0000	0.0000	0.0087	0.0050	0.0000
NO	0.0000	0.0000	0.0020	5 ppm	0.0000
NO_2	0.0000	0.0000	2 ppm	0.0000	0.0000